

# JUACEP Summer Program 2014 at Nagoya University



Japan-US Advanced Collaborative Education Program

Nagoya University

Copyright © JUACEP 2015 All Rights Reserved.

Published in February, 2015

Leaders of JUACEP

Professor Noritsugu Umehara

Professor Yang Ju

Japan-US Advanced Collaborative Education Program (JUACEP)

Graduate School of Engineering

Nagoya University   
NAGOYA UNIVERSITY

Furo-cho, Chikusa-ku, Nagoya, 464-8603, JAPAN

JUACEP@engg.nagoya-u.ac.jp

<http://www.juacep.engg.nagoya-u.ac.jp>

# Table of Contents

## <1> About the Program

a) Overview	...5
b) Participants	...6
c) Schedule	...8

## <2> Classes & Events

a) Japanese Class	...12
b) Handcraft Exercise	...14
c) Field Trip	...15
d) Research Internship	...16
- Research Reports	...18
e) Workshop	
- The 9 <sup>th</sup> Workshop (for UM students)	...106
- The 10 <sup>th</sup> Workshop (for UCLA students)	...131
f) Final Presentation of Medium-term Students	...149

## <3> Reports & Questionnaires on JUACEP Program

a) Reports	...154
b) Questionnaires	...173

## <4> Appendix

a) Pictures	...178
b) Handout Materials	...186



<1>

## About the Program



## 1-a. Overview

This program was designed for graduate and doctoral students of University of Michigan and University of California, Los Angeles. The students had research activities at laboratories of Nagoya University (NU) and worked on the specific research projects under their supervisors at NU.

At the end of the program, they wrote a research report and gave a final presentation at the workshop about the research findings. The report and presentation were evaluated by each NU supervisor and the students got credits (2 or 3 credits depending on the program period) from Nagoya University. The credits were transferred to ME590/ENGR591 at University of Michigan under the agreement.

Also, the optional Japanese language class, handcraft exercise and factory tours were offered during the program.

### ~Program Contents~

[Short Course] May 13 – August 7, 2014 (UM students)

June 17 – August 29, 2014 (UCLA students)

[Medium Course] June 17 – December 18, 2014 (UCLA students)

May		
	13	<b>Orientation for the UM short course students</b>
	14	<b>Research Project, Japanese Language Class</b>
Jun.	12	
	17	<b>Orientation for the UCLA short&amp;medium course students</b>
	18	<b>Research Project, Japanese Language Class</b>
	24	<b>Field Trip to Toyota Factory, INAX Museum and Seafood BBQ in Chita Peninsula</b>
Jul.	1	<b>Handcraft Exercise</b>
	15	
	17	
Aug.	6	
	7	<b>Workshop and Farewell for the UM students</b>
	28	
	29	<b>Workshop and Farewell for the UCLA short course students</b>
?		
Dec.		
	18	<b>Program end of the UCLA medium course students</b>

## 1-b. Participants

	<b>Students from University of Michigan</b>	<b>Advisors at Nagoya University</b>
1	<b>Fu-Long CHANG</b>	Assoc. Prof. Susumu HARA
	Mechanical Engineering	Mechanical Science and Engineering
2	<b>Taehee JANG</b>	Prof. Yang JU
	Electrical Engineering	Mechanical Science and Engineering
3	<b>Songyao JIANG</b>	Prof. Yasuo SUZUOKI
	Electrical Engineering	Electrical Engineering and Computer Science
4	<b>Charles Lesmana SIE</b>	Prof. Nobuo KAWAGUCHI
	Electrical Engineering	Computational Science and Engineering
5	<b>Jin-Gen WU</b>	Prof. Tatsuya SUZUKI
	Mechanical Engineering	Mechanical Science and Engineering
6	<b>Hanyi XIE</b>	Prof. Noritsugu UMEHARA
	Mechanical Engineering	Mechanical Science and Engineering
7	<b>Yang YONG</b>	Prof. Fumihito ARAI
	Biomedical Engineering	Micro-Nano Systems Engineering
8	<b>Yingrui ZHAN</b>	Prof. Takashi ISHIKAWA
	Mechanical Engineering	Materials Science and Engineering
9	<b>Chiyang ZHONG</b>	Prof. Toshiro MATSUMURA
	Electrical Engineering	Electrical Engineering and Computer Science

	<b>Students from UCLA (Short Course)</b>	<b>Advisors at Nagoya University</b>
10	<b>Song DONG</b>	Prof. Koji MIZUNO
	Mechanical and Aerospace Engineering	Mechanical Science and Engineering
11	<b>Jose Eduardo GAVIRIA</b>	Prof. Noritsugu UMEHARA
	Materials Science and Engineering	Mechanical Science and Engineering
12	<b>Zihe HE</b>	Prof. Fumihito ARAI
	Mechanical and Aerospace Engineering	Micro-Nano Systems Engineering
13	<b>Yue HUANG</b>	Prof. Yoji YAMADA
	Mechanical and Aerospace Engineering	Mechanical Science and Engineering
14	<b>Yingxia LIU</b>	Prof. Nobutada OHNO
	Materials Science and Engineering	Electrical Engineering and Computer Science
15	<b>Yuan Hung LO</b>	Prof. Katsutoshi HORI
	Bioengineering	Biotechnology
16	<b>Tait Dewitt MCLOUTH</b>	Prof. Yang JU
	Materials Science and Engineering	Mechanical Science and Engineering
17	<b>Mark Kristopher SEAL</b>	Prof. Toru UJIHARA
	Materials Science and Engineering	Materials Science and Engineering

	<b>Students from UCLA (Medium Course)</b>	<b>Advisors at Nagoya University</b>
18	<b>Elvia CORTES</b>	Prof. Akihiro SASOH
	Mechanical and Aerospace Engineering	Aerospace engineering
19	<b>Antonio MARTINEZ</b>	Prof. Nobuo KAWAGUCHI
	Electrical Engineering	Electrical Engineering and Computer Science



<b>Instructors</b>	
Prof. Yasuhiko SAKAI	Director of Creation Plaza
Asst. Prof. Kazue KANEKO	Creation Plaza
Mr. Masafumi NAKAKIMURA	Chief Technical Staff
Mr. Koji YAMAMOTO	Technical Staff
Mr. Shintaro GOTO	Technical Staff
Mr. Kiyonori SAITO	Technical Staff
Ms. Sumie YASUI	Japanese Teacher

<b>Coordinators of Partner Universities</b>	
Prof. Katsuo KURABAYASHI	Mechanical Engineering, University of Michigan
Prof. Jenn-Ming YANG	Materials Science and Engineering, UCLA





<b>JUACEP Members</b>	
Prof. Yang JU	Mechanical Science and Engineering
Prof. Noritsugu UMEHARA	Mechanical Science and Engineering
Assoc. Prof. Yasumasa ITO	Mechanical Science and Engineering
Tomoko KATO	Administrative Officer
Chiharu YADA	Administrative Officer

# 1-c. Schedule

**JUACEP Summer Program 2014 Schedule**

Date		8:45-10:15	10:30-12:00	13:00-14:30	14:45-16:15	16:15-	
5/12/2014	Mon	Arrival of UM students					
5/13/2014	Tue	Orientation for UM students (10:00 @ ES032)	Lunch @ Chez Jiroud	1. Student insurance, admission fee, in-bound ticket. 2. Passport, out-bound ticket photocopy 3. Introduction to professors, TAs and labs.			
5/14/2014	Wed	Japanese Lang 9:30- (UM)		Stipend & tuition payment@ES031	Introduction to PE II-1	Research at Each Lab	
5/15/2014	Thu	Japanese Lang 9:30- (UM)		Research at Each Lab			
5/16/2014	Fri	Research at Each Lab		Research at Each Lab			
5/17/2014	Sat						
5/18/2014	Sun						
5/19/2014	Mon	Research at Each Lab		Research at Each Lab	Lecture by Prof. Shih		
5/20/2014	Tue	Japanese Lang 9:30- (UM)		Lecture by Prof. Shih	Research at Each Lab		
5/21/2014	Wed	Research at Each Lab		Research at Each Lab	Introduction to PE II-2	Research at Each Lab	
5/22/2014	Thu	Japanese Lang 9:30- (UM)		Research at Each Lab			
5/23/2014	Fri	Research at Each Lab		Research at Each Lab			
5/24/2014	Sat						
5/25/2014	Sun						
5/26/2014	Mon	Research at Each Lab		Research at Each Lab			
5/27/2014	Tue	Japanese Lang 9:30- (UM)		Research at Each Lab			
5/28/2014	Wed	Research at Each Lab		Research at Each Lab	Introduction to PE II-3	Research at Each Lab	
5/29/2014	Thu	Japanese Lang 9:30- (UM)		Research at Each Lab			
5/30/2014	Fri	Research at Each Lab		Research at Each Lab			
5/31/2014	Sat						
6/1/2014	Sun						
6/2/2014	Mon	Research at Each Lab		Research at Each Lab			
6/3/2014	Tue	Japanese Lang 9:30- (UM)		Research at Each Lab			
6/4/2014	Wed	Research at Each Lab		Research at Each Lab			
6/5/2014	Thu	Japanese Lang 9:30- (UM)		Research at Each Lab			
6/6/2014	Fri	University Festival					
6/7/2014	Sat	University Festival					
6/8/2014	Sun	University Festival					
6/9/2014	Mon	Research at Each Lab		Research at Each Lab			
6/10/2014	Tue	Japanese Lang 9:30- (UM)		Research at Each Lab			
6/11/2014	Wed	Research at Each Lab		Research at Each Lab	Introduction to PE III-1	Research at Each Lab	
6/12/2014	Thu	Japanese Lang 9:30- (UM)		Research at Each Lab			
6/13/2014	Fri	Research at Each Lab		Research at Each Lab			
6/14/2014	Sat						
6/15/2014	Sun						
6/16/2014	Mon	Arrival of UCLA students					
6/17/2014	Tue	Orientation for UCLA students (10:00 @ES 021)	Lunch @ Chez Jiroud	1. Student insurance, admission fee, in-bound ticket. 2. Passport, out-bound ticket photocopy 3. Introduction to professors, TAs and labs.			
6/18/2014	Wed	Japanese Lang 9:30- (UCLA)		Stipend & tuition payment@ES032	Introduction to PE III-2	Research at Lab	
6/19/2014	Thu	Japanese Lang 9:30- (UCLA)		Research at Each Lab			
6/20/2014	Fri	Research at Each Lab		Research at Each Lab			
6/21/2014	Sat						
6/22/2014	Sun						
6/23/2014	Mon	Research at Each Lab		Research at Each Lab			
6/24/2014	Tue	Toyota Motor Factory Tour					
6/25/2014	Wed	Japanese Lang 9:30- (UCLA)		Research at Each Lab			
6/26/2014	Thu	Japanese Lang 9:30- (UCLA)		Research at Each Lab			
6/27/2014	Fri	Research at Each Lab		Research at Each Lab			
6/28/2014	Sat						
6/29/2014	Sun						
6/30/2014	Mon	Research at Each Lab		Research at Each Lab			
7/1/2014	Tue	Japanese Lang 9:30- (UCLA)		Handcraft Exersice (Group A)			
7/2/2014	Wed	Research at Each Lab		Research at Each Lab	Introduction to PE IV-1	Research at Each Lab	
7/3/2014	Thu	Japanese Lang 9:30- (UCLA)		Handcraft Exersice (Group B)			
7/4/2014	Fri	Research at Each Lab		Research at Each Lab			
7/5/2014	Sat						
7/6/2014	Sun						
7/7/2014	Mon	Research at Each Lab		Research at Each Lab			
7/8/2014	Tue	Japanese Lang 9:30- (UCLA)		Handcraft Excersice (Group C)			
7/9/2014	Wed	Research at Each Lab		Research at Each Lab	Introduction to PE IV-2	Research at Each Lab	
7/10/2014	Thu	Japanese Lang 9:30- (UCLA)		Research at Each Lab			
7/11/2014	Fri	Research at Each Lab		Research at Each Lab			

62	7/12/2014	Sat						
63	7/13/2014	Sun						
64	7/14/2014	Mon	Research at Each Lab		Research at Each Lab			
65	7/15/2014	Tue	Japanese Lang 9:30- (UCLA)		Handcraft Excercise (Group D)			
66	7/16/2014	Wed	Research at Each Lab					
67	7/17/2014	Thu	Japanese Lang 9:30- (UCLA)		Research at Each Lab			
68	7/18/2014	Fri	Research at Each Lab	Stipend payment@ES031	Research at Each Lab			
69	7/19/2014	Sat						
70	7/20/2014	Sun						
71	7/21/2014	Mon	Marine Day					
72	7/22/2014	Tue						
73	7/23/2014	Wed	Research at Each Lab		Research at Each Lab			
74	7/24/2014	Thu						
75	7/25/2014	Fri						
76	7/26/2014	Sat						
77	7/27/2014	Sun						
78	7/28/2014	Mon						
79	7/29/2014	Tue						
80	7/30/2014	Wed	Research at Each Lab		Research at Each Lab			
81	7/31/2014	Thu						
82	8/1/2014	Fri						
83	8/2/2014	Sat						
84	8/3/2014	Sun						
85	8/4/2014	Mon						
86	8/5/2014	Tue	Research at Each Lab		Research at Each Lab			
87	8/6/2014	Wed						
88	8/7/2014	Thu	Workshop and Farewell Party for UM students @ VBL Hall					
89	8/8/2014	Fri	Departure of UM students					
90	8/9/2014	Sat						
91	8/10/2014	Sun						
92	8/11/2014	Mon						
93	8/12/2014	Tue	Research at Each Lab		Research at Each Lab			
94	8/13/2014	Wed						
95	8/14/2014	Thu	Bon Holidays					
96	8/15/2014	Fri						
97	8/16/2014	Sat						
98	8/17/2014	Sun						
99	8/18/2014	Mon		Stipend payment@account office (3rd floor, ES Bldg.)	Research at Each Lab			
100	8/19/2014	Tue	Research at Each Lab		Research at Each Lab			
101	8/20/2014	Wed						
102	8/21/2014	Thu						
103	8/22/2014	Fri						
104	8/23/2014	Sat						
105	8/24/2014	Sun						
106	8/25/2014	Mon						
107	8/26/2014	Tue	Research at Each Lab		Research at Each Lab			
108	8/27/2014	Wed						
109	8/28/2014	Thu						
110	8/29/2014	Fri	Workshop and Farewell Party for UCLA students (short) @ VBL Hall					
111	8/30/2014	Sat	Departure of UCLA students (short)					
112	8/31/2014	Sun						
113	9/1/2014~ 9/30/2014	-	Research at Each Lab		Research at Each Lab			
114	10/1/2014~ 10/31/2014	-	Research at Each Lab		Research at Each Lab			
115	11/1/2014~ 11/30/2014	-	Research at Each Lab		Research at Each Lab			
116	12/1/2014~ 12/18/2014	-	Research at Each Lab (Submitting research report and final presentation at each lab: date TDB)		Research at Each Lab			
117	12/19/2014	Fri	Departure of UCLA students (medium)					

	Japanese Language Class		Field Trip
	Introduction to Production Engineering (PE)		Workshop
	Handcraft Exercise		Holidays



<2>

## Classes & Events

## 2-a. Japanese Class

Course name	Japanese Language								
Teaching staff	Ms. YASUI Sumie								
Course period	① May 14 - June 12, 2014 for University of Michigan students ② June 18- July 17, 2014 for UCLA students								
Weekly timetable	Tuesday & Thursday, 1st & 2nd period (9 : 30-12 : 00) * May 14, June 18, 25 Wednesday (9 : 30-12 : 00)								
Classroom	#3 Engineering Building, room 441 (4 <sup>th</sup> floor, B3-①)								
Textbook	“GENKI, An Integrated Course in Elementary Japanese” I (The Japan Times) This textbook is a comprehensive approach to developing the four basic language skills (listening, speaking, reading and writing) in order to cultivate overall Japanese-language ability. *Some teaching material will be given in class.								
Course Contents	<p><b>Course outline</b> The purpose of this course is to introduce the most essential Japanese words and expressions for everyday life. Students will learn writing system (Hiragana &amp; Katakana), the basic grammar, expressions of Japanese.</p> <p><b>Classroom activities</b> Basic communication skills required in everyday life will be taught by introducing new vocabulary, new grammar, and practicing listening, conversation and role-playings.</p> <p><b>Homework and Quiz</b> You are expected to submit your homework by the deadline. Quizzes will be given every day in class. 1. Hiragana 2. Katakana 3. Dictation 4. Conjugation</p>								
Evaluation	<table> <tr> <td>1. Homework</td> <td>20%</td> </tr> <tr> <td>2. Quizzes</td> <td>30%</td> </tr> <tr> <td>3. Oral exam.</td> <td>50%</td> </tr> <tr> <td></td> <td><u>100%</u></td> </tr> </table> <p>More than 80% attendance is required.</p>	1. Homework	20%	2. Quizzes	30%	3. Oral exam.	50%		<u>100%</u>
1. Homework	20%								
2. Quizzes	30%								
3. Oral exam.	50%								
	<u>100%</u>								
Course schedule	<p>1. ① 5/14(Wed) ② 6/18(Wed) Greeting Expressions, Hiragana 1 Introducing yourself, Noun sentences 1, Occupation, Nationality, Age, Numbers 1-100</p> <p>2. ① 5/15(Thu) ② 6/19(Thu) Classroom expressions, Hiragana 2 Shopping, Noun sentences 2, Price, Numbers 101-1,000,000</p> <p>3. ① 5/20(Tue) ② 6/25(Wed) Hiragana 3 Describing where things are, Locations Placing an order at a restaurant</p> <p>4. ① 5/22(Thu) ② 6/26(Thu)</p>								

- Hiragana 4  
Talking about your daily life  
Verbal sentences 1, Time reference, Adverbs
5. ① 5/27(Tue) ② 7/1(Tue)  
Hiragana 5  
Invitations, Suggestions, Desires  
Verbal sentences 2, Days/Weeks/Months/Years, Counting
6. ① 5/29(Thu) ② 7/3(Thu)  
Katakana 1  
Talking about your family  
Adjectives, Likes or Dislikes, Degree expressions, Family terms
7. ① 6/3(Tue) ② 7/8(Tue)  
Katakana 2  
Talking about your week-end, Past tense, Time words
8. ① 6/5(Thu) ② 7/10(Thu)  
Katakana 3  
Making a request (Verb-Te-form ), Progressive actions,  
Describing your status
9. ① 6/10(Tue) ② 7/15(Tue)  
Asking permission, Prohibition, Negative request  
Describing two things  
Talking about your interests  
Plain form
10. ① 6/12(Thu) ② 7/17(Thu)  
**The Final Examination (speaking)**

① Class UM	② Class UCLA
Fu-Long Chang	Elvia Cortes
Songyao Jiang	Jose Gaviria
Charles Sie	Zihe He
Hanyi Xie	Yue Huang
Yang Yong	Tait McLouth
Yingrui Zhan	Mark Seal
Chiyang Zhong	Antonio Martinez

## 2-b. Handcraft Exercise

### *“Demonstration of the Internal Combustion Engine”*

Date: Group A - July 1 (Tue)

Group B - July 3 (Thu)

Group C - July 8 (Tue)

Group D - July 15 (Tue)

Time: 13:00-16:00

Place: Creation Plaza (10<sup>th</sup> floor, IB Building)

Staff: Yasuhiko Sakai, Professor, Director of Creation Plaza

Kazue Kaneko, Professor, Creation Plaza

Koji Yamamoto, Technical staff

Masafumi Nakakimura, Technical staff

Shintaro Goto, Technical staff

Kiyonori Saito, Technical staff



### Schedule

--13:00~13:30--

- (1) Opening remarks: By Professor Yasuhiko Sakai
- (2) Self-introduction of Staffs
- (3) Self-introduction of Students: Department, Grade, Name, Motivation
- (4) Lecture of the basis of the Internal Combustion Engine by Teaching Assistants
  - ①History
  - ②Characteristic
  - ③Operation principle
  - ④Practice engine

--13:30~14:30--

- (5) Assembling practice
  - ①Disassembling
  - ②Assembling
  - ③Adjustment

--14:30~15:30--

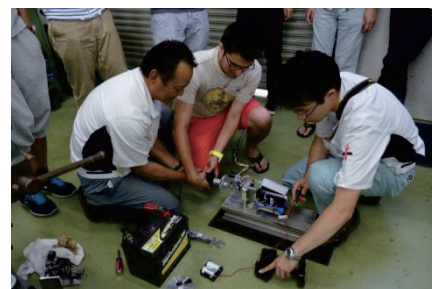
- (6) Performance test

--15:30~15:50--

- (7) Discussion
  - ①Comment
  - ②Discussion
  - ③Questionnaire

--15:50~16:00--

- (8) Closing with taking a memorial photograph





## 2-c. Field Trip

**Date:** June 24 (Mon)

**Visited Places:**

\* Toyota Motor Factory (Motomachi Plant)

[http://www.toyota.co.jp/en/about\\_toyota/facility/toyota\\_kaikan/index.html](http://www.toyota.co.jp/en/about_toyota/facility/toyota_kaikan/index.html)

\* Uotaro (lunch)

\* INAX Museum

<http://www1.lixil.co.jp/ilm/english/>

**Schedule:**

Time	Event
08:30	Departure from Nagoya University
09:30	Arrival at Toyota Motor Factory
09:30-10:40	Bus tour of the factory (assembly and welding shops)
10:40	Departure from Toyota Motor Factory
12:00-14:00	Lunch (seafood BBQ at Uotaro in Chita Peninsula)
14:30	Arrival at INAX Museum
14:30-17:00	Tour of the museum
17:00	Departure from INAX Museum
18:00	Arrival at Nagoya University



## 2-d. Research Internship

### Participants from University of Michigan

	Name	Research Theme	Report Title
1	Fu-Long CHANG	A Novel Control System Design for Robust Assist Systems	Updating Final-State Control Algorithm with Overshoot/Undershoot Prevention Technique for a Connection Control Problem (P.18)
2	Taehee JANG	Design of a Multifunction Probe Used for Microwave AFM	Design of a Multifunction Probe Used for Microwave AFM (P.19)
3	Songyao JIANG	Load-Frequency Control Considering Power Output Fluctuation of Renewable Energy Generators	Dynamic Modelling of Combined Cycle Power Plant for Load Frequency Control with Large Penetration of Renewable Energy (P.20)
4	Charles Lesmana SIE	Human Activity Sensing and Recognition	Exploration of Correlation Coefficient Method Accuracy on Human Activity Sensing Data (P.28)
5	Jin-Gen WU	Design of Automated Collision Avoidance System for Small EV	Automated Steering System for Obstacle Avoidance Based on Potential Field Method (P.34)
6	Hanyi XIE	Friction and Wear of 3D Printed Material	Friction and Wear for 3D Printed Material (P.40)
7	Yang YONG	3D Fabrication of Nanostructure	Assemble of Multi-layer Structured Blood Vessel (P.41)
8	Yingrui ZHAN	Cold Forge Spot-Bonding of Metallic Materials	Cold Forge Spot Bonding of Copper and Aluminum Alloy Sheets (P.48)
9	Chiyang ZHONG	Surge Analysis for Lightning Protection or Switching and Protecting Phenomena	Development of Current Suppression Equipment in Low Voltage DC Distribution System (P.57)

## Participants from UCLA

	Name	Research Theme	Report Title
1	Song DONG	Vehicle Crash Safety	Analysis of Vehicle's Crash Based on Structures' Section Forces (P.65)
2	Jose Eduardo GAVIRIA	Tribology of CNx Including Boron at High Temperature	Manufacture and Characterization of Boron Oxide Solid Lubricant Using Radio Frequency Magnetron Sputtering at Low-Vacuum (P.73)
3	Zihe HE	On-Chip Cell Manipulation	Bonding in Chip Fabrication for Cell Stiffness Measurement (P.81)
4	Yue HUANG	Slip Control for Contact Motion Reproduction: from Human to Dummy Skin	Slip Control for Contact Motion Reproduction (P.87)
5	Yingxia LIU	Analysis of Solder Joints Using an Inelastic Material Model	Thermal Stress and Strain Analysis of TSV and Microbumps in 3D IC Using Abaqus (P.88)
6	Yuan Hung LO	Bacterial Adhesion and Biofilm Formation	Adhesive Bacterionanofiber AtaA and Quorum Sensing in Bacterial Immobilization (P.89)
7	Tait Dewitt MCLOUTH	Quantitative Evaluation of Carbon-fiber Content-rate in GFRP Laminations Using Microwaves	Quantitative Evaluation of Carbon Fiber Content in CFRP Using Microwave Analysis (P.90)
8	Mark Kristopher SEAL	Solution Growth of Cubic SiC	Analysis of Solution Growth Conditions on Silicon Carbide (SiC) Polytype (P.91)
9	Elvia CORTES	Effect of Anode Geometry on Steady-State Magnetoplasmdynamics Thruster	Performance of an Applied-field MPD Thruster (P.100)
10	Antonio MARTINEZ	Indoor Map and Navigation	Acceleration Sensing: Design of Elevator Recognition and Displacement Estimation Algorithm and Implementation on Smartphone (P.101)

# Updating Final-State Control Algorithm with Overshoot/Undershoot Prevention Technique for a Connection Control Problem

Fu-Long Chang

Department of Mechanical Engineering  
University of Michigan  
Ann Arbor, MI 48109-2125 USA

Email: fulong@umich.edu

Supervisor: Susumu Hara

Department of Mechanical Science and Engineering  
Nagoya University  
Nagoya 464-8603

Email: haras@mech.nagoya-u.ac.jp

## ABSTRACT

This paper proposes a method to prevent overshoot and undershoot (OS/US) problems for final-state control (FSC) and updating final-state control (UFSC). The FSC is an optimal feedforward control technique to drive a dynamic system to a specified state in a specific time period by external inputs. The UFSC is a modified version of FSC to deal with the varying final state by updating the FSC control input at each sample time. However, both FSC and UFSC algorithm does not guarantee that no overshoot or undershoot happens on the transient state between the initial state and the final state. This paper proposes an OS/US prevention technique via tuning the FSC or UFSC activated time. The technique is developed by adding a constraint that all the FSC or UFSC control input should be in the same direction. In this paper, the effectiveness of the algorithm is verified by simulations of a plural-cart connection problem. When an operator pushes a cart and attempts to connect with another stationary cart in the front, the front cart should be accelerated to the same velocity and position as those of the rear cart at the moment of connection end in order to realize a smooth connection. Furthermore, the front cart should not have any backward or forward motion during the connection to prevent the collision between the carts or crash something in the front. Therefore, a UFSC algorithm with OS/US prevention technique is highly desired.

# Undisclosed

## **DESIGN OF A MULTIFUNCTION PROBE USED FOR MICROWAVE AFM**

Taehee Jang

Department of Electrical Engineering and Computer Science, University of Michigan  
tjang@umich.edu

Supervisor: Prof. Yang Ju

Graduate School of Engineering, Nagoya University  
ju@mech.nagoya-u.ac.jp

### **ABSTRACT**

A new multifunctional probe used for microwave AFM (M-AFM) which can obtain the morphology and the electrical properties of materials was designed to improve the impedance matching and directivity of the probe. In order to enhance the performance, it is designed on the microstrip transmission line. The thickness of gold was increased to 780nm to reduce the ohmic loss due to the skin depth. The simulation results of the new probe were compared with those of the previous probe. In addition, the three types of tips were designed and simulated.

Undisclosed

# DYNAMIC MODELLING OF COMBINED CYCLE POWER PLANT FOR LOAD FREQUENCY CONTROL WITH LARGE PENETRATION OF RENEABLE ENERGY

Songyao Jiang

Department of Electrical Engineering and Computer Science, Graduate School of University of Michigan  
songyaoj@umich.edu

Supervisor: Associate Prof. KATO, Takeyoshi

Graduate School of Engineering, Nagoya University  
tkato@nuee.nagoya-u.ac.jp

## ABSTRACT

As the concern about climate change and energy shortage grow stronger, the incorporation of renewable energy in the power system in the future is foreseeable. In a hybrid power system with a large penetration of PV generation, PV panel is regarded as a negative load in the power system. With the accurate prediction of PV output power, load frequency control could be done by controlling the thermal and hydro power plant in the system. Combined Cycle Power Plant is widely used because of its great advantages of fast response and high efficiency. This article is focusing on the mathematical modelling and analysing of Combined Cycle Power Plant for the frequency control purpose in a model of hybrid system with large renewable energy generation.

## 1. BACKGROUND

### 1.1 FUTURE OF RENEWABLE ENERGY

Electricity is regard as a kind of clean energy without pollution in utilization. But nowadays, the process to generate electricity is not clean because thermal power plant which combust coal oil and natural gas still hold an important part of the generation. These kind of energy sources are called fossil fuel which are converted from the ancient dead organisms through a long natural process called decomposition. Because the process, millions of years, is significantly longer than any human activities, fossil fuels are generally considered to be non-renewable resources because. In addition, the consumption of fossil fuel always comes together with the emission of pollution to air and water system. Therefore, as concerns of the shortage and pollution of fossil fuel grows stronger, many countries encourage the development of renewable energy. It is expected that the renewable energy could completely replace the traditional fossil fuel and even nuclear in the future.

The World Wide Fund for Nature (WWF), which is an international non-governmental organization working on issues regarding environment, post a famous energy report in 2011. In this report, WWF advocates a 100% renewable energy future in 2050.[1] It analyse the demand and supply of energy and provide and approach to the utilization of renewable energy. It also points out the challenges ahead like equity, land and sea use, lifestyle, innovation and provide some possible solutions. Peoples are motivated by this report that the world is excited for the coming of a foreseeable renewable future. Figure 1 shows the percentage of different energy source from 2000 to 2050.

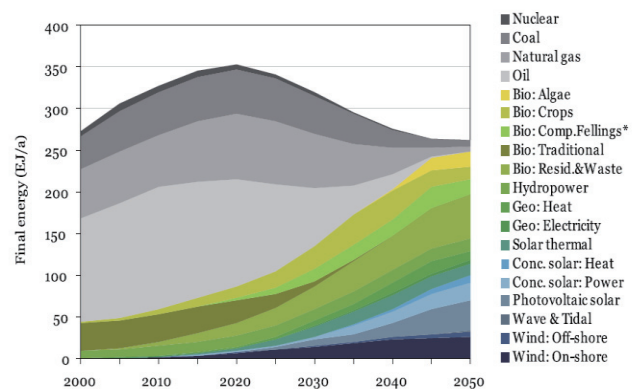


Figure 4: World Energy Supply by Source. The Ecotys Energy Scenario, December 2010

Fig.1 World Energy Supply by Source [1]

The figure shows that in the future renewable energy like biomass, hydropower and solar power will play a major role in the energy consumption. Some countries, for example Germany and Australia are reported targeting switch to the 100% renewable energy in 2050. Because of the consideration of climate changes and energy shortage, replacing traditional fossil and nuclear energy with renewable energy has become a worldwide trend.

## 1.2 RENEWABLES IN POWER SYSTEM

Currently, most of the electricity generation relies on the combustion of fossil fuel. Figure 2 is a pie chart presenting the percentage of power generation by different type of sources for the first four months of 2014. This chart is delivered from the data provided by US energy department.

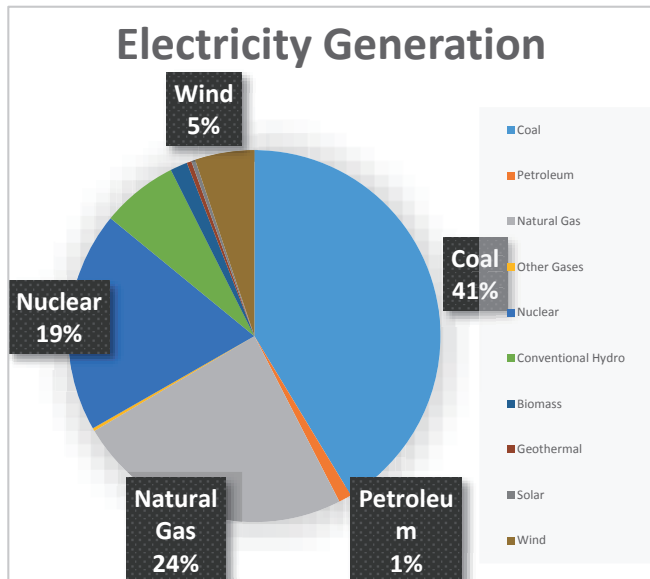


Fig. 2 Electricity Generation by Sources [2]

As shown in the figure, coal and natural gas forms 65% of the total power generation and renewables only forms less than 15% of the generation now. Wind energy and traditional hydropower are two of the most mature renewables in the world. However, wind farm is considered as a project that take large area of land to operate. Wind farm must choose the area where wind is relatively strong and sustaining over the year. This kind of area is always far from the place where the power is majorly used, for example big cities and large factories. Solar power is considered to be one of the most important resources in the future with large potential. As we know, most of the energy on earth comes from the sun. If a very small part of that power could be utilized, human will never suffer the shortage of energy. WWF made an assumption in their energy report that if 0.3% of the Sahara Desert was a concentrated solar plant, it would power all of the Europe. Of course, this idea sounds too idealist. In fact, just like wind farm, PV farm also requires a significantly large area of land to install. This feature increase the cost of PV power and prevents PV farm to be developed further. Recently the development of the idea Micro-grid and Distributed Generation incorporate large usage of solar panel. Unlike the traditional power system that generation and load are separated to be far from each other, Distributed Generation is an ideal that generation is installed at the usage site. PV panel, wind turbine, small natural gas generator and fuel cell are the major generation plant in distributed generation. For example, in a district of living houses, PV panels could be installed on every roof of the buildings, which makes usage of the sunlight that not used currently and solve the issue that PV panels need large area to install. Large

penetration of renewable energy generation is definitely practical and foreseeable in the future.

As renewable energy generation depends mostly on the condition of the weather, for example PV panel depends on the amount of sunlight that received and wind turbine depends on the speed of wind, it is hard to regulate the generation of renewables comparing to traditional generation. While controlling the power output of renewables, the response is much slower than traditional generation with petroleum and natural gas. For a hybrid power system with renewables and traditional fossil fuel power plant, the generation of PV panels is often regarded as negative load in the system. The responsibility of balancing load and generation relies on the control of traditional generation in the system. The load and generation control is discussed in detail in next section. The techniques to predict PV output power is still under development. PV output power could be predicted by imaging processing using satellite images or ground based camera. Many of the students in my lab are currently working on the forecasting of PV power now. Renewable energy generation will definitely play an important role in power system in the future.

## 2. AGC OF HYBRID POWER SYSTEM

As known to all, electricity cannot be stored in significant amount. Therefore, the dynamic balance between generation and demand is one of the most important issue in power system. It is required that load and generation are balanced moment by moment. Load is the usage of electricity in the grid, so in general, it could not be controlled. Therefore, the generation of power plant should be controlled and adjusted frequently to balance the system. Nowadays, this process is controlled automatically and so called *Automatic Generation Control (AGC)*.

In the process of balancing the load and generation, it is difficult to directly measure the load. Instead, as the grid is using AC current nowadays, system frequency is considered to be a very useful indicator of the power mismatch. Power mismatch will have an influence on the system frequency. If the generation is larger than demand, the generation will converted to kinetic energy and therefore increase the frequency of the system. The amount of increase in system frequency depends on the total storage and total inertia of the system. If the generation in the power system could not meet the demand, the kinetic energy will convert to electricity to meet the demand of load. Therefore, if the frequency becomes lower than nominal value, which is 50Hz or 60Hz, it indicates that the generation needs to be increased. If the frequency is higher than the nominal value, the generation needs to be decreased. Continues adjustment need to be implemented in the system to keep the frequency stable. It is because that frequency, as an aspect of system stability, is important for many applications on the grid. Large deviation and fluctuation in frequency will cause potential damage to some precise instruments.

## 2.1 TURBINE-GOVERNOR CONTROL

There are different types of AGC. The first one is called *Turbine-Governor Control*. The kinetic energy talk above is stored in the turbine generator units in the power system. The turbine flows the Newton's second law, which is

$$J\alpha = T_m - T_e \quad (1)$$

When the load suddenly increase, the current will also increase. This will lead the electrical torque  $T_e$  of each turbine unit to increase to supply the increased load. From the equation (2), it could be seen that the acceleration  $\alpha$  then becomes negative. A negative acceleration will cause the drop of speed of the turbine units. Because the system frequency is proportional to the speed of the generating synchronous machine, the frequency also drops.

The Turbine-Governor Control act as a proportional control to compensate the changes in load. It follows the equation:

$$\Delta p_m = \Delta p_{ref} - \frac{1}{R} \Delta f \quad (2)$$

where  $\Delta p_m$  is the change in turbine  $\Delta f$  is the frequency deviation,  $\Delta p_{ref}$  is the change of the setting of reference power.  $R$  is called the droop coefficient. Figure 3 shows a Turbine-Governor Control example.

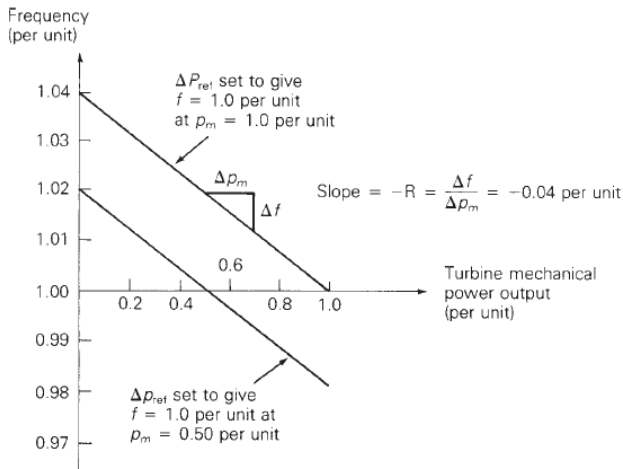


Fig. 3 Turbine-Governor Control [X]

## 2.2 LOAD-FREQUENCY CONTROL

Because the Turbine-Governor Control is proportional control, there exists a steady state error in frequency. The second type of AGC, which is *load frequency control (LFC)*, could further management the output of generators and reset the frequency to its nominal value. Considering a control area in the power system with interconnected tie-lines, the objective of LFC is to absorb its own load changes in the area, regulating the frequency to nominal value and maintaining the power flow in tie-lines as scheduled. There is an important factor in LFC called *area control error (ACE)*. It could be defined using the following equation:

$$ACE = \Delta p_{tie} + B_f \Delta f \quad (3)$$

where  $\Delta f$  is the frequency deviation and  $\Delta p_{tie}$  is the deviation of net tie-line power flow.  $\Delta p_{ref}$  is the change of the setting of reference power.  $B_f$  is called the *frequency bias constant*.

LFC works together with Turbine-Governor that  $\Delta p_{ref}$  could be calculated as the integral of ACE, which is,

$$\Delta p_{ref i} = -K_i \int ACE dt \quad (4)$$

With the integral part in this control process, the frequency deviation will be continuously affect the output of generators to maintain the frequency at its nominal value.

## 3. COMBINED CYCLE POWER PLANT

### 3.1 INTRODUCTION OF CCGT

The gas turbine engine is a complex assembly of different components such as compressors, turbines, combustion chambers, etc., designed on the basis of thermodynamic laws [1]. It is a type of heat engines that absorb the heat of energy source, converting it into mechanical energy, which drives electrical generators. Combined cycle gas turbine is based on the design of single cycle gas turbine. As shown in Figure 4. In single cycle gas turbine, when the gas turbine is operated, air is filtered and then drawn through the inlet of the compressor. The fuel, which is natural gas in this case, is fed into the combustor together with compressed air and combusted. The resulted high-temperature and high-pressure gas is fed into the gas turbine and drives its shaft. Then the mixed gas is exhausted. However, this exhaust gas is still low in its Entropy which means much energy is wasted without utilization. Therefore, it limits the efficiency of single cycle gas turbine, which is about 34% in net Carnot thermo-dynamic efficiency.

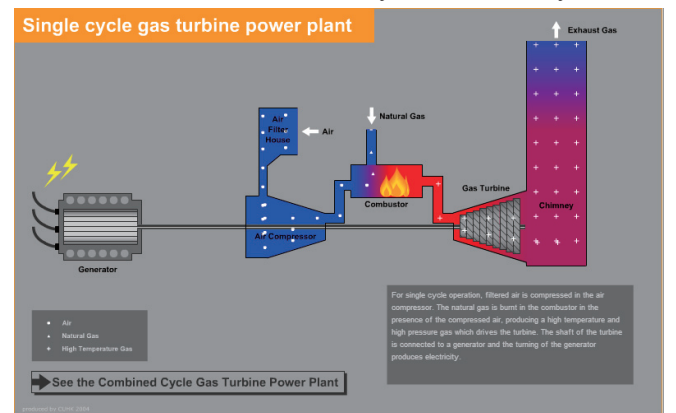


Fig. 4 Single cycle gas turbine power plant

By adding a subsequent heat engine, it may extract energy from the waste heat of the exhaust gas, which could improve the overall efficiency of the plant. A commonly used combination is adding a steam turbine after the cycle of gas turbine. The remaining heat in exhaust gas generate steam in



a special device called *heat recovery steam generator* (HRSG), as shown in Figure 5. The steam is fed into the steam turbine and produce additional mechanical power and therefore electricity. The steam is recycled through condenser and fed into HRSG again. This process could probably improve 50 – 60 percent of the overall efficiency. This is called a Combined Cycle Gas Turbine. It could achieve a thermal efficiency of around 60%. Because of its high efficiency and fast response, many new gas power plants around the world are of this kind.

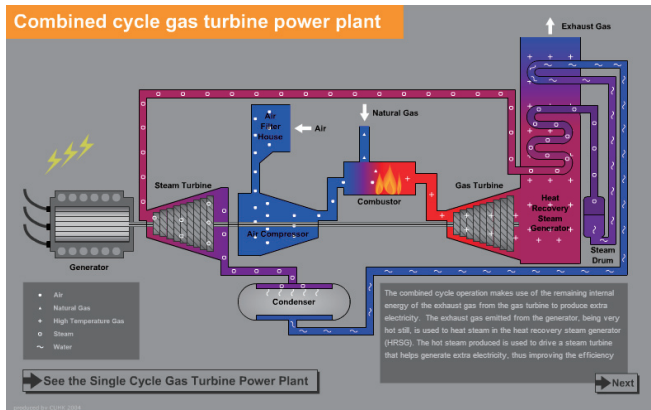


Fig. 5 Combined cycle gas turbine power plant

### 3.2 MATHEMATICAL MODELLING & LITERATURE SURVEY

To simulate load frequency control, the dynamic characteristics of combined cycle power plant is crucial. As a heat engine, thermal effect plays the most important role in modelling combined cycle power plant. There are two major points of control in this kind of power plant, which are air flow and fuel flow. The air flow into the compressor is controlled by inlet of the compressor while the fuel flow into the combustor is controlled by the fuel valve. Air and fuel together determine the temperature and pressure of the resulted gas output from the combustor, which determines the power output of the gas turbine and the temperature of the exhaust gas. To model the dynamic performance of combined cycle, it is better to use the single cycle gas turbine as a basic reference. There is a famous model of gas turbine which is called Rowen's Model. [4]

#### 3.2.1 ROWEN'S MODEL OF SINGLE CYCLE GAS TURBINE.

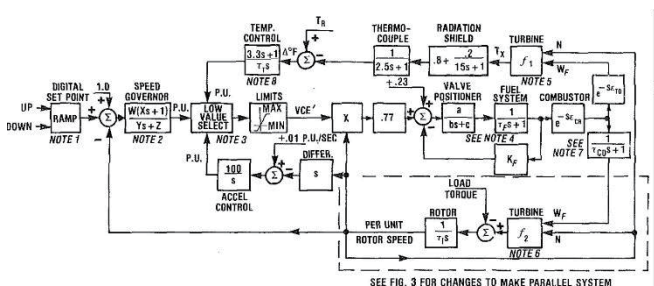


Fig. 1 Simplified single-shaft gas turbine simulation block diagram for isolated operation

Fig. 6 Rowen's model of SCGT [4]

Rowen provided a very detailed explanation of his model. In this model, it could be found that thermal flow and control both play critical roles. As shown in Figure 6, there are three different types of control in his model. The first one is *speed control*. The measured speed from the rotor dynamics is subtracted from the speed set point, which is 1 per unit (pu). The error signal is fed into the speed governor and generate speed control signal. The second one is the *temperature control* circuit. The exhaust temperature is calculated from the gas flow and rotating speed of the turbine. Then the temperature value is transmitted through the blocks of thermocouple and radiation shield. This process simulates the measurement of the exhaust temperature that the resulted temperature is regarded as the measured temperature by devices. The temperature controller controls the temperature of the exhaust gas and set the exhaust temperature at reference value to prevent the gas turbine from overheat. It could also improve the efficiency of the gas turbine. The third one is *acceleration control*. This controller is used to prevent the turbine from accelerate or decelerate too fast. The low value selector compared three control signals and use the lower one to determine the operating condition of the gas turbine. This control signal is regarded as the fuel signal which determine the fuel flow into the combustor. The time constants of fuel system and combustor delay are also considered and included. The resulted gas flow into the turbine together with the system frequency are used to calculate the turbine output force and exhaust temperature. The output force is fed into the block which stands for the rotor inertia. Together with the load torque, regarding the inertia as an integrator, the rotor speed could be calculated easily.

#### 3.2.2 ZHANG'S MODEL OF COMBINED CYCLE GAS TURBINE

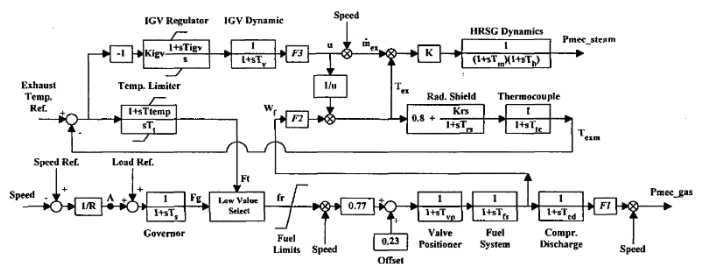


Fig. 2. Combined cycle plant dynamic model

Fig. 7 Zhang's model of CCGT [5]

For combined cycle gas turbine, because of the existence of HRSG and steam turbine. The mathematical model is more complicated than the model of single cycle gas turbine. But the Rowen's model of SCGT could be a great reference. Zhang's model is based on the model build by Rowen. As explained in Zhang's article, the time constant of steam turbine, which is the second cycle in CCGT, is much slower than the constant of gas turbine, which is the first cycle in CCGT. In fact, the exhaust temperature in CCGT is controlled at certain fixed value to maximize the efficiency of

steam turbine. Therefore, as a result, the dynamics of steam turbine have little influence on the overall dynamics of CCGT. As shown in Figure 7, Zhang's model is basically very similar to Rowen's model. Acceleration control is eliminated in Zhang's model, IGV control is added to control the temperature of exhaust gas to maximize the efficiency and the dynamics of HRSG and steam turbine is added. Steam flow is calculated as a function of turbine speed and a coefficient K is added to stand for the efficiency of steam turbine. The output power of gas turbine and steam turbine could be added together to stand for the total power output of CCGT.

### 3.2.3 MANTZARIS & VOURNAS'S MODEL OF COMBINED CYCLE GAS TURBINE

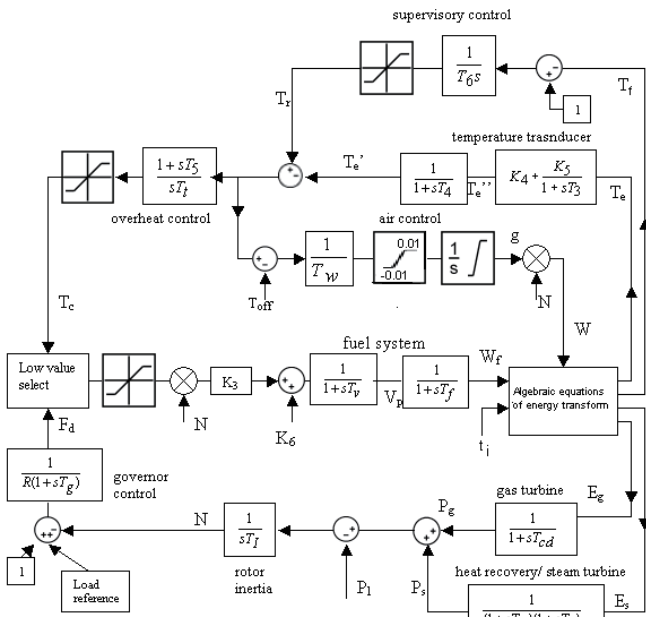


Fig. 8 Mantzaris & Vournas's model of CCGT [6]

Mantzaris & Vournas develop their own model and incorporate the advantages of Zhang's model by making their own modification. As shown in Figure 8, all the mathematical calculation is integrated in a block called *Algebraic Equation of Energy Transform*. This model has a clear flow of signals that the key control variables, which are air flow W and fuel flow Wf are fed into the algebraic block and calculate gas flow and steam flow into the turbines together with the temperature of exhaust gas. There is an additional control circuit in this model called *supervisory control*. It takes the gas turbine inlet temperature into consideration that the inlet temperature will have an influence on reference temperature which is used to regulate exhaust temperature to maintain the plant at maximum efficiency.

Because of the logic structure of this model is clear and the parameters are given in detail. I rebuild my model according to this one. The following's are the equations used in this model [7]:

From the adiabatic compression equation the following relation holds, where x is the ratio of input-output temperatures for isentropic compression:

$$x = \frac{t_{d,is}}{t_i} = (P_r)^{\frac{\gamma-1}{\gamma}} \quad (1)$$

In (1)  $P_r$  is the actual compressor ratio. For nominal airflow ( $W=1pu$ ), this is equal to the nominal ration  $P_{r0}$ . When airflow is different from nominal ( $W \neq 1$ ), the actual compression ratio is

$$P_r = P_{r0}W \quad (2)$$

and therefore:

$$x = (P_{r0}W)^{\frac{\gamma-1}{\gamma}} \quad (3)$$

From the definition of compressor efficiency:

$$\eta_c = \frac{t_{d,is} - t_i}{t_d - t_i} \quad (4)$$

The gas turbine inlet temperature depends on the fuel to air ratio (assuming that air is always in excess). The temperature rises with the fuel injection  $W_f$  and decreases with airflow W.

From the energy balance equation in the combustion chamber, the following normalized equation results:

$$W \frac{t_f - t_d}{t_{f0} - t_{d0}} = W_f \quad (6)$$

or:

$$t_f = t_d + (t_{f0} - t_{d0}) \frac{W_f}{W} \quad (7)$$

Similar to (4), the gas turbine efficiency is given by

$$\eta_t = \frac{t_f - t_e}{t_f - t_{e,is}} \quad (8)$$

For the adiabatic expansion, noting from (3) that the right hand side is the same as in the compression (the mass that enters the compressor is the same with the one in the output of the gas turbine) we have:

$$x = \frac{t_f}{t_{e,is}} \quad (9)$$

from which we obtain for the actual exhaust temperature similarly to (5):

$$t_e = t_f [1 - (1 - \frac{1}{x})\eta_t] \quad (10)$$

$$E_g = K_0[(t_f - t_e) - (t_d - t_i)]W \quad (11)$$

The thermal power absorbed by the heat exchanger of the recovery boiler is proportional to airflow and exhaust temperature.

$$E_s = K_1 t_e W \quad (12)$$

	Parameter	Value
ti0	Ambient temperature (K)	303
td0	Nominal compressors discharge temperature (C)	390
tf0	Nominal gas turbine inlet temperature (C)	1085
te0	Nominal exhaust temperature(C)	532
Pr0	Nominal compressor pressure ratio	11.5
$\gamma$	Ratio of specific heat (Cp/Cv)	1.4
$\eta_c$	Compressor efficiency	0.85
$\eta_t$	Turbine efficiency	0.85
K0	Gas turbine output coefficient (1/K)	0.00303
K1	Steam turbine output coefficient (1/K)	0.000428
R	Speed governor regulation	0.04
Tg	Governor time constant (s)	0.05
K4	Gain of radiation shield	0.8
K5	Gain of radiation shield II	0.2
T3	Time constant of radiation shield(s)	15
T4	Time constant of thermocouple(s)	2.5
T5	Time constant of temperature control (overheat) (s)	3.3
Tt	Temperature control (overheat) integration rate (s)	0.4699
Tc max	Temperature control upper limit	1.1
Tc min	Temperature control lower limit	0
Fd max	Fuel control upper limit	1.5
Fd min	Fuel control lower limit	0
K3	Fuel valve lower limit	0.23
Tv	Valve positioner time constant (s)	0.05
TF	Fuel system time constant (s)	0.4
T6	Time constant of Tf control (s)	60
Tw	Time constant of air control (s)	0.4699
Tcd	Gas turbine time constant (s)	0.2
Tm	Steam turbine time constant (s)	5
Tb	Heat recovery boiler time constant (s)	20
TI	Turbine rotor inertia constant (s)	18.5
Toff	Temperature offset	0.01

Table 1: Parameters used in M&V's Model of CCGT [6]

### 3.3 MODIFICATION & SIMPLIFICATION

I rebuilt the model according to Mantzaris & Vournas's model using Simulink. The model is shown in Figure 9.

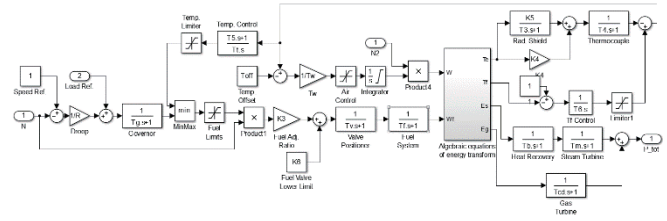


Fig. 9 Model of CCGT in Simulink

There are two input of this sub system, which are frequency and load reference, and one output, which is the overall output of the Combined Cycle Power Plant. In this project, the major concern is the regulation of frequency by adjusting the power output of plants in its normal operating point, which means the speed deviation is small. Therefore, the dynamics of the path from frequency deviation to power output is the most important path in our model. The above model is too complicated for this project because of the consideration about the thermal transform and control paths. The above model must be simplified before implemented.

According to the explanation in Rowen's article. The product of the turbine speed with air flow and fuel flow is not necessary when the speed deviation is small. Therefore, in our application, this product could be eliminated. Furthermore, the supervisory control is not necessary. It is because that the ambient temperature, which is the air inlet temperature is not given in our application. This temperature is considered to be constant which would have no influence on the reference temperature. The simplified version of CCGT model is shown in Figure 10.

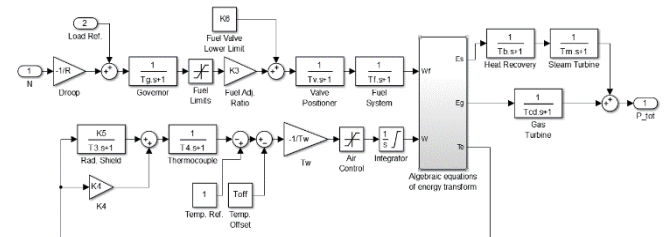


Fig. 10 Simplified CCGT Ver. 1

The logic relationship is clear in this model. The two points of control, which are air flow  $W$  and fuel flow  $W_f$ , are decoupled comparing to the previous model. However, this model still seems to be complicated than expected. After careful consideration, I found that the air control loop is used for maintain the exhaust temperature at desired value to maximize the efficiency of the system. In my application, efficiency is not concerned, so we could make an assumption that the air flow is always at its nominal value, which is 1 pu. In this situation, the control loop of air flow could be completely deleted. In such case, the exhaust temperature will not be fed back and controlled. The further simplified version of model is shown in Figure 11 below.

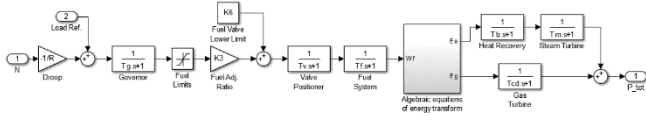


Fig. 11 Simplified CCGT Model Ver. 2

As shown in this model, there is a single loop through which the frequency deviation and power output is connected with many time constants and delays. This version of CCGT model is simplified enough and meets the requirements of this project.

## 4 SIMULATION AND RESULTS

### 4.1 SIMPLE TEST CIRCUIT

After modelling and simplified the dynamic behaviour of CCGT. Simple test must be implemented to examine the assumption I made in simplifying the model. Figure 12 shows a simple test circuit I built in Simulink to test the dynamic behaviour of the model after the sudden change of load.

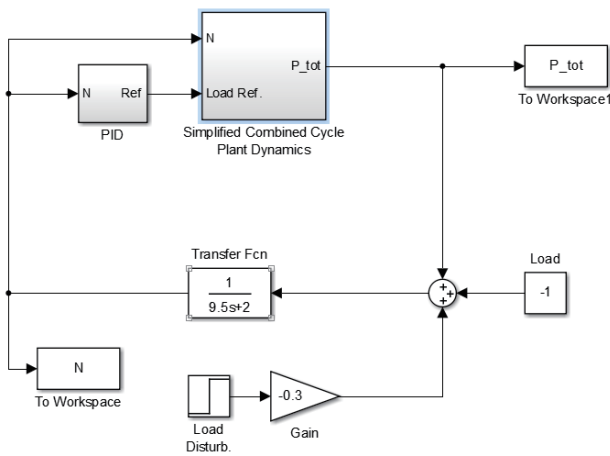


Fig. 12 Simple Test Circuit in Simulink

There is a constant load of 1 pu in the circuit and the load suddenly change to 1.3 pu at 200s using a step function and a gain of 0.3. The output power of CCGT is added to the total load of the system. The resulted mismatch is fed into a transfer function which stands for the total system inertia. The parameters of the inertia is get from the inertia of Matsumoto's model. The output of the inertia dynamics is the speed deviation. This deviation is regulated externally by a simple PI controller which is shown in Figure 13.

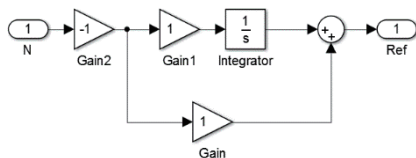


Fig. 13 Simple PI Controller

The control signal output is fed into CCGT model as the load reference signal which is used as an integral control to reset the frequency at its nominal value.

By comparing the dynamic behaviour of the model before and after simplification, the assumption I made during simplification could be therefore verified. Figure 14 shows the result of this simulation. It shows the power output and frequency change of the CCGT. The red line stand for the model before simplification and the blue line stand for the model after simplification. After the sudden change in load at 200s, the frequency suddenly drop by 0.02. Then the controllers, which are both Turbine Governor Control and LFC worked and got the frequency back. Then the output of the CCGT becomes 1.3 pu, which is equal to the total load. It means that the generation and demand are balanced again. There is almost no difference between the model before and after simplification. There is only tiny difference at the start. Starting behaviour is not a concern in this project. Therefore, according to this simple test, the simplified model of CCGT is thought to be valid and sound.

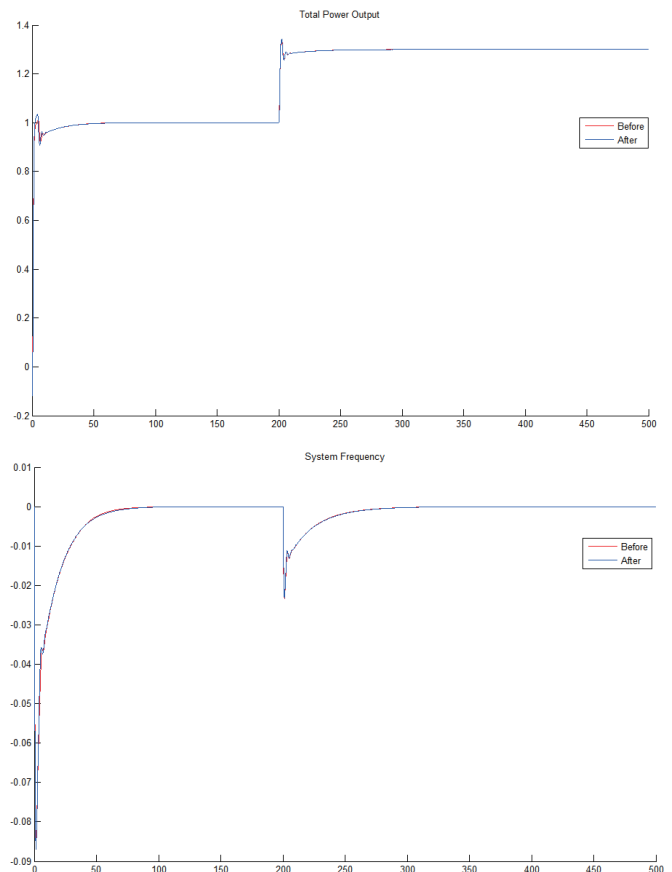


Fig. 14 Comparison of Simulated Results

#### 4.2 IMPLEMENT ON MATSUMOTO'S MODEL

Mr. Matsumoto tested my model of CCGT together with his model. However, in your model, there is energy loss in the simulation block to calculate the exhaust gas temperature and turbine input gas temperature. Therefore, my CCGT model initially did not work as of it in his model. He made a modification to my model that the output gain of the abovementioned block was adjusted to cancel the energy loss. After that, he replaced the steam turbine model to my CCGT model. At this time my CCGT model works fine with his system. As a result, the frequency deviation was reduced because of the quicker response of CCGT than steam turbine.

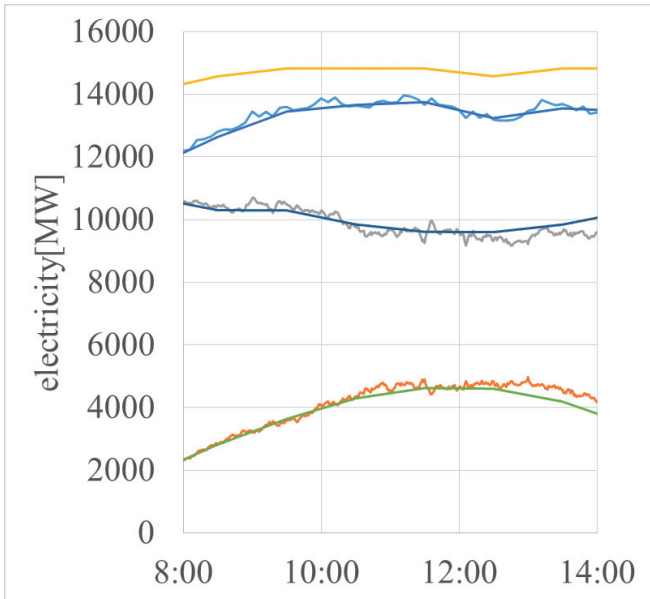


Fig. 15 Total Power of Matsumoto's Hybrid System

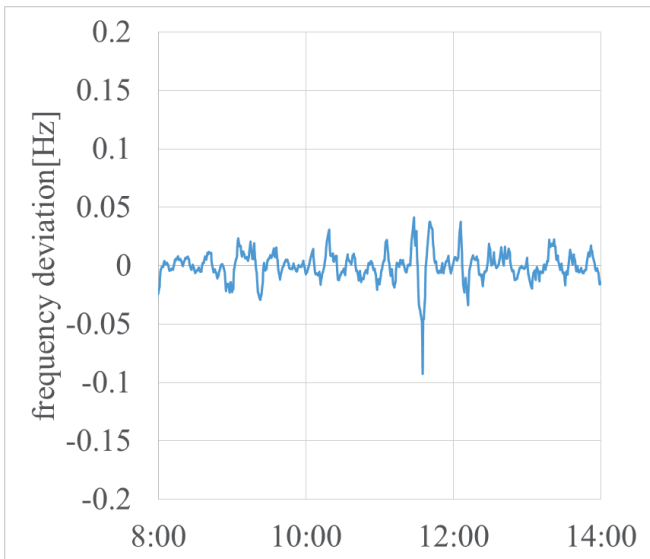


Fig. 16 Frequency Deviation Using the Original Steam Turbine

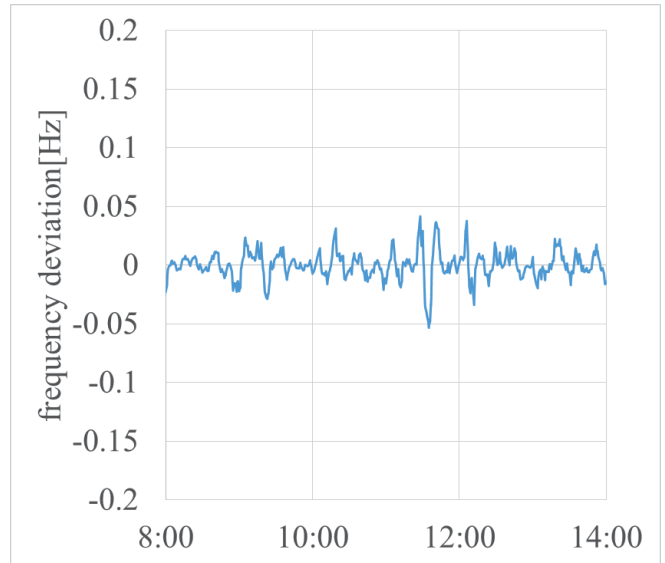


Fig. 17 Frequency Deviation Using the CCGT

#### REFERENCES

- [1]. WWF, The Energy Report, 2011.
- [2]. U.S. Energy Information Administration, Monthly Energy Review Jul 2014, page 95, 2014.
- [3]. H. Cohen, G.F.C. Rogers, H.I.H. Saravanamuttoo, Gas Turbine Theory, 4th Edition, Longman, London, 1996.
- [4]. Rowen, W.I., "Simplified mathematical representations of heavy-duty gas turbines," Journal of Engineering for Power, Vol. 105, pp. 865-869, October 1983.
- [5]. Zhang, Q., So, P. L., "Dynamic Modelling of a Combined Cycle Plant for Power System Stability Studies", IEEE Power Engineering Society Winter Meeting, Vol. 2, pp. 1538-1543, 2000.
- [6]. Mantzaris, J., Vournas, C. "Modelling and Stability of a Single-Shaft Combined Cycle Power Plant", Int. J. of Thermodynamics, Vol. 10 (No. 2), pp. 71-78, June 2007.
- [7]. Spalding, D. B., Cole, E. H., Engineering Thermodynamics, Edward Arnold, London, 1973.

#### ACKNOWLEDGEMENTS

I would like to express my deepest appreciation to all those who provided me the possibility to complete this report. A special gratitude I give Supervisor, Associate Professor. Kato, whose contribution in stimulating suggestions and encouragement, helped me to coordinate my project especially in simplifying the model.

Furthermore I would also like to acknowledge with much appreciation the crucial role of Mr. Matsumoto, who explained me the theories in his model and help me simulate my simplified model with his hybrid system.

# EXPLORATION OF CORRELATION COEFFICIENT METHOD ACCURACY ON HUMAN ACTIVITY SENSING DATA

Charles Lesmana Sie

Department of Electrical Engineering and Computer Science, University of Michigan  
charlsie@umich.edu

Supervisor: Nobuo Kawaguchi, Kei Hiroi, Katsuhiko Kaji

Graduate School of Engineering, Nagoya University  
kawaguti@nagoya-u.jp, k.hiroi@ucl.nuee.nagoya-u.ac.jp, Kaji@nuee.nagoya-u.ac.jp

## ABSTRACT

The introduction of many fitness tracking devices early this year shows manufacturer's interest to gear costumers towards healthier lifestyle. The most essential feature of the device is to count steps taken by the user. Step counting is a basis to develop a human activity sensing algorithm. There are many ways that has been developed to measures steps taken. This paper explores the use of correlation coefficient to statistically measure steps taken based on the acceleration data. The first cycle of the acceleration norm waveform is the sliding window to generate correlation coefficient plot. Each peak in the plot indicates one step taken by the user. The result showed that the correlation coefficient has a better accuracy in counting steps compared to the threshold method. The correlation coefficient method produces an error percentage that is 14.6% lower than the result of threshold method.

## 1. INTRODUCTION

Human activity sensing composed of various methods to identify action, such as walking and jogging, using mathematical algorithm based on the readings of sensors or sensory network. The activity can range from complex measurement of movement of human joint as well as a simpler one such as steps taken in a defined period of time.

Numerous smart phone applications have a feature to count steps taken by using positional information of the Global Positioning System (GPS). These applications can give users estimation on the steps taken; however, most of them are lacking in accuracy in indoor environment. This happens because the direct connection from the device to the satellite may be blocked in indoor environment.

In this project, the correlation coefficient method will be used to measure steps taken from the information given by accelerometer readings only. Thus, it eliminates the needs of direct satellite connection to the user's device. The information on the object unique features, such as age, gender, and height were considered to provide performance analysis on different object groups. The accuracy of this

method was explored to provide knowledge for further research on human activity sensing.

## 2. RELATED WORK

Estimating the number of steps taken from acceleration data is one of the estimation used in Pedestrian Dead Reckoning (PDR). PDR is the process of calculating an object's current position using a sensory data and previously determined location. The process uses acceleration, gyro, and geomagnetism data to estimate number of steps taken, step length and the walking direction.

PDR is used in many navigational systems, such as car GPS and smart navigation apps. Users use navigation application to direct them to desire destination, and it works well in outdoor settings. However, the method is subject to cumulative error since the estimation of current state is based on the previous state. This problem is worse in an indoor setting. Indoor position estimation is harder due to the obstacles that could alter the sensor data.

In order to improve accuracy of indoor positioning, a robust method to estimate the number of steps taken is very crucial. There has been plenty of method used to count steps, such as the threshold method [1]. It uses high and low threshold values to count steps as the acceleration norm waveform pass through the values. However, limitation appears due to its rigid algorithm and static parameters. Another method, developed by First Line Software, is to calculate the angle between sensor's acceleration vectors of current and previous points to detect one step. But, this method is susceptible to noise [2].

The proposed method explored in this paper, tries to provide flexibility by using dynamic parameter without hurting the accuracy. This method is expected to be simpler and cheaper to implement compared to the threshold method.

## 3. BACKGROUND INFORMATION

Step counting is a relatively simple task to do manually. However, the implementation of step counting in PDR

means that the method needs to be automated by calculating readings from sensor, in this case accelerometer.

Correlation coefficient method initially identifies the first step (sinusoidal cycle) from the acceleration waveform, and defines it as a window. The window is used to find correlation coefficient by sliding it to the entire waveform. Each peak presented in the correlation coefficient waveform represents one step taken by the user.

The proposed method uses technique such as correlation coefficient calculation, low pass filtering, and sliding window. To evaluate the performance of this method HASC-IPSC logs [3] are used to provide performance result on different age groups and genders with balanced number of logs.

### 3.1. Correlation Coefficient

Correlation coefficient is a statistical measurement of linear dependence between two variables, in this case between two waveforms. Equation (1) shows the formula used to calculate correlation coefficient.

$$r = \frac{\sum_{i=1}^n (X_i - \bar{X})(Y_i - \bar{Y})}{\sqrt{\sum_{i=1}^n (X_i - \bar{X})^2} \sqrt{\sum_{i=1}^n (Y_i - \bar{Y})^2}} \quad (1)$$

The formula calculates dependencies between the two waveforms X and Y. The numerator of the formula calculates the covariance between the two waveforms. The denominator part of the formula is the product of each waveform's standard deviations.

The coefficient value can range between -1 to +1. The negative value means there is negative correlation between the two waveforms. For this project, the focus is to evaluate the value of positive correlation coefficient, i.e.  $0 < r < 1$ .

Table 1: Correlation coefficient strength

Correlation Coefficient (r)	Strength
> 0.7	Strong
0.4-0.7	Moderate
0.2-0.4	weak
< 0.2	None/minimal

The numerical value of correlation coefficient is normalized and there are some threshold values that differentiate the correlation strength between the two waveforms. Table 1 shows the four different strength level of correlation coefficients based on its numerical value.

### 3.2. Sliding Window

The sliding window method is used by Yoshizawa [4] to sense activity change by observing the acceleration data waveform. The finite sized window slides throughout the waveform and identifies the changing point based on the pre-defined calculation.

Similarly, the finite window in this project slides throughout the waveform. As it slides, the correlation coefficient value is calculated. The window size is determined by identifying the length of the first one-period cycle of the acceleration waveform. The first cycles resembles the first steps taken by the object.

Figure 1 visualizes the method used to determine one period cycle. It measures the two consecutive peaks and defines the length between the peaks as the sliding window length.

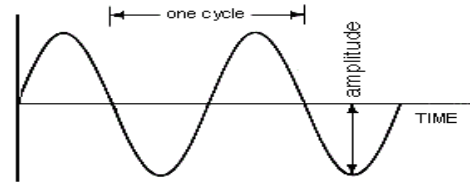


Figure 1: One period cycle identification

### 3.3. Filtering

The waveform of the acceleration data tends to be periodic sinusoidal wave. A simple one-pole low pass filter is used to remove the high frequency noise in the waveform. The filtered waveform provides smoother transition and makes the peaks identification simpler. The low pass filter used in this project removed frequency above 10Hz. This cut off frequency still preserves important acceleration data.

### 3.4. HASC-IPSC

The HASC-IPSC is an Indoor Pedestrian Sensing Corpus that contains logs of acceleration, gyro, and geomagnetism data. The logs in this database are used because it has balanced data from different age groups and gender.

Logs in the database are divided into two main parts: basic activity and route data. These data are collected from 50 male and 50 female users with age distribution ranges from early 20s to late 60s. [5]

In the logs, the basic activity data have recording time of 20 seconds with one specific activity performed such as walking, stepping up and stepping down. The route data recording time depends on the competition of the route. For this project, the route length is approximately 74.9m long. The sampling frequency of the accelerometer is 100 Hz.

Figure 2 shows the 3D visualization of the route with the surrounding environment. The yellow trail showed the path taken by the user as it walks from the lower floor to upper floor in one log entry.

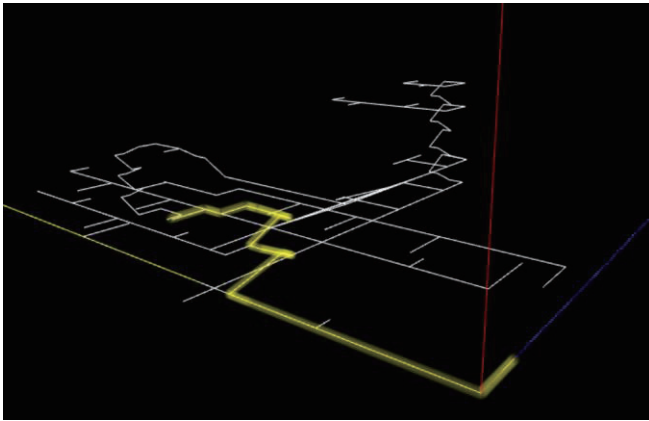


Figure 2: Path of the route logs

### 3.5. Threshold Method

The threshold method was used to count steps using the norm of acceleration data from HASC-IPSC database. It uses the acceleration norm and identifies crossing of both high and low threshold value to identify one step cycle. However, one major problem of the method is there is a scenario where the norm will not cross the threshold values in each cycle.

## 4. STEP COUNTING ALGORITHM

The code developed to perform this method has three main parts. It includes the window size determination, correlation coefficient calculation, and correlation coefficient waveform peaks identification to count the steps taken in each log. The logs from HASC-IPSC have to be checked first and the defects were removed as some of the acceleration data may contain inconsistent recording time and high frequency noise.

Firstly, the filtered waveform was scanned, and then the first sinusoidal cycle of each log was identified. One cycle window is calculated by measuring the first two consecutive peaks. The window contains the acceleration norm data of each log. It represents the first step taken by user in the acceleration norm waveform.

Secondly, the window, that contains the acceleration norm wave of the first step, slides through the entire waveform of the log. As the windows slides through, the correlation coefficient is calculated to generate the correlation waveform. The waveform of the correlation generated from sliding window is a periodical wave that has values between -1 to +1. Figure 3 shows illustration of the sliding window that contains the first cycle (step) in the waveform plot. The arrow shows the direction of the sliding window.

Lastly, the correlation coefficient waveform is observed and each peak is identified as one step. The peaks in one waveform are varying in magnitude; it may range from as low as 0.2 to as high as 0.95. The requirement for the peak to be counted as one step is its value must be equal or larger

than 0.4. This provides assurance that the  $n^{\text{th}}$  step has moderate correlation to the first step taken.

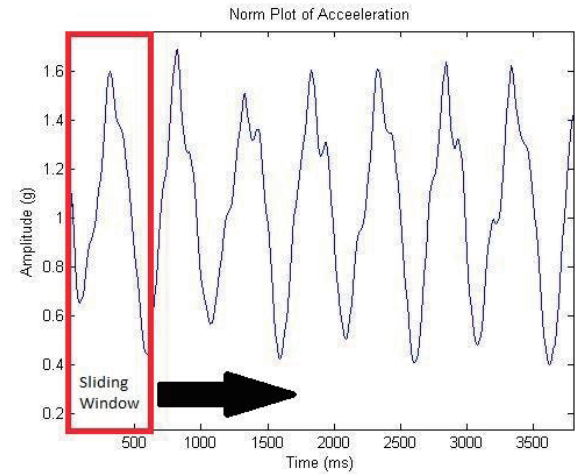
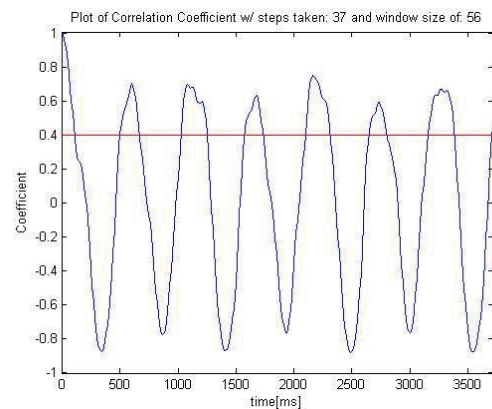


Figure 3: Sliding window

Figure 4 shows one of the correlation coefficient waveforms from basic activity log. The peaks, which are counted as one step, have values above the red threshold line of 0.4. In the end, the total number of peaks in the



correlation waveform represents the total steps taken.

Figure 4: Correlation coefficient plot

## 5. RESULTS & EVALUATION

First, the proposed method was used to measure the steps taken in the shorter logs, where there is only one single activity performed throughout the entire log. These logs are simpler to run as the recording time is shorter and the wave has similar periodic cycles. Thus, the accuracy of the step counting tends to be higher in these basic activity logs.

On the other hand, the route logs contain acceleration data that has more than one activity. The route chosen for this project has a combination of 2 basic activities which are walking and stepping up. Figure 2 showed the actual route taken.

### 5.1 Basic Activity Logs

The correlation coefficient method is used to count steps of the basic activity logs. It performs very well to measures



the number of steps taken. The basic activity is a simple and repetitive activity, thus the pattern of steps taken varies minimally throughout each log recording. Most of the logs generate a correlation coefficient plot with very distinguishable peaks.

The subsections below provide information about the average steps taken and average window size length in each basic activity. Each person has 9 log entries and there are a total of 100 people in each basic activity. The method runs through 900 different logs to calculate the number of steps taken and window sizes.

### Walking

Figure 5 shows two histograms of the number of steps taken and window sizes throughout the walking activity logs. The average calculated number of steps taken in a 20 second walking time is 32 steps with standard deviation of 10 steps. Moreover, the window sizes have an average length of 550 milliseconds with standard deviation of 137 milliseconds.

Figure 6 shows two histograms expressing the steps taken by male and female users. In the 20 second time span, the male gender has an average of 32.28 steps taken and female has an average of 32.47 steps taken. Thus, gender does not affect the average number of steps taken in a 20 second long walking activity.

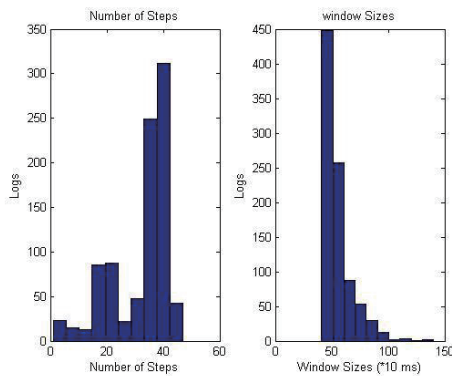


Figure 5: Steps and window sizes histogram (walking)

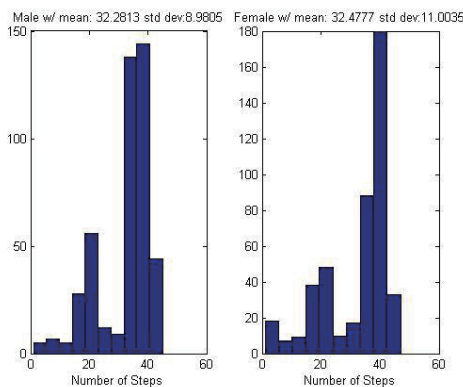


Figure 6: Gender variation of steps histogram (walking)

### Stepping up

Figure 7 shows two histograms of the number of steps taken and window sizes throughout the stepping up activity logs. The average calculated number of steps taken in a 20 second walking time is 29.1 steps with standard deviation of 8 steps. Moreover, the window sizes have an average length of 559 milliseconds with standard deviation of 120 milliseconds.

Figure 8 shows two histogram expressing the steps taken by male and female users. In the 20 second time span, the male gender has an average of 29.5 steps taken and female has an average of 30 steps taken. Similar to walking, the gender does not affect the average number of steps taken in a 20 second long stepping up the stairs activity.

Figure 7: Steps and window sizes histogram (step up)

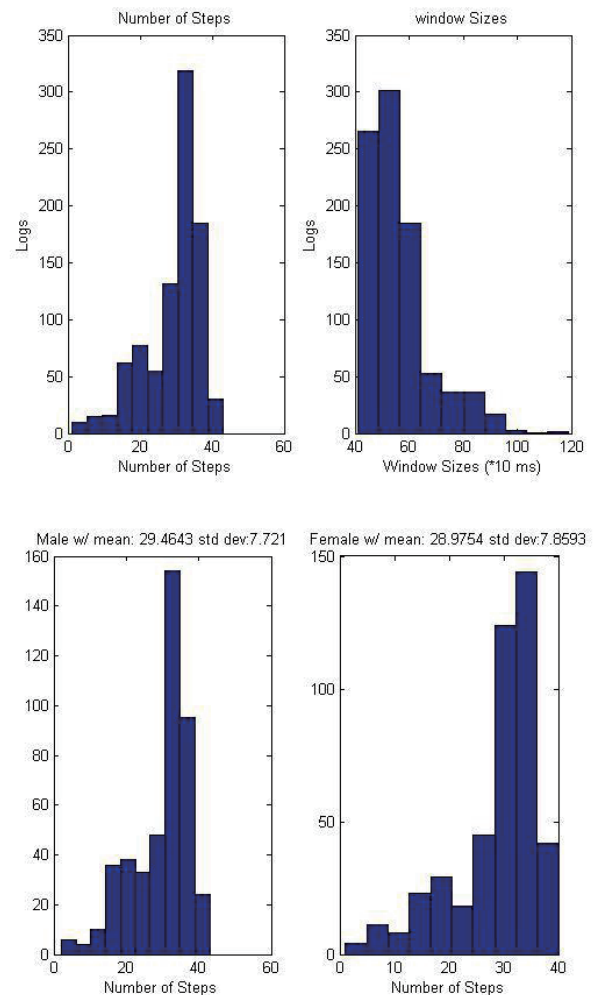


Figure 8: Gender variation of steps histogram (step up)

### Stepping down

Figure 9 shows two histograms of the number of steps taken and window sizes throughout the stepping down activity logs. The average calculated number of steps taken in a 20 second walking time is 29.9 steps with standard deviation of 9 steps. Moreover, the window sizes have an

average length of 564 milliseconds with standard deviation of 139 milliseconds.

Figure 10 shows two histogram expressing the steps taken by male and female users. In the 20 second time span, the male gender has an average of 29.5 steps taken and female has an average of 30 steps taken. Thus, the average number of steps taken in stepping down the stairs activity is not affected by the user's gender.

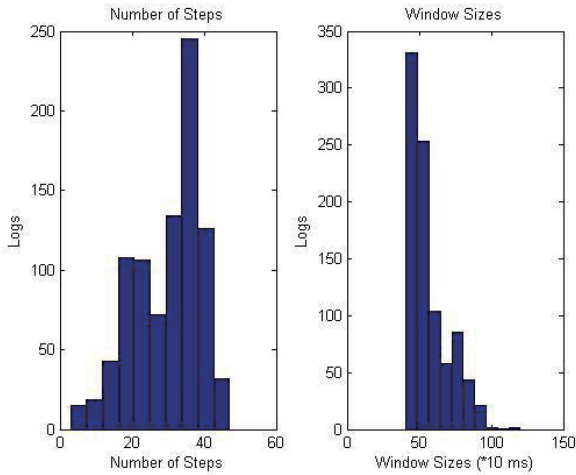


Figure 9: Steps and window sizes histogram (step down)

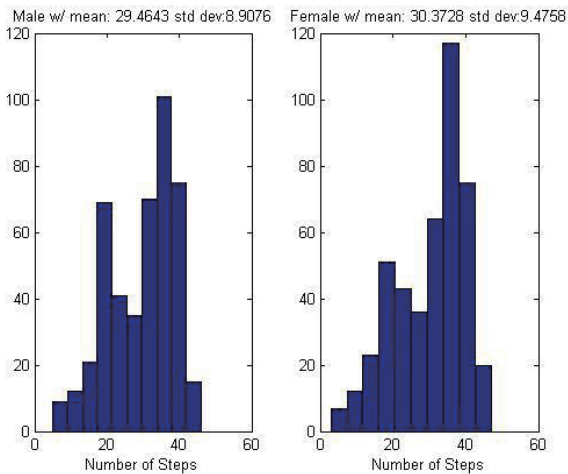


Figure 10: Gender variation of steps histogram (step down)

## 5.2. Route logs

The route logs have longer and varying recording time because the route has *theoretical length of 74.9m*. The proposed method tries to calculate steps taken in the route logs of 5 different users. These logs were also used by Murata [1] to count steps using the threshold method.

In order to provide performance comparison the assumption made must be identical. The proposed method, similar to threshold method, assumes that the step length is 45% of the height for people below the age of 65. In the other hand, people who are older than 65 has a step length of

40% of their height. Table 2 provides the pedestrian information used in this experiment.

Table 2: Pedestrian information

	Height (cm)	Age	Gender
Person 1207	178	20	Male
Person 1208	171	20	Male
Person 1217	168	30	Male
Person 1234	174	50	Male
Person 1296	147	60	Female

The measured distance travelled is the product of the step length of each person and their respective calculated number of steps taken to complete the route. Then, the error of the measurement is calculated by finding the difference between the theoretical route length (74.9m) and the measured distance travelled.

The error from this method is important to compare the accuracy of the correlation coefficient method and the threshold method. Table 3 shows the error comparison between the proposed method and threshold method result of distance travelled.

Table 3: Comparison of errors between two methods

	Method error [m]		Error Improvement [m]
	Threshold	Correlation Coefficient	
Person 1207	28.4	34.8	-6.4
Person 1208	42.0	7.9	34.8
Person 1217	22.6	23.38	-1.2
Person 1234	16.7	2.9	13.8
Person 1296	23.3	9.8	13.5
<b>Average</b>	26.6	15.8	10.9
<b>Standard Deviation</b>	9.6	13.1	16.1

Improvement is observable as the correlation coefficient method yield smaller error compared to the threshold method. The average error of the threshold method is 35.6%, while the average error of the correlation coefficient is 21.0%. Thus, the correlation coefficient method is more accurate in identifying the steps taken compared to the earlier method.

Keep in mind that these calculations were taken without the knowledge of changes in activity performed. The only known data is the acceleration data readings and the assumed activity performed is walking.

### 5.3. Evaluation

This method provides a lower cost alternative to accurately count steps based on the acceleration data readings. Counting steps in the basic activity logs is very simple as the method shows a reasonable number of steps for a 20 seconds recording time for each activity.

However, some logs contain very volatile acceleration data. The norm of the acceleration tends to fluctuate even after the low pass filter is applied to the waveform. This may happen because of sudden change of movement that is significantly different than the previous one.

Moreover, the method algorithm assumed that the steps in the entire waveform would be relatively similar to the very first step identified in the waveform. This assumption can be wrong as some people might change their walking speeds within the 20 seconds log recording period.

The performance of the proposed method in calculating the number of steps in route logs was very satisfying. For the same five logs, the correlation coefficient produces a better accuracy in calculating the distance travelled based on the readings of the acceleration data. There is more than 10% improvement in accuracy compared to the results of threshold method.

However, the precision to detect route log is still lacking since the proposed method does not incorporate activity recognition algorithm to identify the changes in activity performed. If the changes can be identified, the accuracy can be increased as the sliding window waveform and length can be adjusted depending on the requirement.

### 6. CONCLUSION

Human activity sensing is a complicated process composed of combination of simple processes. One of them is step counting to detect distance travelled. The correlation coefficient method is one of the ways to count steps by sliding a finite acceleration window length to generate correlation coefficient waveform. Then, the peaks are counted to determine the number of steps taken.

The HASC-IPSC data were used to test the performance of the proposed method, and the result showed that correlation coefficient is an effective way to count steps. For comparison purpose, the results of the step counting using threshold method on the same log files were compared. The correlation coefficient yield smaller average error in estimating the distance travelled. Based on the five route logs used, the method explored in this project has an average error percentage of 21.0%, significantly lower than the threshold method that yields error of 35.6%.

### 7. FUTURE WORK

- *Activity recognition* can be integrated in this method. One of the most common ways is to include a machine learning technique to identify

change of activity based on the acceleration data reading.

- *Step length estimation* method can be developed to measure the length of each step taken. This paper used a static assumption of the step length. It depends on the height of each person. There is a need to accurately measures step length. It will improve the precision of the calculated distance travelled significantly.

### ACKNOWLEDGEMENTS

This paper will be used to fulfill research report requirement of JUACEP 2014 summer course in Nagoya University.

### REFERENCES

- [1] Murata, Y., Kaji, K., Hiroi, K., Kawaguchi, N., Pedestrian Dead Reckoning Based on Human Activity Sensing Knowledge. UbiComp '14, pp. 4-8(2014)
- [2] First Line Software\_ (Counting Steps with MEMS). <http://www.firstlinesoftware.com/outsourcery/16-counting-steps>
- [3] Kaji, K., Wanatabe, H., Ban, R., Kawaguchi, N., HASC-IPSC: Indoor Pedestrian Sensing Corpus with a Balance of Gender and Age for Indoor Positioning and Floor-plan Generation Researches. International Workshop on Human Activity Sensing Corpus and Its Application (HASCA2013), pp. 606 -608(2013)
- [4] Yoshizawa, M., Takasaki, W., Ohmura, R., Parameter Exploration for Response Time Reduction in Accelerometer-based Activity Recognition. International Workshop on Human Activity Sensing Corpus and Its Application (HASCA2013), pp. 654-658(2013)
- [5] HASC Tool. <http://hasc.jp/tools/hasctool-en.html>.

# AUTOMATED STEERING SYSTEM FOR OBSTACLE AVOIDANCE BASED ON POTENTIAL FIELD METHOD

Jin-Gen Wu

Department of Mechanical Engineering, College of Engineering, University of Michigan  
jingen@umich.edu

Supervisor: Professor Tatsuya Suzuki

Graduate School of Engineering, Department of Mechanical Science and Engineering, Nagoya University  
t\_suzuki@nuem.nagoya-u.ac.jp

## ABSTRACT

The primary idea of this research project is to use the Potential Field Method [1] and apply it to construct an automated steering system for obstacle avoidance on a small electrical vehicle (COMS). A real-time potential field is generated by detecting the location of obstacles including humans and side walls in driving environment using Laser Range Finder (LRF) in experiment. A reference path is generated using real-time potential field gradient in control program with different weight values for obstacles and side walls. By using the reference path and the look-ahead point control [2], error between the reference angle and output angle are calculated and used as a feedback signal to the steering control system. The weight values and PID gains are tuned in the experiment so that the vehicle can follow smoothly.

## INTRODUCTION

Due to fast-paced nature of technological development, driver assistance systems are cutting edge technology studied in various research institutes and automotive industry. In particular, automated driving and steering assistance systems provide safety and convenience to drivers and passengers. Automated steering and steering assistance system are implemented on modern vehicles because electrical power steering has become popular nowadays and drivers need safer driving conditions in emergency. Sometimes there are many accidents happened when the vehicle is travelling too fast and a pedestrian suddenly steps into the vehicle's path. To prevent tragedy and to ensure safety, automated steering system is installed in modern vehicles.

In previous researches, small electric vehicles can be controlled with basic automated steering control program by using predetermined potential field representing a

simplified narrow road consisting of an obstacle in the middle and walls on both sides. However, driving environment is more complicated in the real world. Therefore, in this research project, detecting the real driving environment in real-time is needed to create proper reference path for vehicles.

## EXPERIMENT SET UP

In this experiment, a small electric vehicle (COMS, Toyota Auto Body Co.Ltd.) is used. For safety concern, only slow speed experiments are done because control program is not fully developed. Digital encoders on rear wheels of COMS provide the position and yaw angle of the vehicle. Potentiometer on the steering column measures the steering angle. The LRF on the front of COMS detects all of objects in front of the vehicle. The main control program of COMS has already been developed and works in hybrid with the automated steering control program developed in this research project.

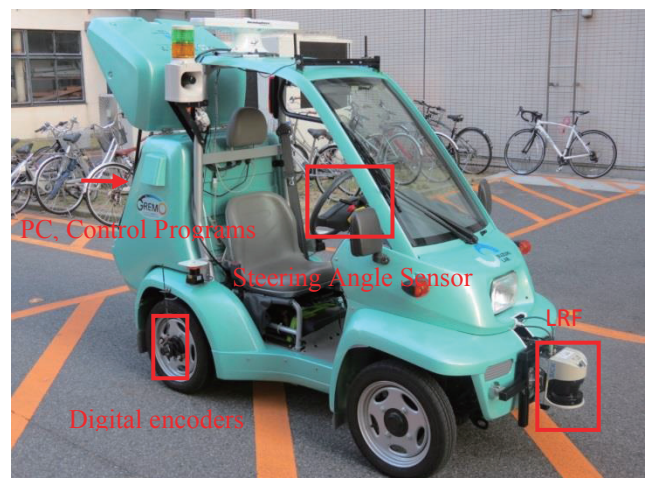


Figure 1: COMS set up

## ALGORITHM

The goal for classifying the obstacles, which include pedestrians and side walls using the proposed algorithm, is assigning different weight values for obstacles and side walls. While large weight value is used in obstacles, it can generate safer reference path for people on the driving environment by potential function. There are two algorithms to achieve this goal. One is the distance method, and the other is the k-means method.

In this experiment, Laser Range Finder (LRF) is used to detect all the obstacles in front of the vehicle. The information which provides from LRF is angle ( $r$ ) and distance ( $\theta$ ). Each distance data correspond to each angle data which detect range from 95 degree to -95 degree with 0.25 degree resolution. The XY coordinate is calculated by using following equation. Origin of coordinate at (0,0).

$$x_n = r_n * \cos \theta_n \quad (1)$$

$$y_n = -r_n * \sin \theta_n \quad (2)$$

$n$  : from 1 to 760.

The distance method algorithm has two steps for separating the obstacles from the side walls. The first step is calculating the distance between consecutive points. When the distance between consecutive points large than specific value (0.3m), the later point will be classified to another cluster. The second step is determining the number of data in cluster more than threshold value (15), it means this cluster can assume to be a side wall (Figure 2) and vice versa (Figure 3). Advantage for distance method is easy to compute and simple code is used. However, this method still has two shortages. One is the original same cluster side wall data facile to split for several cluster due to noise. The other is classification errors which means the obstacle data be classified as side wall data. This phenomenon are caused by when the obstacle volume is too large, the number of data for representing this obstacle easy more than threshold value.

After separating the obstacles from the side walls by distance method, the K-means method is applied on obstacles data (Figure 4). It provides center position of each cluster used for creating potential functions. However, when the k-means method is applied, it needs to know the number of clusters. There is a drawback for K-means method in this experiment which driving environment is too complicated to get how many clusters in this experiment.

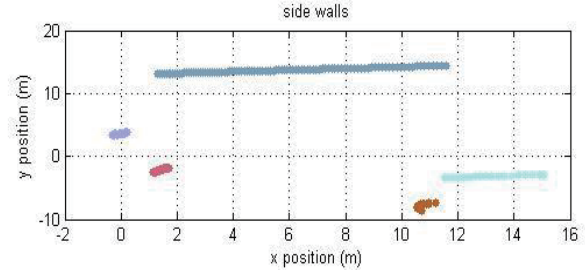


Figure 2: side walls after distance method

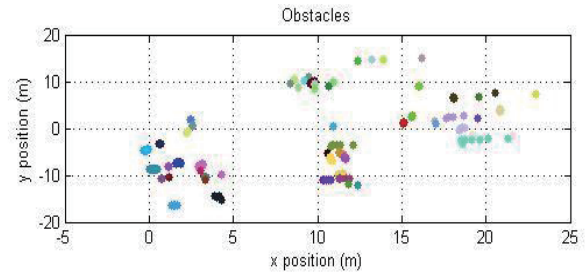


Figure 3: obstacles after distance method

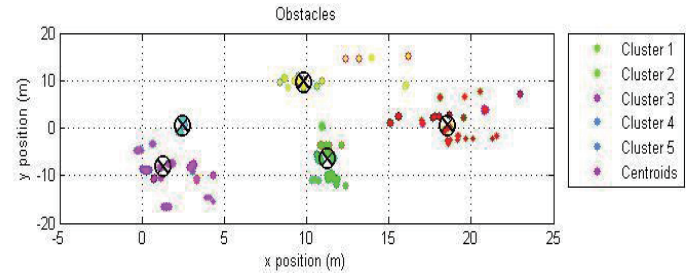


Figure 4: clusters computed using the K-means method

## POTENTIAL FIELD & REFERENCE PATH

After analyzing the data from LRF, reference path (Figure 5) is generated according to the potential field of driving environment shown in figure 9 (using one step in real raw data from LRF as an example). In this experiment, vehicle moving direction is defined as positive x direction and there are side walls at both sides (y direction). The high potential on the vehicle path represents the side walls at both sides and obstacles in front of vehicle. According to the potential field method, the heading direction of the vehicle should always point to the low potential at every time step. The reference path is calculated as follows:

Given the potential function:

- Attractive potential from the goal
- $$U_g(x, y) = -W_g * X \quad (3)$$

- Repulsive potential from the side wall

$$U_w(x, y) = w_w \sum_n \exp \left\{ -\frac{(y-y_{wn})^2 + (x-x_{wn})^2}{\sigma_w^2} \right\} \quad (4)$$

- Repulsive potential from the obstacle

$$U_c(x, y) = w_c \exp \left( -\frac{(x-x_c)^2}{\sigma_{cx}^2} - \frac{(y-y_c)^2}{\sigma_{cy}^2} \right) \quad (5)$$

- The total potential field

$$U(x, y) = U_g + U_w + U_c \quad (6)$$

The heading direction vector of the vehicle at time t is:

$$[v_{x_t}, v_{y_t}]^T = -\nabla U(x_t, y_t) = \left[ \frac{\partial U(x, y)}{\partial x}, \frac{\partial U(x, y)}{\partial y} \right]_{x=x_t, y=y_t}^T \quad (7)$$

The vehicle location at time t+1 is then:

$$x_{t+1} = x_t + d \cos \left( \tan^{-1} \left( \frac{v_{y_t}}{v_{x_t}} \right) \right) \quad (8)$$

$$y_{t+1} = y_t + d \sin \left( \tan^{-1} \left( \frac{v_{y_t}}{v_{x_t}} \right) \right) \quad (9)$$

$d$  : a small distance interval.

$w_g$  : The weight of  $U_g$

$w_w$  : The weight of  $U_w$

$n$  : Number of data

$\sigma_w$  : The standard deviation of  $U_w$

$w_c$  : The weight of  $U_c$

$\sigma_{cx}$  : The standard deviation of  $U_c$  in  $x$  axis

$\sigma_{cy}$  : The standard deviation of  $U_c$  in  $y$  axis

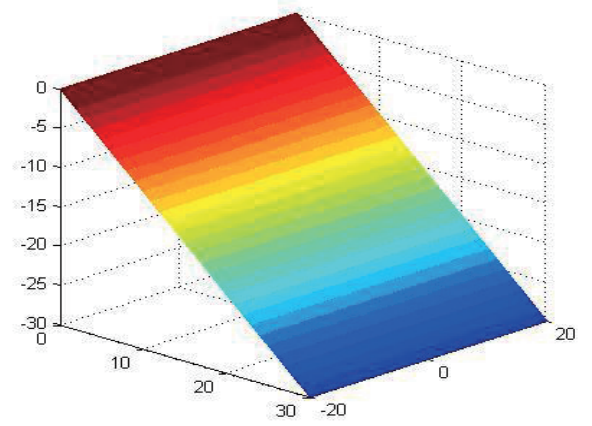


Figure 6: potential function of the goal

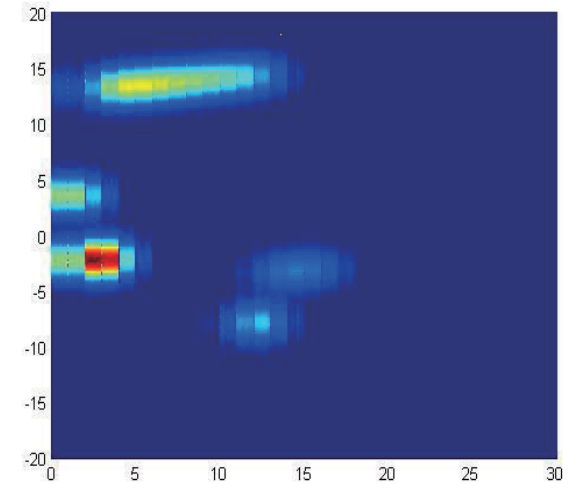
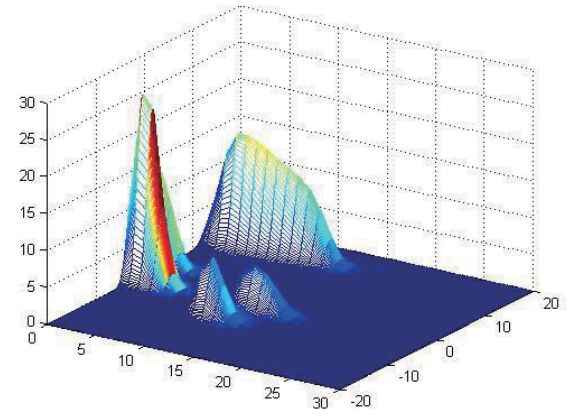


Figure 7: potential function of the side walls

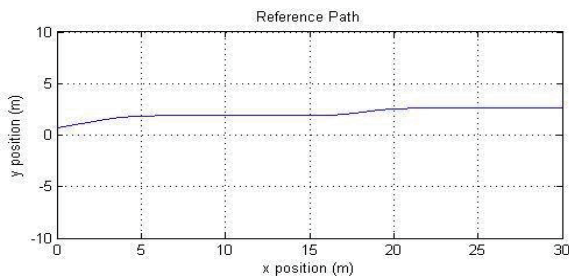


Figure 5: reference path calculated from potential field

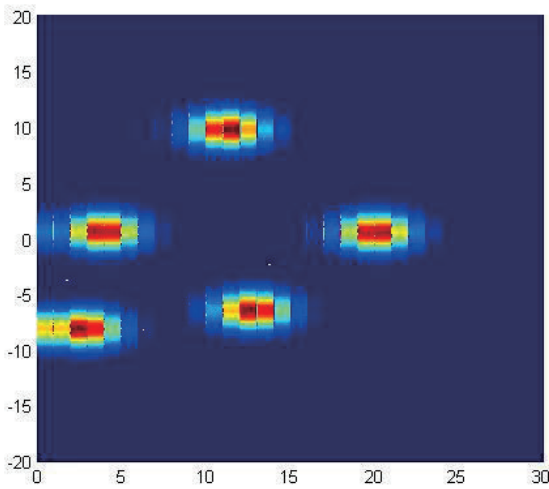
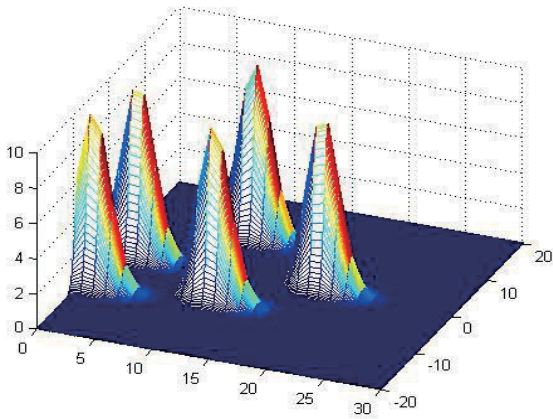


Figure 8: potential function of the obstacles

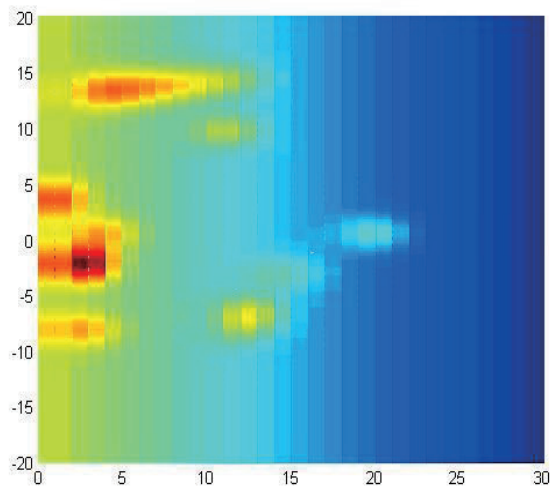
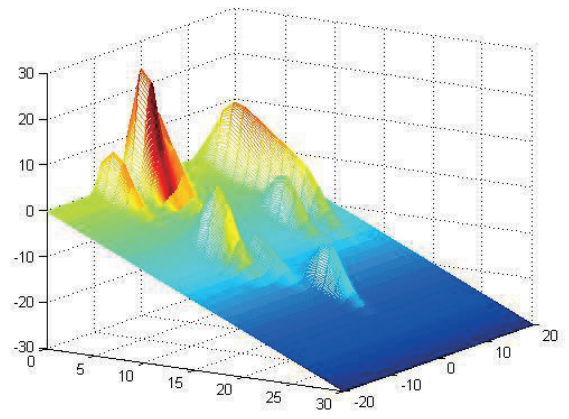


Figure 10: potential field of the driving environment

## CONTROL ARCHITECTURE

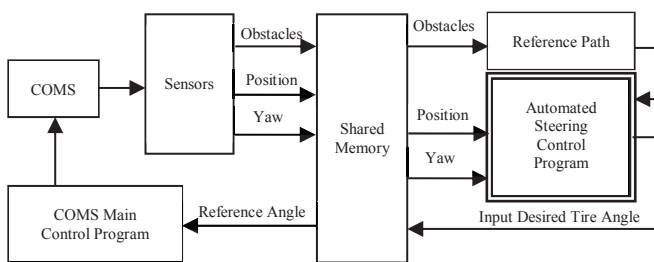


Figure 9: automated steering system block diagram

Figure 7 shows the data flow of the automated steering system control program. At first, the sensor provides information of the position, yaw angle and obstacles of the vehicle to the shared memory. In addition, the shared memory not only stores all the information of the vehicle but also shares all information to both the main control program and automated steering control program (double-lined box). Then, the automated steering control program

gets the position and yaw angle from the shared memory, and calculates the desired tire angle from the reference path which is generated by real-time data from LRF and potential gradient. The desired tire angle is then sent back to the shared memory as a reference angle for the main control program. Finally, the main control program drives the steering motor to the desired angle. This process is repeated every 0.02 second (50Hz), meaning that the steering angle is updated in each time step.

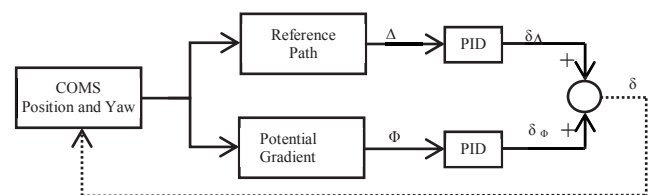


Figure 11: automated steering control program block diagram

The steering angle (tire angle) is computed by the look-ahead observation (figure 9) and PID control. The look-ahead point, generated according to the vehicle speed, is a prediction of the vehicle position based on the current steering angle. The angle deviation ( $\Phi$ ) is the difference between the vehicle yaw angle and the potential gradient direction. The distance deviation ( $\Delta$ ) is the shortest distance from the look-ahead point to the reference path. The angle deviation and distance deviation are measured at each time step and sent to PID controllers as shown in figure 8. The steering angle is calculated by multiplying different gain values to the derivatives, integrals of  $\Delta$  and  $\Phi$  and to themselves, and then summing all up. First order backward difference quotient and trapezoidal rule are used to calculate derivatives and integrals in the program. The parameters of the PID controller gains are tuned in the experiment to let the vehicle follow a smooth path [2].



Figure 12: look-ahead observation

## EXPERIMENT

In the experiment, the test speed is not as fast as practical driving because control program is not fully developed. However, the result shows that the control algorithm successfully avoids obstacles in real-time.

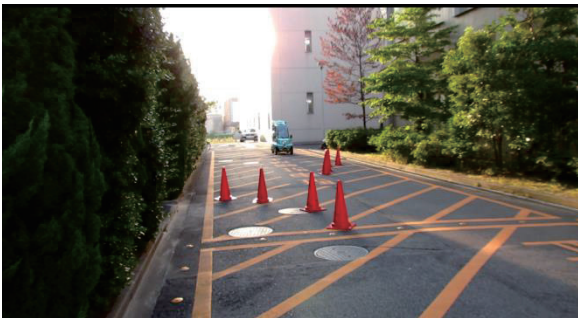


Figure 13: driving environment set up

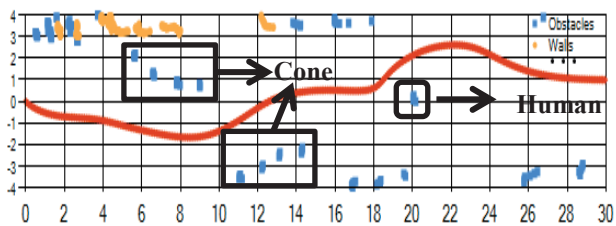


Figure 14: obstacles and reference path

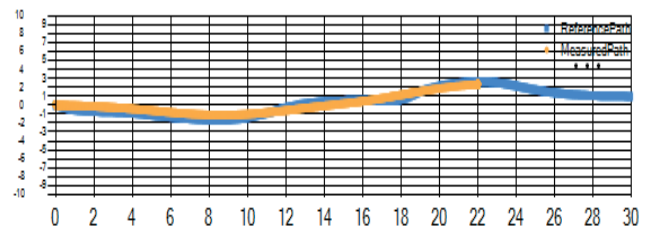


Figure 15: reference path and measure path

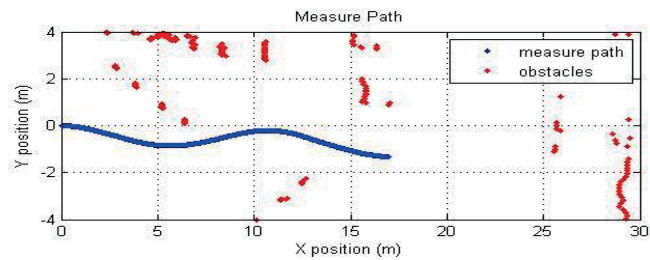
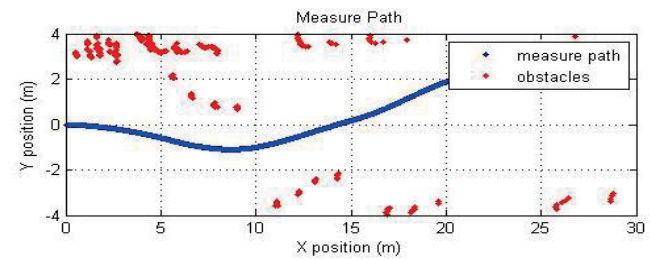


Figure 16: obstacles and measure path

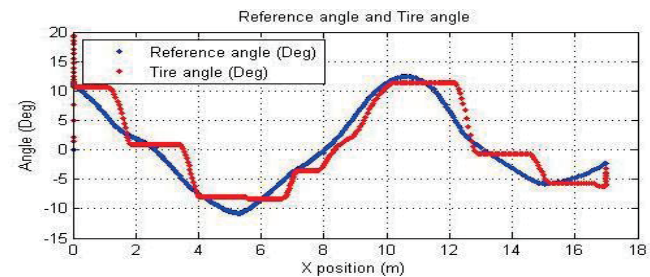
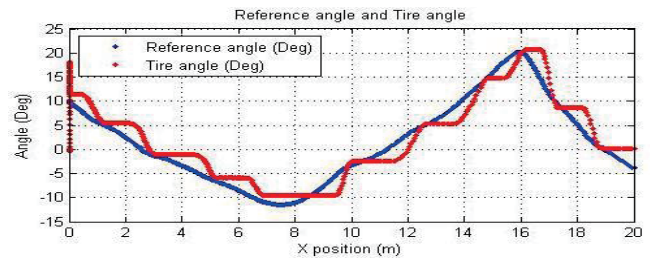


Figure 17: reference angle and tire angle



Figure 14 shows all the obstacles in driving environment and reference path for avoiding all the objects in front of vehicle. In control program, the reference path is generated according to the data from LRF every time step which means it will change every time step, so only first reference path can be recorded. Figure 15 indicates that COMS followed the reference path precisely only using the distance deviation which is the shortest distance from the look-ahead point to the reference path.

Figure 16 and 17 show the results of the vehicle practical path and obstacles and reference angle and tire angle separately. In these two experiments, the measure paths of COMS successfully pass through all the obstacles in front of vehicle. Besides, the tire angle can follow the desire angle closely but it still has a step behavior in our experiment result. This delay to steering phenomenon maybe is the main reason for difficulty of controlling the vehicle to follow a desired path in this research project. Possible reasons for the delay are: backlash of the gears inside the steering system, communication delay between the steering control program and the main control program, or steering motor controller delay.

## DISCUSSION

This automated steering control program just be built in basic structure, therefore it still need more testing to be done to find the PID control gains and look-ahead distances for better performance.

Applying the K-means method for detecting data can successfully generate reference path in Matlab, but it can't be used in real driving environment which is too complicated to generate the proper reference path. In addition, for a better reference path by using K-means method, it needs to know how many obstacles in front of vehicle which is unknown for practical environment. Maybe others algorithms can solve this problem.

Our goal is to assign different weight values for obstacles and side walls. However, we still use the same value for them in the practical experiment. When the value of weight is different, unreasonable reference path can be generated. The possible reason for causing weird reference path with same weight value is driving environment potential function be created by every environment data points. When the amount of data is too much, even just slight difference on weight values, the corresponding reference path will change significantly.

## CONCLUSION

In this research project about automated steering system, the theory of potential method has been implemented in constructing the real-time reference path and tested in the control program. The program now has a basic structure and can work in parallel with the main

control program on COMS. It can avoid a pedestrian suddenly steps into the vehicle's path. Although only slow speed test and look-ahead observation are done in this experiment. The next step of this research project should have more tests and data are required for control program to fully work.

## REFERENCES

- [1] Noriyasu Noto, Hiroyuki Okuda, Yuichi Tazaki and Tatsuya Suzuki, Steering Assisting System for Obstacle Avoidance Based on Personalized Potential Field, 2012 15<sup>th</sup> International IEEE Conference on Intelligent Transportation Systems, Anchorage, Alaska, USA, September 16-19, 2012.
- [2] Yan Zhang, Automated Steering System for Obstacle Avoidance Based on Potential Field Method, JUACEP Independent Research Report, Nagoya University, Japan, summer 2013.

## Friction and Wear for 3D printed Material

**Hanyi Xie**

Department of Mechanical Engineering, University of Michigan  
xiehy@umich.edu

**Prof. Noritsugu Umehara**

ume@mech.nagoya-u.ac.jp  
Department of Mechanical Science and Engineering, Nagoya University

**Prof. Albert Shih**

shiha@umich.edu  
Department of Mechanical Engineering, University of Michigan

### ABSTRACT

Fused deposition modeling (FDM), a prominent method of additive manufacturing, has been extensively adopted in the industry for its capacity to build complex structures with less time and cost. In FDM, thermoplastic material such as acrylonitrile butadiene styrene (ABS), polycarbonate (PC), and polyetherimide (PEI), among others, is guided through a heated nozzle with a temperature just above the melting point of the material. The partially liquefied (semisolid) material is deposited from an extrusion head in the areas within the bounds of a specific cross section of the computer aided design (CAD) model. After deposition, the material solidifies and welds to the previous layer. This layer by layer FDM building process affects the material properties. Extensive research has been conducted in dimensional accuracy, surface roughness, and mechanical strength characterization for FDM.

The tribological aspects of FDM material, however, have not been well understood. Friction induced wear resistance is a material property in applications where mating surfaces are subjected to sliding. The friction force and heat result in surface degeneration and failure. Equbal et al. investigated the sliding wear performance of FDM-processed ABS parts. Effects of five parameters including layer thickness, part build orientation, raster angle, raster width and air gap, on the wear resistance of the parts built via FDM were studied, based on which an equation was developed to predict the wear rate. Among all thermoplastic suitable for FDM, only ABS was addressed. Sood et al. advanced Equbal et al.'s study by including the optimization of FDM process parameters, but they gave little emphasis on the resulting wear properties of the FDM-produced parts, comparing with traditional plastic parts from injection molding. Igus® inc. (East Providence, R.I.) is a supplier of engineered polymer components and assemblies featured of self-lubrication and wear resistance. Igus® developed iglide® tribo-filament which was claimed to be the first filament for 3D

printers developed for dynamic applications and to be more wear resistant, though no relative publications were found.

In this study, the wear resistance of FDM generated parts was examined by pin-on-disk friction tests. A comparison of wear resistance between FDM printed parts and off-the-shelf plastic stock material was made using profilometer to determine the wear rates. Friction induced wear mechanisms were analyzed by scanning electron microscope (SEM) observation, Energy-dispersive X-ray spectroscopy (EDX), and Vickers hardness test. Three types of polymers were chosen for study: ABS and Ultem. ABS is one of the most commonly used polymers because it is sturdy and hard and has long lifespan. Ultem is the thermoplastic PEI and used in medical and chemical instrumentation due to their heat resistance, solvent resistance and flame resistance. Two types of specimens were prepared out of each material: one was FDM printed, and the other was machined from off-the-shelf stocks by injection molding, namely: ABS\_FDM, ABS\_stock, Ultem\_FDM and Ultem\_stock.

The paper first illustrates specimen preparation, pin-on-disk friction test, wear rate determination, and wear track examination. Results including hardness, wear rate, SEM images and EDX analysis are then presented. Wear rate comparison and wear mechanism are discussed in the third part. And the last section provides the conclusions.

UNDISCLOSED

# ASSEMBLE OF MULTI-LAYER STRUCTURED BLOOD VESSEL

Yong, Yang

Department of Biomedical Engineering, College of Engineering, University of Michigan  
yongy@umich.edu

Supervisor: Professor Arai, Fumihito  
Tutor: Yamagishi, Yuka

Department of Micro-Nano Systems Engineering, Graduate School of Engineering, Nagoya University  
arai@mech.nagoya-u.ac.jp

## ABSTRACT

Cardiovascular diseases are the leading cause of death in the world and lots of cases require coronary and peripheral bypass surgeries [1]. Autograft is by far the optimum choice, whereas this choice is not available for a large group of patients. Although synthetic grafts have been developed and shown positive clinical outcomes, graft failure usually happens in the graft less than 6 mm in diameter or in the areas of low blood flow [2-5]. Moreover, the purely synthetic materials lack growth potential and long-term results have shown more complications [4, 5]. Vascular tissue engineering has become a promising approach for small diameter blood vessel regeneration. In this report, we fabricated small diameter blood vessels (ranged in 2-6 mm) inside of PLCL (poly (L-lactide-co-caprolactone)) scaffold that aims to mimic the biological and mechanical properties of native tissues. The chosen cells are fibroblasts, smooth muscle cells (SMCs) and vascular endothelial cells which are major components of natural blood vessels.

*Key words: Vascular tissue engineering. Vascular grafts. Tissue Engineered Blood Vessel (TEVB). PLCL scaffold. Multi-layered tissue. Mechanical properties.*

## 1. INTRODUCTION

Cardiovascular diseases are still the leading cause of death in the world. In 2008, cardiovascular diseases contribute to 30% of global death, that is, around 17.3 million people; in which, 7.3 million were due to coronary heart disease [1]. Low and middle-income countries are mainly affected that over 80% of cardiovascular related deaths happen in these countries [1].

Coronary heart disease is caused by plaque building up along the walls of the arteries, which leads to narrowed arteries and decreased blood flow to the heart. This condition usually requires vascular reconstruction, which can be achieved by bypass surgeries [2, 4]. The standard clinical substitutes for coronary and peripheral bypass

procedures are autografts, such as saphenous vein, arm vein, mammalian artery, or radial artery, especially for replacing small diameter blood vessels with inner diameter less than 6 mm [3, 4]. Arterial autografts are commonly used for coronary bypass surgeries due to their high mechanical properties; internal mammary artery showed a higher patency rate than saphenous vein, that is, 85% versus 61% after 10 years [4, 5]. However, harvesting autografts is a harsh process leading to side effects, infections or even patient death [4]. Moreover, autograft is not available in over 10% of the patients due to injuries, diseases or previous surgeries [6].

Synthetic materials were first engineered to serve as blood vessel substitutes. PET (polyethylene terephthalate), and ePTFE (expanded polytetrafluoroethylene) are successfully used for the replacement of medium-large diameter blood vessels of inner diameter larger than 6 mm [3, 6]. However, synthetic grafts show a low patency rates in the long term for small diameter blood vessel usage, for example, coronary bypass and lower-the-knee peripheral bypass [3, 5-7]. Using PET or ePTFE for small diameter blood vessels leads to several complications like aneurysm, intimal hyperplasia, thrombosis, etc. Long-term use also shows material-related failures, such as calcification and infection. Moreover, the material has no growth potential for paediatric application and the patient has to replace the substitute multiple times over the age. These drawbacks are mainly due to non-functional cell structure and a mismatch between the mechanical properties of synthetic grafts and native blood vessels [6]. Thus, the desired graft is biocompatible with growth potential and has mechanical properties fit the native environment.

A promising solution for these clinical gaps is tissue engineering. The general principle of tissue engineering (Fig. 1) is seeding functional cells on suitable scaffolds, “followed by *in vitro* culture and *in vivo* implantation” [8]. Ideally, the scaffold will be degraded and absorbed over time, leaving the tissue generated by the cells, which can be integrated into the natural environment. Thus, this approach relies on the seeding cells, the scaffolds and the construction

technique. Many attempts have been done to generate a tissue engineered blood vessel (TEVB) and considerable improvements have been made in the field regard to cell lines, scaffold and construction technique. By now, TEVBs

can be constructed *in vitro*, and several have successfully repaired the vascular defects in animal models. However, only few reached clinical translation and there are a lot to improve for this promising approach.

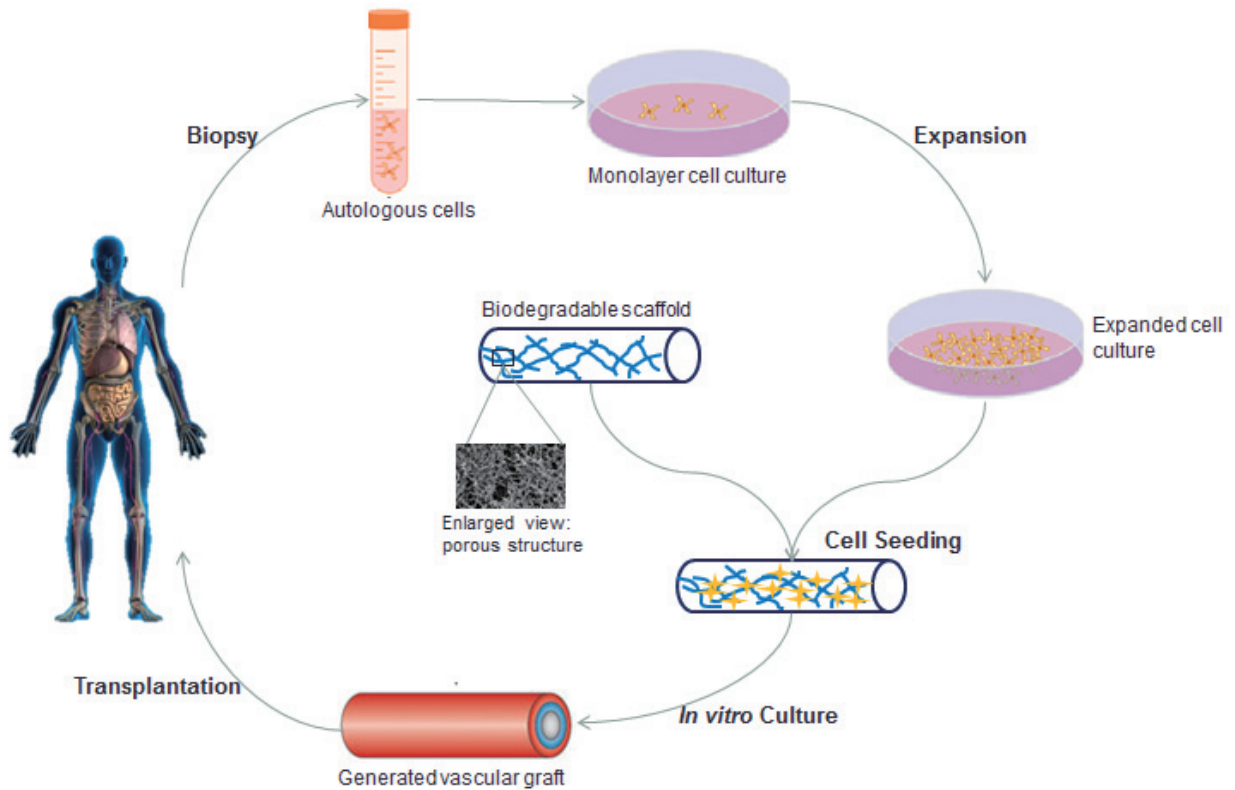


Figure 1 Schematic principle of vascular tissue engineering.

In this report, we fabricated a small diameter artery-like tubular tissue using biocompatible PLCL scaffold and three cell lines using the assembly technique proposed by Yamagishi, *et al* [9]. The tubular tissues automatically reconstructed by the residual stress of the PLCL scaffolds after cell seeded on the surface. As a result, we obtained the tubular cell membranes inside the scaffolds. The fabricated TEVB was aiming at clinical attempts, so that we first determined the fabricating conditions for the PLCL scaffold to match the mechanical properties of the natural blood vessels. Secondly, we seeded three different cell lines on the scaffold as the composition of a natural blood vessel: tunica adventitia (mainly composed of layers of fibroblasts, collagen and ECM), tunica media (mainly composed of layers of SMCs) and tunica intima (single layer of endothelial cells, which is key component of an ideal vascular graft) from outside in.

## 2. MATERIAL AND METROD

### 2.1 Design Concept

Figure 2 shows the step-by-step procedure of the fabrication of blood vessel graft. First, the tubular PLCL scaffold is fabricated using dip-coating method. Meanwhile, assemble the multilayered tissues using Layer-by-Layer

(LbL) technique. Then, fix the cut-opened and flat PLCL scaffold in a jig and use it as a culture device; seed the coated cells onto the scaffold. Repeat this step for multiple cell lines. After certain time of culture, release the scaffold from the jigs and it automatically recovers to tubular shape by its residual stress. Lastly, bond the two free edges using a biocompatible adhesion and the vascular graft is complete.

### 2.2 Fabrication of PLCL Scaffold

The chosen material for scaffold is PLCL, which is biocompatible and biodegradable, rubber-like elastic and has mechanical characteristics mimicking natural blood vessel using certain fabrication condition [10]. Moreover, the surface can be modified to reach over 90% porosity and supports cell attachment and proliferation [11].

The PLCL tubular scaffolds were manufactured by dip-coating followed by salt leaching technique. First, 3 wt.% and 5wt.% of PLCL solution dissolved in chloroform were prepared. To generate the porous surface, grounded NaCl particles (53-100  $\mu\text{m}$ ) were added to the polymer solution at a ratio of 20 wt.%, 40 wt.% and 60wt. %. After dip-coating (pull-up speed of 3 mm/s) 2-6 times, the resulting PLCL/NaCl composite tubular scaffolds were leached in distilled, deionized water with shaking overnight and freeze-dried.

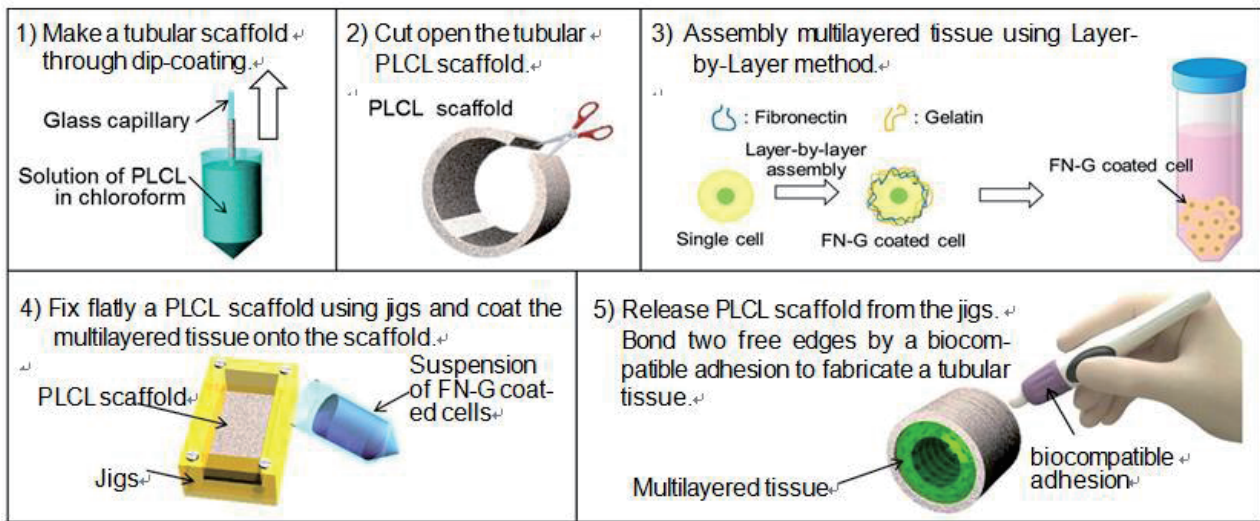


Figure 2 Procedure of fabricating a tubular tissue using PLCL scaffold. (retrieved from Yamagishi, *et al.* 2014 with permission)

The thicknesses of the PLCL scaffolds at the middle of the glass capillary were measured using an inverted optical microscopy after sliced into rings. The Young's module ( $E$ ) of the scaffolds were calculated using equation (1), in which,  $P$ : Force,  $t$ : Thickness,  $d$ : Width,  $A$ : Cross-section Area,  $L$ : Test piece's circumference,  $L_1$ : Jig's circumference,  $\Delta l$ : Displacement.  $P$  and  $\Delta l$  were measured using Tensile Testing Machine compliant to JIS K6251 with tension speed of 30 mm/min (Fig. 3).

$$E = \frac{\sigma}{\varepsilon} = \frac{P/A}{(L - L_0)/L_0} = \frac{P \times L_0}{(2\Delta l + L_1 - L_0) \times 2 \times t \times d} \quad (1)$$

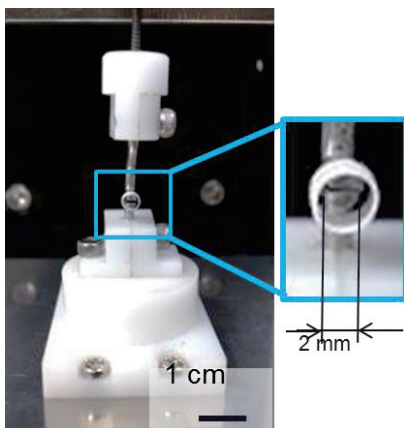


Figure 3 Setup of the tensile test (ring type) for the fabricated scaffold

The morphology and pore diameter of scaffolds were studied with a scanning electron microscope (SEM, Hitachi, Japan).

## 2.3 Fabrication of Multilayered Tissues

Multilayered tissues were fabricated using the Layer by Layer (LbL) method [12, 13]. This method can not only maintain high cell viability after rounds of centrifugation, but also generate nano-scale thin films on the single cell surface. We deposited fibronectin-gelatin (FN-G) nanofilms onto single cell surfaces in order to promote cell-cell interactions as in natural ECM.

Cells were alternatively immersed in 0.04 mg/ml fibronectin and gelatin in 50 mM Tris-HCl (pH = 7.4). After each procedure, the cells were washed with 50 mM Tris-HCl (pH = 7.4) to remove unabsorbed polymers. The coated cells were then seeded onto the PLCL scaffold at an appropriate density.

The cells were cultured in a standard cell culture incubator (Panasonic, Japan) in a 5% CO<sub>2</sub> atmosphere at 37°C. The cells were passaged twice per week.

We first fabricated a 2-cell-type tubular tissue by seeding  $4.5 \times 10^6$  cells/well of MOVAS 7 (smooth muscle cells) first, than  $2 \times 10^5$  cells/well of UV $\square$ 2 (vascular endothelial cells). They were stained with DAPI and Calcein AM, respectively.

Secondly, we seeded  $1.1 \times 10^6$  cell/well of NIH3T3 (fibroblasts) first, than seeded  $2.2 \times 10^6$  cells/well of MOVAS 7 (smooth muscle cells). Last, we seeded  $2.2 \times 10^5$  cells/well of UV $\square$ 2 (vascular endothelial cells) to mimic the three-tissue-layered structure of natural blood vessels. NIH3T3 and UV $\square$ 2 were stained with Hoechst 33342 (blue), and MOVAS 7 were stained with Calcein AM (green).

We observed the cells on the scaffold by confocal fluorescence microscope. Live/dead assay was also performed.

## 2.4 Recovering of the Tubular Structure

After three days of cell culturing on the scaffold, the scaffold was released to fabricate the final construct. Because of the high flexible and elastic features of PLCL, it recovered to the tubular shape automatically after releasing

from the jigs. The biocompatible adhesion used to seal the two ends of the flat PLCL scaffold was DERMABOND<sup>®</sup> (Ethicon, Johnson-Johnson), which is indicated for skin closure. After applying the DERMABOND to the indicated position, polymerization was completed in approximately two minutes 30 seconds.

Previous data has shown (the details are not included in this report) that DERMABOND distributes tension along the entire incision, that the healing organization strength is equal to the nodule tensile strength of the 4-0 suture thread.

### 3. RESULT AND DISCUSSION

An ideal TEBV should meet two important requirements, supporting regeneration of a functional endothelium and reaching similarity between the mechanical properties of TEVG and natural blood vessels [2]. Lacking of these two requirements contributes to the failure of PET and ePTFE made small diameter grafts [2, 4].

The mechanical behavior of an artery is complex and the concept of “compliance” is used to simplify the physics by “encompassing the changing mechanical properties depending on the hemodynamic pressure within the graft” [14].

At a given pressure  $P$  in a vessel of diameter  $d$  and wall thickness  $t$ :

$$E = \frac{\text{stress}}{\text{strain}} = P \frac{d/2t}{\Delta d/d} \quad (2)$$

Rearranging equation (2),

$$\text{Compliance} = \frac{d}{2Et} \quad (3)$$

The initial mechanical properties of a graft are mainly determined by the scaffold. We modified the fabricating conditions of the scaffold to find a best match to the natural small blood vessel regard to the basic mechanical properties. The reference blood vessel is the external carotid artery of a healthy person, with Diameter  $\approx 3 \sim 4$  mm, Young’s module  $\approx 0.8$  MPa and Thickness  $\approx 380 \mu\text{m}$  [15].

Figure 4 is the Young’s modulus of the fabricated PLCL scaffold using different compositions of the dip-coating solution ( $n = 3$ ). It clearly shows the properties of PLCL scaffold can be easily controlled by the composition of PLCL solution. High concentration of PLCL directly leads to high tension of the scaffold.

Figure 5 illustrates the relationship between the thickness of the scaffold and the dip-coating counts ( $n = 3$ ). As expected, it shows a linear positive correlation between the thickness and coating counts. The correlation coefficient depends on the composition of the PLCL solution.

Based on the reference parameters, the chosen fabricating conditions are as follows (Table 1). Fig. 6 is the images of the fabricated tubular scaffold using this condition. This fabricated PLCL scaffold is 3 mm in diameter and  $380 \mu\text{m}$  in thickness, Young’s modulus of 0.78MPa. By equation (3), the compliance is about 5.1, which fits the range for a natural artery [14].

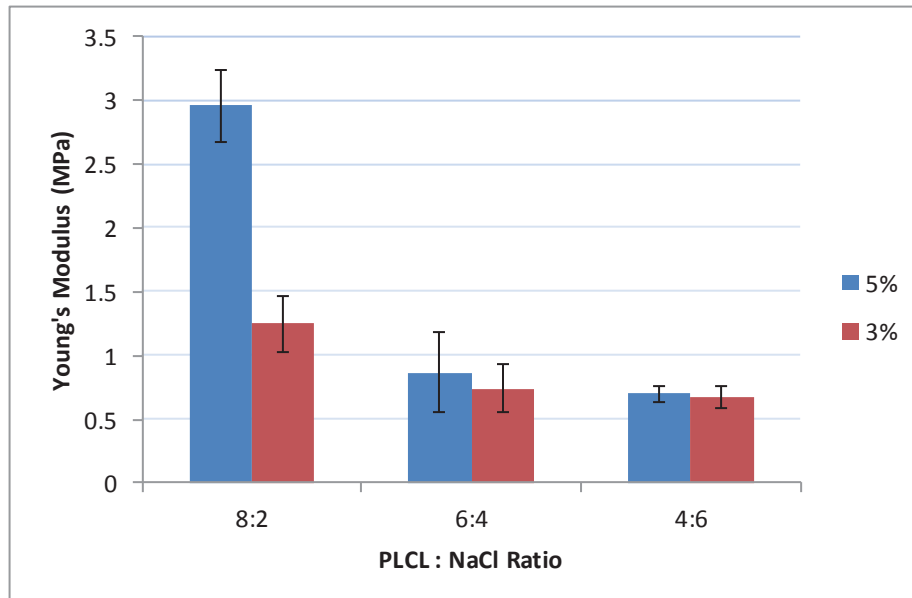


Figure 4 Young’s modulus of PLCL scaffolds under different fabrication conditions.

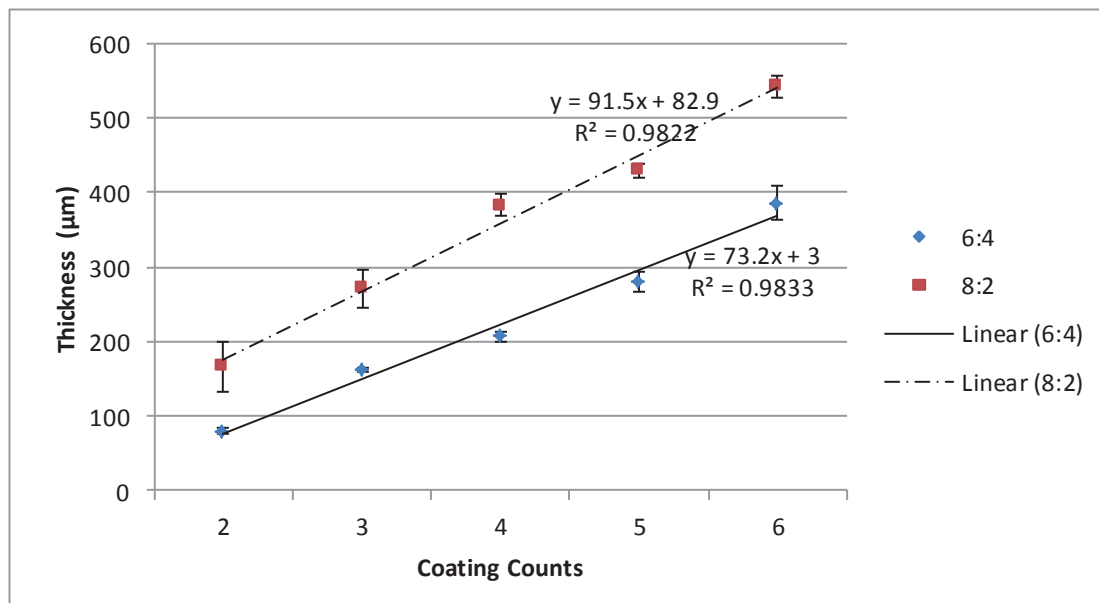


Figure 5 Relationship between scaffold thickness and counts of dip-coating. Blend ratio of NaCl are 20 wt.% (red) and 40 wt.% (blue), respectively. Both are 5 wt.% of PLCL dissolved in chloroform.

Table 1 Fabrication conditions of PLCL scaffold.

Chloroform : PLCL	95 : 5
PLCL : NaCl	6 : 4
Particles diameter of NaCl	53 - 100 µm
Number of coating	6
Pull-up velocity	3.0 mm/s

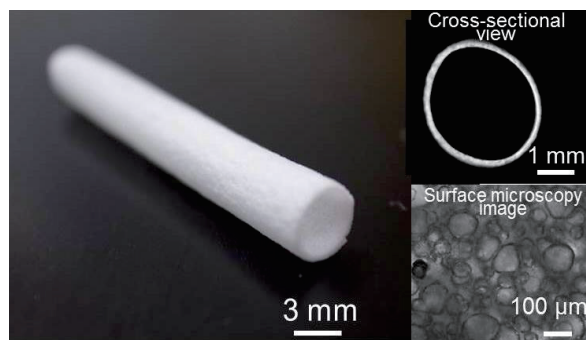


Figure 6 Images of the fabricated PLCL scaffold.

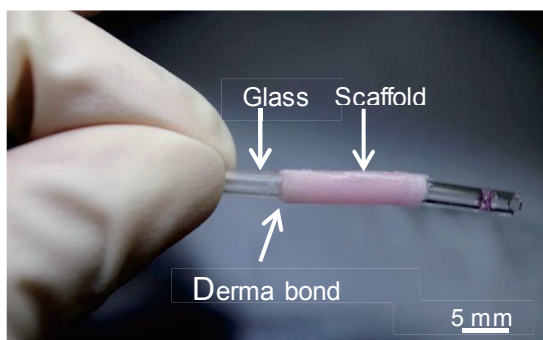


Figure 7 Fabricated tissue engineered blood vessel.

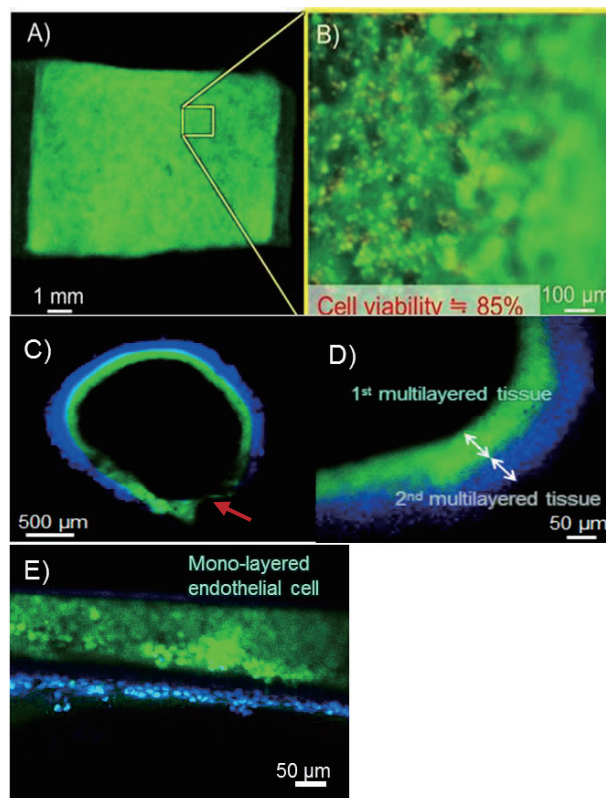


Figure 8 A) Image of tissues on the surface of PLCL scaffold. Live and dead cells were stained with green and red color, respectively. C) Fluorescent cross-section image of tubular tissue with hollow 2-layer-structure. E) Fluorescent side-section image of tubular tissue with hollow 3-layer-structure. B) and D) are enlarged views of A) and C), respectively. Red arrow in C) points to a discontinuous site of the cellular layers.

Fig. 7 is a picture of the final constructed TEBV; it has a length of 15mm and diameter of 3mm. Fig. 8 gives the fluorescent images of the final constructed tissues (A-D are images from a tubular tissue constructed with two cell lines, E is from a tubular tissue constructed with all three cell lines). The live/dead cell assay gives a result of around 85% cell viability on the final construct.

These results confirm that the proposed technique can be used to construct multilayered tubular tissues inside the PLCL scaffolds with controlled mechanical parameters.

In Fig. 8 C), the cross-section image of the constructed tissue layers, there is a gap on the circular cell layers (point by red arrow) where the DERMABOND was applied. Even though the mechanical parameters and the structural integrity were well restored by the DERMABOND, the tissue structure was not continuous. Moreover, the cell layer around the gap area is also significantly thinner than the rest of the tubular tissues. This might be caused by the stretching and pressing of the scaffold by the jigs, where the pressed area shows ununiformed properties that cells were hard to well-attached to. The technique might need to be slightly modified to allow an elongated scaffold area for being stabilized in the jigs while not to be included for the final construct tubular tissue. More experiments should be done to improve the final construct because the continuity of the endothelium is crucial for the functionality of the graft *in vivo*.

#### 4. CONCLUSION AND FUTURE WORK

In this short project, we successfully fabricated a multilayer structured blood vessel. It mimics the basic cellular structure of natural blood vessel and different cells were well attached to each other and the scaffold in static station. The mechanical characteristics of the fabricated graft match the external carotid artery by manipulating the fabrication conditions of the PLCL scaffold directly.

This is only a preliminary step of a research. A perfusion culture experiment should be conducted to test the graft's compatibility of shear stress caused by high flow rate, and monitor the cell attachment and cell viability after providing different biological (growth factors), chemical (NO) and mechanical cues.

For long-term study, the degradation rate of the PLCL, the change of the mechanical properties and its effects on cells should be monitored as well. These are better to be conducted by implanting the final construct made by animals' cells into the animal model itself. In the long-term study, the functionality of the graft can also be tracked.

For clinical translation of the proposed technique, the first concern is difficulty of automation, that is, the assembly step should be engineered and optimized. Different growth factors, for example, VEGF (Vascular Endothelial Growth Factor) can be incorporated in the graft to support the growth of endothelium, maximize the functionality and integration of the graft to the recipient's blood vessel system. If the graft is prepared for animal/clinical trial, immunogenicity tests will also be necessary to avoid toxicity or other side effects.

#### ACKNOWLEDGEMENT

This experiment is done at Arai Lab, Nagoya University, and fully supported by Professor Fumihito Arai, Dr. Taisuke Masuda, Yuka Yamagishi and Mitsuhiro Ukiki. My sincere appreciations to them, Professor Katsuo Kurabayashi at University of Michigan, the JUACEP staff at Nagoya University and IPE (International Programs of Engineering) staff at University of Michigan.

#### REFERENCES

- [1] Shakouchi, T., Tsujimoto, K., Sugimoto, H., Flow and Heat Transfer of Impinging Jet with Low Nozzle-Plate Spacing and Their Control, *JSME*, 69-686 B, pp. 2305-2312 (2003).
- [1] World Health Organization, Cardiovascular diseases, Fact Sheet No. 317, 2013.
- [2] V. Catto, S. Farè, G. Freddi, and M. C. Tanzi, Vascular Tissue Engineering: Recent Advances in Small Diameter Blood Vessel Regeneration, *ISRN Vascular Medicine*, vol. 2014, 27 pages, 2014.
- [3] L. Bordenave, P. Menu, and C. Baquey, Developments towards tissue-engineered, small-diameter arterial substitutes, *Expert Review of Medical Devices*, 5 (3): 337-347, 2008.
- [4] A. Rathore, M. Cleary, Y. Naito, K. Rocco, and C. Breuer, Development of tissue engineered vascular grafts and application of nanomedicine, *Wiley Interdisciplinary Reviews: Nanomedicine and Nanobiotechnology*, 4(3): 257-272, 2012.
- [5] S. Goldman, K. Zadina, T. Moritz et al., Long-term patency of saphenous vein and left internal mammary artery grafts after coronary artery bypass surgery: results from a department of veterans affairs cooperative study, *Journal of the American College of Cardiology*, 44 (11): 2149-2156, 2004.
- [6] Piccone V. Alternative techniques in coronary artery reconstruction. In: Sawyer PN, editor. Modern vascular grafts. New York: McGraw-Hill, 1987.
- [7] Zhang, W. J., Liu, W., Cui, L. and Cao, Y. Tissue engineering of blood vessel. *Journal of Cellular and Molecular Medicine*, 11: 945-957, 2007.
- [8] Sorrentino, S. and Haller, H. "Tissue Engineering of Blood Vessels: How to Make a Graft", in "Tissue Engineering, From Lab to Clinic". New York: Springer, 263-278, 2011
- [9] Yamagishi, Y., et al., Microfluidic perfusion cultivation system for multilayer structured tubular tissues, The 17th international conference on miniaturized systems for chemistry and life sciences, no. 1213, 2013.
- [10] Jeonga, S., Kima, B., et al. In vivo biocompatibility and degradation behavior of elastic poly(l-lactide-co-ε-caprolactone) scaffolds. *Biomaterials*, 25, pp.5939-5946, 2004
- [11] Jeong, S., Kim, S.H., Kim, Y.H., Jung, Y., Kwon, J.H., Kim, B.S., Lee, Y.M. "Manufacture of elastic biodegradable PLCL scaffolds for mechano-active vascular tissue engineering". *J Biomater Sci Polym Ed*.15(5):645-60. 2004
- [12] M. Matsusaki, H. Ajiro, T. Kida et al., Layer-by-Layer Assembly Through Weak Interactions and Their



- Biomedical Applications, *Advanced Materials*, 24 (4): 454-474, 2012.
- [13] A. Nishiguchi, H. Yoshida, M. Matsusaki *et al.*, Rapid Construction of Three-Dimensional Multilayered Tissues with Endothelial Tube Networks by the Cell-Accumulation Technique, *Advanced Materials*, 23 (31): 3506-3510, 2011.
- [14] S. Sarkara, H.J. Salacinskib, G. Hamiltonc, A.M. Seifalian. The Mechanical Properties of Infrainguinal Vascular Bypass Grafts: Their Role in Influencing Patency, *European Journal of Vascular and Endovascular Surgery*.31(6): 627–636, 2006
- [15] Riley, WA, Barnes, RW, Evans, GW and Burke, GL. Ultrasonic measurement of the elastic modulus of the common carotid artery. The Atherosclerosis Risk in Communities (ARIC) Study. *Stroke*.; 23: 952-956. 1992

# **COLD FORGE SPOT BONDING OF COPPER AND ALUMINUM ALLOY SHEETS**

Yingrui Zhan

Department of Mechanical Engineering, University of Michigan  
redblaze@umich.edu

Supervisor: Professor Takashi Ishikawa

Department of Materials Science and Engineering, Graduate School of Engineering, Nagoya University  
ishikawa@numse.nagoya-u.ac.jp

## **ABSTRACT**

Cu alloys have great thermal and electric conductivity while Al alloys have low density and good resistance to corrosion. Therefore, joining of Cu and Al alloy sheets preserves advantages of two materials and lowers the cost. It could be applied in electric industry, power industry, marine industry and aerospace industry. However, as it may be difficult using traditional methods to join different materials because of different melting points, cold forge spot bonding process is a possible option. In this work, cold forge spot bonding process was applied to join C1100P Cu alloy sheets and Al050 Al alloy sheets. The joint strength was measured by cross tension testing. Then fracture surfaces were evaluated by Scanning Electric Microscope. Finite Element Analysis was conducted to consider deformation behavior during process. In general, as the amount of punch indentation increased, the bonding effect of Cu and Al alloy sheets was improved.

## **1. Introduction**

Copper is easily stretched, molded, and shaped; is resistant to corrosion; and conducts heat and electricity efficiently. Aluminum weighs about one-third as much as steel or copper; is malleable, ductile, and easily machined and cast; and has excellent corrosion resistance and durability<sup>(1)</sup>. Copper and Aluminum sheets joining has drawn a growing interest for cost and weight reduction, especially, combining the advantages of high specific conductivity and good resistance to corrosion. The joined sheets possess high formability, electrical and thermal conductivity, making it a chosen material for specific application in automobile, electronics and marine industry<sup>(2)</sup>.

Traditional fusion welding is inapplicable for joining of dissimilar metal sheets because of different melting points. Several processes have been used to achieve joining of dissimilar metal sheets. They are generally divided into two categories, metallurgical joining and mechanical joining. Metallurgical joining includes cold welding, friction stir welding, resistance welding, etc. Mechanical joining includes self-pierce riveting, mechanical clinching, fastening, etc. The main difference between metallurgical and mechanical joining is in the mechanical joining processes the contacting surfaces are not bonded<sup>(3)</sup>.

Cold forge spot bonding is a method of backward extrusion used for joining metal sheets, which belongs to metallurgical joining. Two layered cylindrical cup of dissimilar metals are formed and joined. Surface pressure and surface expansion are necessary to obtain strong bonding<sup>(4)</sup>. Compared to other bonding processes, cold forge spot bonding has lower cost and requires simple equipment.

## 2. Experiments

### 2.1 Background

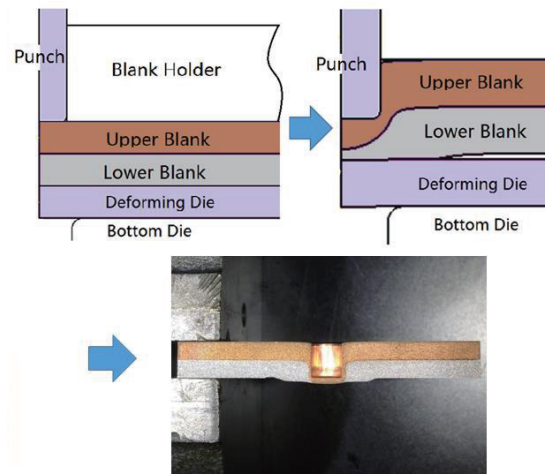


Fig. 1 Diagram of cold forge spot bonding process

As shown in Fig.1, two blanks, one is Aluminum alloy and the other is Copper alloy, are sandwiched between a blank holder and a bottom die. A plastic-deformable and disposable deforming die is seated between the lower blank and the bottom die. The punch is moving downward and pressing the upper blank against the lower blank. As the upper blank pushes the lower blank, both blanks are deformed locally and bonded together by the high surface pressure and large surface expansion.

### 2.2 Materials and experimental conditions

C1100P is used for upper sheet. Al050 is used for lower sheet. S45C is used for deforming die. Mechanical properties of these materials are shown in Table 1. Flow stress in Hollomon's equation is calculated from results of tensile tests. Upper sheets and lower sheets are all cut in 150mm × 50mm × 3mm and perforated in order for cross tension tests. The contacting surfaces between punch and upper sheet and those between deforming die and lower sheets are lubricated by Boron nitride. The contacting surfaces between upper and lower sheets are polished by emery paper #180 right before spot bonding process. 800kN Mechanical Link Servo Press is used for experiment, as shown in Fig.2. The diameter of punch is 5.0mm. The amount of punch indentation is changed from 4.0mm to 6.0mm.

Table 1 Mechanical properties of materials in experiment

Material	Part	Thickness /mm	Ultimate tensile strength /MPa	Flow stress /MPa
C1100P	Upper sheet	3.0	234.32	$\sigma=367\varepsilon^{0.189}$
Al050	Lower sheet	3.0	121.58	$\sigma=160\varepsilon^{0.120}$
S45C	Deforming die	3.0	—	$\sigma=1568\varepsilon^{0.21}$



Fig.2 800kN Mechanical Link Servo Press

### 3. Results and discussion

#### 3.1 Cross tension testing

After experiments, Cu and Al alloy sheets were bonded as shown in Fig.3. The deformation area was in a round shape and the diameter was around 18mm at 4.0mm punch indentation and around 20mm at 6.0mm punch indentation. Consequently spot bonding process may not result in a severe deformation outside punch area. As standardized in ISO 14272, cross tension testing was conducted, which is shown in Fig.4. And joint strength was evaluated by cross tension strength and maximum load value. The results are shown in Fig.5. It is clear that the joint strength is getting higher as the amount of punch indentation increases.

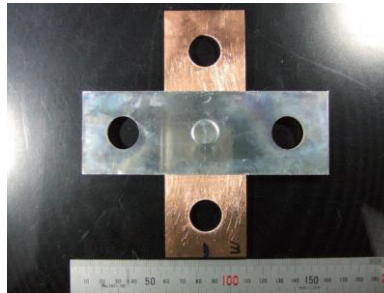


Fig.3 Specimen of bonded Cu and Al alloy sheets

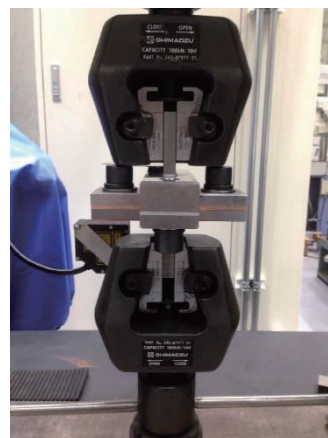


Fig.4 Cross tension testing process

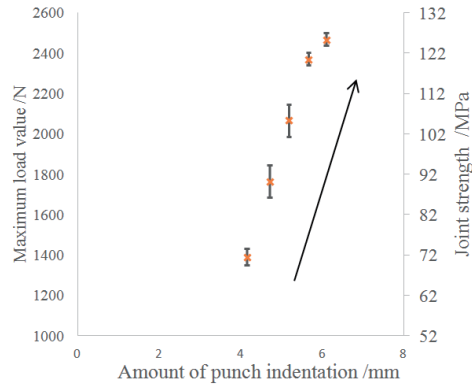


Fig. 5 Maximum load value and joint strength of each condition

### 3.2 Microstructure of fracture surfaces

Fracture surfaces of both Copper and Aluminum sheets in different amount of punch indentation after cross tension testing were investigated by SEM. Two modes, SEI and BEC, are used to obtain photos. Photos are taken from top view and oblique view, shown in Fig.6.

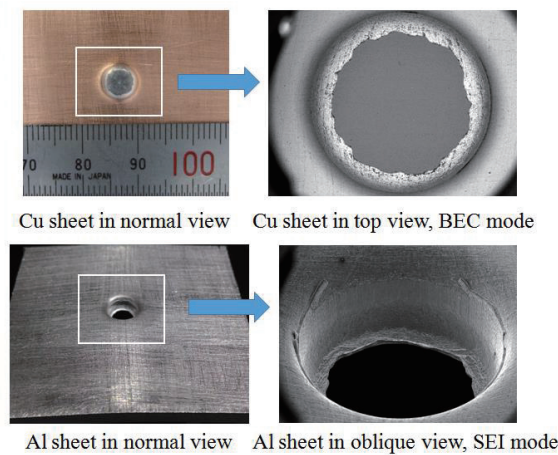


Fig.6 Diagram of modes and views in SEM

The compositional images of top view of Copper sheets are shown in Fig.7, where dark areas represent Aluminum and light areas represent Copper. Obviously more Aluminum were attached on Copper surface as the amount of punch indentation increases. In addition, a thin layer of Aluminum began to exist on the center of deformation area of Copper when the amount of punch indentation reached 5.5mm. This leads to one crucial fact that the detaching mechanism, which was the separation of Cu and Al sheets at first, changed into the fracture of Al sheet as punch went deeper. This fact is according with the joint strength obtained from cross tension testing.

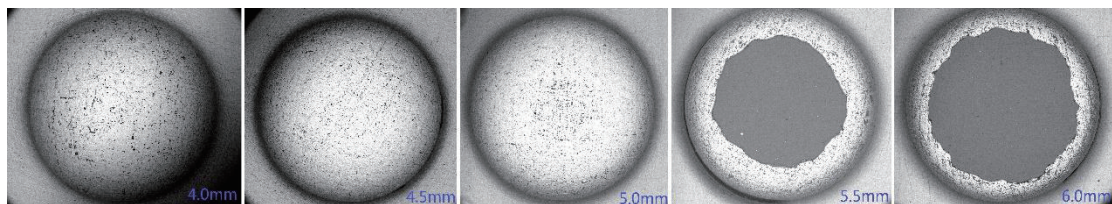


Fig.7 The compositional images of top view of Copper sheets

The compositional images of oblique view of Copper sheets are shown in Fig.8. Besides Aluminum left on the top, it also began to exist at the bottom position of the upside-down cup shape. With the increasing of amount of punch indentation, Aluminum at this position was getting more and thicker. This tendency is according to previous observation.

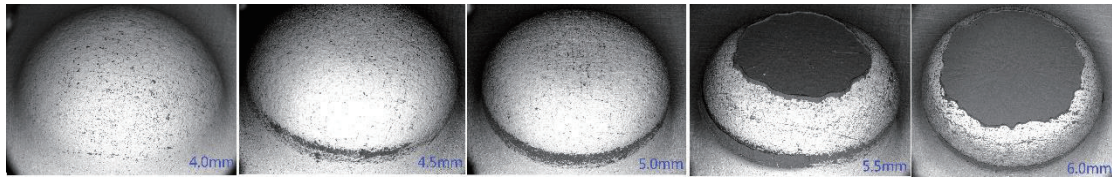


Fig.8 The compositional images of oblique view of Copper sheets

For Al sheets, SEI mode was used to produce images shown in Fig.9, as little Copper was left on Aluminum sheets. In these images, corresponding characteristics were obvious.

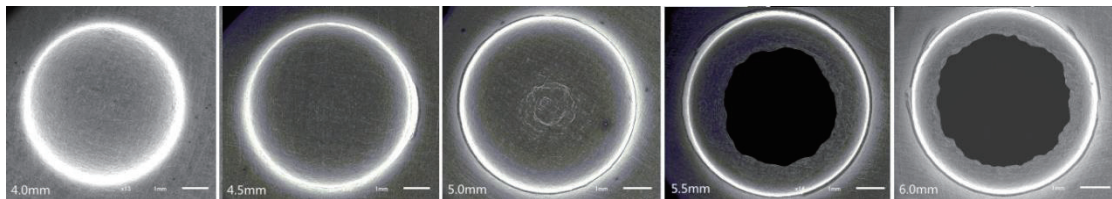


Fig.9 Images of top view of Copper sheets in SEI mode

The fracture mode changed from surface fracture to base metal fracture and resulted in increase of joint strength. In Fig.10, the change of bonding area is shown.

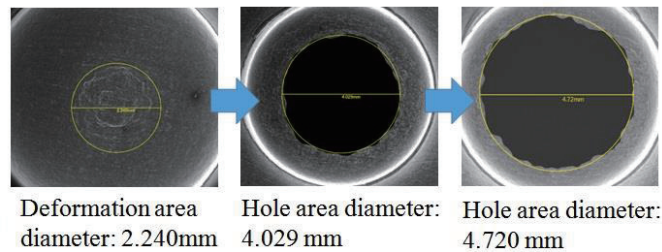


Fig.10 Change of the bonding area

From oblique view of Al sheets, the characteristics of side wall of the "center hole" could be observed, as shown in Fig.11.

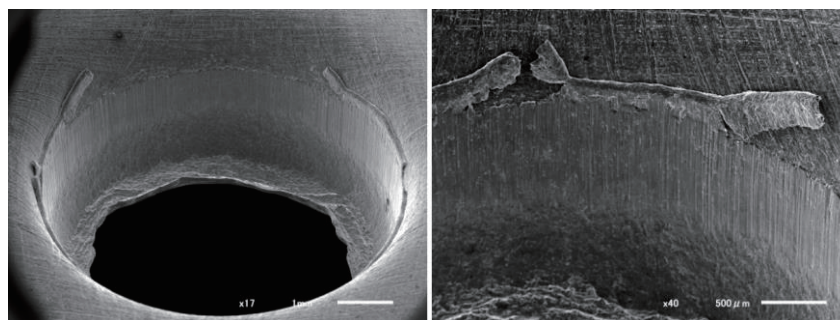


Fig.11 Oblique view of Al sheets in SEI mode(left) and amplified view

Fig.11 shows the important characteristics of bonding area during cross tension testing when the amount of punch indentation was 6.0mm. The strip of Aluminum shown at the edge is the result of metal flow caused by shear effect of cross tension testing. Since the cross tension testing was not conducted ideally, the strip of Aluminum was fractured and part of it was left on Copper side while most of it were on Aluminum side. Also, from the mark of the wall it was clear that ductile fracture occurred during cross tension test.

### 3.3 Finite Element Analysis

In order to consider the deformation behavior of cold forge spot bonding process, finite element analysis was performed by DEFORM-2D. Punch, blank holder and bottom die were modeled as rigid while upper sheet, lower sheet and deforming die were set to be elasto-plastic. The friction coefficient  $\mu$  of the interfaces between tool and sheets was set to be 0.1 and type is Coulomb friction. That of

interfaces between two sheets was set to be the function of surface expansion ratio. When the surface expansion ratio is lower than 4, shear friction coefficient is 0.15 while the ratio is larger than 4, friction coefficient is 1.00. These values were obtained by geometry fitting of experiment and simulation.

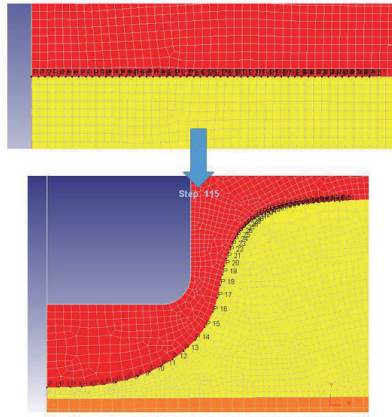


Fig.12 Diagram of point tracking in DEFORM-2D

For simulation results, Points spaced 0.1mm apart at the interface between Cu and Al sheets were created. Relevant parameters of cold forge spot bonding process at these points were obtained by point tracking function of DEFORM-2D. The x-axis values of these points representing radius changed as the spot bonding process went, as shown in Fig.12.

Distribution of surface expansion ratio of lower sheet,  $S_{Al}$  is shown in Fig.13. The equation of  $S_{Al}$  is given as follows.

$$S_{Al} = A/A_0 \quad (1)$$

$A_0$  is initial area and  $A$  is the final area of surface element. Large surface expansion ratio areas are concentrated for  $r < 3\text{mm}$ . Also, distribution of maximum surface pressure  $p_{max}$ , and relative slippage of two sheets were shown in Fig.13. Obviously all these parameters increased when the amount of punch indentation was increasing.

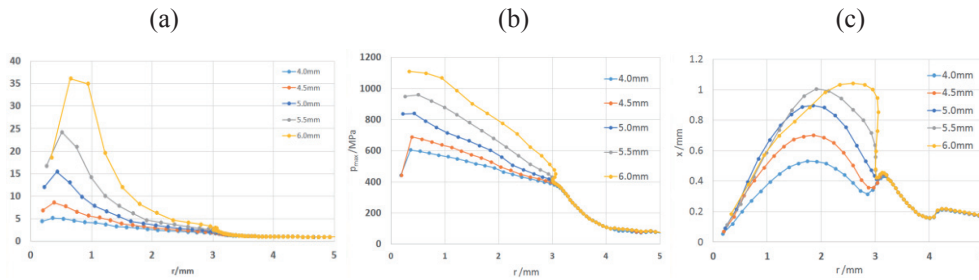


Fig.13 Each parameter's distribution at interfaces during spot bonding process, (a)lower sheet surface expansion ratio  $S_{Al}$ , (b)maximum surface pressure  $p_{max}$ , (c)relative slippage of two sheets.

Besides, bonding region is evaluate by utilizing the analysis results. In the case of solid phase bonding, it is necessary to put the surface energy to achieve bonding of two metals. Total friction work  $W$  is calculated by time-integrating the product of friction factor  $m$ , surface pressure  $p$  and relative

$$W = \int m p v dt \quad (2)$$

Total friction work evaluates the energy of friction force on the contact surfaces during bonding. The amount of punch indentation mostly affects areas where  $r < 3\text{mm}$ .

Another parameter, distribution of evaluation factor of real contact area,  $\Pi$ , which was used to evaluate bonding region where large surface expansion ratio but little relative slippage of sheets existed.  $\Pi$  is calculated by the maximum value of the product of surface pressure and expansion ratio of Al sheet divided by the 0.2% proof stress of Al alloy.

$$\Pi = (S_{AlP})_{MAX} / \sigma_{0.2(Al)}, \quad (3)$$

$\Pi$  is a dimensionless parameter for the degree of real contact with virgin metals. Both  $W$  and  $\Pi$  increased as the amount of punch indentation was increasing, as shown in Fig.14.

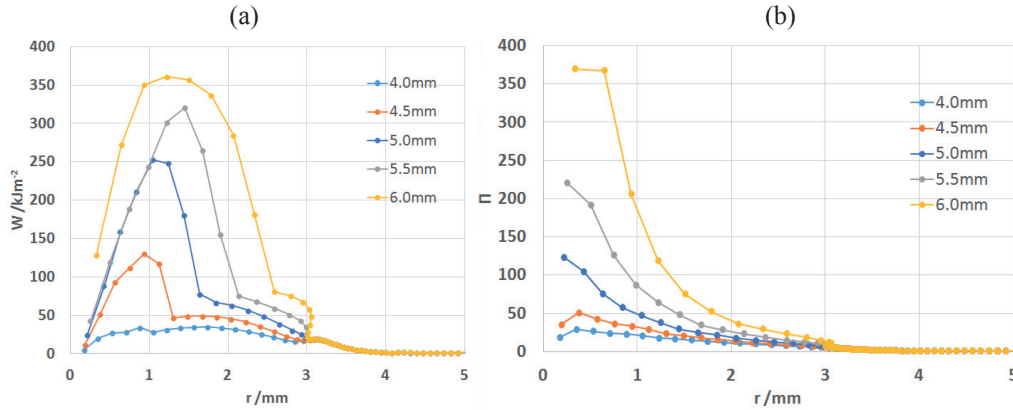


Fig.14 Distribution of (a) total friction work,  $W$ ; (b) evaluation factor of real contact area,  $\Pi$

The bonding area of specimen whose punch indentation was 5.5mm, had a radius of 2.015mm. This value was corresponding to x-axis of distribution of friction work. Then the corresponding point was found, and the total friction work is around 100kJm<sup>-2</sup>. These value could be considered as the minimum friction work in order to achieve effective spot bonding, which is shown in Fig.15(a).

The same procedure was done for specimens with punch indentation of 5.0mm and 6.0mm and similar results were obtained. Thus area with total friction work over 100kJm<sup>-2</sup> were bonded strongly because of the effect from large relative slippage between interfaces.

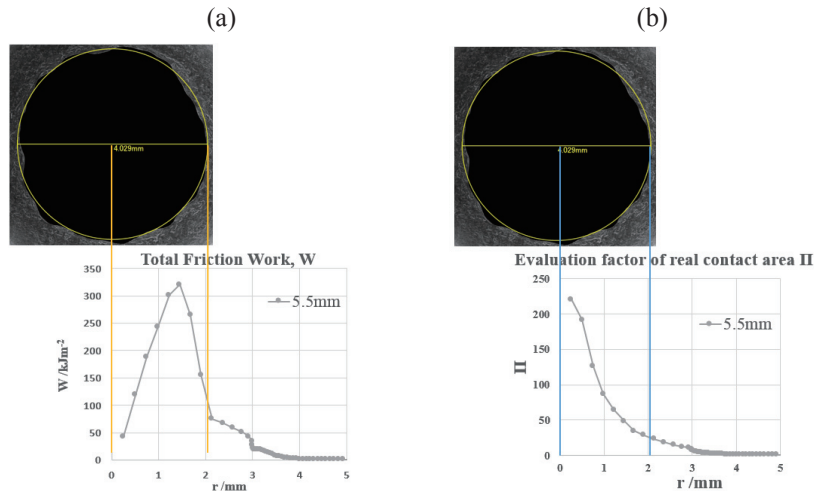


Fig.15 Diagram of relationship between bonding area and (a) total friction work,  $W$ ; (b) evaluation factor of real contact area,  $\Pi$

Same process was done regarding distribution of evaluation factor of real contact area,  $\Pi$ . Then the corresponding point was found, and the evaluation factor is around 28. These value could be considered as the minimum evaluation factor of real contact area in order to achieve effective spot bonding, as shown in Fig.15(b).

Specimens with punch indentation of 5.0mm and 6.0mm were also evaluated and similar results were obtained. Thus area with evaluation factor of real contact area over 28 were bonded strongly because of the effect from large surface expansion with little relative slippage.

#### 4. Conclusions

Cold forge spot bonding method was applied in joining of Cu and Al alloy sheets. By cross tension testing and SEM observation, joint strength and microstructure of fractures surfaces were evaluated. In addition, by finite element analysis, deformation behavior of bonding area was revealed. The following



results were obtained.

1) Joining of Cu and Al alloy sheets is successfully achieved at room temperature by cold forge spot bonding technology.

2) When the amount of punch indentation reached about 4.0mm, Cu and Al sheets were able to be bonded. As it continued to be higher, the bonding area and bonding strength were increasing.

3) Base metal fracture started after the amount of punch indentation reached 5.0mm.

4) Compared to Steel-Al condition, Cu-Al bonding needs lower load and the most bonded area was closer to center line.

In all, cold forge spot bonding technology could be a suitable and low-cost method of joining dissimilar metal sheets. It does not require complex machines or procedures and the parameters of bonding effect are easy to be found. The amount of punch indentation is one of the most important factors that could influence the joint strength. After punch indentation reaches a certain value, the joint strength rely more on the strength of lower sheets than on the strength of contacting surface bonding.

## **Acknowledgement**

I would like to express my gratitude for JUACEP, Professor Ishikawa and his Material Deformation and Processing Laboratory for all the guidance and help given to me. I learned a lot from Professor Ishikawa and my fellow students regarding academic attitudes, knowledge and skills. This experience is my lifelong treasure.

## **Reference**

- (1) U.S. Geological Survey
- (2) Li, X., Zu, G., Ding, M., Mu, Y., & Wang, P. (2011). Interfacial microstructure and mechanical properties of Cu/Al clad sheet fabricated by asymmetrical roll bonding and annealing. *Materials Science and Engineering: A*, 529, 485-491.
- (3) Mori, Ken-ichiro, et al. "Joining by plastic deformation." *CIRP Annals-Manufacturing Technology* 62.2 (2013): 673-694.
- (4) Yuri Miwada, Taikahiro Ishiguro, Eiji Abe, Nobuki Yukawa, Takashi Ishikawa, Tomoaki Suganuma. Cold forge spot-bonding of high tensile strength steel and aluminum alloy sheets. 11<sup>th</sup> International Conference on Technology of Plasticity, 2014.

# Development of Current Suppression Equipment in Low Voltage DC Distribution System

**Chiyang Zhong**

Department of Electrical Engineering, University of Michigan  
zchiyang@umich.edu

**Prof. Toshiro Matsumura**

matumura@nuee.nagoya-u.ac.jp  
Graduate School of Engineering, Nagoya University

**Associate Prof. Yasunobu Yokomizu**

yokomizu@nuee.nagoya-u.ac.jp  
Graduate School of Engineering, Nagoya University

## ABSTRACT

Grounding faults occur in a DC low-voltage distribution system could cause large currents through transmission lines, which may damage devices in the system. Hence reducing the sudden rush current important and fault current limiters (FCLs) are used. Most of the existing FCLs are expensive because of the components and materials used. The aim of this research is to develop FCLs consisting of passive elements that are simpler and cheaper. Different topologies of the device are analyzed and compared for their performances on current suppression. In addition, based on the existing topologies, a new topology has been proposed. With simulations, it has been proven to have better characteristics during the fault periods over the others.

## I. INTRODUCTION

The DC low-voltage distribution systems are widely employed in some parts of the world, especially in Japan nowadays. More are expected to be constructed, so protecting them from faults and contingencies is an important task. Grounding is the most common fault that takes place at the distribution level of the power system. Under a grounding situation, short current is drawn through the line. If the current was too large, end equipment would be badly damaged. Surge current caused by lightning strikes also requires some level of reduction. Therefore, low-voltage DC fault current limiters are researched by people around the world. Currently, many FCLs are built using controlled components, which need control schemes to be implemented to work properly, or expensive superconductive materials.

FCLs consisting of only passive elements are also considered. They are not only simpler to make, but also less expensive compared to the other types of FCL.

Analyses on some topologies have been done in some previous works. In [1] and [2] the L-R topology is looked into, including its operation and installation. Namba *et al.* have also compared the L-R topology with the L-RC topology in [3] and [4].

This report can be divided in two parts. In the first part, four different FCL topologies developed from the L-R topology are simulated and compared with each other. They are proven to be equivalent to the L-R topology in their best case scenarios after a series of tests. Based on the L-R and L-RC topologies, a new topology is proposed in the second part of the report. Details are given to describe how the L-RD topology is brought up. With respect to both the current suppression period and the current interruption period, the newly proposed L-RD topology has been proven more promising than the other FCL topologies.

The rest of the report is organized as follows. Section II describes the four new topologies modified from the L-R topology, followed by their current suppression performance in the next section. In Section IV, how the L-RD topology is originated is elaborated. Its development and comparison with the L-R and L-RC topologies is presented in Section V. Conclusions are drawn in Section VI.

## II. L-R BASED FCL TOPOLOGIES

From literature [1], the L-R FCL topology is made up of an inductor in parallel with a resistor. It is given in Fig. 1, together with the other four new structures modified based on it.

Clearly the simplest topology is the L-R topology in Fig. 1 (a). The others are added with extra elements. Topology A shown in Fig. 1 (b) consists of an inductor, two resistors, and a capacitor. Fig. 1 (c) shows Topology B, which uses one resistor and two inductors

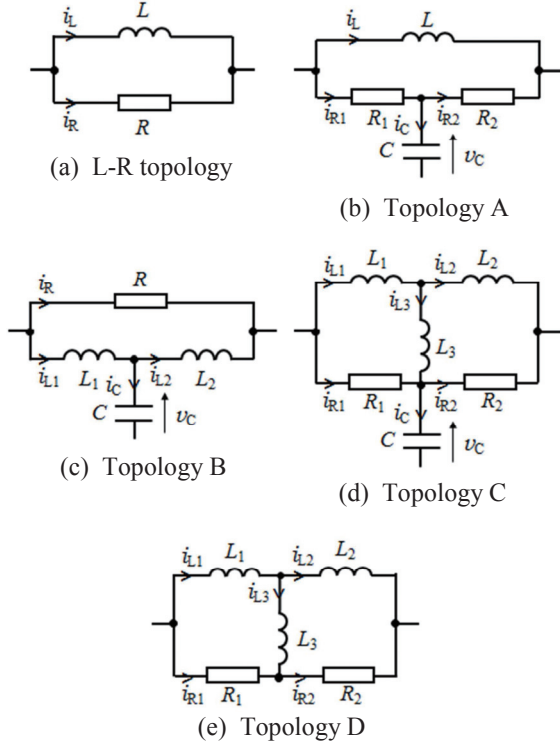


Fig. 1 Different FCL topologies

instead. The connection of the capacitor does not change. A bridge circuit can be seen in Topology C that is in Fig. 1 (d). It has three inductors with one on the bridge, two resistors, and a capacitor at the same place as the previous cases. Fig. 1 (e) gives Topology D, which is the same as Topology C except that the capacitor connected to ground has been removed.

For simplicity, the baseline values used in the simulations, which is described in the next section, for the inductance and resistance in the L-R topology are  $2.0 \Omega$  and  $3.0 \text{ mH}$  respectively. In order to compare the topologies, the other four have to meet the following constraints,

$$\sum_{i=1}^{N_L} L_i = 3.0 \text{ mH} \quad (1)$$

$$\sum_{i=1}^{N_R} R_i = 2.0 \Omega \quad (2)$$

where  $N_L$  and  $N_R$  are the numbers of inductors and resistors in each FCL topology respectively. Thus sum of all inductance values is  $3.0 \text{ mH}$ , while the resistance values should add up to  $2.0 \Omega$ .

### III. CURRENT SUPPRESSION PERFORMANCE

Simulations were done to test out the four topologies proposed. The circuit is given in Fig. 2. It

has a DC source with internal resistance  $R_S$  and inductance  $L_S$ . Resistor  $R_L$  is used to represent the load in a power system. The switch  $S$  simulates the grounding fault, which occurs at  $25 \text{ ms}$ . The total simulation time is  $50 \text{ ms}$  for each run. The first  $25 \text{ ms}$  is needed for the circuit to reach its steady operating state. At  $25 \text{ ms}$ , the switch closes to provide a path to ground for the current, thereby shorting the system load. When the L-R FCL is used, the current goes through the inductor  $L$  and no voltage drop would appear across it during the steady state. But after  $S$  closes, the impedance of the loop decreases, increasing the current dramatically, which induces a large voltage across the inductor. As the inductor stores energy, the resistor  $R$  is used for consuming the stored energy after the circuit breaker operates to protect the circuit. The circuit breaker is not analyzed here, but it will appear in Section IV. Due to its existence, the current can be largely reduced compared to the case without FCL.

In the simulations, the values of the components within the test circuit shown in Fig. 2 are given in Table I. During normal operation, the steady-state current is  $10 \text{ A}$ . The simulation result for the L-R topology is given in Fig. 3. Clearly the current passing through the FCL does not increase as quickly compared to the circuit without the device.

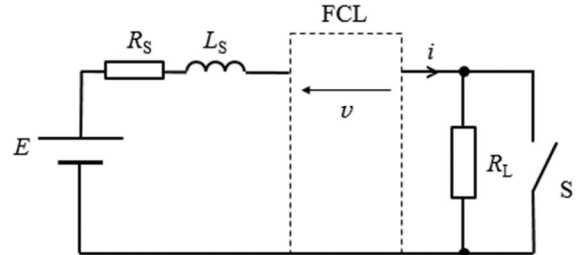


Fig. 2 Simulation circuit for testing the current suppression performance of different topologies

TABLE I

SIMULATION CIRCUIT COMPONENT VALUES

Component	Value
Source Voltage $E$	$120 \text{ V}$
Source Resistance $R_S$	$0.6 \Omega$
Source Inductance $L_S$	$1.5 \text{ mH}$
System Load $R_L$	$11.4 \Omega$

Topology A has two resistors. According to constraint (2), the total resistance should be  $2.0 \Omega$ . For illustrational purpose, two scenarios are presented in

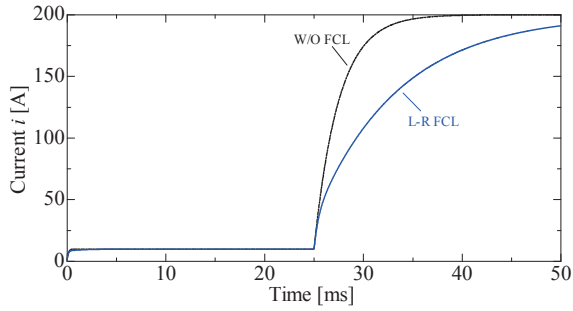
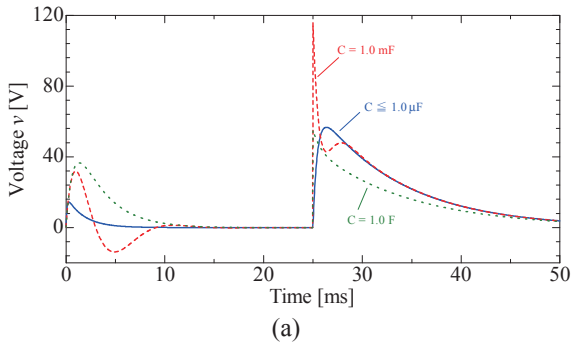
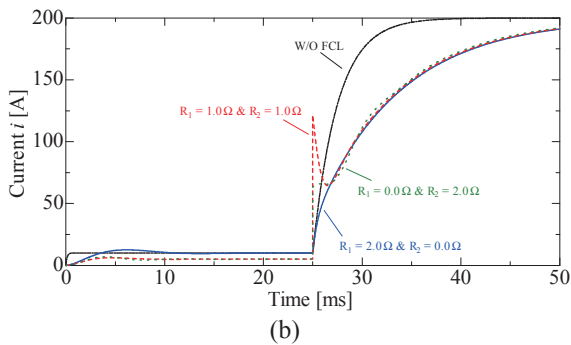


Fig. 3 Current suppression of L-R topology

Fig. 4. In Fig. 4 (a), the influence of the capacitor has on the circuit was tested with both resistors equaling  $1.0 \Omega$ . It can be seen that a smaller capacitor gives a better current limitation result. With a capacitor that is smaller than or equal to  $1.0 \mu\text{F}$ , the branch has a very large impedance that does not draw current through it. Therefore all the current would be going through the inductor and the resistor after the fault occurs. It is the same as making  $R_1 = 2.0 \Omega$  and  $R_2 = 0.0 \Omega$  due to the constraint, shorting the capacitor branch. The scenario shown in Fig. 4 (b) used  $1.0 \text{ mF}$  as the capacitor value. In both cases, there is no current going through the capacitor to ground, thus they are equivalent to the L-R topology. These are the two configurations of the topology that gives the whole circuit the best current limitation performance. As for Topology B, the two



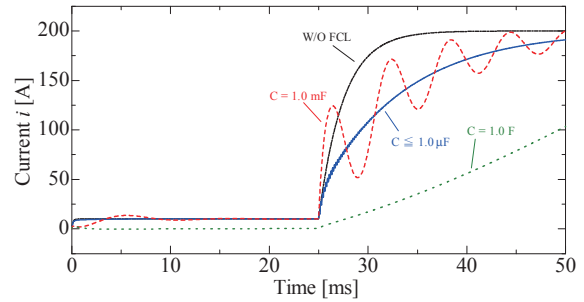
(a)



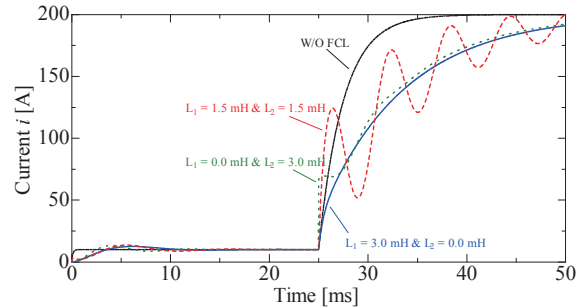
(b)

Fig. 4 Current suppression of Topology A

inductors should sum up to  $3.0 \text{ mH}$ . Similar analysis can be done. According to Fig. 5 (a) in which both inductors are  $1.5 \text{ mH}$ , using a smaller capacitor is better for the performance. Clearly in the plots, oscillation can be observed when the capacitor is  $1.0 \text{ mF}$ . This value was used in Fig. 5 (b) to see how the resistors affect the current characteristic. It turns out that the best case scenario is also equivalent to the L-R topology when no current is drawn through the capacitor.



(a)



(b)

Fig. 5 Current suppression of Topology B

With the bridge circuit in Topology C, the  $3.0 \text{ mH}$  total inductance is divided into three parts. The result given by equally divided inductance and resistance is shown in Fig. 6 (a). In Fig. 6 (b) the inductance of  $L_3$  is the variable when the other two inductor values are equal.  $R_1$  and  $R_2$  are the same as well, and the capacitance is  $1.0 \mu\text{F}$ . The values of  $L_1$ ,  $L_2$ ,  $L_3$ , and  $C$  are  $2.5 \text{ mH}$ ,  $0.5 \text{ mH}$ ,  $0.0 \text{ mH}$ , and  $1.0 \mu\text{F}$ , respectively in Fig. 6 (c). Those three scenarios give an insight into how the circuit works. Apparently the best performance is achieved when no current is drawn through either  $L_3$  or  $C$ . In order to make this happen, the two nodes connected to  $L_3$  should have the same potential, while the capacitor value should be small enough. Without the capacitor, the modeling of Topology D was much simpler. The outcomes are similar to that of Topology C when the capacitor used is small enough. Thus, the best case scenario is exactly

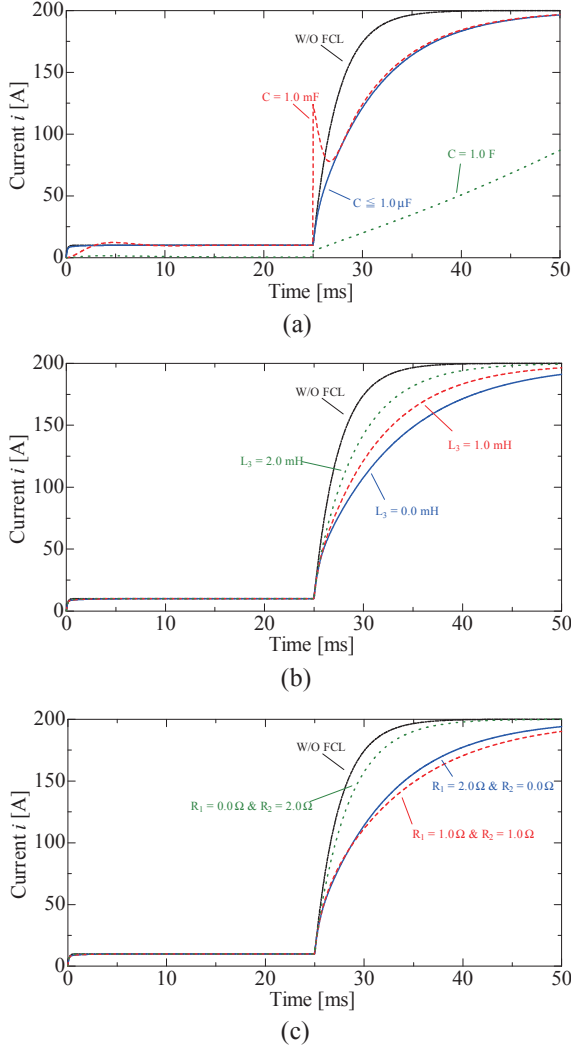


Fig. 6 Current suppression of Topology C

the one found in the previous design, without the existence of the capacitor. Fig. 7 and Fig. 6 (b) are the same because they have the same configuration when the capacitor in Topology C is neglected.

Each topology has its own best case scenario, which gives the most desired current suppression performance. The configuration of every topology is listed in Table II. For the first two topologies, they both have two scenarios that achieve the same best performance. Thus there are two configurations 1 and 2 for each shown in the table. The aim for achieving this result is to prevent any current from flowing through either the capacitor to ground or the inductor on the bridge. Therefore, they can all be transformed into the L-R topology to optimize their current limiting effects when constraints (1) and (2) are considered. The current would be only going through a total inductance

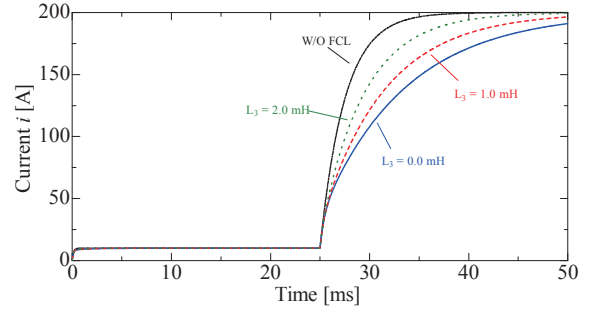


Fig. 7 Current suppression of Topology D

of 3.0 mH in parallel with a total resistance of 2.0 Ω. Any extra components or branches added to the L-R topology would degrade its capability to reduce surge current. In general, the four proposed topologies are not worth implementing as their best performances can be achieved by the circuit in Fig. 8 with the L-R FCL applied. It has less components, thereby is more economical to implement in practice.

TABLE II

BEST CASE SCENARIO OF EACH TOPOLOGY

Topology	Configuration
A	1. $R = 2.0 \Omega$ , $L_1 = 3.0 \text{ mH}$ , $L_2 = 0.0 \text{ mH}$ 2. $R = 2.0 \Omega$ , $C \leq 1.0 \mu\text{F}$
B	1. $R_1 = 2.0 \Omega$ , $R_2 = 0.0 \Omega$ , $L = 3.0 \text{ mH}$ 2. $R = 2.0 \Omega$ , $C \leq 1.0 \mu\text{F}$
C	$R_1 = 1.0 \Omega$ , $R_2 = 1.0 \Omega$ , $L_1 = 1.5 \text{ mH}$ , $L_2 = 1.5 \text{ mH}$ , $L_3 = 0.0 \text{ mH}$ , $C \leq 1.0 \mu\text{F}$
D	$R_1 = 1.0 \Omega$ , $R_2 = 1.0 \Omega$ , $L_1 = 1.5 \text{ mH}$ , $L_2 = 1.5 \text{ mH}$ , $L_3 = 0.0 \text{ mH}$

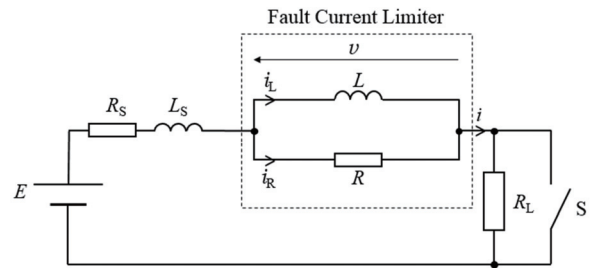


Fig. 8 Simulation circuit with equivalent L-R FCL

#### IV. ORIGIN OF THE L-RD TOPOLOGY

This section describes the development of a new topology, the L-RD topology. It is inspired by the L-

RC topology mentioned in literatures [3] and [4]. Although the L-R FCL topology has been proven better than the others in the previous section, the L-RC topology given in Fig. 9 has an even better current suppression effect after the fault occurs. It has a capacitor connected in series with a resistor, which as a whole is paralleled to an inductor.

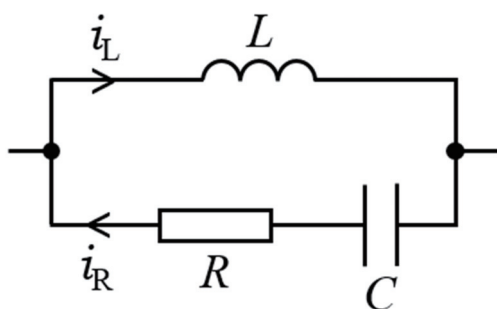


Fig. 9 L-RC FCL topology

In this section, the simulation circuit shown in Fig. 10 is slightly modified from that in Fig. 2, with an unideal circuit breaker added. One type of this device is described and analyzed in [5]. It is used to protect the circuit from longer exposures to large current flows. By disconnecting the transmission lines, it protects the end equipment from being damaged. However it has a time delay ranging from 3 ms to 10 ms depending on the device itself. In the new simulation circuit, the switch S representing the grounding fault closes at 10 ms and the circuit breaker operates 10 ms after that, which is at 20 ms. Due to its unideal characteristic, the resistance of the device within the breaking period does not increase from 0 to infinite immediately. This one here instead of acting exactly like a switch, it actually operates like a variable resistor that exponentially increases its resistance from 0  $\Omega$  to infinite within a time span. To better understand how the circuit breaker works, its response to the fault was tested without an FCL. There are three models corresponding to different operating times, 2 ms, 5 ms, and 7 ms. After using the resistance varying data concluded from previous experiments, the results of each is given in Fig. 11, including the current

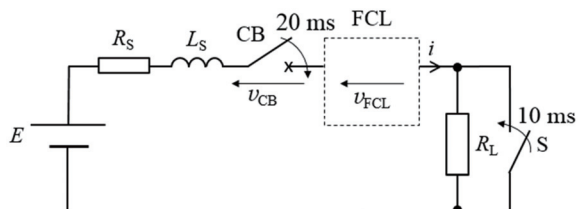


Fig. 10 Simulation circuit for developing the L-RD FCL topology

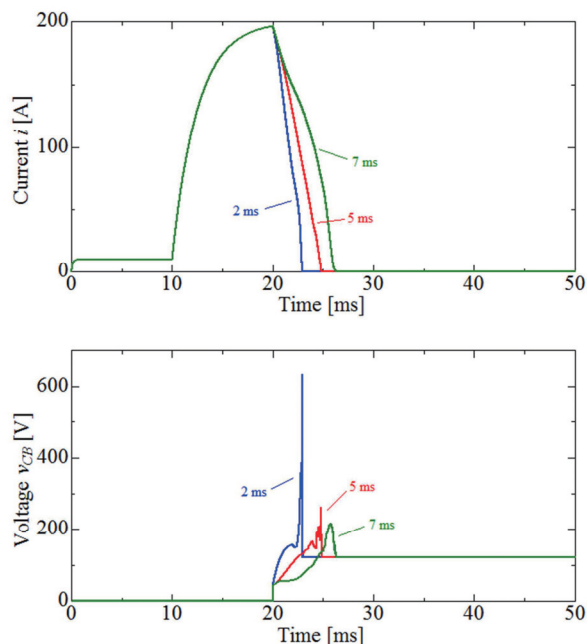


Fig. 11 Responses of three circuit breaker decreasing rate and the voltage drop across the circuit breaker.

From Fig. 11 it is clear to see that the larger the operating time is, the smaller the maximum voltage applied across the circuit breaker is, thus the less likely the device is damaged. However, shorter time duration is desired in real operation for faster response. The duration between 10 ms and 20 ms is the delay time of the operation of the circuit breaker. At 20 ms, it opens the circuit, which may easily induce an arc over the space. This phenomenon is looked into in literature [5]. The instant power usage and accumulated energy consumption of the operating time models are also plotted and they are given in Fig. 12. Apparently a shorter operating time model consumes less energy over time, but it has the highest maximum power drawn. For the 7 ms model, it does not draw as much power at every time instant, its long time duration gives the highest energy consumption within the breaking action. Considering the tradeoff between the voltage drop and the operating time, as well as the power and energy graphs, the 5 ms model is chosen for the following simulations.

By applying the 5 ms circuit breaker model to the test circuit, the L-RC topology was simulated. With the results shown in Fig. 13, the influence of the capacitor value can be observed. It can be seen that a small capacitor gives better current limitation effect, but at the same time induces larger maximum voltage across

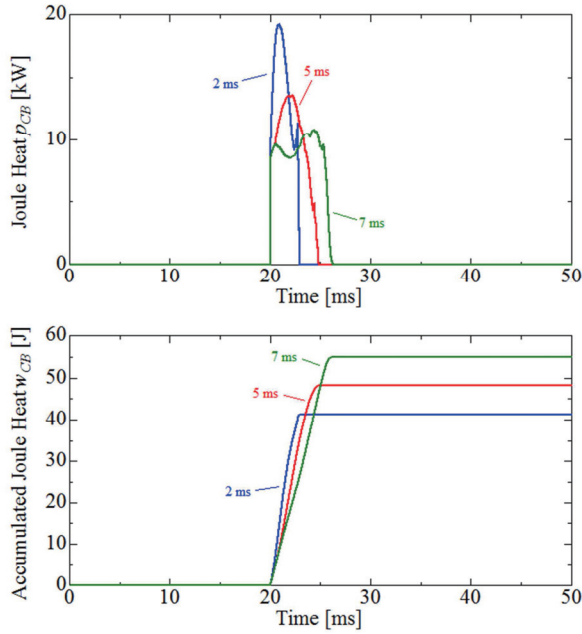


Fig. 12 Instant power drawn and accumulated energy consumption over time

the circuit breaker after it operates. During the current limitation period, which is between 10 ms and 20 ms, the L-RC FCLs with 1.0  $\mu\text{F}$  and 1.0 nF capacitors have the same performance, both better than the 1.0 mF case. The current suppression effect produced by the L-RC topology outperforms that produced by the L-R topology. However during the current interruption period that starts at 20 ms, a smaller capacitor clearly

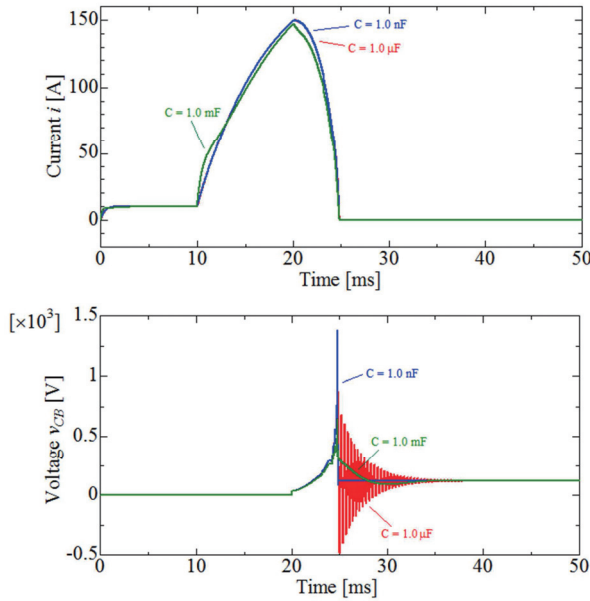


Fig. 13 Characteristics of the L-RC topology

induces a larger maximum voltage across the circuit breaker. The case with a 1.0 nF capacitor generates a maximum voltage drop of about 1400 V, which can fry the device easily. As for the 1.0  $\mu\text{F}$  scenario, the maximum voltage produced is only about half of much, although the voltage oscillation is much more serious. It is generated by the energy stored being released from the inductor, and then flowing back and forth between it and the capacitor. Thus 1.0  $\mu\text{F}$  is used as the capacitance for the L-RC topology in the later tests. The frequency of the voltage oscillation observed in Fig. 12 is calculated as follows,

$$f = \frac{1}{2\pi\sqrt{LC}} \approx 2906 \text{ Hz} \quad (3)$$

where  $L$  and  $C$  are the components in the L-RC topology with values of 3.0 mH and 1.0  $\mu\text{F}$  respectively.

## V. DEVELOPMENT AND ANALYSIS

When considering the current suppression period, the simulation results show that the larger the impedance of the resistor branch is, the better the performance gets. Therefore to achieve this goal, the FCL topology with an inductor in parallel with a branch of infinite impedance, like the one shown in Fig. 14, is desirable. As for the current interruption period, a resistor in parallel with the inductor is required because the energy stored needs to be consumed. If there was path for the current to flow after the circuit breaker operates, an arc would be very likely to occur, and this is extremely dangerous in practice. Although the L-RC topology gives infinite impedance under a DC condition, it produces voltage oscillation and large voltage drop across the device as demonstrated in the previous section. Therefore to find a topology that has infinite impedance on the resistor branch for current limitation, while keeping a path for the current to flow after the circuit breaker opens and reducing the magnitude of the voltage drop mentioned, the L-RD topology is thought of. It is given Fig. 15. This new topology has a diode replacing the capacitor in the L-RC topology, with its cathode facing the resistor. With

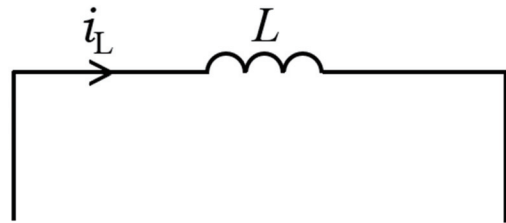


Fig. 14 Inductor in parallel with an infinite impedance branch



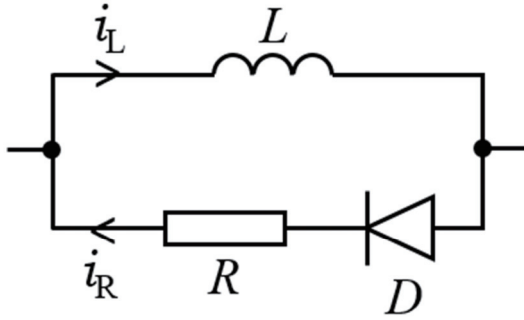


Fig. 15 L-RD FCL topology

this configuration, the diode is able to block the current from flowing through the resistor during the current limitation period, while providing the path for current to flow from the inductor to the resistor after the circuit breaker breaks.

Theoretically speaking, the L-RD topology holds the merits of both L-RC topology and L-R topology. Simulations were done to prove it. The comparisons between these three topologies are given in Fig. 16, in which two time periods are observed. One period is between 20 ms and 30 ms when the current limitation effect is concerned the most. The other time duration that matters is after 30 ms, which focuses on the current interruption effect. The current plot is used to compare the current suppression effect of the three topologies, while the voltage plot is used to see the corresponding voltage drops across the circuit breaker. The resistance and inductance used during simulations

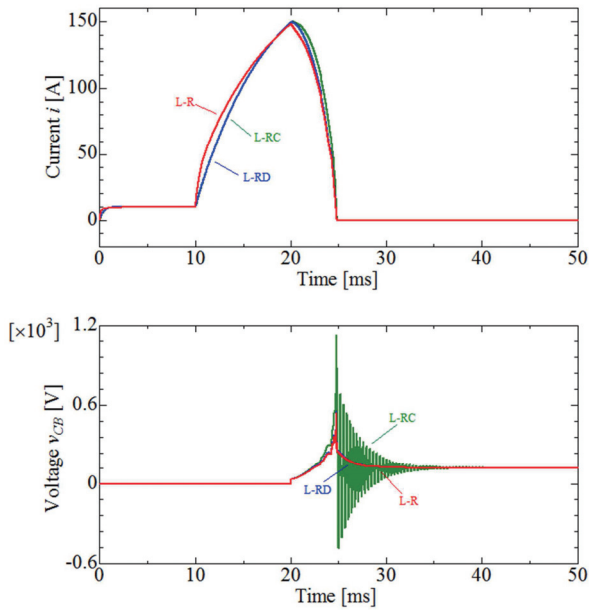


Fig. 16 Comparisons between three topologies

are  $2.0 \Omega$  and  $3.0 \text{ mH}$ , respectively. After analyzing the results from Fig. 16, Table III is produced and it clearly shows which topology is the best among the three in which time period. An X is put under the corresponding row and column to represent the best performance. When there are two or more topologies equally good under a certain circumstance, an X is marked correspondingly for each topology. Obviously, The L-RD and L-RC topologies outperform the L-R topology with the same current limitation characteristic. The L-RD and L-R topologies have similar current interruption performance that exceeds the L-RC topology. Hence the L-RD topology is most promising over the whole process.

TABLE III

COMPARISONS OF THREE TOPOLOGIES UNDER TWO CIRCUMSTANCES

Topology	Current Limitation	Current Interruption
L-RC Topology	X	
L-RD Topology	X	X
L-R Topology		X

## VI. CONCLUSIONS

This report has explored the characteristics of fault current limiters used in DC low voltage distribution systems. Four new topologies constructed based on the L-R topology are analyzed. The configuration of each topology for achieving the best current suppression performance has been found. The simulation results show that all topologies can be transformed into the L-R topology in order to excite the most desirable current limitation effect. Therefore they are not practical to implement in real systems due to extra components only to achieve the same performance that can be provided by the simple L-R topology.

More effort has been put into developing a new topology. The L-RD topology is proposed in this report, inspired by the L-RC and L-R topologies. The L-RC topology gives a great current limitation effect within the time after the fault occurs and before the circuit breaker operates, but it induces serious voltage oscillation and large maximum voltage drop across the device. Although the L-R topology does not have a capacitor so the problems are eliminated, its performance in the current suppression period is not as good as the L-RC topology. The proposed L-RD FCL

overcomes the shortfall in each time period. It has been proven to have better current suppression and interruption performances over the whole process. As a result, the L-RD topology is more promising than the other two topologies.

In future work, tests can be conducted to fully understand the newly proposed L-RD FCL topology. In addition, more thoughts can be given to develop other promising topologies.

### ACKNOWLEDGEMENTS

I would like to thank Kohei Namba for being the teaching assistant to help me with my research, as well as Prof. Matsumura and Associate Prof. Yokomizu for giving me helpful advice, throughout the whole time.

### REFERENCES

- [1] K. Namba, Y. Yokomizu, T. Matsumura, "Fundamental approach to installation of fault current limiter for low voltage DC system and its current limiting effect," in *Rec. Tokia-Section Joint Conf. on Elec. and Related Eng.*, D4-6, 2013.
- [2] K. Namba, Y. Yokomizu, T. Matsumura, "Fundamental approach to current limiting effect by means of installation of fault current limiter in low voltage DC system," in *Rec. IEEJ Annual Meeting*, 6-269, 2014.
- [3] K. Namba, Y. Yokomizu, T. Matsumura, "Comparative discussion about current limiting effect due to different fault-current-limiters for low voltage DC system," *Rec. Tokia-Section Joint Conf. on Elec. and Related Eng.*, B3-2, 2014.
- [4] K. Namba, Y. Yokomizu, T. Matsumura, "Suggestion of circuit configuration of fault current limiter for low voltage DC system and comparative discussion about its current limiting effect," in *Rec. IEEJ Annual Meeting*, E-12, 2014.
- [5] Y. Yokomizu, T. Matsumura, Y. Taniguchi, "Direct-current breaking performance of molded-case circuit breaker and its dependence on source voltage and principal components," *Frontier of Applied Plasma Technology*, vol. 3, no. 1, pp. 5-10, Jan. 2010.

# ANALYSIS OF VEHICLE'S CRASH BASED ON STRUCTURES' SECTION FORCES

Dong, Song

Department of Mechanical Engineering, Graduate School of Engineering, UCLA  
dongsong@ucla.edu

Supervisor: Mizuno Koji

Graduate School of Engineering, Nagoya University  
kmi zuno@mech.nagoya-u.ac.jp

## ABSTRACT

This paper presents the relation between vehicle deceleration and the structure section forces in the process of frontal crash. By using a 2010 Toyota Yaris full car finite element model, the frontal crash simulation was carried out in LS-DYNA, and the results including the structures' section forces, contact forces, the deceleration of the passenger compartment, and the force changes at different initial velocities are attained. The deceleration of the passenger compartment was generated by the force transmitted to the firewall – the structural forces and the engine contact forces. These force levels were compared with impact velocities. The force paths could be evaluated by cross section forces of members. The collapse of the passenger compartment is important since it relates with survival space of occupants. A high speed impact simulation was conducted to make the passenger compartment collapse. This paper introduced a definition of the compartment collapse using the cross section force, and provided a new method of predicting the passenger compartment collapse.

**Keywords: section forces, deceleration, collapse of the passenger compartment**

## 1. Introduction

Crashworthiness is one of the most important factor for design of passenger vehicle bodies. The vehicle body structure is required to be both stiff at some parts (to prevent intrusions to the passenger compartment) and soft at other parts (to absorb the impact energy). Many researchers have studied the vehicle crashworthiness by using component tests, full-car crash tests and computer simulations [1] [2].

In this paper, crash simulations of a finite element (FE) model based on a 2010 Toyota Yaris passenger sedan without the dummy impacting a rigid wall were

conducted. The passenger compartment deceleration and the structure section forces and internal contact forces were examined at various velocities. The FE simulation provided important information describing the force transmitting paths in the process of frontal impact at various impact velocities.

The collapse of the passenger compartment is important problem in frontal impact at high speed since it relates with survival space of occupants. The definition of the passenger compartment collapse at high speed frontal impact is developed and can be used for predicting collapse. It provides the theoretical reference for the studies of the crash process and the crashworthiness design of vehicles.

## 2. Vehicle's Crash Model

The small car model used in this paper was developed through the process of reverse engineering at the National Crash Analysis Center (NCAC) of The George Washington University (GWU). It is constructed by 974,383 elements, including full functional capabilities of the suspension and steering subsystems. The car model was validated by comparing the simulation of the NCAP (New Car Assessment Program) frontal wall impact tests at 56 km/h. Figure 1 shows the comparison of the actual and FE model. [3]

Figure 2 shows the details of the model for the frame and drive train for this vehicle. The material density for the engine was defined such that the mass is similar to the one measured from the actual engine. [3]

The mass, moments of inertia, and center of gravity (CG) locations of the FE model are shown in Table 1. [3]

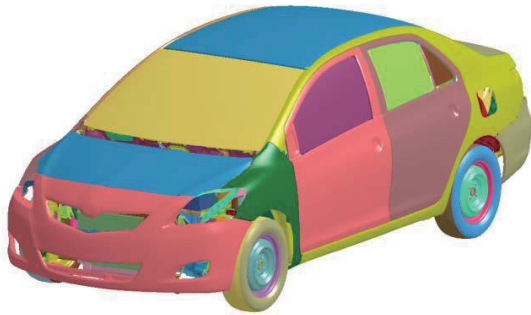


Fig. 1 – Actual and FE Model of a 2010 Toyota Yaris Sedan

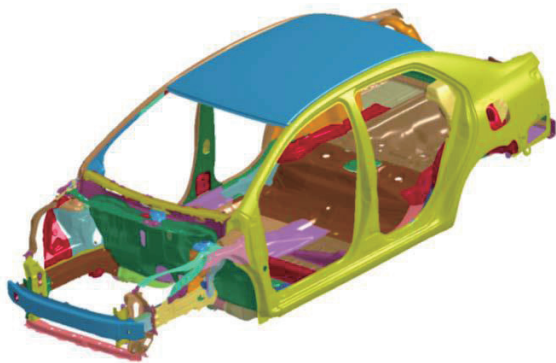


Fig. 2 – Details of the Modeled Vehicle Frame and Drive Train

Table 1– The Mass, Inertia, and CG Data of the FE Model

	FE Model
Weight, kg	1100
Weight of the Passenger Compartment, kg	830
Pitch inertia, kg-m <sup>2</sup>	1566
Yaw inertia, kg-m <sup>2</sup>	1739
Roll inertia, kg-m <sup>2</sup>	395
Vehicle CG X, mm	1004
Vehicle CG Y, mm	-4.4
Vehicle CG Z, mm	569

For this simulation, accelerometers were positioned in 7 locations (Figure 3), which are the left and right rear seats, the intersections of the B-pillars and the side sills, the engine top and bottom, and the CG of the vehicle.

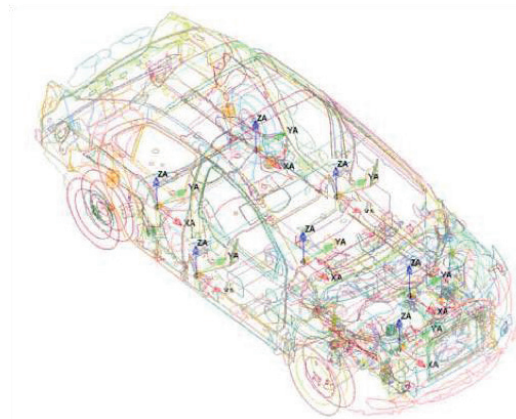


Fig. 3 – Accelerometer Locations in FE Model

### 3. The Deceleration of the Passenger Compartment and the Force paths Analysis

#### 3.1 Fundamental

In the process of the frontal crash, the collision impact from the rigid wall will start from the front frame. And then, the forces will transmit to the other parts of the vehicle along some particular paths (Figure 4) [4].

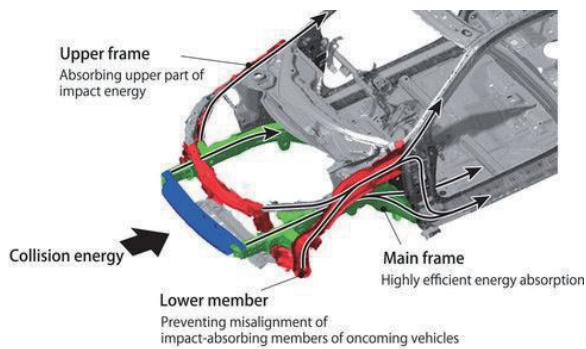


Fig. 4 – Force Transmitting Paths

In order to analyze the transmitting path of the forces, the sections such as figure 5 had been defined before calculating. Then, the section-force's changing along with the time in the main structures can be obtained from the simulation.

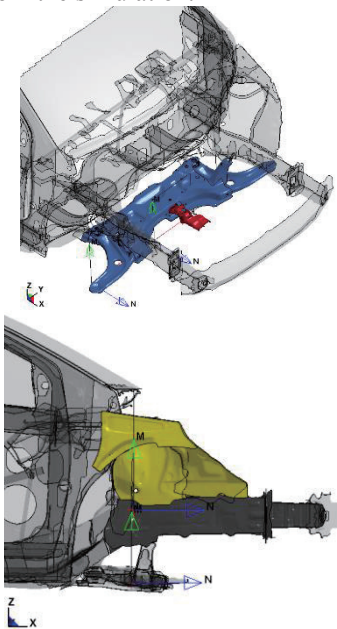


Fig. 5 – Sections Defined in the Main Structures

As the deceleration of the passenger compartment was generated by the force transmitted to the firewall – not only the structural forces, but also the engine contact forces. However, the contact forces transmitting paths from the engine to the firewall cannot be easily figured out, because the movement of the engine during the collision will be related to the initial velocity of the crash.

In order to understand the contact force paths, the frontal crash into a rigid wall of the car at about 56 km/h was simulated according to the EuroNCAP standard. Figure 6, 7 and 8 show the deformation behavior of the engine room at 40 ms. The deformation behavior of the vehicle showed that the engine started to contact with the

other parts at 40ms. The engine hit the suspension member strongly from 40ms, as well as the steering rod. And from the figure 7, the left part of the engine hit the brake booster which is in blue and brown color in the figure. Figure 9 shows schematic diagram of the transmitting paths of the contact forces to the firewall. The figure represents that the contact forces mainly come from the contact between the suspension member and the engine.

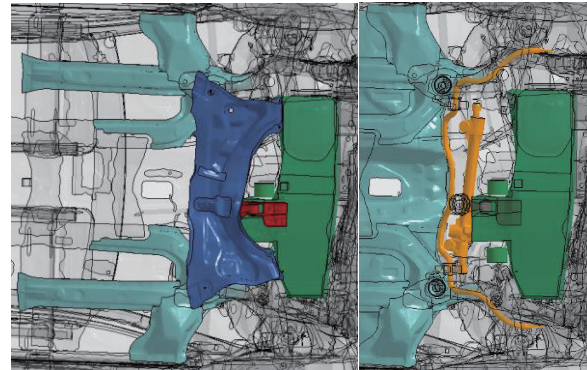


Fig. 6 – Vehicle Dynamic Simulation Result 40 ms (Bottom View)

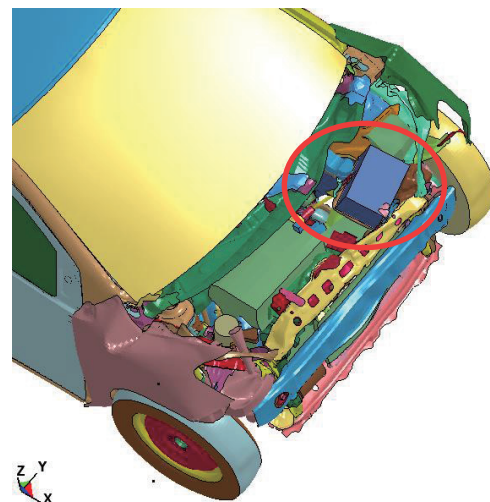


Fig. 7 – Vehicle Dynamic Simulation Result 40 ms (Top View)

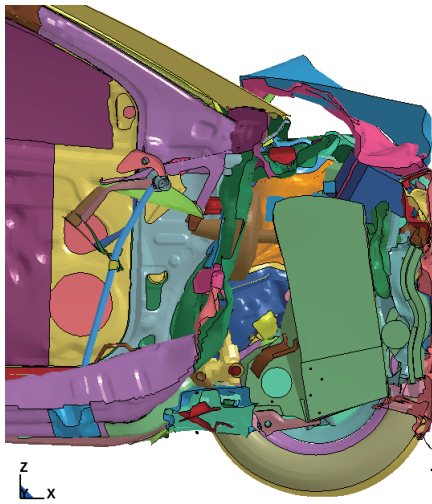


Fig. 8 – Vehicle Dynamic Simulation Result 40 ms (Section View)

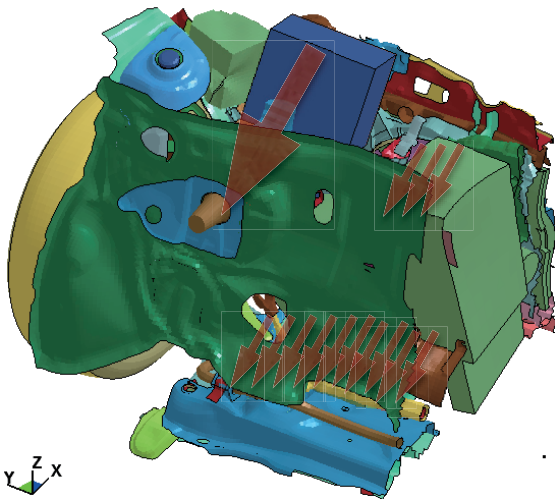


Fig. 9 – Contact Force Transmitting Paths

To understand the deceleration of the passenger compartment, the relation between the deceleration and the sum of the section forces and the contact force were examined. Designating the mass of the passenger compartment as  $m_c$ , the deceleration of the compartment

as  $a_c$ , and the sum of the section forces and the contact force to the firewall as  $F_{total} (= \Sigma F_{section} + \Sigma F_{contact})$ , the motion of equation of the passenger compartment is expressed as:

$$F_{total} = m_c a_c \quad (1)$$

Figure 11 shows the simulation results of the total force in comparison to the product of the deceleration and the mass of the passenger compartment (830 kg). The deceleration was measured by an accelerometer element located at the intersections of the B-pillars and the side sills. The total force ( $F_{total}$ ) and the inertial force ( $m_c a_c$ ) were comparable, which indicates that Eq.(1) is valid.

The main and upper frames suffered most of the forces before 30ms. At 40ms, the total force increased because of the backward strike of the engine. The forces then transmitted to the extension of the carline and also spread to the front floor and side panels as shown in figure 4. The deviations of the curves reveal the vibrations of the vehicle during the frontal crash. As shown in figure 10, the forces that influence the deceleration of the compartment were changing with the velocity. At the low velocity (30 km/h), the structural forces are the main forces, and the engine contact forces almost can be neglected. However, when the velocity is increased, the engine contact forces cannot be neglected, and even larger than the structural forces. As the contribution of the engine contact forces increasing, the deviations were build up due to the vibration of the engine. The accumulation of the deviations can be found through the next section in figure 12.

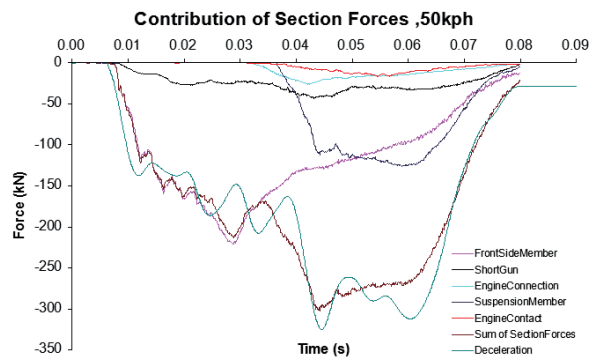
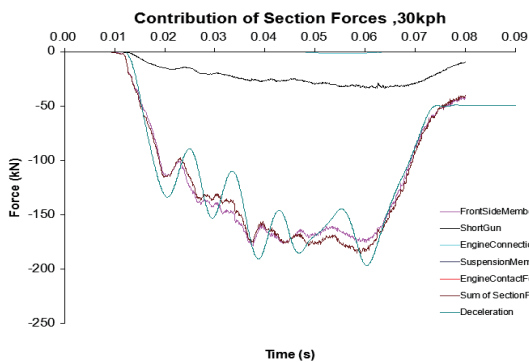


Fig. 10 – Contribution of Section Forces

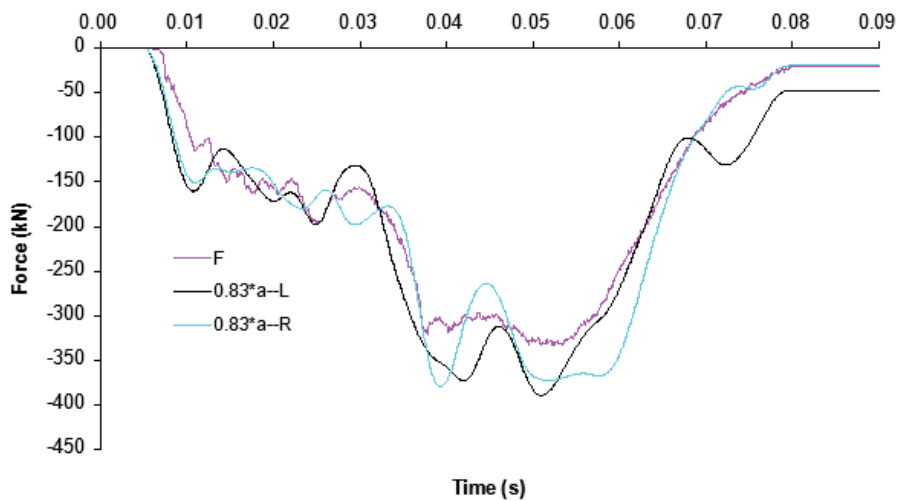


Fig. 11 – Force-Deceleration Relation ( $F_{total} = m_c a_c$ )

### 3.2 The Force Paths Associated with the Impact Velocities

As shown in the previous result (figure 11), the force and deceleration are divided into two phases at 56 km/h impact velocity. The engine hit the other parts in 30 - 40 ms. Before 30 ms, the forces are mainly structural forces, which are transmitted in the main and upper frames. After 40ms, the engine contact forces are the major force that transmitted into the firewall.

At different impact velocities, these two phases would be changed. From 20 to 50 km/h, the simulation results showed that the force transmitting paths are associated with the impact velocities. The results are shown in figure 12 (1) (2).

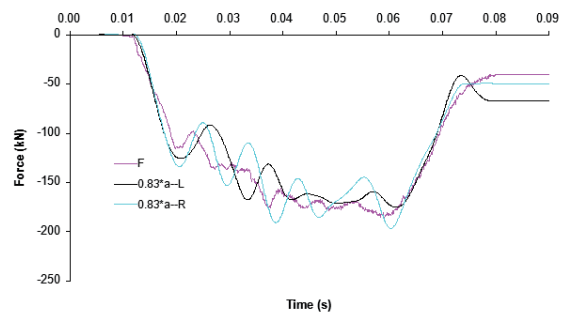
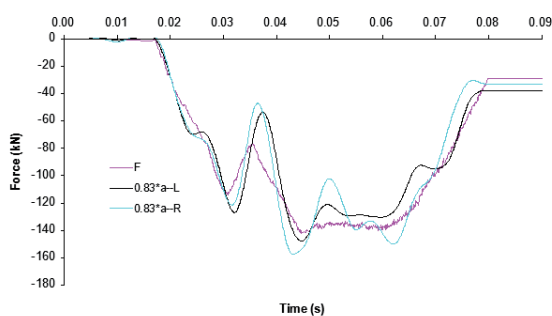


Fig. 12 – F -  $m \cdot a$  Relations at Different Velocities (1)

From the simulation results and the car deformation behavior, the engine effects were little at low velocities. At 20 or 30 km/h, the forces that transmitted to the firewall mainly were structural forces from the longitude. As the velocity increased to 40 or 50 km/h, the effects of the engine became more and more significant. The force levels at high velocities compared with low impact velocities were determined by the engine contact forces.

Compared with the result of figure 11, the engine vibrations would be increased with the velocities, which would lead to the larger deviations.

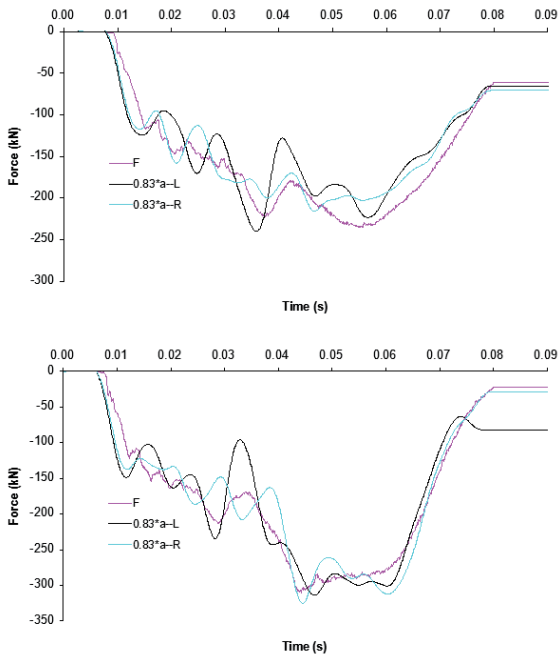


Fig. 12 – F - m\*a Relations at Different Velocities (2)

### 3.3 Passenger Compartment Collapse

The collapse of the passenger compartment is important since it relates with survival space of occupants. A high speed impact simulation was conducted to make the passenger compartment collapse. By analyzing the section forces in the side sills, we can define the collapse of the passenger compartment with these section forces changing along the displacement.

The frontal crash simulations at 50 km/h and 100 km/h were conducted as a comparison. At the high speed collision, the tires will contact with the bottom of the A-pillars and exert the axis forces and the moments to the side sills. Figure 13 shows the deformation behavior in the crash at 50 and 100 km/h at 60 ms. In the figure, at 50 km/h, the tires hit the bottom of the A-pillars slightly, however, the tires hit it strongly at 100 km/h. The side sills did not deform at 50 km/h, while they significantly deformed at 100 km/h at the rear part of the sills (figure 14).

Figure 16 shows force-displacement characteristics of the vehicle in frontal impact at 50 and 100 km/h. In order to measure the section forces at the deformation parts, the sections were set as in figure 15. The displacement of the vehicle was measured by the accelerometers located at the rear seats, which will give the displacement data behind the deformation parts. The location of the accelerometers is important because the displacement behind the deformation parts would be changed compared with the displacement of the non-deformed parts. [5]

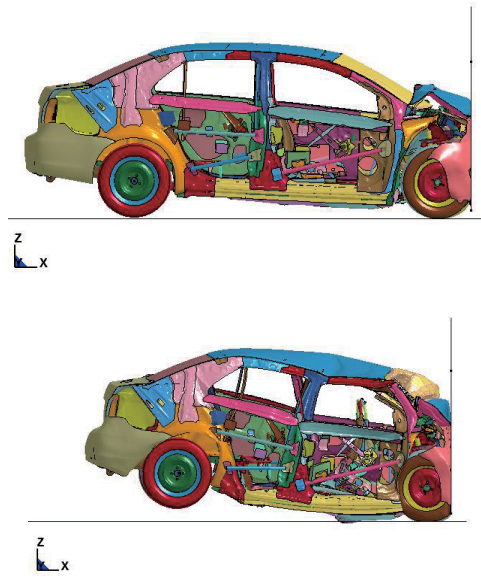


Fig. 13 – High Speed Simulations' Comparison at 50 and 100 km/h, 60ms

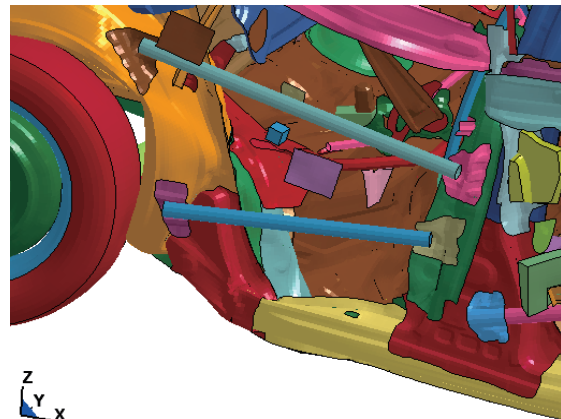


Fig. 14 – The Deformation of the Side Sill at 100 km/h

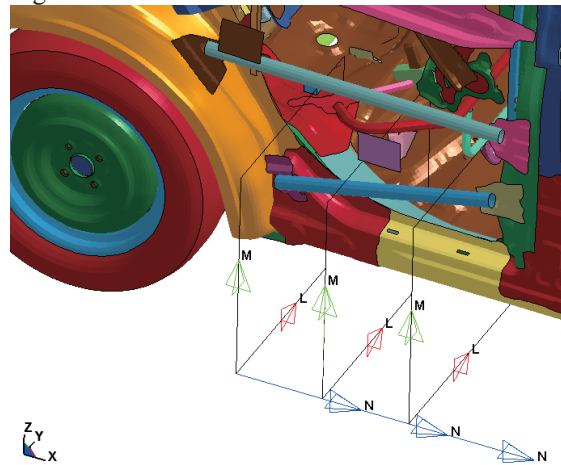


Fig. 15 – The Sections Created in the Sills



When the side sills deformed, the section forces would drop before the maximum displacement. This drop can be used to define the collapse of the passenger compartment, which means that the side sills were significantly deformed.

At 100 km/h simulation result, the section forces started to drop at around the displacement of 900 mm (figure 17). So that, the collapse of the passenger compartment was indicated by this drop before the maximum displacement around 1000 mm.

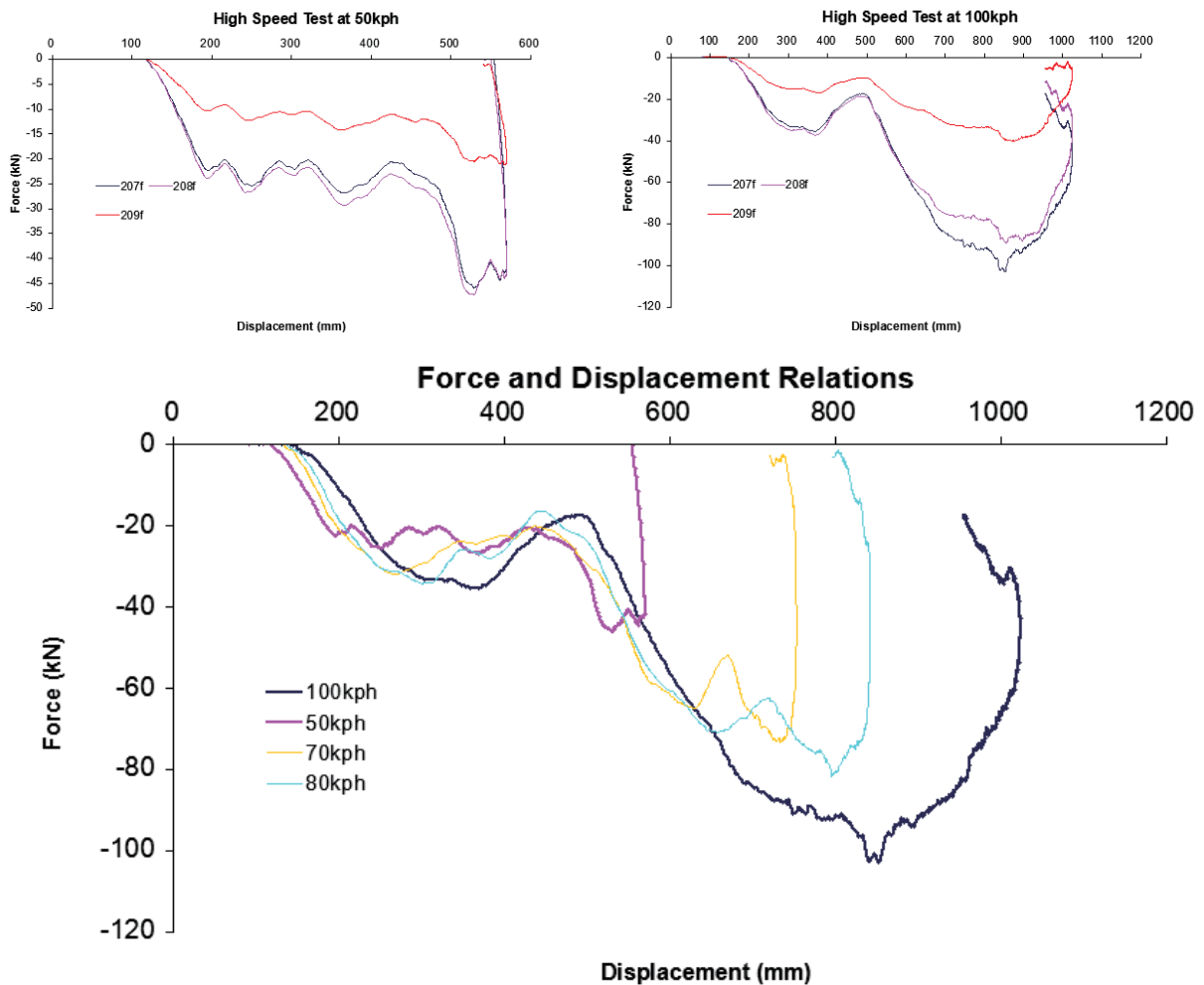


Fig. 16 – Force and Displacement Relations

#### 4. Conclusions

The vehicle deceleration and the structure section forces in the process of frontal crash were analyzed to figure out the force transmitting paths. The force levels were also compared with impact velocities. The force paths could be evaluated by cross section forces of members. The results can be used as the vehicle structure design. Furthermore, the occupant survival space during the frontal crash was determined by the collapse of the passenger compartment. The collapse can be predicted by the definition of the side sill section forces changing along the displacement. The design of the carline can be

improved according to the simulation results. All these achievements are very valuable to go on the research of the crashworthiness design of the body.

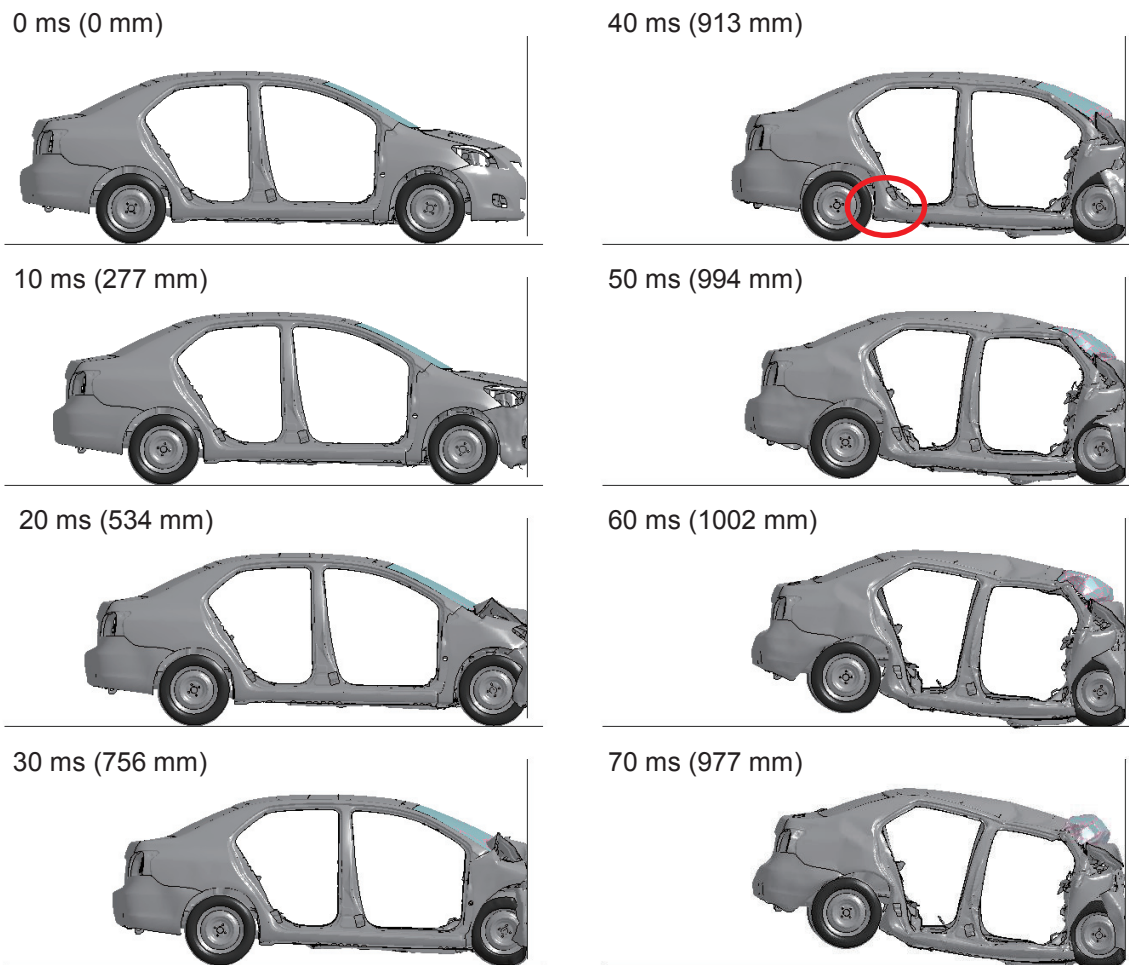


Fig. 17 Deformation behavior in frontal impact at 100 km/h

### Acknowledgments

I am using this opportunity to express my gratitude to everyone who supported me throughout this project. I am thankful for their aspiring guidance, invaluable constructive criticism and friendly advice during the project work. I am sincerely grateful to them for sharing their truthful and illuminating views on a number of issues related to the project.

I express my warm thanks to Mr. Mizuno and Mr. Ito for their support and guidance. I would also like to show gratitude to my committee, including Mr. Yamada, Ms Chen, Mr. Miyoshi, Mr. Oida, Mr. Iwanaka and Mr. Mizuguchi.

### References

- [1] Xie, S., Xu, L., Fang, K., Wu, S.R., Discussion on strain rate effects in numerical simulation of vehicle crash. SAE Technical Paper No. 2008-01-0504 (2008).
- [2] Griškevičius, P., Žiliukas, A., The crash energy absorption of the vehicle front structures. *Transport*, vol. 18 (2), pp. 97-101 (2003).
- [3] NCAC, Development & Validation of a Finite Element Model for the 2010 Toyota Yaris Passenger Sedan, NCAC Technical Summary (2011).
- [4] Ying Yang, Guangyao Zhao, Jianwei Di, Analysis of Vehicle's Frontal Crash Based on Structures' Section Forces, *IEEE*, pp. 1-4 (2006).
- [5] Aleksandra Krusper, Robert Thomson, Energy-absorbing FUPDs and their interactions with fronts of passenger cars, *International Journal of Crashworthiness*, pp. 635-647 (2010).

# MANUFACTURE AND CHARACTERIZATION OF BORON OXIDE SOLID LUBRICANT USING RADIO FREQUENCY MAGNETRON SPUTTERING AT LOW-VACUUM

Jose Eduardo Gaviria

Department of Material Science and Engineering, Graduate School of Engineering, University of California Los Angeles  
gavi6354@g.ucla.edu

Supervisor: Noritsugu Umehara

Graduate School of Engineering, Nagoya University  
ume@mech.nagoya-u.ac.jp

## ABSTRACT

Characterization of boron based coatings on silicon substrate using radio frequency (RF) magnetron sputtering onto silicon substrate. Manufacturing issues that arose through the length of the project are discussed. The possible explanation for their appearances are discussed in conjunction with the possible solutions. Initially problems with residual stresses and chemical stability of boron based coatings were observed. These issues were partly resolved by multiple applications of the boron coating. Auger electron spectroscopy and Raman spectroscopy were undertaken in order to characterize the produced coatings. Difficulties with characterization methods made it impossible to determine the exact chemical composition of the coating. Hardness of the coating was sub-par for tribological application; however, a reduction of friction coefficient was achieved in some coatings in both high and ambient temperatures. Further research could yield an alternative to diamond like carbon coatings for high temperature applications in oxidizing environments.

## 1. INTRODUCTION

The use of coatings in engineering applications is evident in most industries. Automotive industries use coatings to protect their products from corrosion. Some coatings are polymeric paints, while others are nickel electroplating used to protect parts. However, there are further applications for coatings than just corrosion prevention. Diamond like carbon (DLC) coatings, in development for use on materials to improve tribological properties, have been shown to increase the lifetime of parts with minimal difficulty of manufacture [1]. The following project tries to develop an alternative to DLC coatings for applications that are limited by the inherent nature of DLC coatings.

## 1.1 BORON COATINGS

Elemental boron has similar properties as to carbon. Like carbon, boron also displays catenation [2]. Because of this property, boron can produce structures similar to DLC [2]. The main advantage of boron based coatings over DLC coatings is due to the fact that boron doesn't readily react with ferrous materials as DLC materials do [2]. Another advantage of boron based coatings over DLC coatings is their thermal stability in oxidizing atmosphere [2, 3]. This is mainly due to the fact that carbon reacts with oxygen when exposed to temperatures over 300-400°C. Furthermore, boron has a better chemical stability than carbon [3,4]. Desired properties of coating materials are usually mechanical properties. The main two properties of main interest are hardness of the coating as well as the frictional coefficient of the material. The main types of boron that are of most interest to research are as follows:

- Boron Oxide – most common form of boron in atmosphere. Mostly amorphous and non reactive in regular atmosphere. Literature explains that there is a possibility that high pressure and humidity transform the boron oxides into boric acid, a known compound that reduces friction in liquid lubricants [3].
- Boron Nitride – This type of boron compound has both hexagonal and cubic structures. The hexagonal structure shares the same molecular structure as graphite and has the possibilities of having lubricating properties [2,3].
- Boron Carbide – Boron carbide has high hardness properties only second to diamond [2].
- Boron-Nitrogen-Carbon (BNC) – Hybrid structure of boron and carbon that has little research and could have potential properties advantageous to the application as a tribological film [2].

Boron carbide and boron nitride share the distinction of being the two hardest materials known to man behind

diamond [2-4]. As such, they are of high interest to researchers for possible application to steel tooling to increase their wear life [3]. Boron oxide may not have the high hardness of the other boron compounds; however, it has been found to be of interest due to the fact that it can be used as an additive in liquid lubricants to decrease friction [3]. Furthermore, it has been shown that it can be used as a solid lubricant as a replacement for liquid lubricants [3]. This is only done when liquid lubrication is unfeasible. An example of such an application is for low gravity environments [2, 3]. BNC is also of interest because of the little research into the material. Furthermore, the possibilities of hybrid structures that may share properties of both materials and further improve the systems it where tribological coatings are applied.

## 1.2 COATING MANUFACTURE METHOD SELECTION

The manufacture of coatings has many different manufacturing technologies in use. The technology is usually dependent on the material of choice. DLC coatings are usually made using chemical vapour deposition (CVD) methods; however, due to boron's high melting point, CVD cannot be used easily to manufacture coatings at room temperature. Therefore, another manufacturing methods need to be considered and explored. Radio frequency (RF) magnetron sputtering was selected to manufacture the boron coatings. This is mainly due to the fact that this method is a physical deposition method that doesn't require high temperature for the manufacture of high melting point materials. Further reasons for the selection of RF magnetron sputtering are as follows:

- Top-down manufacturing
- Low maintenance
- High adhesion

Furthermore, the use of RF magnetron sputtering is widespread in the semiconductor industry. Making the use of a common technology will ease the application of the boron coatings in many industries. RF magnetron sputtering also posses many distinct variables that will further help in modifying the resulting coating molecular structure and give researchers the ability to study the possibility of modifying coatings for distinct applications. For this project, the manufacturing parameters will not be a main focus of the research; however, they will be recorded in order to determine possible causal links between the manufacturing parameters and subsequent properties of the resulting film.

## 2. EXPERIMENTAL

### 2.1 MANUFACTURING

Boron based coating will be manufactured RF magnetron sputtering using a custom made rig. A picture of which can be seen as Figure 1.

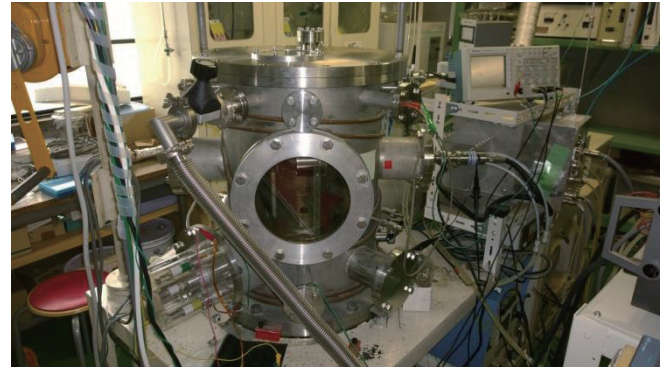


Figure 1. Custom magnetron sputtering rig with oscilloscope attached to measure voltages across the system. Voltage bias is provided by a second DC power supply. Furthermore, the chamber has two inlet lines for argon and nitrogen gas.

The custom magnetron sputtering rig uses a NRF model NR3NP-03 200V power supply. A signal modulator from NRF was also connected in series to the chamber to phase shift the signal as to maximize the plasma energy. The target will be 99.5% pure Boron target made by Kurt J. Lesker Company. The substrate for the coating will be a silicon wafer provided by industry cut into quarters using a diamond tipped pen. Table 1 outlines the manufacturing parameters used to deposit the coating onto the substrate through the length of the project.

Table 1. Table showing the different parameters of manufacture and their settings.

Parameter	
Power Supply Power (Watts)	100-200
Distance from Sputtering Target (mm)	10-30
Target Bias Voltage (Negative Volts)	0-100
Ar/N Ratio	5/1, 5/3, 1/1
Sputtering Time (minutes)	5-25

The reason for the range of parameters is due to the fact of attempting to optimize the manufacturing parameters using trial and error. In the end, the samples with coatings that were tested were mostly made using the following parameters: 200 Watt power supply setting, 30 mm sputtering distance, -5 volt target bias, and 3/5 Nitrogen to Argon gas mixture.

After manufacture, some samples showed signs of instability. Figure 2 shows a boron coating sample just removed from the chamber and after several hours after removal.

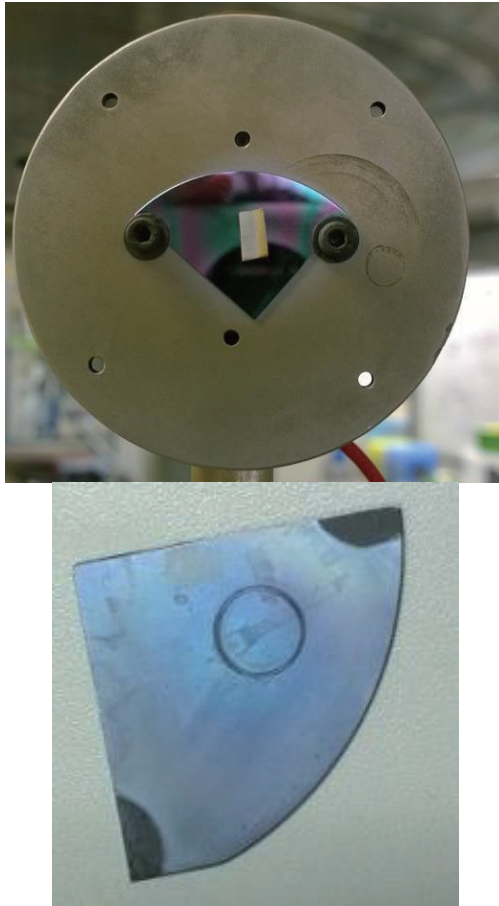


Figure 2. The top most picture show a boron coating after removal from the vacuum chamber. This sample is somewhat shiny after removal. The bottom picture is a boron coating after several hours of exposure. It is evident that there was a physical change due to the opacity of the coating.

To show if these were due to residual stresses caused by thermal expansion, a sample was made and then allowed to cool to room temperature slowly in the chamber. Decomposition of the coating was still evident after this sample was made. It then became clear that the decomposition of the coating was due to the exposure to the atmosphere. There was several changes made to the manufacture to try to resolve the issue; however, the most successful methods of reducing the rate of chemical decomposition were to grow the film by multiple layers and the addition of a carbon interlayer. Multiple layers were manufactured by stopping and starting the sputtering of the boron film while in the chamber.

## 2.2 CHARACTERIZATION

To characterize the physical properties of the coating, the following tests will be undertaken with the following equipment:

- Friction Test – Friction testing was conducted using a custom made ball on substrate rotating test. This test was conducted at room temperature and high temperature for 10 minutes and at 100 revolutions

per minute (RPM) using a silicon nitride ball as the second contacting surface.

- Annealing Test – This test was performed using an infrared lamp set to 300-350°C for 30 minutes. Pictures were taken before and after the test to show qualitatively the effect of high temperature on the coating.
- Micro-Hardness – Micro-hardness was taken on these samples to determine their hardness. This test was conducted using an Elionix ENT-1100a tester.
- Profilometer – Profilometry was taken to determine the roughness of the coating as well as to determine the coating thickness using a modified procedure. This was conducted by a Mitutoyo Surftest SV-3100.
- Raman Spectroscopy – This test was performed to determine the chemical structure of the sample.
- Optical Microscopy – Optical microscopy was done in order to see physical changes of the sample as well as to see the sample's coating.
- Auger Electron Spectroscopy (AES) – AES was undertaken in order to determine the chemical composition of the coating on manufactured substrates.

Profilometry is conducted mainly to measure the coating thickness and the curvature of the sample and coating. Curvature was measured to attempt to calculate the residual stress of the sample [5]. Raman spectroscopy was attempted on many of the samples manufactured; however, it seems that the samples had a specific molecular structure that gave the coating fluorescence [6, 7]. This fluorescence resulted in Raman spectroscopy being unable to help determine the chemical composition of some of the coatings [7, 8]. AES was also conducted; however, the results were inconclusive. This could possibly be due to calibration error or to the AES method being near the limit of detection [8].

## 3. RESULTS

### 3.1 PROFILOMETRY

Profilometry was taken of the samples in the course of the project. This was conducted on some of the samples manufactured to determine the thickness of the coating. This was accomplished by protecting an area of the substrate from coating and measuring the difference of the step of the substrate to the top of the coating.

Table 2. Average measured thickness of coatings based on sputtering time and applied power to the RF magnetron sputterer and differing Ar/N ratio.

Sputtering Time (min)	Average Thickness (μm)	STDEV	Applied Power (W)
25	1.80675	0.322426	200
25	1.4535	0.282867	200
25	2.479625	1.35224	200

Furthermore, some sample substrates' curvature profile was taken for the use to determine the residual stresses of the coating [5]. This was done by using a fifth-order polynomial fit. This due to the fact that the first integral of the polynomial fit represents the deflection of a uniformly loaded beam [5]. The use of the deflection value can be plugged, along with other parameters, into an equation that can be used to calculate the residual stress in the coating.

$$\sigma = \delta/r^2 * E/3(1 - \nu) * d_s^2/d_f \quad (1)$$

Where  $\delta$  is wafer deflection in cm,  $r$  is radius of the profilometry scan in cm,  $E$  is the young's modulus of the substrate,  $\nu$  is the Poisson coefficient of the substrate,  $d_s$  is the thickness of the substrate and  $d_f$  is the thickness of the film. With  $\sigma$  equalling the residual stress found in the coating using equation (1). An example of a surface profile and the polynomial fit can be seen as Figure 3.

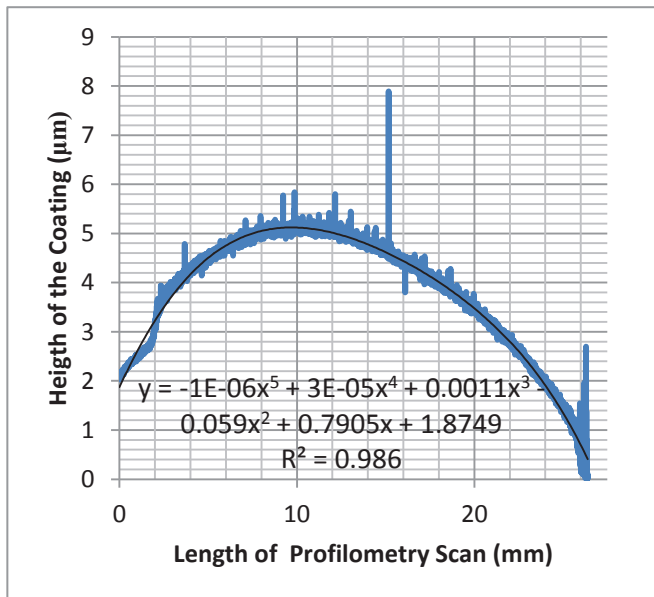


Figure 3. Full profilometry scan of the coated surface of a silicon sample. A fifth order polynomial fit is calculated and the equation is displayed on the graph area with an R value of 0.986.

From these profilometry profiles taken and the polynomial fits gathered, residual stresses were calculated for some of the coating systems. Table 3 shows the

deflection of the coatings before and after coating as well as the calculated residual stresses.

Table 3. Calculated deflection from the first integral taken from the surface profile of various samples. These profiles are taken before and after coating in order to calculate the residual stress found in the coating.

Coating System	Deflection of Substrate (μm) X/Y	Deflection of Coating (μm) X/Y	Calculated Residual Stresses (MPa) X/Y
Bi-layer application of boron film	3.18458 44.9837	-9.83636 -38.1061	-5.312185357 -13.15258943
Tri-layer application of boron film	217.647 247.693	44.9474 15.8539	-0.730689693 -7.639383222
Bi-layer application of boron film with carbon interlayer	135.4 66.732	-29.613 -15.7694	-8.283334112 -5.142000619

Negative numbers in residual stresses means a compressive residual stress. Positive deflection of the substrate means a tensile residual stress.

### 3.2 MICRO-HARDNESS

Micro-hardness testing was undertaken to determine the hardness and strength. This was conducted on mostly the last samples using bi-layer solution to the issue with the physical change in the coating. Furthermore, the micro-hardness test curve shows that there are several layers of the coating. This can be seen by multiple layers breaking and seen by the flattening of the curve. This is due to the fact that the diamond tip is not loaded due to the material breaking until finding the next hard layer. Figure 3 shows a clear loading graph that shows the breaking of the different layers in the coating.

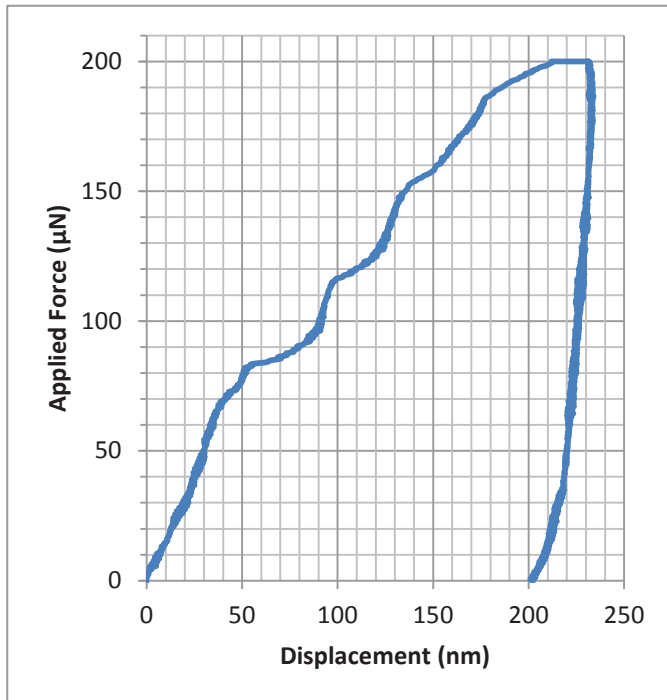


Figure 4. Load versus displacement graph of the micro-hardness test conducted. This graph is interesting due to the several steps evident in the graph. These steps show the multi-layer application of the coating and how they affect the strength of the coating.

From all the different compositions' micro-hardness testing, an average hardness was calculated. Table 4 shows a summary of the hardness of the coatings.

Table 4. Micro-hardness resulting hardness from the different samples. It is evident that the calculated hardness numbers are not very reliable due to the high standard of deviation. Furthermore, the calculated hardness values are low in comparison to other tribological coatings [3, 9]. This points to the coatings very high wear rate [9].

Sample Composition	Calculated Hardness (MPa)	STDEV
Bi-layer application of boron film	1151.815385	297.0653
Bi-layer application of boron film with carbon interlayer	615.24	124.999

Large standards of deviation can be attributed to the variance on density of coating due to the low packing of the coating. None of these coatings generated have higher hardness than DLC coatings [3]. This is probably due to the low density of the coating. Probable increasing of the density of the coating would probably lead to higher hardness more in line with boron compounds and closer to the DLC hardness.

### 3.3 CHEMICAL CHARACTERIZATION

Chemical characterization of the coating was conducted by two different methods. Initially Raman spectroscopy was conducted on a range of samples that were initially manufactured using the magnetron sputtering method. However, there seems to be a fluorescence effect that may be due to the molecular structure of the coating [6, 8]. Because Raman spectroscopy is not the method to easily determine the molecular structure of the material such as electron diffraction or x-ray diffraction. Figure 5 shows an example of both a correct Raman spectrum and a spectrum that shows fluorescence in the sample.

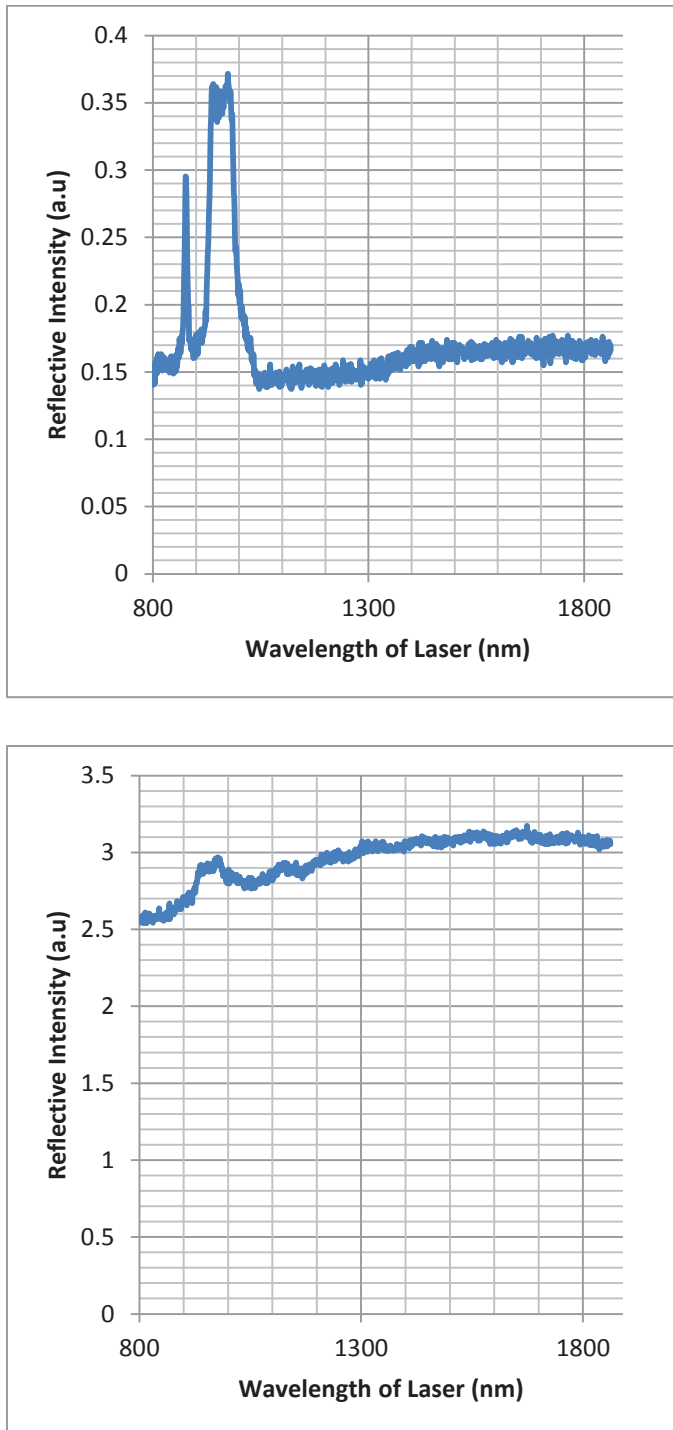


Figure 5. The top most graph is the Raman spectra of one of the boron coatings made during the course of project. In the spectra, the secondary silicon peak around 950 nm is evident; furthermore, there is another peak around 870 nm that corresponds with boron oxide compound. The bottom graph is a spectrum of another boron coating. This spectrum has no useful information and nothing can be done to improve the spectra.

Because of the failure of the Raman spectroscopy to help us determine with a high degree of certainty what the chemical composition of the coating, AES was undertaken

on a selected sample. AES also had issues in determining the chemical composition of the sample. This is seen by the spectra of the AES having wide peak or non-corresponding peaks to the elements that might be present in the coating. This might be due to the equipment not properly calibrated or the elements that need to be detect being at the limit of detection of the machine. Figure 6 shows one of the faulty AES spectra.

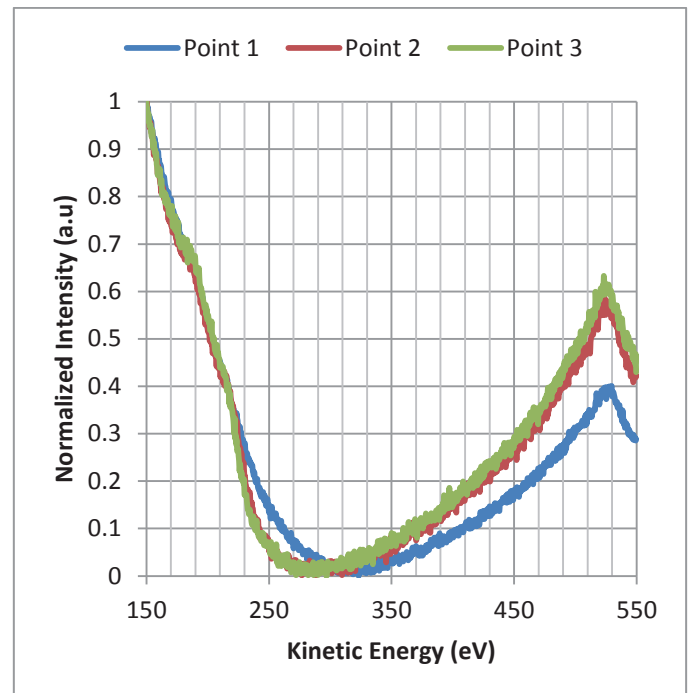


Figure 6. Auger electron spectroscopy spectrum of a boron oxide coating. In the spectrum, it is evident that the peaks of the spectrum are too wide and difficult to use to determine the chemical composition of the coating. The peak around 520 eV is most likely corresponding with oxygen [8]. The peak at the beginning of spectrum doesn't correspond with an element present in the chamber during sputtering. There are three different spectra of three points of the same sample showing that the spectra is not an operator error and is repeatable.

### 3.4 FRICTION TEST

Friction test was conducted using a custom rig. A single test was conducted on each sample. Each sample test was only conducted once on each sample unless a high temperature friction test was performed on the same sample. These tests were conducted for 10 minutes at a 100 RPM with a 0.5N load on the ball. Figure 7 shows a profile of the friction coefficient of the friction test.



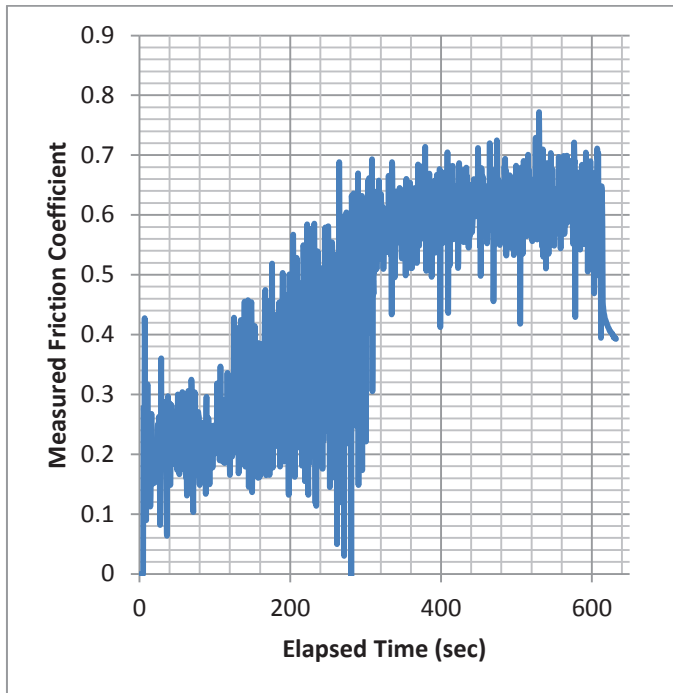


Figure 7. Friction test of the boron-carbon bi-layer coating at room temperature. The friction coefficient fluctuates around two different averages. The first average friction coefficient is most likely the friction coefficient of the material. The second friction coefficient is most likely due to the debris from the coating.

For the different friction test, Table 6 shows the resulting average friction coefficient calculated from the data of the tests conducted.

Table 6. Several average friction coefficient of different coating compositions as well as the substrate for comparison. The boron carbon friction coefficient is the lowest; however, it is not stable and the coating has a small amount of thermal instability.

Sample Composition	Average Friction Coefficient	STDEV	High Temp (Y/N)
Boron/Carbon	0.377793443	0.013399267	N
Silicon	0.448360286	0.024986064	N
Boron/Carbon Bi-layer	0.252241451	0.07682761	N
Boron Bi-layer	0.457073479	0.057005396	N
Boron Tri-layer	0.535857676	0.114671187	N
Carbon	0.228873881	0.012164858	N
Boron/Carbon Bi-layer	0.1689904	0.099322597	Y

#### 4. CONCLUSION AND DISCUSSION

After the length of the project, the following information was determined from the results of the tests conducted. Firstly, manufacture of boron nitrates is difficult using RF magnetron sputtering without using a boron nitrate target. Second, the control of the boron film is highly dependent on the control of the deposition conditions within the chamber [2, 4]. A high standard on the control of the chamber is a necessity when using low-vacuum pressure to make sure that the control of the elemental composition is maintained. This is mainly due to the belief that the bi-layer system is helpful to the chemical stability and residual stress of the coating due to the fact that the residual stresses are lower due to the smaller layers formed by sopping and starting the sputtering [10].

Third, the use of multiple layer applications can help reduce the residual stress found in the coating [10]. This is possibly due to the added impurities creating a better surface for growth of the film material. Fourth, the thermal stability of the boron coating is there; however, there seems to be some issues that might have to do to oxidation or oxygen release of the coating. Further work into reducing the oxygen content could help solve this issue. Furthermore, the use of coatings of boron nitride might be better options for high temperature applications in atmosphere. Lastly, the high temperature friction test taken of the Boron-Carbon coating shows that there is still a reduction of friction coefficient; furthermore, the coating was still stable after 30 minutes of exposure to the high temperature unlike other boron coatings manufacture during the length of the project and unlike carbon coatings in high temperature in an oxygen containing atmosphere.

After all the results are taken into consideration, it is evident that the possibilities for boron film application for high temperature are possible. The technology is still young and further improvements in the technology are necessary for actual implementations in tribological applications. Further improvement in manufacturing films as well as determining the fundamental molecular structure will help determine the desired properties and the corresponding molecular structure that correspond with desired material properties necessary for the maturity of the technology.

#### ACKNOWLEDGEMENTS

Special thanks to Dr. Albert Lukas, Deng Xingrui, K. Ichimura, and S. Senda in Professor Umehara's laboratory for advice and guidance thought the length of the project. Thank you to the JUACEP program at Nagoya University and JASSO grant that funded the research and exchange program.

#### REFERENCES

- [1] Erdemir, A., & Donnet, C. (2006). Tribology of diamond-like carbon films: recent progress and future prospects. *Journal of Physics D: Applied Physics*, 39(18), R311.

- [2] Zhou, Z. F., Bello, I., Lei, M. K., Li, K. Y., Lee, C. S., & Lee, S. T. (2000). Synthesis and characterization of boron carbon nitride films by radio frequency magnetron sputtering. *Surface and Coatings Technology*, 128, 334-340.
- [3] Donnet, C., & Erdemir, A. (2004). Solid lubricant coatings: recent developments and future trends. *Tribology Letters*, 17(3), 389-397.
- [4] Cofer, C. G., & Economy, J. (1995). Oxidative and hydrolytic stability of boron nitride—a new approach to improving the oxidation resistance of carbonaceous structures. *Carbon*, 33(4), 389-395.
- [5] Thomas, M. E., Hartnett, M. P., & McKay, J. E. (1988). The use of surface profilometers for the measurement of wafer curvature. *Journal of Vacuum Science & Technology A*, 6(4), 2570-2571.
- [6] Kubota, Y., Tanaka, S., Funabiki, K., & Matsui, M. (2012). Synthesis and fluorescence properties of thiazole–boron complexes bearing a  $\beta$ -ketoiminate ligand. *Organic letters*, 14(17), 4682-4685.
- [7] Shreve, A. P., Cherepy, N. J., & Mathies, R. A. (1992). Effective rejection of fluorescence interference in Raman spectroscopy using a shifted excitation difference technique. *Applied spectroscopy*, 46(4), 707-711.
- [8] Trehan, R., Lifshitz, Y., & Rabalais, J. W. (1990). Auger and x-ray electron spectroscopy studies of hBN, cBN, and N<sup>+</sup> 2 ion irradiation of boron and boron nitride. *Journal of Vacuum Science & Technology A*, 8(6), 4026-4032.
- [9] Marino, M. J., Hsiao, E., Chen, Y., Eryilmaz, O. L., Erdemir, A., & Kim, S. H. (2011). Understanding run-in behavior of diamond-like carbon friction and preventing diamond-like carbon wear in humid air. *Langmuir*, 27(20), 12702-12708.
- [10] Kemi, H., Sasaki, C., Kitamura, M., Satomi, N., Ueda, Y., & Nishikawa, M. (1999). Internal stress induced in the process of boron coating. *Journal of nuclear materials*, 266, 1108-1112.

# BONDING IN CHIP FABRICATION FOR CELL STIFFNESS MEASUREMENT

Zihe He, Hirotaka Sugiura

Department of Mechanical Engineering, Graduate School of Engineering, UCLA  
martinhe@g.ucla.edu

Supervisor: Fumihito Arai

Graduate School of Engineering, Nagoya University  
arai@mech.nagoya-u.ac.jp

## ABSTRACT

To measure the stiffness of cells, it is necessary to build a microchip that is able to keep one cell at fixed position and apply force to it. That is the function of the chip we are building now. During fabrication of the chip, bonding between glass layers and wafer has been a problem and we tried different intermediate layers to fix it. Though there are many kinds of bonding, mostly we focus on anodic bonding because that's the easiest method and applicable to our purpose. The intermediate layers we tried include chromium, aluminium and copper. In the end, we did bonding successfully with copper intermediate layer, which is not used very often.

## INTRODUCTION

Cell stiffness can help identify disease cells and sort them out. A number of pathophysiological states of individual cells result in drastic changes in stiffness in comparison with healthy counterparts. Mechanical stiffness has been utilized to identify abnormal cell populations in detecting cancer and identifying infectious disease. For example, several studies have shown a reduction in cell stiffness with increasing metastatic efficiency in human cancer cell

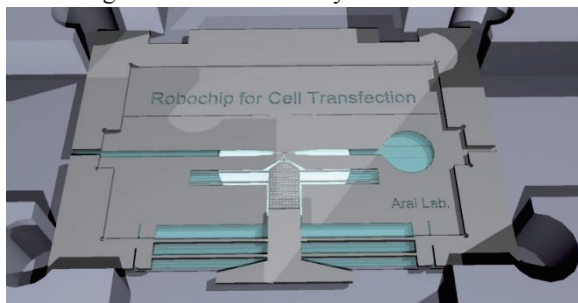


Fig 1. CAD image of chip (Former version)

Figure 1 shows former version of the microfluidic chip we need to fabricate. Current version of the chip has some modification from the former version, but function and working theory are the same. Cells will be conveyed through the central channel and compressed by the outer probe. The outer probe is

driven by a piezoelectric actuator (Fig 3). By observing the deformation of cell and force applied by the actuator, we can get stiffness of the cell with hertzian contact theory (Fig 4). As for structure of the chip, it has three layers: Cover glass layer, device layer and holding glass layer. To make the chip able to do cell stiffness measurement, we need to etch certain patterns on both glass layers and the SOI (Silicon on Insulator) device layer, and the processing of three layers consists of several main steps: mask design, photolithography, etching and sputtering. The final step to attach the three layers together is bonding. Flow chart of fabrication of the chip is shown in fig 2.

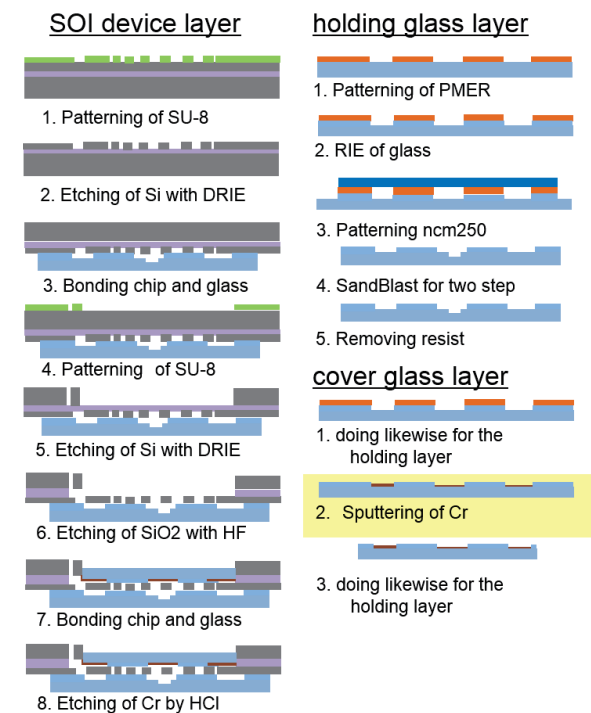


Fig 2. Flowchart of Chip Fabrication

Bonding process is very important in chip fabrication because it determines hermeticity of the chip. If the device layer is not sealed very well, there could be severe problem like leakage when cells are

pushed through the channel. Also, the clearance of packaging is supposed to so accurate that the probe can move freely while other parts are fixed.

Since we had much trouble bonding the three layers, special attention is desired on this issue. There are three most common methods of bonding: fusion bonding, anodic bonding and eutectic bonding. In these three kinds, fusion bonding or direct bonding, is usually used in the bonding of Pyrex glass and silicon. Also, pre-treatment is required to make the attachment surface so smooth that Si-O-Si bonding can form. Theory of anodic bonding is to apply high voltage and temperature to generate electrostatic force and attach glass layer, intermediate layer and silicon layer. Eutectic bonding is even more complicated but the requirement in vacuum and temperature is less strict. In the experiment, we need metallic intermediate layer to perform as circuit, so anodic bonding is the most feasible method.

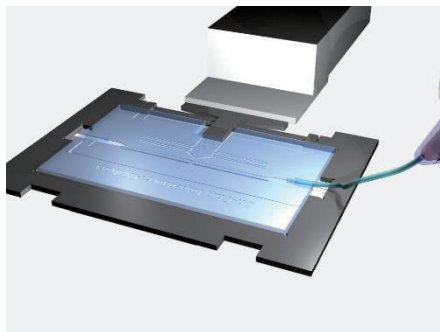


Fig 3. Piezoelectric Actuator & Cell Injection Device

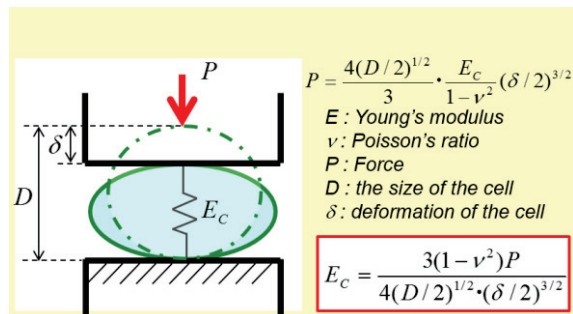


Fig 4. Hertzian contact theory

## SPUTTERING

Sputtering is a very important step before bonding. Since a metallic intermediate layer is applied to contact surface between cover glass layer and wafer, we need some method to deposit thin metal layer on cover glass. Two methods available are CVD (chemical vapor deposition) and PVD (physical vapor deposition). Compared to chemical vapour deposition, PVD can generate smoother and thinner film, so we used PVD to apply metallic film to cover

glass. PVD includes several methods: Thermal Evaporation, E-beam Evaporation and sputtering. Among these three methods, thermal evaporation is easy but the film deposited has low uniformity and reliability. E-beam evaporation is able to address more kinds of evaporant but requires high temperature. Sputtering is more reliable than thermal evaporation and costs less than E-beam evaporation. We don't need to deal with metal rarely used so sputtering is enough in our case. Comparison among thermal evaporation, E-beam evaporation and sputtering are shown in the two charts below.

Deposition	Material	Typical Evaporant	Impurity	Deposition Rate	Temperature Range	Cost
Thermal	Metal or low melt-point materials	Au, Ag, Al, Cr, Sn, Sb, Ge, In, Mg, Ga, CdS, PbS, CdSe, NaCl, KCl, AgCl, MgF <sub>2</sub> , CaF <sub>2</sub> , PbCl <sub>2</sub>	High	1 ~ 20 A/s	~ 1800 °C	Low
E-Beam	Both metal and dielectrics	Everything above, plus: Ni, Pt, Ir, Rh, Ti, V, Zr, W, Ta, Mo, Al <sub>2</sub> O <sub>3</sub> , SiO <sub>2</sub> , SiO <sub>2</sub> , SnO <sub>2</sub> , TiO <sub>2</sub> , ZrO <sub>2</sub>	Low	10 ~ 100 A/s	~ 3000 °C	High

Table 1. Features of Thermal and E-beam [2]

Evaporation	Sputtering
Low energy atoms (~ 0.1 eV)	High energy atoms / ions (1 ~ 10 eV)
High Vacuum	Low Vacuum
• directional, good for lift-off	• poor directionality, better step coverage
• lower impurity	• gas atom implanted in the film
Point Source	Parallel Plate Source
• poor uniformity	• better uniformity
Component Evaporate at Different Rate	All Component Sputtered with Similar Rate
• poor stoichiometry	• maintain stoichiometry

Nonconformal, Line of sight process

Conformality Depends on Plasma Conditions

Table 2. Features of Evaporation and Sputtering [2]

Basic theory of sputtering is shown below. Though there are different types of sputtering, the fundamental concept of these kinds are the same.

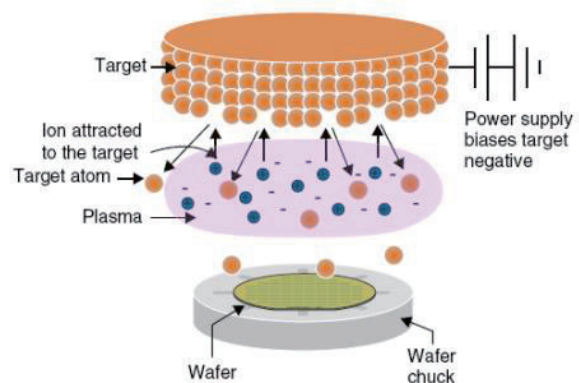


Fig 5. Basic Theory of Sputtering [2]

Sputtering is technique used to deposit thin films of a material onto a surface (a.k.a. "substrate"). By first creating a gaseous plasma and then accelerating the ions from this plasma into some source material (a.k.a. "target"), the source material is eroded by the arriving ions via energy transfer and is ejected in the form of neutral particles - either individual atoms, clusters of atoms or molecules. As these neutral particles are ejected they will travel in a straight line unless they come into contact with something - other particles or a nearby surface. If a "substrate" such as a Si wafer is placed in the path of these ejected particles it will be coated by a thin film of the source material.[3]

The two sputtering systems we used in the chip fabrication are both magnetron sputtering system. Fig 6 and fig 7 display the RF confocal sputtering system we used. A sputtering system configuration where multiple magnetron sputtering sources are arranged in a specific circular pattern and are aimed at a common focal point. When a substrate is placed in the vicinity of this focal point and rotated on its own axis, it is possible to deposit highly uniform single layers, multi-layers and co-deposited alloy films. [3]

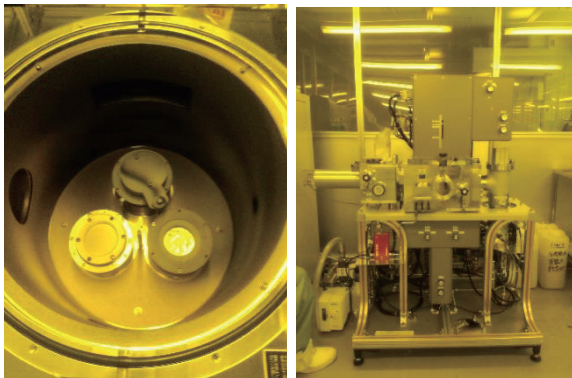


Fig 6 & Fig 7. RF confocal Sputtering System

However, unfortunately, this confocal sputtering system didn't work very well due to some unknown reason. We tried sputtering aluminium and copper onto two pieces of cover glass, but the results we got turned out not to be very stable. First we sputtered copper on the glass, and the copper films we got on the three pieces glass were uneven or not uniform. Then we changed the copper target into aluminium target. We did sputtering with aluminium target twice, one time the aluminium film came out fine while the other time with some cloudy ring as shown in fig 8.



Fig 8. Cloudy ring of aluminium sputtering

The possible reason for getting this cloudy or mossy ring is that we were probably getting a columnar morphology, which gives a "mossy" white or grey appearance. The columnar structure develops when the film is deposited on a grainy (not smooth) surface or when the film thickness exceeds several hundred nanometers (and there is no concurrent bombardment during deposition) [4].

Bonding of these two pieces of cover glass with aluminium sputtered to the wafer had various problems and was a failure. Then we continued with copper sputtering using another sputtering device, the DC magnetron sputtering system (Fig 9 & Fig 10).

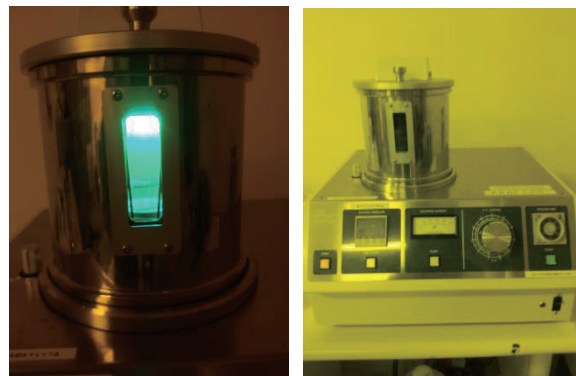


Fig 9 & 10. DC magnetron sputtering system (left), sputtering in process (right)

This DC magnetron sputtering system is direct sputtering system. A sputtering system configuration where the substrate is positioned or moving directly in front of and parallel to the magnetron sputtering source targets. As a rule, target diameters (or "lengths" as in the case of rectangular magnetron sputtering sources) should be about 20% to 30% larger than the substrate to achieve reasonable uniformity. For example a 100 mm wafer would require a 150 mm sputter target to achieve +/- 5% deposition uniformity. Although this configuration is much less flexible and generally more expensive than con-focal sputtering, it has its place in production applications which require maximum deposition rates (semiconductor wafer metallization), applications which utilize large substrates (e.g. flat panel displays) and a few techniques that demand "line-of-sight deposition" (e.g. "lift-off") [3]. Compared to confocal sputtering system, this direct sputtering system can handle only one sample one time, but the processing was much faster than

confocal sputtering system. While it took 30 min to process the three samples for confocal sputtering system, it took about 10 min to process one sample in direct sputtering system.

Luckily, the result we got was very good. As shown in figure 11, the film on the cover glass layer was shiny and uniform, which is acceptable in further bonding process.

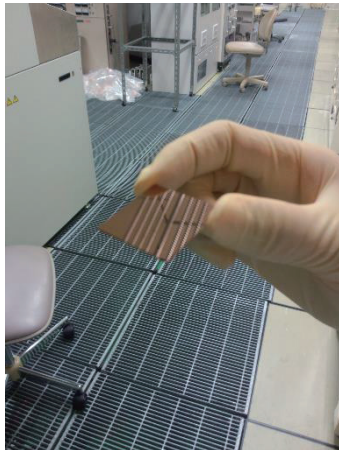


Fig 11. Cover glass with copper sputtered

## BONDING

As mentioned in the introduction part, usually there are three bonding methods. Fusion bonding or direct bonding works for Si to glass bonding, but not a good choice for bonding with intermediate layer. Eutectic bonding, also referred to as eutectic soldering, describes a wafer bonding technique with an intermediate metal layer that can produce eutectic system. Those eutectic metals are alloys that transform directly from solid to liquid state, or vice versa from liquid to solid state, at a specific composition and temperature without passing a two-phase equilibrium, i.e. liquid and solid state. The fact that the eutectic temperature can be much lower than the melting temperature of the two or more pure elements can be important in eutectic bonding. [5] Though eutectic bonding is an option, it's hard to control the ratio of different metal in eutectic alloy to achieve eutectic temperature. Compared with these two methods, anodic bonding is qualified for the goal we need to achieve and the device for anodic bonding is easy to operate.

Fig 12 and Fig 13 show the system we used for anodic bonding. Fig 14 shows concept of bonding between silicon and glass. At an elevated temperature,  $\text{Na}^+$  ions in the glass become so mobile that they are attracted toward the cathode as a result of the applied voltage. This leaves behind relatively immobile oxygen anions at the glass side of the Si-glass interface, at which a space charge region is

formed. This in turn creates an equivalent positive charge (image charge) on the Si side of the Si-glass interface (as illustrated in Fig. 13), resulting in a high electric field (magnitude of up to  $10^6 \text{ V cm}^{-1}$ ) across the Si-glass interface. Under the high electric field, oxygen anions are drifted away from the  $\text{Na}^+$  depletion region to the Si surface. As this happens, oxidation of Si by the oxygen anions is presumed to occur and a thin oxide layer is formed at the interface, which contributes to the migration of the bonding front[6].

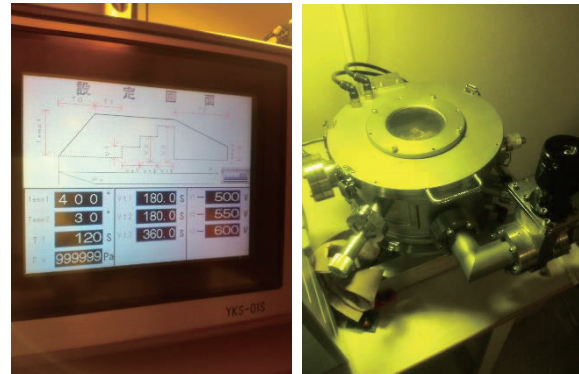


Fig 12 & Fig 13. Applied voltage and corresponding time in bonding (left), chamber of bonding system (right)

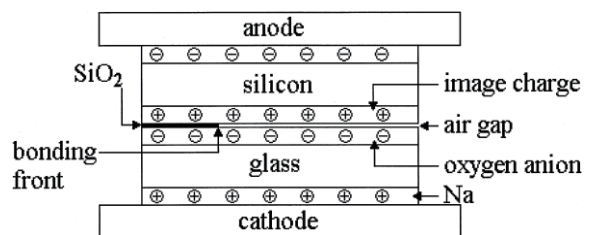


Fig 14. Diagram of anodic bonding [6]

Bonding between holding glass layer and wafer is simply anodic bonding between silicon and glass because there is no intermediate layer. However, the metallic layer between cover glass layer and wafer can cause some problems.

Before we start anodic bonding, some pretreatment of both cover glass layer and wafer is necessary. First we used CUTE low pressure plasma system to remove organic contaminants on the surfaces. Next we put the glass layer and chip into supersonic cleaning system to do further cleaning (Fig 14 & Fig 15). When the chip and cover glass are dry, they are ready for bonding.



Fig 14 & Fig 15. CUTE low pressure plasma system (left), supersonic cleaning system (right)

For the first time we used cover glass with smooth chromium and aluminum layers (Fig 16). The bonding was successful but there was contamination inside the cover glass as shown in Fig 17 which could not be removed easily. That contamination could be the combination of diffused aluminum and oxygen anions, aka aluminum oxide. We also tried using the cover glass in Fig 8 with mossy aluminum layer, but it could not be bonded to the wafer at all.

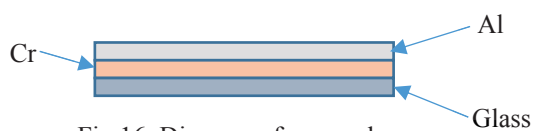


Fig 16. Diagram of cover glass

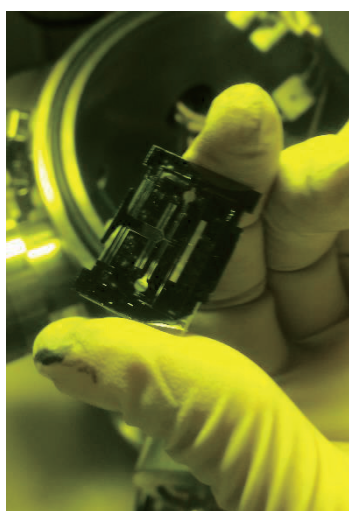


Fig 17. Bonding with aluminium intermediate layer

Actually, diffusion of aluminium and contamination in the cover glass should not have happened because chromium is not only the adhesive but also diffusion barrier. Chromium has excellent adhesion to many materials because of its reactivity. Its affinity for oxygen forms a thin stable oxide coat which prevents further oxidation and provides inertness to corrosive environment. Chromium early popularity in thin films was due to its ease of deposition by sublimation in less than perfect evaporators, while retaining good adhesion [7]. In this case, one possible reason of diffusion would be that the chromium layer is not thick enough to stop diffusion. However, it can't be too thick because chromium layer thicker than 300nm can cause some side effect due to high stress.

For the second time, we used cover glass with copper. The whole bonding process cost 30 mins, and the result was very satisfactory. Some organic contaminant got extracted on the surface of cover glass, but they could be easily cleaned with piranha solution. Ratio of  $H_2SO_4$  and  $H_2O_2$  in the piranha solution we used was 1:1. Finally the chip we got is shown in Fig 18.

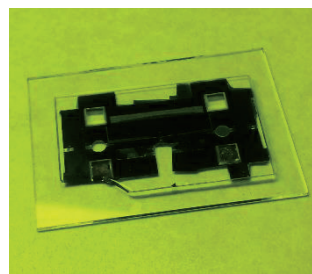


Fig 18. Chip with copper intermediate layer

The bonding was successful, but, unfortunately, due to uneven force on the chip, one corner of the chip was broken. Thus, we could not continue the following experiment with this chip.

## CONCLUSION

On one hand, anodic bonding with copper intermediate layer was a success but more consideration is desired in the process. First, we didn't pay enough attention to the diffusion. After anodic bonding, the cover glass got dirty and contaminant showed up on top of cover glass. Though piranha solution could clean the contaminant completely, where the contaminant was from remained unknown. Also, there could be diffusion of copper into the wafer that we didn't notice. Some researchers did wafer to wafer bonding with copper intermediate layer. Cu diffusion in silicon and silicon dioxide is a known problem and the diffusion is enhanced at high temperature. During Cu thermo-compression bonding, temperature in the range of 300-400 °C is applied. It is hence important to ensure that Cu does not diffuse into the surrounding oxide layers during bonding and annealing [8]. They used Ta as diffusion barrier and worked out fine. In anodic bonding we did, the temperature applied was 400 °C, so diffusion might have happened.

On the other hand, though bonding with chromium and aluminium films was a failure, we can still correct the combination and make bonding work. For example, TiN is a good diffusion barrier which can take the place of Chromium. Due to its thermal stability and low electrical resistivity, TiN is widely used in the microelectronics industry as a diffusion barrier material for Al interconnects in ultra large-scale integrated devices (ULSI). TiN prevents Al

atoms from diffusing into either dielectric materials or into Si substrates. At high temperatures, Al atoms diffusing into TiN films contact oxygen (O), which is present as an impurity, and form aluminum oxides, such as Al<sub>2</sub>O<sub>3</sub>, in the grain boundaries of TiN columnar structures [8]. Aluminum oxides should be able to refrain Al atoms from diffusing into the glass.

In fact, other methods of bonding are still worth investigation. We used anodic bonding basically because it's fast and easy compared to other kinds. There is no evidence saying that eutectic bonding could not work, and researchers have found wafer to wafer bonding with copper bonding layer possible in thermo-compression bonding. Though eutectic bonding and thermo-compression bonding are more complicated, they are still worth a try if we can find solutions to our problem.

Usually it takes 30mins to finish the anodic bonding process in our past experience. According to some research, we can reduce the duration of bonding by change doping of the wafer. In the experiment, we used n-type wafer. As shown in table 3, if we change the doping from n-type to p-type, the bonding time can be reduced dramatically, which can definitely accelerate our research. This is a detail modification that can be helpful.

Wafer	p-type Si	n-type Si	Poly Si/Si
Bonding time (min) <sup>a</sup> at 500 V	4	> 20	20
Bonding time (min) <sup>b</sup> at 500 V	1	–	5
Bonding time (min) <sup>b</sup> at 400 V	15	–	30

<sup>a</sup> Pre-cleaned with acetone.

<sup>b</sup> Pre-cleaned with H<sub>2</sub>SO<sub>4</sub>–H<sub>2</sub>O<sub>2</sub> and HF.

<sup>c</sup> HF dip was excluded for this wafer.

Table 3. Comparison of p-type and n-type

## ACKNOWLEDGEMENTS

Professor Fumihito Arai and members in Nagoya University Arai Lab

## REFERENCES

[1] Wang G, Mao W, Byler R, Patel K, Henegar C, et al. (2013) Stiffness Dependent Separation of Cells in a Microfluidic Device. PLoS ONE 8(10): e75901. doi:10.1371/journal.pone.0075901

[2] <http://www.ece.uah.edu/courses/material/EE410-Wms/Part%206%20%20Thin%20Film%20Deposition.pdf>

[3] <http://www.ajaint.com/whatis.htm>

[4] <http://www.linkedin.com/groups/Bright-coating-aluminum-sputtering-10-1390797.S.150650823>

[5] [http://en.wikipedia.org/wiki/Eutectic\\_bonding](http://en.wikipedia.org/wiki/Eutectic_bonding)

[6] Thomas M.H Lee, Debbie H.Y Lee, Connie Y.N Liaw, Alex I.K Lao, I-Ming Hsing, Detailed characterization of anodic bonding process between glass and thin-film coated silicon substrates, Sensors and Actuators A: Physical, Volume 86, Issues 1–2, 30 October 2000, Pages 103-107, ISSN 0924-4247, [http://dx.doi.org/10.1016/S0924-4247\(00\)00418-0](http://dx.doi.org/10.1016/S0924-4247(00)00418-0).

[7] [http://www.wafer-bumping.com/documents/techno/thin\\_film.html](http://www.wafer-bumping.com/documents/techno/thin_film.html)

[8] Diffusion barrier property of TiN and TiN/Al/TiN films deposited with FMCVD for Cu interconnection in ULSI, Young-Hoon Shin and Yukihiro Shimogaki 2004 *Sci. Technol. Adv. Mater.* 5 399



# **SLIP CONTROL FOR CONTACT MOTION REPRODUCTION**

Yue Huang

Department of Mechanical Engineering, Graduate School of Engineering, UCLA  
yueaptx@ucla.edu

Supervisor: YAMADA Yoji, Professor

Graduate School of Engineering, Nagoya University  
yamada-yoji@mech.nagoya-u.ac.jp

## **ABSTRACT**

It is significant to estimate the risk associated with such emerging technology as wearable robots. One of the hazards identified in their use, which leads a high risk - low severity but high frequency - is abrasion caused by cuffs directly contacting human skin. This threat also requires safety verification/validation tests for the robots. However, using human skin for the tests conceives an ethical problem and it becomes necessary to use dummy skin as a substitution. How to reproduce the cuff motion on the body of a human wearing a robot to that of dummy is of technical interest. To realize it, we construct friction and surface deformation models both for human and dummy skin. Experiments are conducted to analyze the mechanical behaviour of the dummy skin using the models. A basic control is further designed for simulating the overall system performance.

# **UNDISCLOSED**

# **THERMAL STRESS AND STRAIN ANALYSIS OF TSV AND MICROBUMPS IN 3D IC USING ABAQUS**

Yingxia Liu

Department of Materials Science and Engineering, Graduate School of Engineering, UCLA  
liuyingxia@ucla.edu

Supervisor: Nobutada Ohno

Graduate School of Engineering, Nagoya University  
ohno@mech.nagoya-u.ac.jp

## **ABSTRACT**

3D IC is a promising technology to sustain current computing trend for the next generation. TSV and microbumps are important components in 3D IC. In this work, the stress and strain distribution in TSV and microbumps has been studied by Abaqus. Mises stress, axial stress and radial stress change with aspect ratio have been investigated. Also the difference between free surface TSV and free surface TSV with microbump has been compared. Fixed surface plastic model was used to study the stress and strain distribution in our test sample. The results have shown its importance in the reliability study of 3D packaging circuit.

# UNDISCLOSED

## **Adhesive Bacterionanofiber AtaA and Quorum Sensing in Bacterial Immobilization**

Yuan Hung Lo

Department of Bioengineering, Graduate School of Engineering, UCLA  
y1lo@ucla.edu

Supervisor: Dr. Katsutoshi Hori

Department of Biotechnology, Graduate School of Engineering, Nagoya University  
khor@nubio.nagoya-u.ac.jp

### **ABSTRACT**

The toluene-degrading bacterium *Acinetobacter* sp. Tol 5 exhibits autoagglutinating nature and noteworthy adhesiveness to various abiotic surfaces. Previous studies have attributed those features to the highly adhesive cell-surface nanofibers called AtaA. In this study we began the search for a method to control the expression of *ataA* gene through the application of quorum sensing. We grew *ataA*-deficient Tol 5 mutant strain 4140 containing engineered *ataA* plasmid in supernatants from Tol 5 WT, ADP1, PAO1 and *E. coli* sp. BL21, and found that different *ataA* promoter sequences generated different transcriptional activities. In another project, we attempted to optimize the method of isolating and purifying AtaA proteins from the surface of Tol 5 cells by focusing on three main steps: cell growth conditions, AtaA cleavage reaction, and AtaA precipitation and collection.

# **UNDISCLOSED**

# QUANTITATIVE EVALUATION OF CARBON FIBER CONTENT IN CFRP USING MICROWAVE ANALYSIS

Tait McLouth

Department of Materials Science and Engineering, University of California, Los Angeles  
tmclouth@ucla.edu

Supervisor: Yang Ju

Graduate School of Engineering, Nagoya University  
ju@mech.nagoya-u.ac.jp

## ABSTRACT

A method for the determination of carbon fiber volume fraction using microwave analysis is proposed. Six short carbon fiber reinforced polymer samples were tested at a frequency of 110GHz to determine conductivity using the surface reflection coefficient. From there, the conductivity was used to estimate the fiber volume fraction based upon material properties such as fiber conductivity, matrix conductivity, aspect ratio, and the percolation threshold. The fiber volume fractions calculated from the measured conductivities did not agree with those calculated using the conductivities as determined by a four point probe method. This would suggest that the surface reflection coefficient cannot be used to accurately determine the conductivity of the samples.

# UNDISCLOSED

## Analysis of Solution Growth Conditions on Silicon Carbide (SiC) Polytype

Mark Seal

Department of Materials Science and Engineering, Graduate School of Engineering, UCLA  
markkseal@gmail.com

Supervisor: Toru Ujihara

Graduate School of Engineering, Nagoya University  
ujihara@nagoya-u.jp

### Abstract

Large areas (1 cm<sup>2</sup>) of 3C-SiC crystals have been grown on 6H-SiC seed crystals heteroepitaxially, using a top seeded solution growth method. The impact of growth conditions such as growth time and mixing rates are presented. Raman spectroscopy was used to determine the polytype of SiC grown, and electron backscatter diffraction analysis is presented to investigate areas composed of twinned 3C-SiC variants to determine the prevalent domain in the grown crystal.

### Introduction

Silicon carbide (SiC) is an attractive option for the next generation of semiconductor materials due to its superior material properties such as electron mobility, thermal conductivity, large band gap, and high breakdown voltage. One potential use is as the channel material for metal-oxide-semiconductor field-effect transistors (MOSFET), which take advantage of the superior mobility of SiC compared to silicon (Si), the classic device material. A schematic

of a typical MOSFET structure is shown in Figure 1.

SiC exists in a range of polytypes, and a variation of material properties is exhibited between each. Much effort has been expended in the study of mainly the 4H-SiC polytype as a semiconductor material due to its' superior breakdown voltage, mobility, and band gap compared against other polytypes. However, in the MOSFET application, the 3C-SiC polytype exhibits superior performance due to the low density of near-interface electron traps in the SiO<sub>2</sub>/SiC layer [SOURCE 1]. Despite these results, synthesis of high quality of MOSFET devices remains difficult. 3C-SiC is typically grown on a Si substrate by chemical vapor deposition (CVD), and a high density of stacking faults is produced due to the large lattice mismatch (~20%). Si and 3C-SiC also have large a difference in coefficient of thermal expansion and this leads to induced strain at growth temperatures which are typically close to 2000 °C.

The growth rate of common SiC polytypes can be seen in Figure 2. To preferentially grow 3C-SiC the growth temperature should be lowered to thermal equilibrium, around

1600 °C. Solution growth is a synthesis technique that allows for lower growth temperatures without the high density of stacking faults seen in CVD. Top seeded solution growth (TSSG) has been shown to successfully yield large areas (1 cm<sup>2</sup>) of SiC material [SOURCE 2].

A 4 °C off-axis 6H-SiC substrate was used as the seed to preferentially grow the 3C-SiC polytype. Previous work has indicated that the growth mechanism for 6H-SiC is via spiral growth from screw dislocations within the seed, while the 3C-SiC polytype follows a 2D nucleation mode. Previous work also indicated that by flowing the solution of molten Si opposite the offcut direction, a surface with lower RMS roughness could be obtained. [SOURCE 3]

An additional challenge for 3C-SiC solution growth is the presence of competing domains during growth. The 6H-SiC seed can support of 3C-SiC along two domains, as pictured in Figure 3 and the interface between these crystal types create double positioning boundaries (DPBs) which induce a leakage current in devices and must be avoided. The growth rate of these domains depends on the step flow direction and velocity, therefore the Si solvent velocity was controlled via seed and crucible rotation rates.

### Experimental Conditions

A radiofrequency-heated graphite hot-zone furnace (DAI-ICHI KIDEN Co, Ltd) was used to perform the TSSG, heating a graphite crucible which served as the carbon (C) source for SiC growth with a temperature gradient of around 20 °C from the bottom of the crucible to the seed. Electronic grade

silicon (99.9999999%, OSAKA Titanium technologies Co., Ltd.) was used as the solvent in an ambient atmosphere of He:N<sub>2</sub> (100:1). The furnace was heated to 1450 °C and held for an hour to homogenize the Si solvent and stabilize the C concentration. The rod was dipped and the crucible temperature was raised to ~1650 °C in order to initiate 3C-SiC growth.

Prior to growth, the Si material and SiC seed surface were prepared by ultrasonic cleaning with water, acetone, methanol and finally an HF acid rinse. After cleaning, the seed was mounted on top of a graphite rod using carbon adhesive (Nisshinbo). After growth, the seed was extracted from the solvent, and a mixture of HF:HNO<sub>3</sub> (2:1, volume) was used to wet etch the seed from the rod.

SiC polytype was determined by Raman scattering (NRS-3100), and crystal domain was confirmed by electron back scatter diffraction (EBSD) performed by TexSEM Lab system installed on a Zeiss Ultra 55 scanning electron microscope with Orientation Imaging Microscopy software.

### Results and Discussion

3C-SiC growth for 15 hours with crucible and seed rotation rates of 40 and 20 rpm had been previously performed [SOURCE], and their Raman and EBSD images can be seen in Figures 4 AND 5. From the Raman spectra, the 20 rpm sample shows less 6H-SiC (green) and more 3C-SiC (red). From the EBSD spectra, it appears that the 20 rpm sample also has less DPBs (depicted as the intersection of red and blue domains). It is believed that the crucible and seed rotation rate of 40 rpm was

too high to allow the C to reach the center of the sample, promoting 3C-SiC growth only at the edges but not in the center.

Therefore crucible and seed rotation rates of 10 and 5 rpm were carried out. The Raman and EBSD spectra of these samples are pictured in Figures 6, 7, AND 8. From the Raman spectra, we can see that the 10 rpm sample contained only a small area (~15%) of 3C-SiC as shown in Figure 6. This area also contained a large number of DPBs. Crucible and seed rotation rates of 5 rpm yielded similar results as shown in Figure 7. The small area of 3C-SiC (~20%) and the large number of DPBs shown in Figures 6 AND 7 indicate that for growth times of 15 hours, rotation speeds of 10 and 5 rpm are too low to selectively grow a single domain of 3C-SiC.

Growth time was also considered as a variable in this experiment, and a growth with crucible and seed rotation rates of 10 rpm was performed for 30 hours. The Raman spectrum indicates that the surface contains only 3C-SiC, and the EBSD spectrum shows a large number of DPBs as shown in Figure 8. Further testing of this sample is required to understand how the longer growth time affected the final surface.

Cross section analysis was carried out samples grown for 15 hours, the results of which can be found in Figure 9. The cross section was taken such that the center of rotation would be located at the center of the cross section sample. From this analysis, it is seen that the thickness of the grown samples is not uniform across the area, but depends on the rpm of the crucible and seed. Furthermore, the thicknesses of the samples vary, and this variation in thickness

corresponds to the ratio of 6H-SiC and 3C-SiC present.

The sample grown with rotation rate of 40 rpm has a bowed profile, with 3C-SiC present at the edges of the sample but not in the middle. This indicates that the mixing rate was too high to allow for adequate C diffusion to the center of the seed to produce the supersaturation conditions where the 3C-SiC polytype growth rate is dominant.

The sample grown with rotation rate of 20 rpm has a flat profile, with predominantly 3C-SiC observed across the surface. This indicates that the mixing rate was adequate to create supersaturation conditions favorable for 3C-SiC growth.

The samples grown with a mixing rate of 10 and 5 rpm both had film thicknesses of about half of those samples grown at 40 and 20 rpm. They also contained a lower ratio of 3C-SiC to 6H-SiC. Therefore favorable supersaturation conditions for predominantly 3C-SiC growth were not reached within the 15 hour growth time.

For the sample grown at rotation rate of 10 rpm for 30 hours (thickness is shown in Figure 10), predominantly 3C-SiC is observed on the surface. This suggests that during the longer growth time, growth conditions changed from 6H-SiC favorable to 3C-SiC favorable. The difference in thickness between the 15 hour and 30 hour growth time at 10 rpm suggests that the growth rate of 3C-SiC is approximately twice as large as the growth rate of 6H-SiC.

## Conclusion

In this study, 3C-SiC was selectively grown on 6H-SiC seed using the top-seeded

solution growth method. The grown samples contain a mix of 6H-SiC and a large number of DPBs, but trends in growth conditions were observed. A possible explanation of these results is that the crucible and seed rotation rates of 10 and 5 rpm are too low to allow adequate C mixing from the crucible to the sample. During 3C-SiC growth, the C near the seed is consumed and the rate of 6H-SiC growth becomes dominant. The results from the sample grown for 30 hours is that because the growth rates of 6H-SiC and 3C-SiC were allowed to continue for a longer time, the 3C-SiC rate eventually became dominant due to favorable temperature and C concentration conditions.

For mixing rates of around 10 rpm, longer growth times (~30 hours) are required to provide the C supersaturation conditions necessary to allow the 3C-SiC polytype growth rate to dominate over the 6H-SiC. Once these conditions are met, the growth rate of the 3C-SiC is approximately twice that of the 6H-SiC.

Due to time constraints more data could not be collected, however the results presented here indicate that further testing is necessary. Firstly, to ensure the reproducibility of the results, growth for 15 hours with crucible and seed rotation rates of 10 rpm should be performed and analyzed again. Because growth with rotation rates of 20 rpm and 10 rpm yielded the best yield of a single domain and 3C-SiC, growth with crucible and seed rotation rates of 15 rpm for 15 hours should also be performed and analyzed. A transmittance cross sectional analysis of the 10 rpm sample grown for 30 hours may reveal that layers buried beneath

the surface contain 6H-SiC and should therefore be carried out.

### Acknowledgements

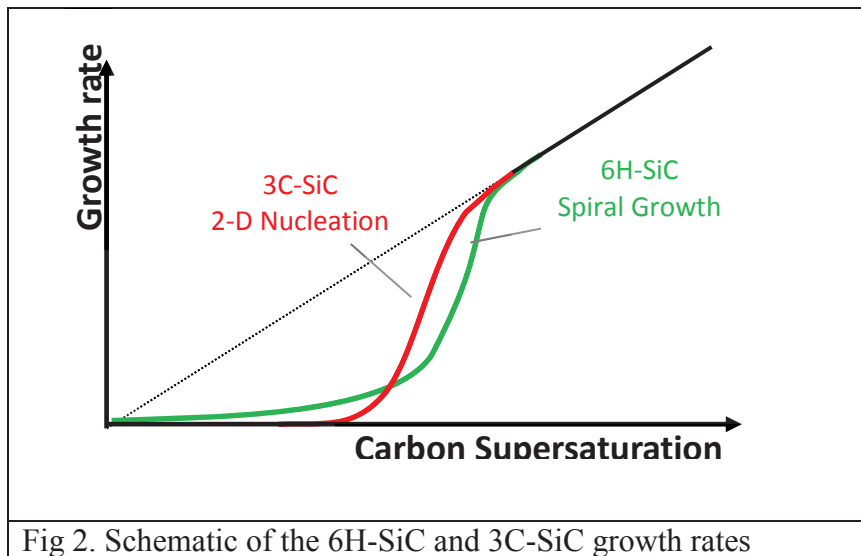
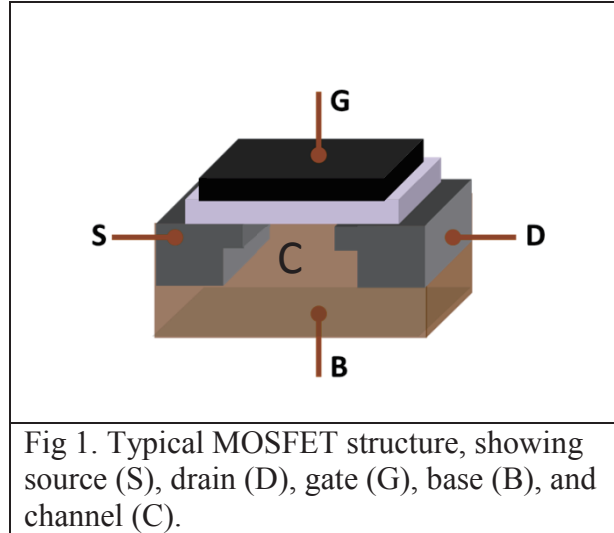
I would like to thank Professor Ujihara for accepting me into his laboratory for the summer, and the entire Crystal Growth group for being so welcoming and eager to help. Especially I would like to thank my mentor and friend Shota Yamamoto for helping every day with the experiments and data collection.

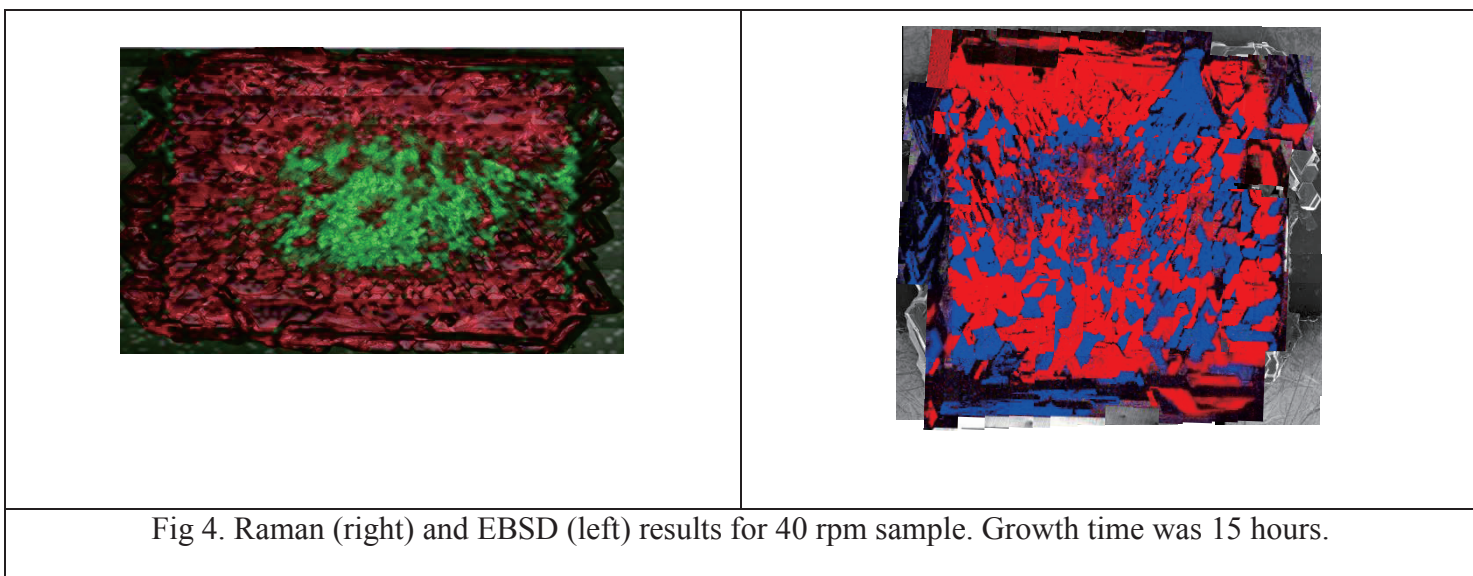
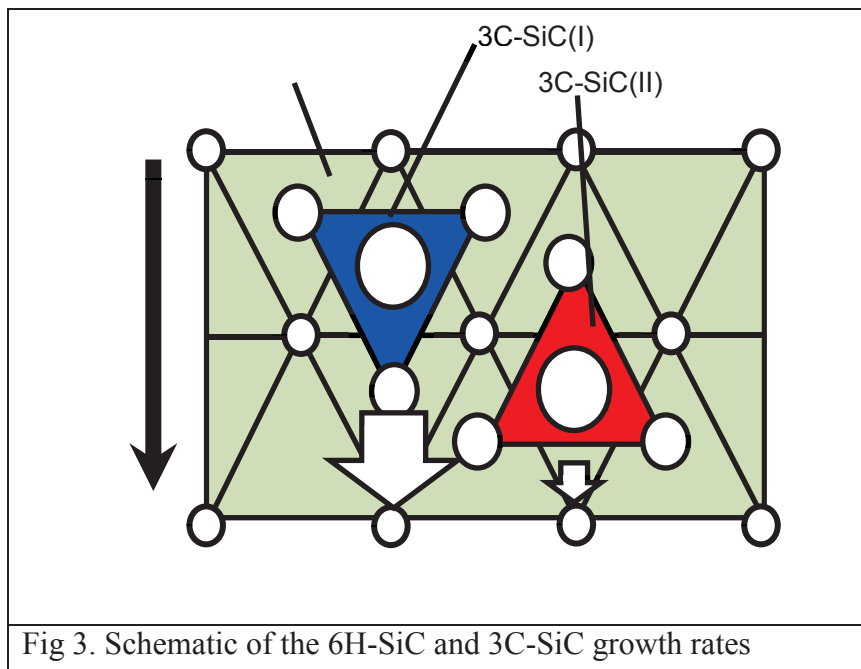
### References

1. E. Okuno, T. Endo, J. Kawai, T. Sakakibara, S. Onda, (11-20) Face channel FMOSFET with low on-resistance, Materials Science Forum 600-603 (2009) 1119-1122.
2. H. Uchida et al., Materials Science Forum, 717-720 (2012) 1109.
3. K. Seki et al., Formation process of 3C-SiC on 6H-SiC by low-temperature solution growth in Si-Sc-C system, Journal of Crystal Growth 335 (2011) 94-99
4. T. Ujihara et al, High-quality and large area 3C-SiC growth on 6H-SiC, Journal of crystal growth 318 (2011) 389-393.
5. M. Mukherjee et al, Dynamic Characteristics of III-V and IV-VI Semiconductor Based Transit Time Devices in the Terahertz Regime: A Comparative Analysis, Terahertz Science and Technology, (September 2010), 1941-7511



## Figures





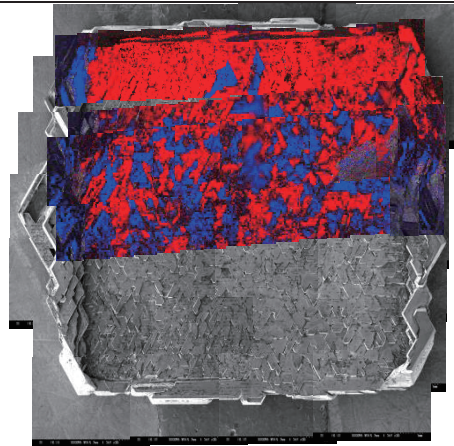
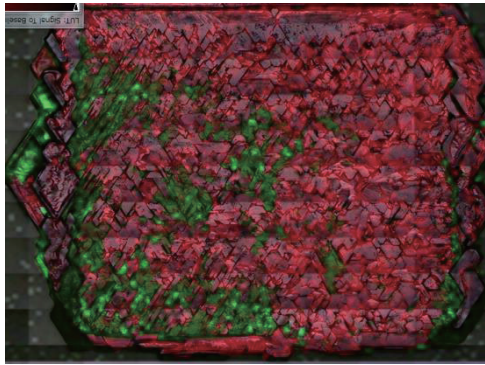


Fig 5. Raman (right) and EBSD (left) results for 20 rpm sample. Growth time was 15 hours.

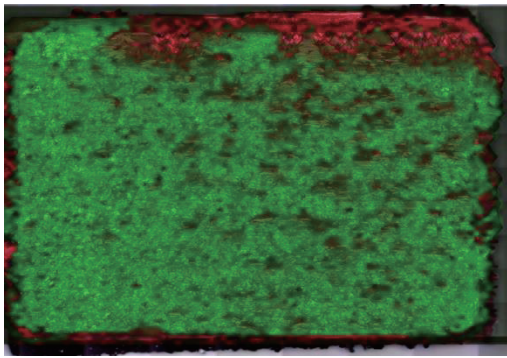


Fig 6. Raman (right) and EBSD (left) results for 10 rpm sample. Growth time was 15 hours.

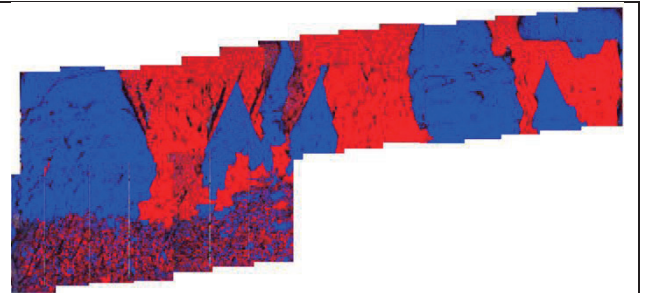
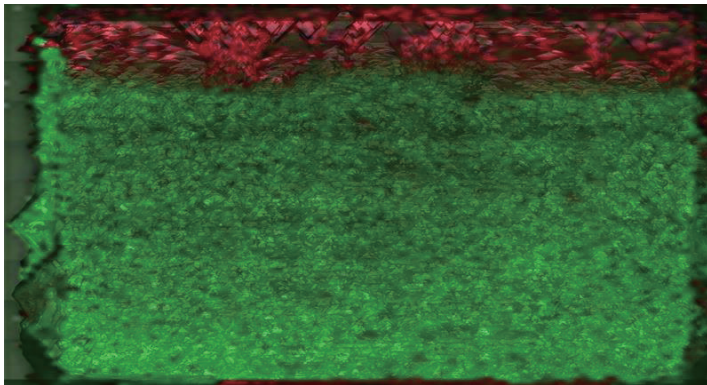


Fig 7. Raman (right) and EBSD (left) results for 5 rpm sample. Growth time was 15 hours.

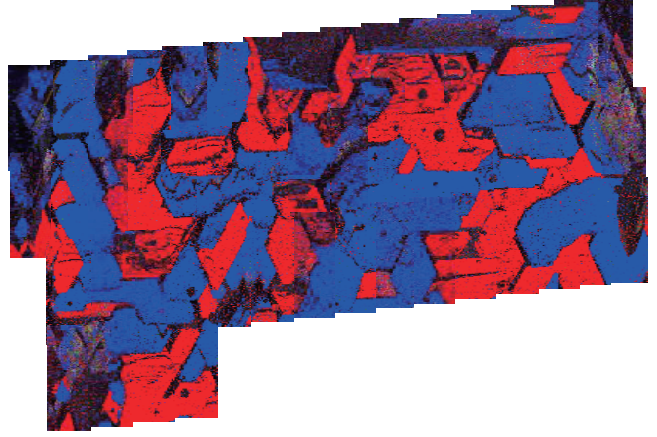
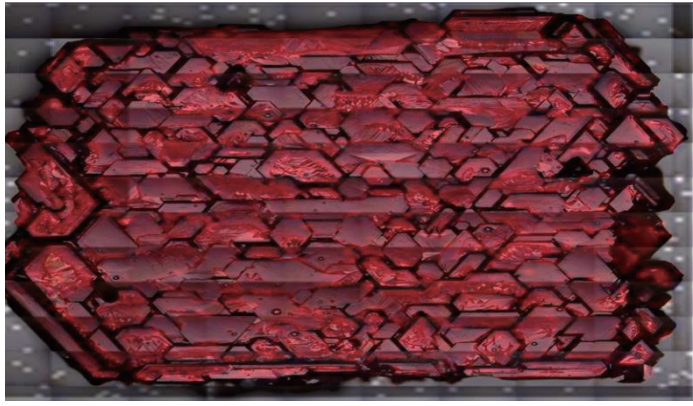


Fig 8. Raman (right) and EBSD (left) results for 5 rpm sample. Growth time was 15 hours.

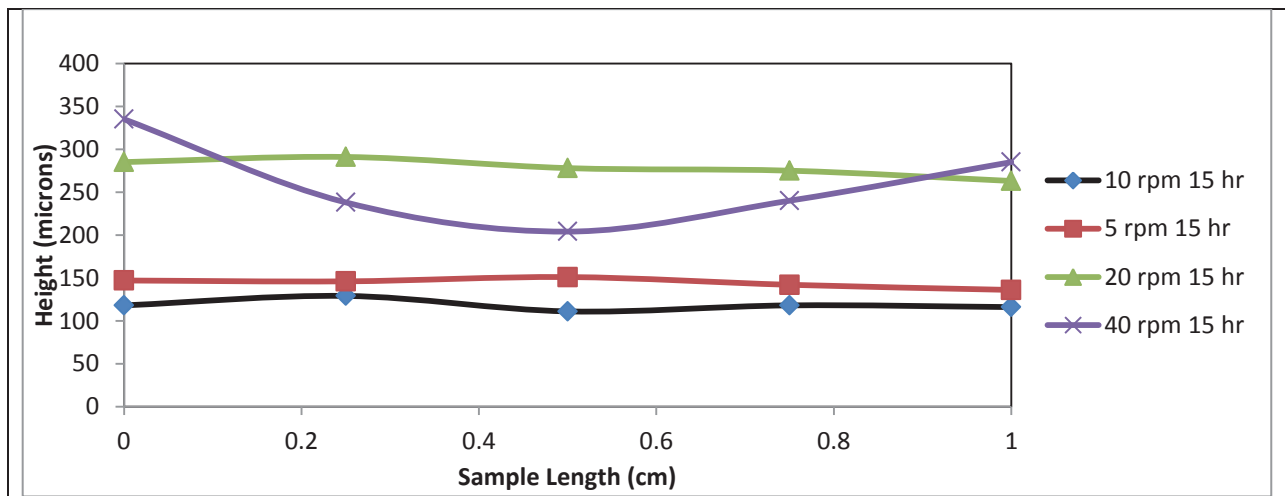


Fig 9. Comparison of cross section thickness for grown 3C-SiC layers grown at 15 hours

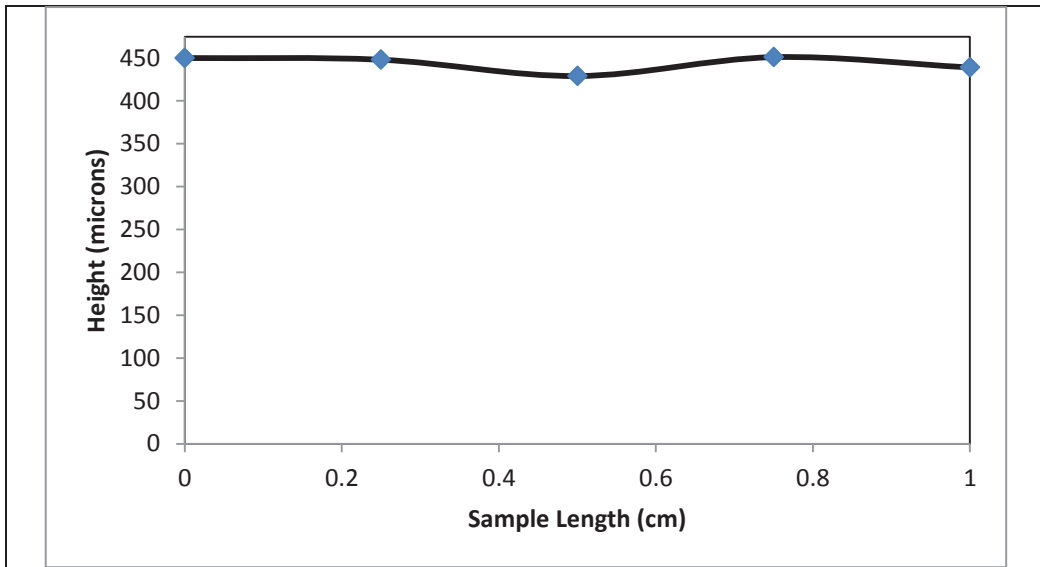


Fig 10. Comparison of cross section thickness for grown 3C-SiC layer at 10 rpm for 30 hours

## **PERFORMANCE OF AN APPLIED-FIELD MPD THRUSTER**

Elvia Cortes

Department of Mechanical and Aerospace Engineering, Graduate School of Engineering, UCLA  
siela@ucla.edu

Supervisor: Akihiro Sasoh

Graduate School of Engineering, Nagoya University  
sasoh@nuae.nagoya-u.ac.jp

### **ABSTRACT**

Electrode erosion and low thrust performance of the magnetoplasmadynamic (MPD) thruster are the two main problems that need to be solved in order to achieve high power electric propulsion in the future. Previously the performance of an applied-field MPD thruster at Nagoya University was measured under a small current operation. A larger thruster has now been developed providing additional propellant injection methods. In this study, the performance of the larger Af-MPD thruster was measured. The cathode to total mass flow rate ratio was varied and it was found that thrust efficiency improved when the ratio was kept at about 0.5. The total mass flow was also varied and the results show that a smaller mass flow rate is more efficient. For this MPD thruster, a maximum thruster efficiency of 12.6% was obtained at a specific impulse of 2500 seconds using a total mass flow of 56 sccm.

**UNDISCLOSED**

# ACCELERATION SENSING: DESIGN OF ELEVATOR RECOGNITION AND DISPLACEMENT ESTIMATION ALGORITHM AND IMPLEMENTATION ON SMARTPHONE

Antonio Martinez

Department of Electrical Engineering, Graduate School of Engineering, UCLA  
writeantonio@gmail.com

Supervisor: Professor Nobuo Kawaguchi

Department of Computer Science and Engineering, Graduate School of Engineering, Nagoya University  
kawaguti@nagoya-u.jp

## ABSTRACT

Since the advent of smartphones equipped with sophisticated sensing hardware, human activity recognition research is trending to move from utilizing dedicated sensing devices to using commercial smartphones. This paper presents the design of an algorithm to recognize and estimate displacement on an elevator and its corresponding implementation within an app for a smartphone. This is an initial attempt towards the building of a robust, but simple and fast real-time human activity recognition service on this wearable platform.

Keywords: accelerometer, elevator, human activity recognition, smartphone, iOS, wearable.

## 1. INTRODUCTION

With the massive deployment of smartphones, these days, research involving their built-in sensors is increasing rapidly since they are becoming more accurate and reliable. Accelerometer, gyroscope, and magnetometer produce signals that can be harvested and processed to obtain or improve information such as location and movement of the user possessing the smartphone. They have become a powerful platform for wearable context recognition [1]. Research areas related to navigation, location, tracking, and human activity are benefiting greatly from the current advances in smartphone sensing. Human activity recognition, for example, can contribute in an important manner to the fields of security, logistics, and especially medicine. Currently, extensive research and implementation of human activity recognition applications such as patient monitoring for rehabilitation or surgery recovery and assisting services for the elderly and disable are gaining great interest within the medical community.

Human activities like walking, running, sitting, climbing stairs, and riding elevators, among others can be

recognized by processing the signals of the smartphone's various sensors and utilizing algorithms designed for the specific activity. Moreover, information such as average speed or distance displaced can be extracted using the said algorithms.

The work that this paper describes is focused on utilizing only the accelerometer sensor signal while the algorithm tries to estimate as highly accurate as possible the displacement of a given elevator without the help of any other sensing resource. However, this is an initial part of a larger research project that aims to use the smartphone to ultimately recognize and obtain information about any activity that involves an elevator, on any type of elevator, anywhere in the world by having a robust app running on the background and automatically sending out accurate results to the cloud or to another app installed in the smartphone for real-time utilization.

To achieve the objective of this paper, a user-friendly mobile application for Apple's iOS mobile devices was developed. The initial version of the app only collected acceleration data while riding the elevator with the smartphone in hand and it had the capability to export the data via email. The recognition and displacement estimation algorithm was designed in parallel but tested and improved after analyzing the collected acceleration data, and then implemented in a consequent version of the app. The current version of the app includes the link that shows the estimated results right after the elevator ride is completed: the estimated displacement of the elevator in meters, whether the elevator ride was to a higher or lower floor, estimated time the ride took, maximum speed of the elevator, and initial acceleration. The estimated displacements were compared to the actual displacements and very small errors in the range of 1% were found.

Below, in section 2, related research work on elevator recognition is discussed; section 3 describes the iOS app in more detail; section 4 introduces the algorithm design and implementation; section 5 shows the results and error analysis; and section 6 proposes future improvements to conclude the paper.

## 2. RELATED RESEARCH WORK

Many research papers focus on recognizing which activity the user is performing at a given time by using one [2] or more sensing devices in the smartphone [3], but since these algorithms are designed for multi-activity recognition, the success rates may be not that high and the information extraction may be limited. Other papers aim to construct more robust algorithms by focusing their research on a specific activities [4], for example, riding on an elevator, thus allowing the design of more sophisticated algorithms and potentially obtaining better results.

The work presented in this paper is of the latter kind; but here the focus is even narrower, that is, only the accelerometer sensor signal is being used and the algorithm tries to estimate as highly accurate as possible the displacement of one specific elevator without relying on any additional sensing resources.

## 3. SMARTPHONE APPLICATION

### 3.1 Overview

The mobile application for Apple's iOS mobile devices was developed using Objective-C programming language

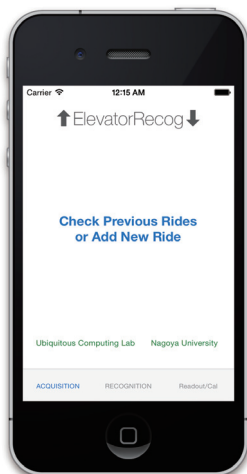


Fig. 1 iPhone App

and Apple's Xcode IDE [5]. This app can be used on an iPhone or an iPad running iOS versions 6.0 and higher. Three devices were used to test the app: an iPhone 3GS running iOS 6.0, an iPhone 4S running iOS 6.2, and an iPad running iOS 7.1. From figure 1, the app actually consists of 3 tabs, named "Acquisition", "Recognition", and "Readout/Calibration"; however in this paper, only the "Acquisition" phase was developed, which consists of the algorithm that

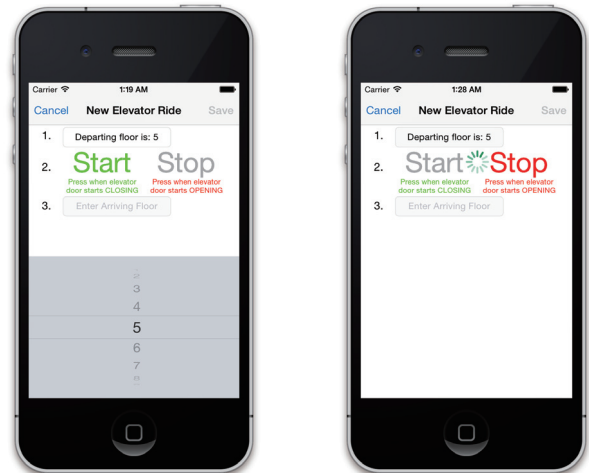


Fig. 2 Elevator ride data collection in action

recognizes and estimate elevator displacement. It is important to note that, although the next phase has the name "Recognition", the "Acquisition" phase also includes a recognition feature, that is, it can recognize from the acceleration signal that an elevator ride has taken place. But the "Recognition" phase, which will be developed on future papers to follow up this study, is meant to recognize an elevator ride automatically, without the interaction of the user, in other words, it will be running on the background and automatically sending out accurate results to the cloud or to another app installed in the smartphone for real-time utilization.

The "Acquisition" phase consists of a user-friendly front-end interface which was built along with a back-end infrastructure that includes an embedded SQLite database to store the collected data. An export feature is available for data export via email, thus data can be stored somewhere else for future use. In an initial stage of the app development phase, the app consisted of the above only, that is, the elevator recognition and displacement estimation algorithm was not implemented yet. Data was being collected by performing elevator rides and exported using this first version of the app. After approximately 60 elevator rides were taken, data was analyzed and the algorithm, which was being designed in parallel, was given the last touches before being implemented into the app's second version. This version included an information page for each elevator ride, which can be linked from the lists of elevator rides.

### 3.2 App Modules

#### 3.2.1 Data Collection

Figure 2 shows the form for collecting data from the 3-axis accelerometer. User takes elevator rides with smartphone while following app's directions to collect data. The steps to follow are as follows: Fill out "departing floor" number by using a picker that contains floor numbers. Press "Start" button for the app to start extracting acceleration



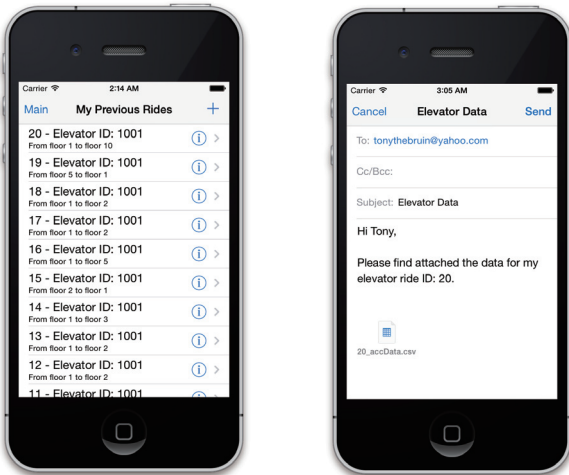


Fig. 3 Data storage and data export

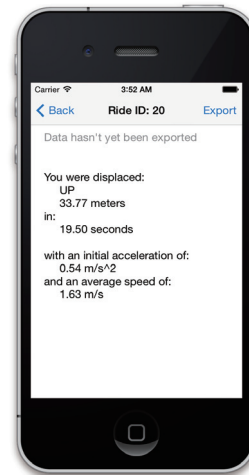


Fig. 4 Page showing results after elevator ride was taken

readings from smartphone's 3-axis accelerometer. Press "Stop" button for the app to end data extraction. And, enter "arriving floor" number. The user has the option of pressing "Cancel" at anytime in order to cancel a ride gone wrong, or "Save" the elevator ride at the end of it. The data collection sampling rate is set to the maximum allowed by iOS devices, that is, 100 samples per second, therefore each acceleration sample is read every 10ms.

### 3.2.2 Data Storage

Each ride is stored in the app's embedded SQLite database that was created for this purpose. In the left screenshot of figure 3, a view of the list of rides extracted from the database file can be seen.

The app also converts the acceleration data into a comma separated value (.csv) file in order to allow the data export via email. The right screenshot on figure 3 shows the pre-formatted email developed for that purpose.

### 3.2.3 Data Processing

The designed algorithm for in-phone data processing is implemented. Using collected accelerometer data, algorithm ultimately estimates displacement of elevator. The process flow is as follows: Raw 3-axis acceleration data is combined and filtered; critical points of typical elevator acceleration curve are identified; acceleration/deceleration are calculated in corresponding intervals; velocity is calculated by integrating acceleration over time; similarly, displacement is calculated by integrating velocity over time.

### 3.2.4 Display of Results

Results are displayed on page that is linked from the list of rides page. This information page shows the estimated results right after the elevator ride is completed: the estimated displacement of the elevator in meters, whether the elevator ride was to a higher or lower floor, estimated time the ride took, maximum speed of the elevator, and initial acceleration. This page is shown in figure 4.

## 4. ALGORITHM DESIGN

### 4.1 Raw Data Filtering

The raw acceleration data received from the sensor is first combined into a total acceleration, thus the position of the phone will not make any difference when extracting the acceleration induced by the elevator. This is accomplished using equation (1).

$$a_{total} = \sqrt{a_y^2 + a_x^2 + a_z^2} \quad (1)$$

Then the acceleration, shown in figure 5a, is filtered using a custom running average equation with an interval of 40 units. The data becomes more readable and easier to process as it can be seen in figure 5b.

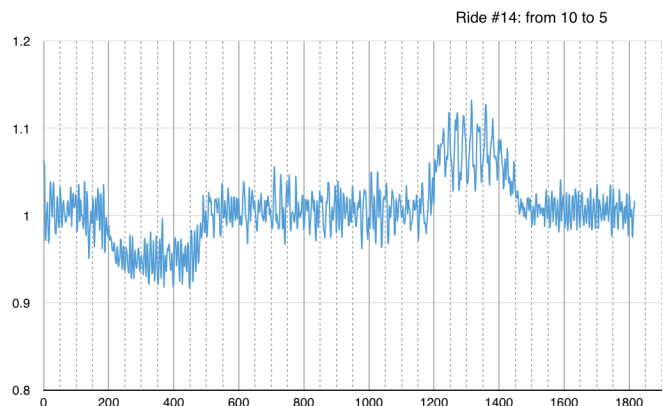


Fig. 5a Acceleration curve *before* filtering

### 4.2 Critical Points

Acceleration data is binned in windows of length equal to 500ms, that is, the size of 50 samples, as it can be seen on figure 6. Once that is accomplished, the variance of each window is calculated and compared to a set threshold that

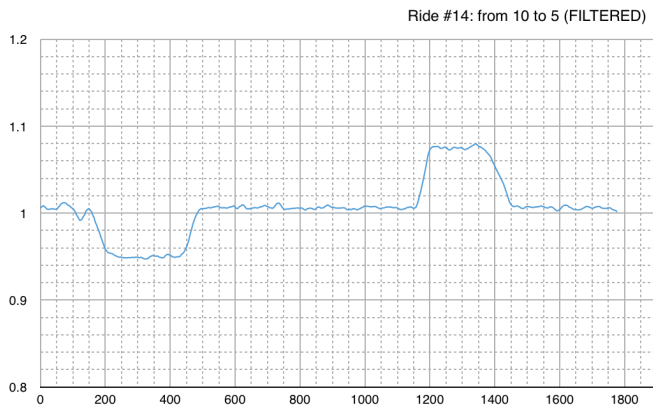


Fig. 5b Acceleration curve after filtering

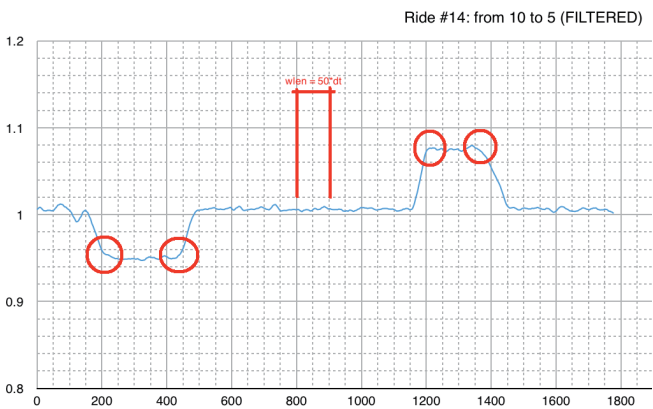


Fig. 6 Window size and four critical points

was obtained a priori when analyzing the data; therefore the index of the windows that pass the threshold are stored in an array and then analyzed again to finally obtain the 4 critical points that define the curve, as it is shown on figure 6.

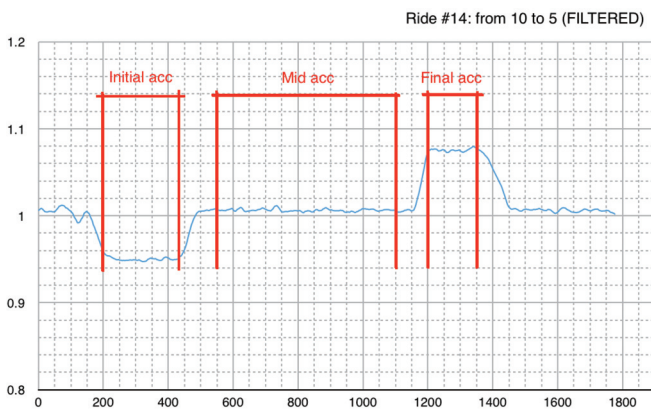


Fig. 7 Acceleration sections

### 4.3 Acceleration and deceleration calculation

The acceleration curve is divided in three segments as it can be seen in figure 7, here called initial acceleration, mid acceleration, and final acceleration. They correspond to the initial acceleration of the elevator, the “zero” acceleration while the elevator is at constant speed, and the deceleration that brings the elevator to a stop, respectively. Then, they all are stored for later use by the algorithm.

$$\Delta x = \int_0^t v_x(t') dt' = \int_0^t \left[ \int_0^{t'} a_x(t'') dt'' \right] dt' \quad (2)$$

### 4.4 Displacement Estimation

Figure 8 shows a typical simplification of an acceleration curve, its corresponding integration to obtain the velocity curve, and its second integration to obtain its displacement curve in order to avoid complex calculations using equation (2), thus minimizing processing time and power consumption. However, this paper proposes an approach where the acceleration curve is transformed to a geometrically equivalent as seen in figure 9 for an even more simplified calculation of integrals over time that

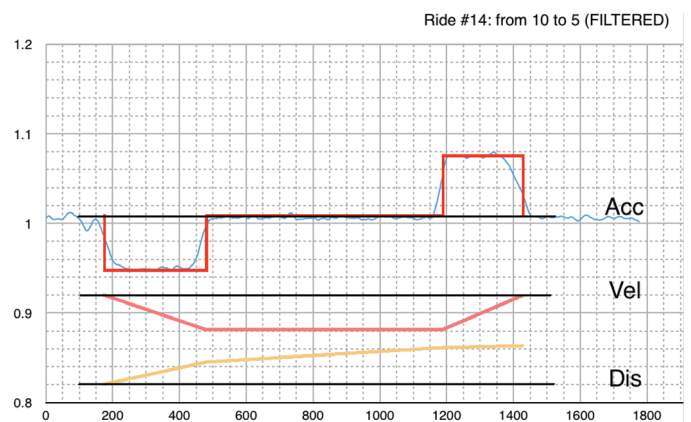


Fig. 8 Typical simplification of acceleration curve

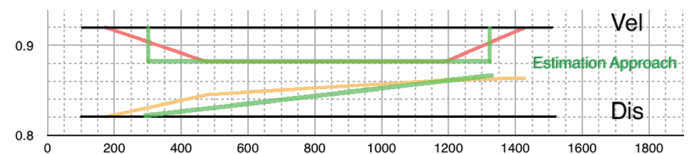


Fig. 9 Simpler approach to displacement estimation

ultimately only requires the calculation of a rectangular area. Mid acceleration is subtracted from initial acceleration, thus net acceleration is obtained. Velocity corresponding to initial acceleration segment is calculated using the net acceleration and integrated over whole span to estimate displacement. Final acceleration is discarded, however its end time is

utilized to set the end of the time span mentioned above. Based on testing and error analysis, post-processing adjustment is needed in order to minimize error between actual and estimated displacement. Second degree polynomial curve fitting is used for this purpose. Since errors trends are different when elevator heads up and when it heads down, two separate error adjustment equation are implemented in the algorithm. More details are presented in the section corresponding to error analysis.

## 5. RESULTS AND ERROR ANALYSIS

After testing the displacement estimation algorithm, errors found between the actual and estimated values were analyzed in order to further improve the algorithm.

By observing the absolute errors on 6 upwards and 6 downwards elevator rides, a pattern was discovered. On the short rides (2-floor displacement) and long rides (9-floor displacement), the errors were relatively large and trending towards the negative side, that is, the estimations had less magnitude than the actual displacements; however for medium rides (4 or 5-floor displacement), errors were slightly negative or positive, as shown in figure 10. These

pattern was somewhat different on upwards rides compared to downwards rides, a separate set of coefficients for each direction was implemented to improve even more the accuracy of the results. A graph showing the absolute errors after the adjustment is shown in figure 11.

A more detailed comparison of the actual and estimated displacements is presented on table 1.

	Departing Floor	Arriving Floor	Direction	ACTUAL Length between floors	ESTIMATED Displacement	Error BEFORE adjustment	ADJUSTED Displacement	Error AFTER adjustment
Ride #18	1	5	UP	9.00	8.55	-5.0%	8.98	-0.2%
Ride #21	1	5	UP	17.30	17.82	3.0%	17.57	1.6%
Ride #10	5	10	UP	19.00	18.96	-0.2%	18.76	-1.3%
Ride #12	5	10	UP	19.00	19.17	0.9%	18.98	-0.1%
Ride #13	1	10	UP	36.30	33.35	-8.1%	36.20	-0.3%
Ride #16	1	10	UP	36.30	33.49	-7.7%	36.39	0.2%
Ride #19	3	1	DOWN	9.00	8.38	-6.9%	9.00	0.0%
Ride #20	5	1	DOWN	17.30	17.12	-1.0%	17.32	0.1%
Ride #14	10	5	DOWN	19.00	18.81	-1.0%	19.05	0.3%
Ride #15	10	5	DOWN	19.00	18.71	-1.5%	18.95	-0.3%
Ride #22	10	1	DOWN	36.30	33.87	-6.7%	36.26	-0.1%
Ride #23	10	1	DOWN	36.30	33.98	-6.4%	36.40	0.3%

Table 1 Detail of errors before and after adjustment

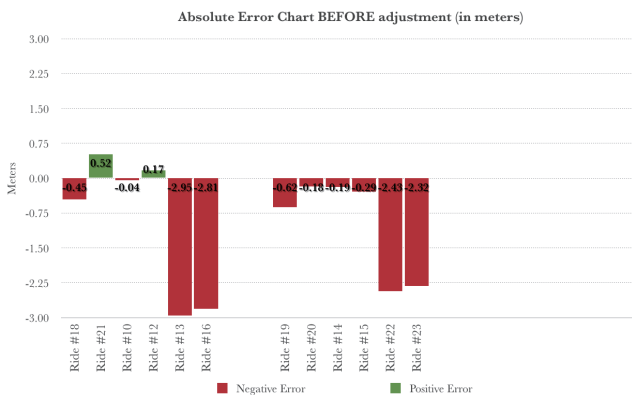


Fig. 10 Displacement estimation errors *before* adjustment

observations led to think of a parabola-shaped correction adjustment, in other words, a second-degree polynomial equation could be used to very accurately minimize errors across all rides lengths. Moreover, since this observed

## 6. FUTURE DEVELOPMENT

Perform further testing on various elevators. Improve app user-friendliness based on feedback received from users. Implement accelerometer calibration to improve displacement estimation. Improve algorithm after a larger amount of data has been taken. Implement “Recognition” tab and all what this implies as explained in the introduction section.

## REFERENCES

- [1] Berchtold M., Budde M., Gordon D., Schmidtke H. R., Beigl M., ActiServ: Activity Recognition Service for Mobile Phones, 2010 International Symposium on Wearable Computers (ISWC), 1-8, 2010.
- [2] Brezmes, T., Gorricho, J.L., and Cotrina, J., Activity Recognition from accelerometer data on mobile phones, IWANN '09: Proceedings of the 10th International Workshop Conference on Artificial Neural Networks, 796-799, 2009.
- [3] Gyorbiro, N., Fabian, A., and Homanyi, G., An activity recognition system for mobile phones, Mobile Networks and Applications, 14(1), 82-91, 2008.
- [4] Koshimizu, K., Kamioka, E., Estimation of User's Behavior for Realizing Just-in-time Services, IEICE-MoMuC2009, 108, 2009.
- [5] Apple iPhone and Apple iPad app development. 2013. Apple Inc. [www.apple.com](http://www.apple.com).

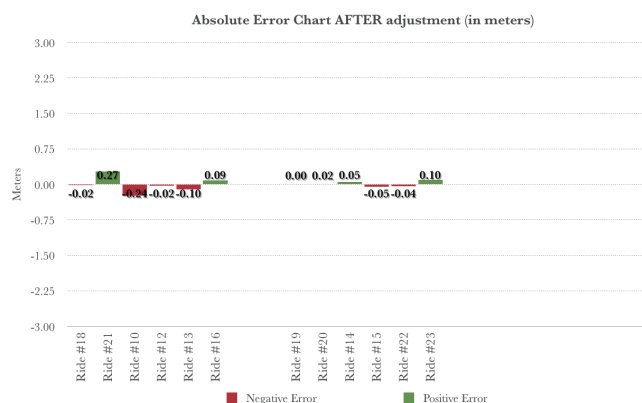


Fig. 11 Displacement estimation errors *after* adjustment

## 2-e. Workshop

### *The 9th JUACEP Workshop*

**Date:** August 7 (Thu)

**Venue:** VBL Hall, Nagoya University

**Timetable:**

14:00            Opening ~Address from Prof. Ju~  
14:10 - 17:40   Presentations by UM students  
                  (15 mins. presentation + 4 mins. Q&A each)  
17:40 - 17:50   Award Ceremony  
18:00 -           Farewell Banquet

**~Presentation Title~**

**1: Chiyang Zhong (P.107)**

*"Development of Current Suppression Equipment in Low Voltage DC Distribution System"*

**2: Charles Lesmana Sie (P.111)**

*"Exploration of Correlation Coefficient Method on Human Activity Sensing Data"*

**3: Jin-Gen Wu (P.115)**

*"Automated Steering System for Obstacle Avoidance based on Potential Field Method"*

**4: Hanyi Xie (N/A)**

*"Friction and Wear of 3D Printed Material"*

**5: Yingrui Zhan (P.118)**

*"Cold Forge Spot Bonding of Copper and Aluminum Alloy Sheets"*

**6: Songyao Jiang (P.123)**

*"Dynamic Modelling of Combined Cycle Gas Turbine"*

**7: Taehee Jang (N/A)**

*"Design of a Multifunction Probe Used for Microwave AFM"*

**8: Yang Yong (P.127)**

*"Assembly of Multi-Layer Structured Blood Vessel"*

**9: Fu-Long Chang (N/A)**

*"Updating Final-State Control Algorithm with Overshoot/Undershoot Prevention Technique for a Connection Control Problem"*

## JUACEP Research Presentation

### Development of Current Suppression Equipment in Low Voltage DC Distribution System (Electrical Engineering)

#### Student

Chiyang Zhong

Department of Electrical Engineering, University of Michigan  
zchiyang@umich.edu

#### Supervisors

Prof. Toshiro Matsumura

matumura@nuee.nagoya-u.ac.jp

Graduate School of Engineering, Nagoya University

Associate Prof. Yasunobu Yokomizu

yokomizu@nuee.nagoya-u.ac.jp

Graduate School of Engineering, Nagoya University

### Introduction

Low Voltage DC Distribution System:

- Widely employed in some areas
- Applications of DC deliveries used
- High reliability and high efficiency for electricity delivery
- Requires protection from faults

Fault Current Limiter (FCL):

- Reduce circuit breaker interruption duty
- Reduce current magnitude during faults

### Introduction

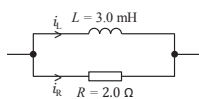
FCL Researched:

- Simple structure with no control part
- No detector for fault occurrence needed
- No additional voltage source needed

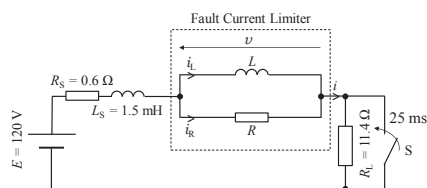
FCL Types:

- L-R topology
- L-RC topology
- L-RD topology (Developed in this research)

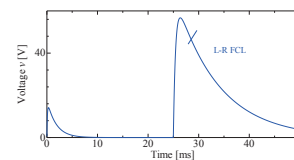
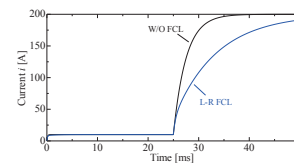
### L-R FCL Topology



- Steady state  
Current only flows through the inductor  
No voltage drop across FCL
- After fault occurs (25 ms) & Current suppression  
Inductor reduces current  
Voltage drop induced

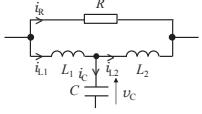
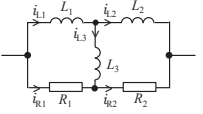


### L-R FCL Topology



### New FCL Topologies

Developed from the L-R topology

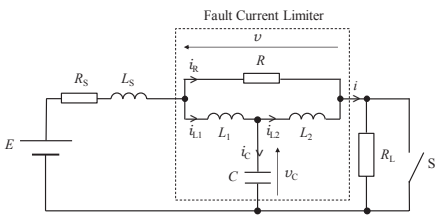
**Constraints**

$$\sum_{i=1}^{N_R} R_i = 2.0 \Omega$$

$$\sum_{i=1}^{N_L} L_i = 3.0 \text{ mH}$$

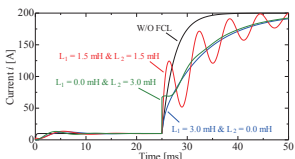
### New FCL Topologies

Topology A



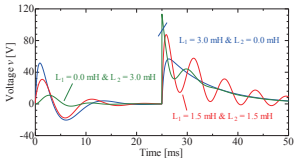
### New FCL Topologies

Topology A



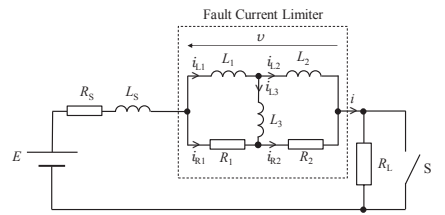
**Best Case Scenario**  
(Equivalent to the L-R Topology)

I	II
R = 2.0 Ω	R = 2.0 Ω
L1 = 3.0 mH	C ≤ 1.0 μF
L2 = 0.0 mH	



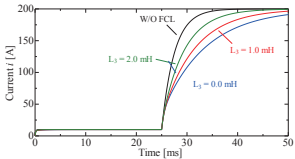
### New FCL Topologies

Topology B



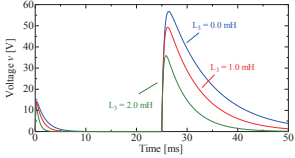
### New FCL Topologies

Topology B



**Best Case Scenario**  
(Equivalent to the L-R Topology)

L1 = 1.5 mH
L2 = 1.5 mH
L3 = 0.0 mH
R1 = 1.0 Ω
R2 = 1.0 Ω



### New FCL Topologies

Conclusions

Topologies A & B:

- Best configuration **equivalent to L-R FCL**
- **More components**

L-R FCL:

- **Less components**
- **Simple and economical configuration**
- **Better performance**

### L-RC FCL Topology

- Current suppression (10 – 20 ms)  
*Almost no current going through resistor*
- Current interruption (> 20 ms)
  - Energy stored in inductor released
  - Current going back and forth between inductor and capacitor
  - Oscillation occurs

### L-RC FCL Topology

C	10 – 20 ms	> 20 ms
1.0 nF	Good	Bad
1.0 μF	Good	Okay
1.0 mF	Bad	Good

Capacitor Value Chosen  
1.0 μF

### Development of L-RD FCL

Current Limitation Period (10 – 20 ms)

Best configuration is ...

Infinite impedance branch

+

Current Interruption Period (> 20 ms)

Best configuration is ...

No capacitor present

### Development of L-RD FCL

#### L-RD Topology

- Current suppression (10 – 20 ms)  
*No current going through resistor*
- Current interruption (> 20 ms)
  - Energy stored in inductor released
  - Current going through diode and resistor
  - Resistor consuming stored energy

### Development of L-RD FCL

#### Comparisons

Variable	Value
L	3.0 mH
R	2.0 Ω
C	1.0 μF

### Development of L-RD FCL

#### Comparisons

FCL	10 – 20 ms	> 20 ms
L-R	Bad	Good
L-RC	Good	Bad
L-RD	Good	Good

Best FCL Topology  
L-RD

## **Development of L-RD FCL**

### Conclusions

#### L-RD FCL:

- Proposed in this research
- Inspired by & developed from L-RC topology
- **Better current suppression performance**
- **Better current interruption performance** (low voltage drop)
- **Simple** configuration
- Proven to be **more promising** than others

# **Thank You**

## **Questions & Answers**




## EXPLORATION OF CORRELATION COEFFICIENT METHOD ON HUMAN ACTIVITY SENSING DATA

Research Report

Charles Lesmana Sie

1


### Navigation System



2

### Project Motivation

- ▶ Provide useful information to improve accuracy in Pedestrian Dead Reckoning (PDR)

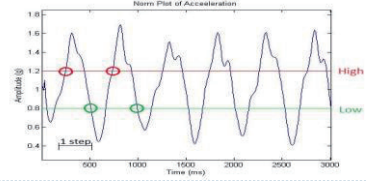


- ▶ Test the performance of correlation coefficient to count steps
- ▶ Alternate method to threshold and angular acceleration method to improve accuracy.

3

### Step Counting Techniques

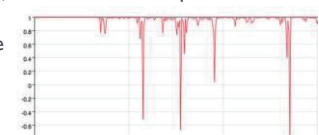
- ▶ Threshold method
  - ▶ Count one step when norm of acceleration cross high and low threshold value consecutively.
  - ▶ Acceleration norm may not cross the different threshold values consecutively.



4

### Step Counting Techniques

- ▶ Angular acceleration method (First Line Software, Inc)
  - ▶ Calculate angle between current and previous point acceleration vector
  - ▶  $\mathbf{a} \cdot \mathbf{b} = |\mathbf{a}| \times |\mathbf{b}| \times \cos(\theta)$
  - ▶ At rest the  $\cos(\theta)=1$ , lower value to represent user movement
  - ▶ Sensitive to noise



5

# Proposed Method

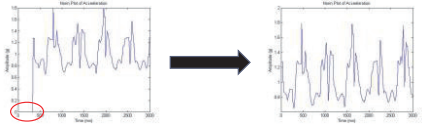

6

### Correlation Coefficient Method

- ▶ The proposed method count the steps taken by statistically measuring the correlation of the first step taken with the  $n^{\text{th}}$  steps. (matlab)
- ▶ HASC-IPSC acceleration data were used to test the performance of the method.
  - ▶ 100 Hz sensor sampling rate
  - ▶ 100 People:
    - ▶ 50 male
    - ▶ 50 female
    - ▶ Age: 20-60

▶ 7

### Adjustment and Filtering

- ▶ Eliminate zero entries
 
- ▶ Remove noise (low pass filter)
 

▶ 8

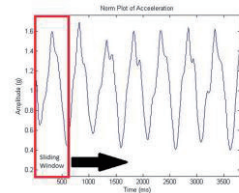
### One Cycle Identification

- ▶ One cycle of acceleration norm = one step taken
- ▶ Length of one cycle is determined by the length of consecutive peaks.

▶ 9

### Sliding Window

- ▶ Defined window length containing parts of acceleration norm
- ▶ It slides through the acceleration waveform to generate correlation coefficient plot



▶ 10

### Correlation Coefficient

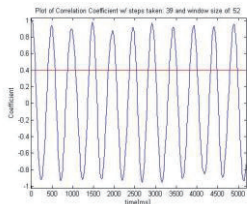
- ▶ Correlation can be positive or negative
- ▶ Larger magnitude means stronger correlation

Correlation Coefficient (r)	Strength
> 0.7	Strong
0.4-0.7	Moderate
0.2-0.4	weak
< 0.2	None/minimal

▶ 11

### Steps Calculation

- ▶ Peaks above 0.4 is counted as one step taken
- ▶ Moderate strength of correlation between the first step and the  $n^{\text{th}}$  step taken is achieved.



▶ 12

# Results

▶ 13

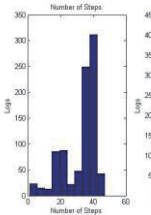
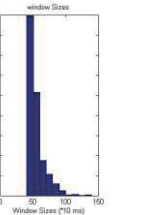
## Basic Activity

- ▶ One activity in each log
  - ▶ Walking
  - ▶ Stepping up (stairs)
  - ▶ Stepping down (stairs)
- ▶ Length:  $\pm 20$  second

▶ 14

### Walking

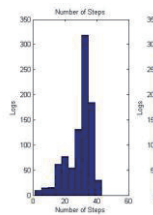
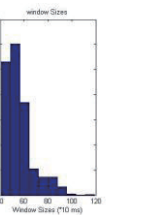
- ▶ Average number of Steps: 32 steps. Standard deviation: 10 steps.
- ▶ Average window size: 550 ms. Standard deviation: 137 ms.

▶ 15

### Stepping Up (Stairs)

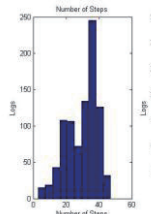
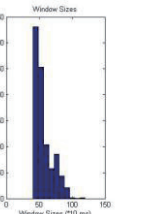
- ▶ Average number of Steps: 29 steps. Standard deviation: 8 steps.
- ▶ Average window size: 559 ms. Standard deviation: 120 ms.

▶ 16

### Stepping Down (Stairs)

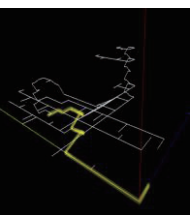
- ▶ Average number of Steps: 30 steps. Standard deviation: 9 steps.
- ▶ Average window size: 564 ms. Standard deviation: 139 ms.

▶ 17

### Route Logs (multiple activities)

- ▶ Combination of simple activities: walking and stepping up (stairs)
- ▶ The theoretical distance traveled in the log route is 74.9m
- ▶ Step length assumption:
  - ▶ 45% of person's height (below 65)
  - ▶ 40% of person's height (above 65)



▶ 18

### Threshold Method vs. Proposed Method

- ▶ Average error:
  - ▶ Threshold method: 35.6%
  - ▶ Proposed method: 21.0%

	Estimated step length [m]	Method error [m]		Error Improvement [m]
		Threshold	Correlation Coefficient	
Person 1207	0.801	28.4	34.8	-6.4
Person 1208	0.770	42.0	7.9	34.8
Person 1217	0.756	22.6	23.38	-1.2
Person 1234	0.783	16.7	2.9	13.8
Person 1296	0.662	23.3	9.8	13.5
Average	0.754	26.6	15.8	10.9
Standard Deviation	0.054	9.6	13.1	16.1

▶ 19

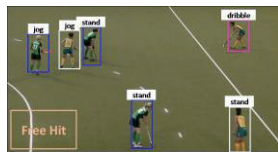
### Conclusion

- ▶ Proposed method is an inexpensive and simple way to measure steps taken
- ▶ Dynamic window sizes provides flexibility.
- ▶ The proposed method is more accurate in counting steps compared to the threshold method.

▶ 20

### Future Work

- ▶ Integration of activity recognition



- ▶ Step length estimation




▶ 21

QUESTIONS?

▶ 22


Thank you for  
your attention

▶ 23




## Automated Steering System for Obstacle Avoidance based on Potential Field Method

Jin-Gen Wu




## Introduction


- Automated driving and steering assist systems are cutting edge technology which be implemented on modern vehicles.
- They provide safety and convenience to the driver and passengers



Automated driving (BMW)



Pedestrian avoidance Steer Assist (Toyota)



## Motivation

- The goal of this research project is to avoid obstacles which can be detected by LRF in real-time in front of the vehicle.
- Improving the behavior of the steering assist system from predetermined obstacles (Yan Kun did last year) to real-time detect obstacles.
- By algorithm implement in controller to classify boundary(side walls) and obstacles which assign different weight values for potential function form sensor's data.

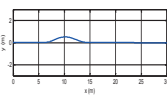


Figure 1: know the position of obstacles and generate the reference path from potential field

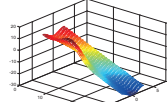





Figure 2: potential field of the driving environment



## COMS set up

- A small electric vehicle (COMS) is used in the research. Only low speed experiments are done to ensure safety.

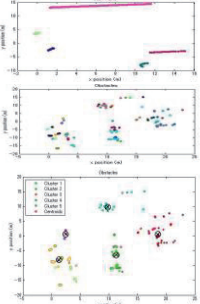





## Algorithm for classify boundary and obstacles

- Distance method :  
When the distance of two points large than one specific value, the later point will be classify to another cluster.
- K-means :  
Apply the K-means method on obstacles data which be classify by "Distance method".

Pors : Define the position of the obstacles  
Cons : Number of clusters which is unknown for us.

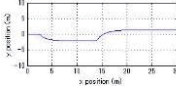


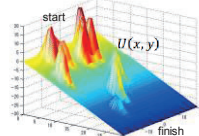


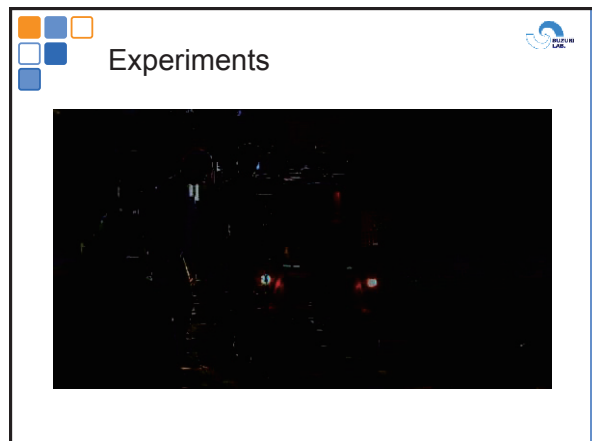
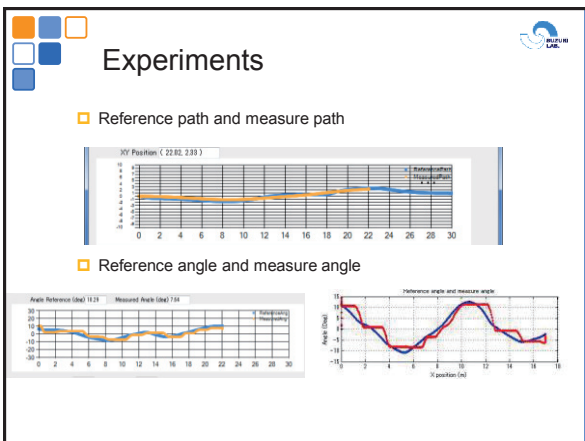
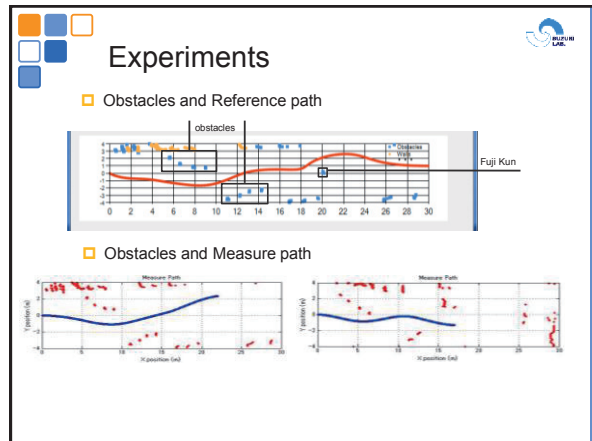
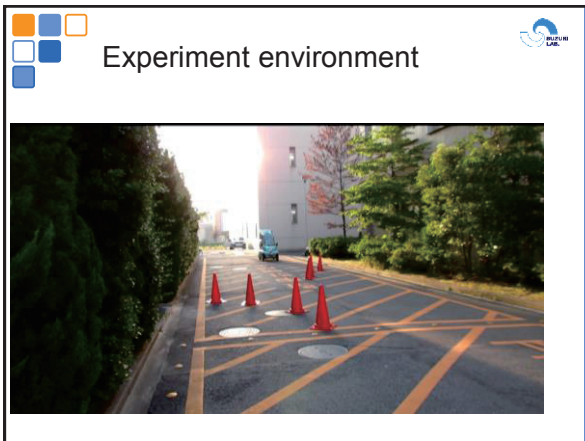
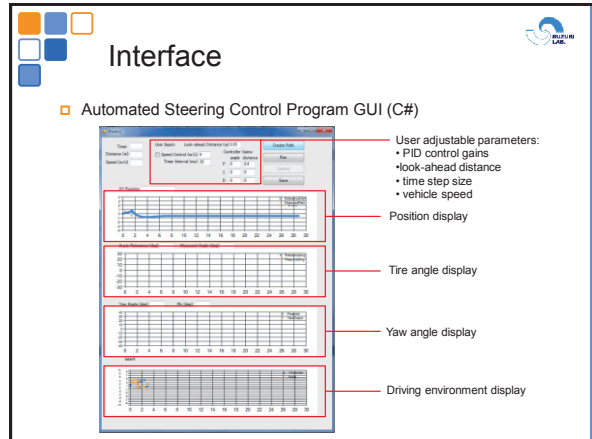
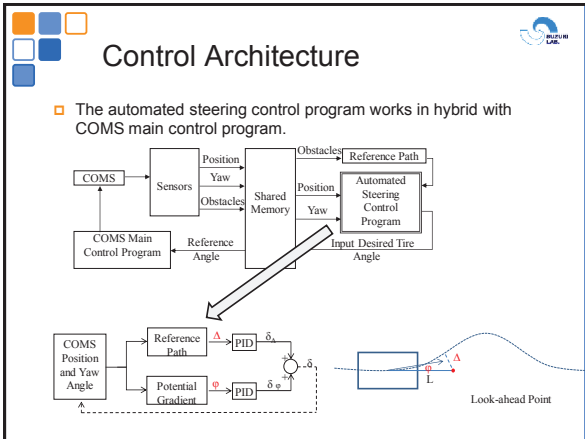
## Basic Idea of potential function



- Detecting the location of the obstacles and boundary of the road by LRF, the potential field function of the driving environment is determined.
- The reference path is calculated as:
  - Given the potential function:  $U(x,y)$
  - The direction vector at time t is:  $[v_{x_t}, v_{y_t}]^T = -\nabla U(x_t, y_t) = \left[ \frac{\partial U(x,y)}{\partial x}, \frac{\partial U(x,y)}{\partial y} \right]^T_{x=x_t, y=y_t}$
  - The vehicle location at time t+1 is then:  

$$x_{t+1} = x_t + d \cos \left( \tan^{-1} \left( \frac{v_{y_t}}{v_{x_t}} \right) \right) \quad y_{t+1} = y_t + d \sin \left( \tan^{-1} \left( \frac{v_{y_t}}{v_{x_t}} \right) \right)$$
 ,where d is a small distance interval.











## Discussion and Conclusion

- This experiment still need more testing to be done to find the PID gains and look-ahead distances for better performance.
- K-means method can successfully generate reference path in Matlab, but it can't use in real driving environment which is too complicated to generate the proper reference path.
- Our goal is using different weigh values in obstacles and side walls. However, we still use the same value for them in the particle experiment. The reason for using same weight value is potential function creating by each points and reference path will change significant even just a slight change for weight value.



Q&A

MICHIGAN ENGINEERING  
UNIVERSITY OF MICHIGAN • COLLEGE OF ENGINEERING

## Cold forge spot bonding of Copper and Aluminum alloy sheets

Nagoya University  
Department of Materials Science and Engineering  
Ishikawa and Yukawa Laboratory  
Yingrui Zhan

2014/8/7 1

MICHIGAN ENGINEERING  
UNIVERSITY OF MICHIGAN • COLLEGE OF ENGINEERING

## Category


- Introduction
- Cold forge spot bonding
- Experimental conditions
- Cross tension testing
- Microstructure of fracture surfaces
- Finite Element Analysis in DEFORM-2D
- How to determine friction coefficient
- Simulation results
- Discussion and Conclusion

2014/8/7 2

MICHIGAN ENGINEERING  
UNIVERSITY OF MICHIGAN • COLLEGE OF ENGINEERING

## Introduction

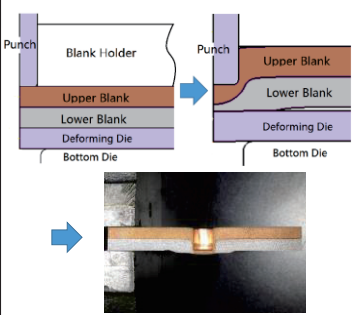
- Joining of Copper and Aluminum sheets greatly enhances the conductivity and resistance to corrosion while maintaining the light weight and low cost.
- This technology could be applied in marine industry, power industry, aerospace industry and so on.



2014/8/7 3

MICHIGAN ENGINEERING  
UNIVERSITY OF MICHIGAN • COLLEGE OF ENGINEERING

## Cold forge spot bonding



- A method of back extrusion for joining dissimilar metal sheets.
- As punch is moving downward, the upper blank pushes the lower blank and both are deformed locally. Then they are bonded together by the high surface pressure and large surface expansion.
- Compared to other methods, it does not require complicated machines or preparations and has low cost.

2014/8/7 5

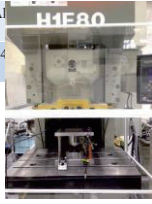
MICHIGAN ENGINEERING  
UNIVERSITY OF MICHIGAN • COLLEGE OF ENGINEERING

## Experimental Conditions

Material	Part	Thickness /mm	Ultimate tensile strength /MPa	Flow stress /MPa
C1100P	Upper sheet	3.0	234.32	$\sigma = 367e^{-0.152}$ $\sigma = 160e^{-0.100}$ $\sigma = 1568e^{0.21}$
AlS4	Lower sheet	3.0		

300kN Mechanical Link Servo Press

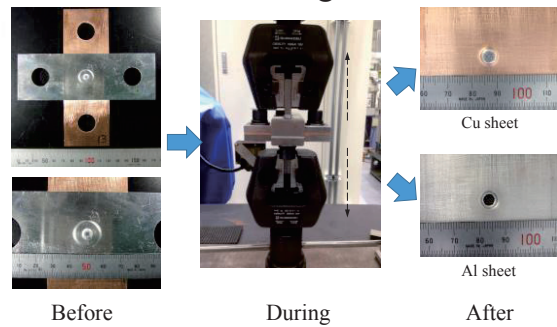
- Punching speed: 1.35spm
- Punch diameter: 5.0mm
- Amount of punch indentation: 4.0mm; 4.5mm; 5.0mm; 5.5mm; 6.0mm.
- Maximum load during experiment: 40.32kN



2014/8/7 6

MICHIGAN ENGINEERING  
UNIVERSITY OF MICHIGAN • COLLEGE OF ENGINEERING

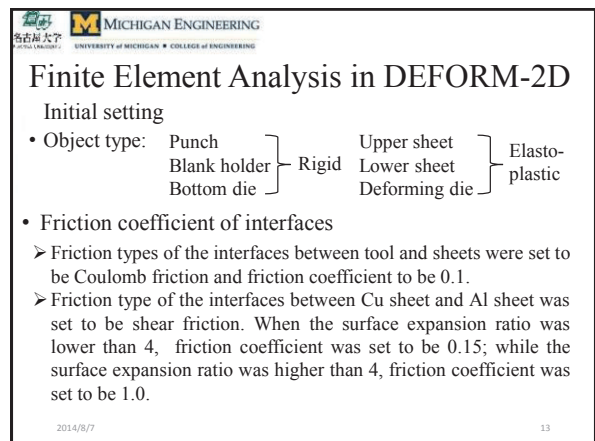
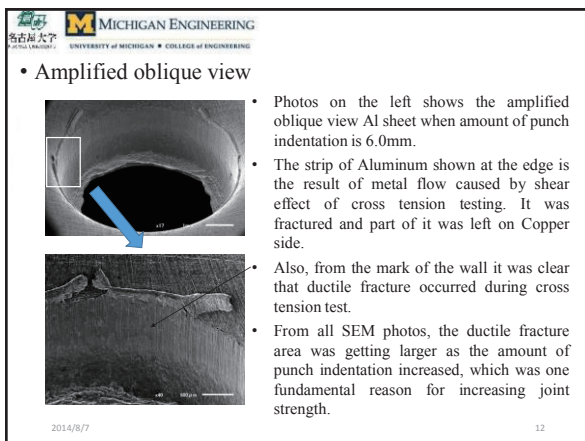
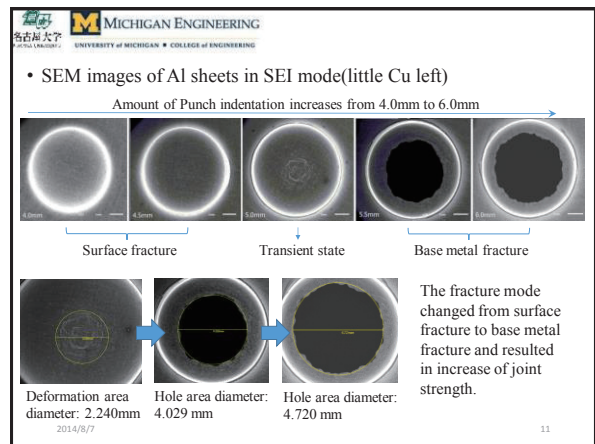
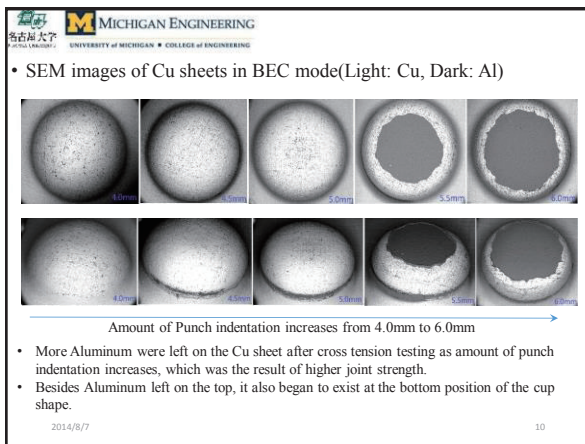
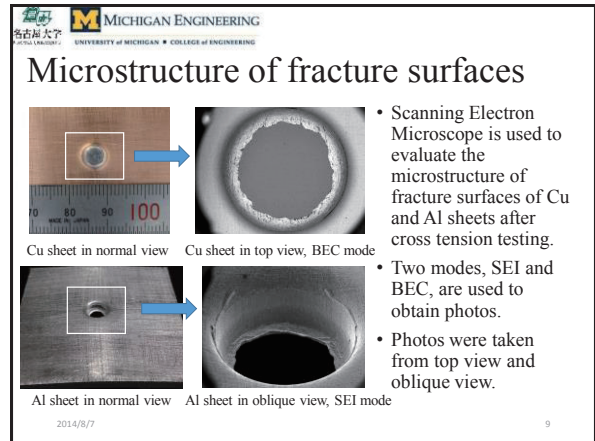
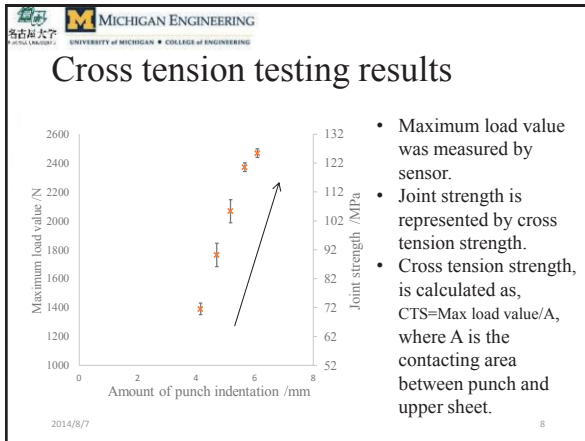
## Cross tension testing



Before During After

2014/8/7 7





**How to determine friction coefficient**

The friction coefficient of interface between Cu and Al is the most important factor in simulation, compared to other friction coefficient. Friction coefficient of other interfaces were set to be 0.1, which was according to previous work<sup>(1)</sup>.

1, Assume the friction coefficient is according with the model on left. a and b are unknown parameters.

Friction coefficient, m

Surface expansion ratio, S

$S \leq a, m = b$   
 $S > a, m = 1.0$

©1 for Minerva, Tadatoshi Ishiguro, GJ Aba, Nobuki Takano, Takashi Ishikawa, Tetsuro Suganuma. Cold-chamber spot bonding of high-tensile strength steel and aluminum alloy sheets. 11<sup>th</sup> International Conference on Technology of Plasticity, 2014. 2014/8/7

2, Use SEM to measure the diameters of strongly bonded area of different punch indentation in experiment, which was shown in previous slide.

3, Measure the dimension of dead zone of Cu and Al sheets after spot bonding process. Also obtain that from simulation.

2014/8/7

**Max Surface Expansion Ratio of Al sheet**

4, Try out different combinations of a and b. When the dimensions of experiment and simulation are roughly close to each other, obtain the data as shown on left and make sure of a.

5, Try out different b in simulation and continue to compare the dimensions until they are very similar to each other. Then b is figured out. So a=4, b=0.15. When surface expansion ratio is 4, friction coefficient changes from 0.15 to 1.

2014/8/7

**Simulation Results**

- Points spaced 0.1mm apart at the interface between Cu and Al sheets were created.
- Relevant parameters of cold forge spot bonding process at these points were obtained by point tracking function of DEFROM-2D.
- The x axis values of these points representing radius changed as the spot bonding process went.

2014/8/7

**Distribution of surface expansion ratio of lower sheet,  $S_{Al}$**

**Max Surface Expansion Ratio of Al sheet**

- $S_{Al} = A/A_0$ ,  $A_0$  is initial area and A is the final area of surface element.
- Max surface expansion ratio for Cu-Al bonding is greatly higher than that for Steel-Al bonding.
- Large surface expansion ratio areas are concentrated for  $r < 3mm$ .

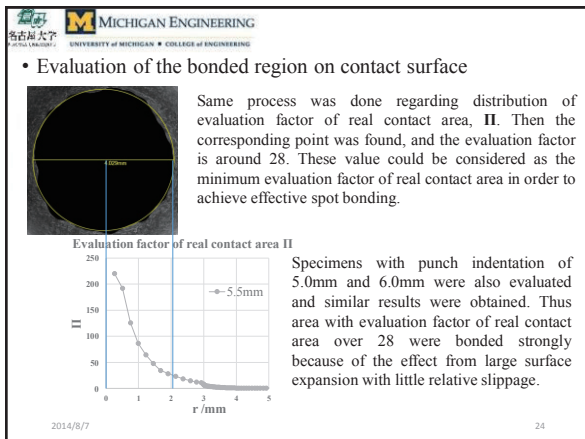
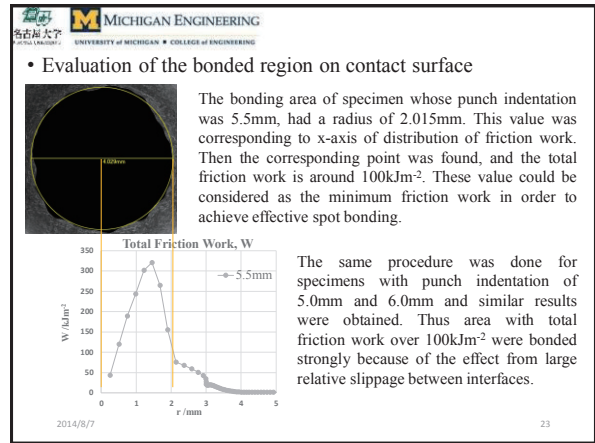
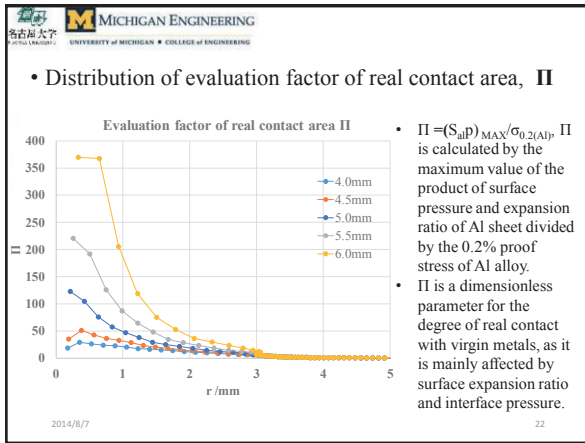
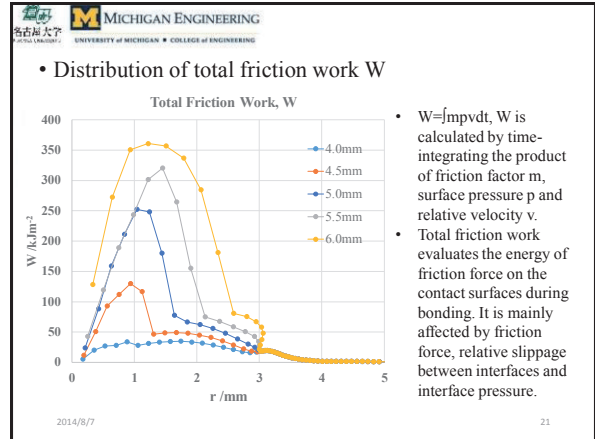
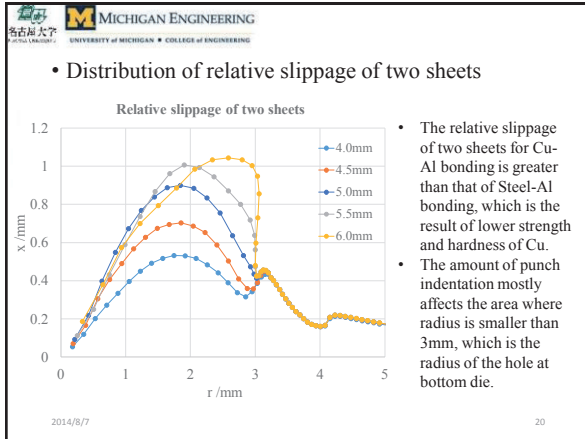
2014/8/7

**Distribution of maximum surface pressure  $p_{max}$**

**Maximum Surface Pressure**

- Max interfaces pressure increases as the punch goes deeper, while decreases as the point is further away from center.
- This parameter is lower compared to the Steel-Al bonding, mainly because the strength of Cu alloy is much lower than that of high tensile strength steel.


2014/8/7



**Discussion and Conclusion**

1. Joining of Cu and Al alloy sheets is successfully achieved at room temperature by cold forge spot bonding technology.
2. When the amount of punch indentation reached around 4.0mm, Cu and Al sheets were able to be bonded. As it continued to be higher, the bonding area and bonding strength were increasing.
3. Base metal fracture began to exist after cross tension testing when the amount of punch indentation reached 5.0mm. Before that, the bonding form of two sheets were more like adhesion than metallurgical bonding.

2014/8/7 25

 MICHIGAN ENGINEERING  
UNIVERSITY OF MICHIGAN • COLLEGE OF ENGINEERING

## Acknowledgements

I would like to express my gratitude for JUACEP, Professor Ishikawa and his Material Deformation and Processing Laboratory for all the guidance and help given to me. I learned a lot from Professor Ishikawa and my fellow students regarding academic attitudes, knowledge and skills. This experience is my lifelong treasure.

2014/8/7 26

 MICHIGAN ENGINEERING  
UNIVERSITY OF MICHIGAN • COLLEGE OF ENGINEERING



감사합니다 Natick  
Danke Ευχαριστίες Dalu Obrigado  
Thank You Köszönöm  
Grazie Tack  
Спасибо Dank Gracias  
谢谢 Merci Seé ありがとう

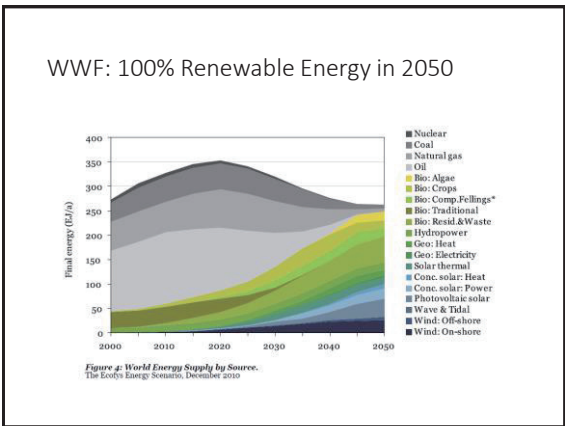
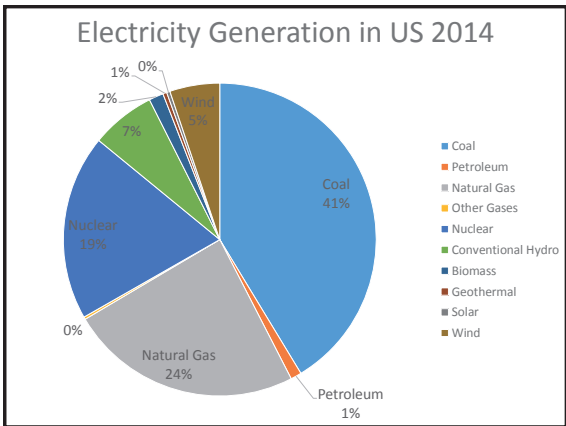
2014/8/7 27

## Dynamic Modelling of Combined Cycle Gas Turbine

For Load Frequency Control Considering Power Output Fluctuation of  
Renewable Energy Generators

### Background

- Renewable energy is generally defined as energy that comes from resources which are naturally replenished on a human timescale such as sunlight, wind, rain, tides, waves and geothermal heat.
- Usage: Power Generation, Heating and Transportation (EV)
- Types of Renewables:
  - Hydropower, wind power, PV, solar thermal, geothermal and biomass
- Growth of renewables:
  - 10-60% annually for many technology
- Economic trends:
  - Renewable energy are getting cheaper



### Characteristics of Renewable Energy Gen.

- Characteristics depend on type of renewables
- Generally difficult to predict and control
- Large penetration of renewables need
- Power Generated by renewable energy generators depend greatly on the condition natural environment.
- Many renewable energy plants need a large place to implement
- The idea of micro-grid and distributed generation also encourage the installation of PV panels and wind turbines.

### Load Frequency Control (LFC)

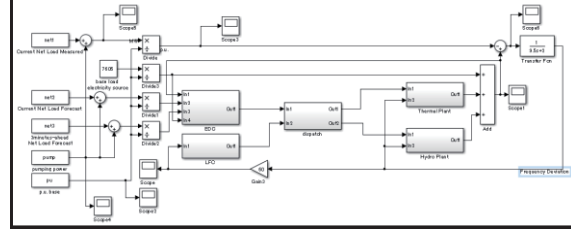
- Power grid requires that generation and load closely balance moment by moment, frequent adjustments to the output of generators are necessary.
- Unbalance between Load and Generation lead to the fluctuation of frequency in the grid:
  - Generation > Load + Loss → Frequency +
  - Load + Loss > Generation → Frequency -
- Therefore, frequency fluctuation act as a sign of the mismatch of generation and load. LFC could be seen as a Process of Rebalancing

### Economic Dispatch Control (EDC)

- Cost is one of the most major concerns in power system.
- Economic dispatch is the short-term determination of the optimal output of a number of electricity generation facilities, to meet the system load, at the lowest possible cost, subject to transmission and operational constraints.
- Main Idea:  
The set of generators with the lowest marginal costs must be used first
- Basic Method of EDC:  
Solving a group of mathematical equations considering the cost of generation together with system constraints.

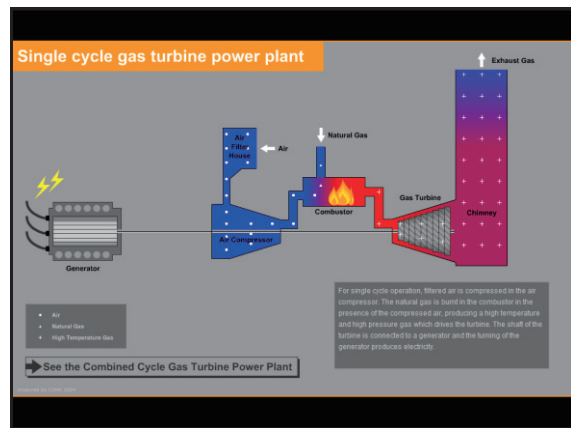
### Matsumoto's Model

- Hybrid System: PV, Thermal, Hydro Plants
- Load Frequency Control and Economic Dispatch Control
- PV Forecasting, Load Measurement and Forecasting



### Introduction of Combined Cycle Power Plant

1. Single Cycle Gas Turbine (SCGT)
  - Major Components:  
Air inlet, compressor, fuel valve system, gas turbine, combustor, electric generator
  - Overall Thermal Efficiency: 35%
2. Combined Cycle Gas Turbine (CCGT)
  - Heat Recovery Steam Generator (HRSG)  
Make use and extract energy from the exhaust gas  
Improve efficiency by 50%
  - Overall Thermal Efficiency: 60%



### Rowen's Model (Single Cycle Gas Turbine)

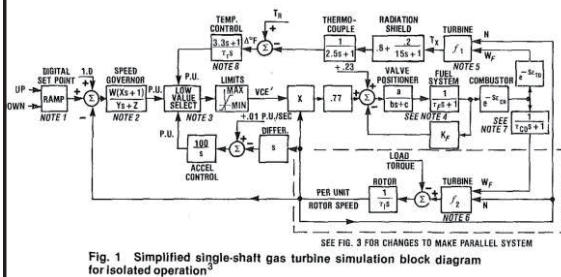
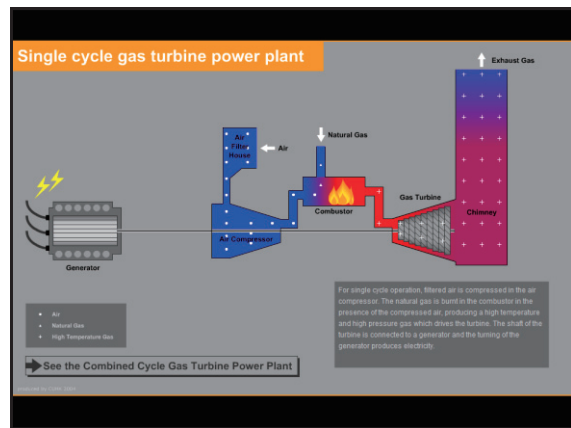
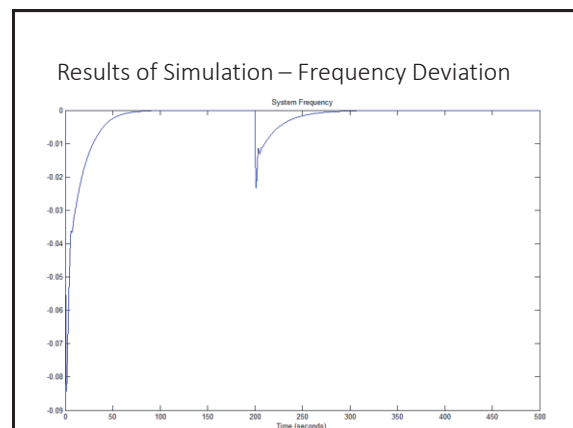
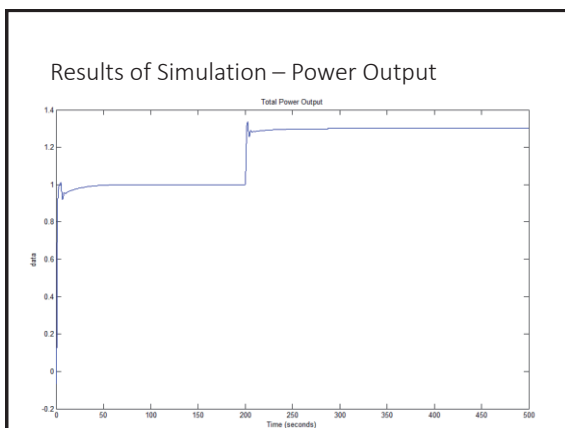
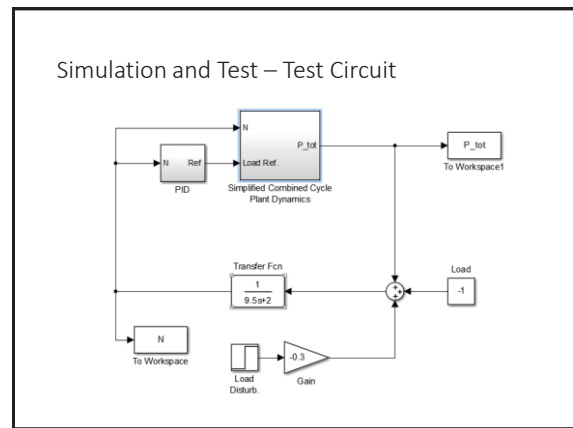
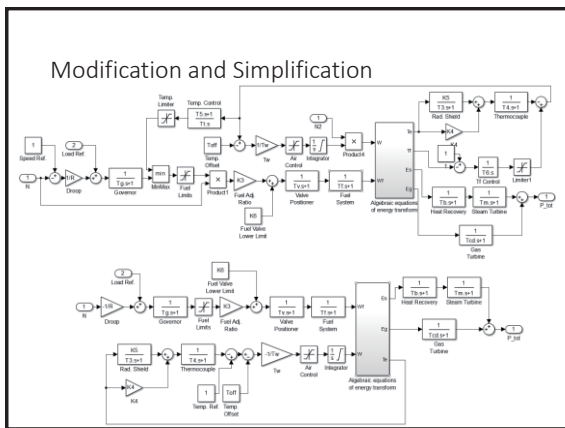
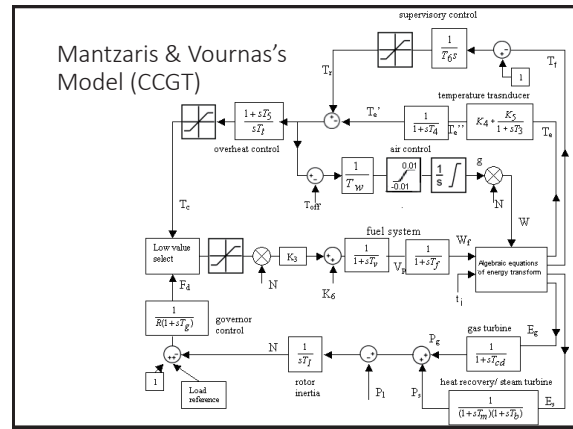
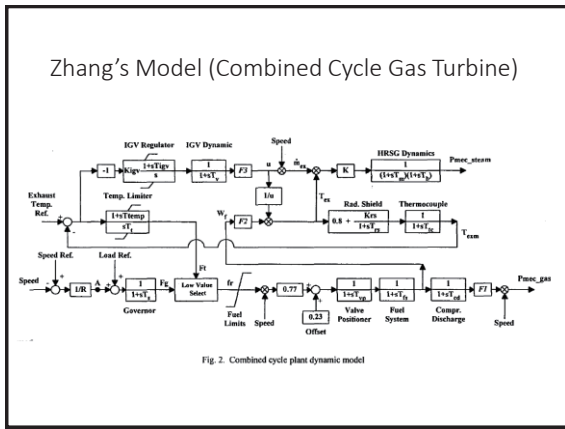
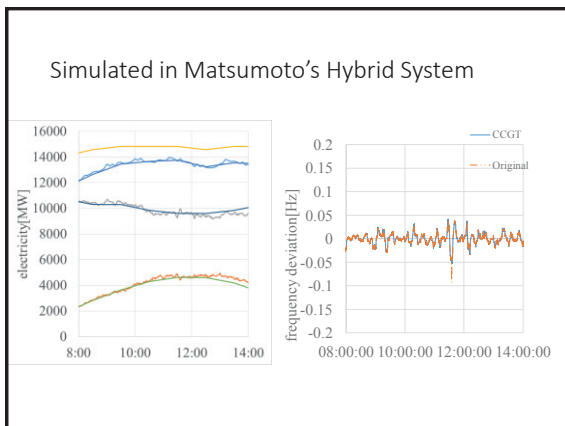
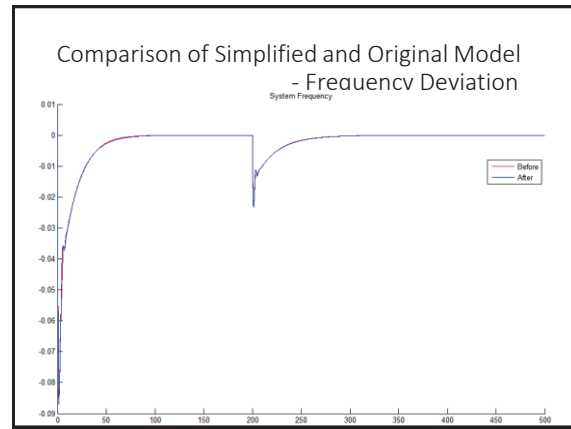
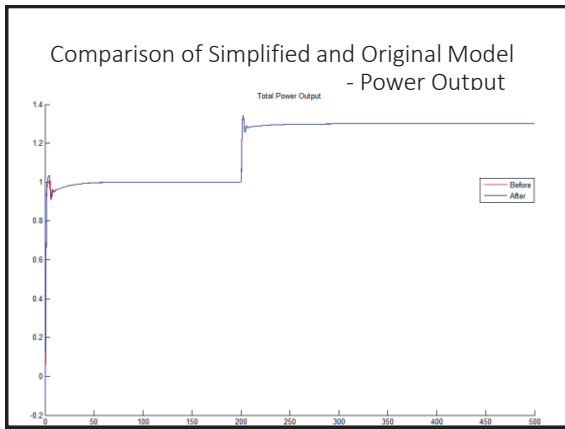


Fig. 1 Simplified single-shaft gas turbine simulation block diagram for isolated operation








References

- WWF, "The Energy Report", page 24, 2011.
- U.S. Energy Information Administration, "Monthly Energy Review Jul 2014", page 95, 2014.
- Rowen, W.I., "Simplified mathematical representations of heavy-duty gas turbines," Journal of Engineering for Power, Vol. 105, pp. 865-869, October 1983.
- Zhang, Q., So, P. L., "Dynamic Modelling of a Combined Cycle Plant for Power System Stability Studies", IEEE Power Engineering Society Winter Meeting, Vol. 2, pp. 1538-1543, 2000.
- Mantzaris, J., Vournas, C. "Modelling and Stability of a Single-Shaft Combined Cycle Power Plant", Int. J. of Thermodynamics, Vol. 10 (No. 2), pp. 71-78, June 2007.

Q & A




1




**JUACEP** Japan-US Advanced Collaborative Education Program  
 Gain Engineering Research Experience in Nagoya and USA

## ASSEMBLY OF MULTI-LAYER STRUCTURED BLOOD VESSEL

**YONG, Yang**  
 Department of Biomedical Engineering,  
 University of Michigan


**M MICHIGAN ENGINEERING**  
 UNIVERSITY OF MICHIGAN • COLLEGE OF ENGINEERING

Supervisor: Prof. ARAI, Fumihito  
 Tutor: YAMAGISHI, Yuka  
 Department of Micro-Nano Systems  
 Engineering, Nagoya University



**Biorobotics LAB**  
 NAGOYA UNIVERSITY

2

## OVERVIEW

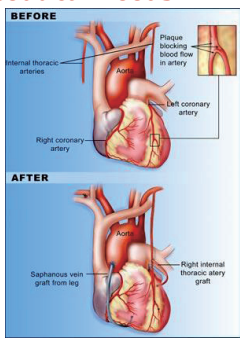
- > Background
  - Clinical needs
  - Vascular tissue engineering
  - Structure and mechanical characteristics of blood vessels
  - Previous research
- > Experiment and Result (2)
  - Layer-by-layer technique
  - Cell lines and dyes
  - Fabricated blood vessels
- > Discussion and Conclusion
  - Future plan
  - Barrier for clinical translation
- > Acknowledgement
- > References
- > Appreciation

- > Goal
- > Experiment and Result (1)
  - Design Concept of Bio-assembly
  - PLCL scaffold and dip-coating method
  - Scaffold fabrication condition

3

## Clinical and Pharmaceutical Needs

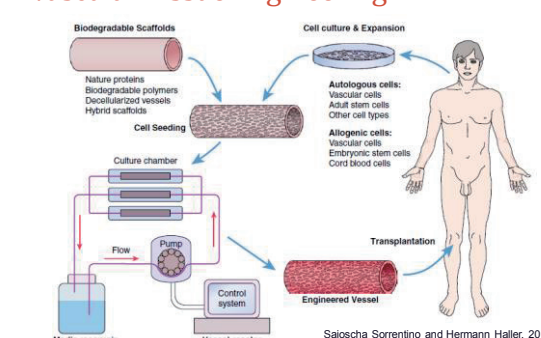
- **Cardiovascular Diseases**
  - leading cause of death worldwide
  - Coronary Artery Disease (40%)
- **Treatment:**
  - Coronary/peripheral bypass surgery
- **Vascular grafts** (small blood vessels with inner diameter < 6 mm):
  - *Autograft:* not available in up to 40% of the patients
  - *Synthetic:* thrombosis, graft failure, no growth potential, etc.
  - *Promising Solution:* Vascular Tissue engineering



Columbus University Medical Center, 2012

4

## Vascular Tissue Engineering

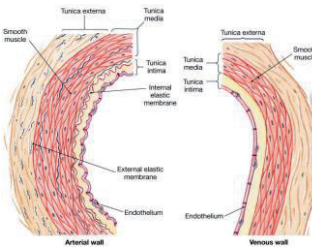


Sajoscha Sorrentino and Hermann Haller, 2011

5

## Structure of Blood Vessel

- **Tunica Adventitia:**
  - fibroblast, collagen, and ECM matrix
  - cell trafficking, immune response mediation and vascular remodeling
- **Tunica Media:**
  - smooth muscle cell (SMC)
  - maintaining homeostasis and remodeling, mechanical support
- **Tunica Intima:**
  - endothelial cells
  - semi-permeable membrane



Robert Droual, 2011


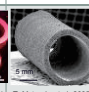
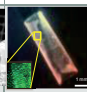
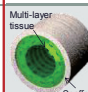
Target blood vessels

Multilayered structure

High cell density

Three different cells

## Previous Research

	Inkjet	Scaffold	3D tissue assembly	Scaffold & 3D tissue
	 <small>Y. Matsunaga et al., 2011</small>	 <small>T. Matsuda et al., 2005</small>	 <small>Y. Yamagishi et al., 2013</small>	 <small>Multi-layer tissue Scaffold</small>
Stiffness	High	High	Low	High
Cell Density	Low	Low	High	High
Size	mm	mm	µm~mm	mm

### Goal

- To fabricate a blood vessel with multi-layer structure that mimics natural small blood vessel biologically (composition, functionality) and mechanically (compliance similar to artery).
- Composed of fibroblast (multi-layer), SMCs (multilayer) and endothelial cells from outer to inner layer, among which, ECM components should also be incorporated.

**Reference blood vessel:**  
**External Carotid Artery (ECA)**  
 Diameter ≈ 3~4 mm  
 Young's module ≈ 0.8 MPa  
 Thickness ≈ 380 μm

### Design Concept

- 1) Make a tubular scaffold through dip-coating. (Glass capillary, Solution of PLCL in chloroform)
- 2) Cut open the tubular PLCL scaffold.
- 3) Assembly multilayered tissue using Layer-by-Layer method. (Fibroblasts, Gelatin, Layer-by-layer assembly, Single cell, FN-G coated cell, FN-G coated cell)
- 4) Fix flatly a PLCL scaffold using jigs and coat the multilayered tissue onto the scaffold. (PLCL scaffold, Jigs, Suspension of FN-G coated cells)
- 5) Release PLCL scaffold from the jigs. Bond two free edges by a biocompatible adhesion to fabricate a tubular tissue. (Multilayered tissue, biocompatible adhesion)

### PLCL (Poly-(L-lactide-co-ε-caprolactone))

- Biocompatible and Biodegradable (slow)
- Mechanical characteristics mimic natural blood vessel
- Flexible and highly elastic
- Highly porous that supports cell attachment (previous: fibroblast and SMC)

SEM of PLCL with 90% porosity

Schematic diagram of chemical structure of the PLCL copolymer:  
 L-Lactide(LA) + ε-Caprolactone(CL) → PLCL

Jeong, et al. 2004

### Dip-Coating Technique

**Dip-coating:**  
 Mold (Glass capillary) → Dip coating → PLCL NaCl → Salt leaching → PLCL

Salt leaching: to create porous structure

- Control the scaffold properties by dip-coating times and composition of PLCL solution
- Control the porosity by amount and size of NaCl crystal

### Material tests of PLCL scaffold

Test conditions (N = 3)

Ratio of PLCL to chloroform	5 wt%, 3 wt%
Composition ratio of NaCl : PLCL	2:8, 4:6
Dip coating number	2 ~ 6

**Tension test (ring type)**  
 JIS K 6251 compliant

P: Force, t: Thickness, d: Width, A: Cross-section  
 L: Test piece's circumference  
 L<sub>1</sub>: Jig's circumference,  
 Δl: Displacement

$$Young's\ module\ E = \frac{\sigma}{\epsilon} = \frac{P/A}{(L - L_0)/L_0} = \frac{P \times L_0}{(2\Delta l + L_1 - L_0) \times 2 \times t \times d}$$

Tension speed = 30 mm/min

### PLCL scaffolding Condition

**Young's module**

**Thickness**  
 (5wt% PLCL in chloroform, NaCl : PLCL = 4 : 6)

Chloroform : PLCL	95 : 5
NaCl : PLCL	4 : 6
Particles diameter of NaCl	53 ~ 100 μm
Number of coating	6
Pull-up velocity	3.0 mm/s

13

### Layer-by-Layer (LbL) Assembly

- High viability (b) compared to (a) because of reduced physical stress caused by centrifugation
- High cell density
- Thickness of tissue layers
- Arbitrary shapes
- Multilayers structure with different cell types

*Fibronectin*: ECM protein  
*Gelatin*: Gel, assist cell adhesion

Layer-by-layer assembly  
Single cell → FN-G coated cell → Cell accumulation → 1 day → 3D multilayered tissue

M. Matsusaki, et al., 2011  
Y. Yamagishi, et al., 2014

### Fabricated Blood Vessels

Cell lines and dyes:

	Fibroblasts	SMCs	Endothelial cells
Cell line	NIH3T3	MOVAS 7	UV-9.2
Dye	Hoechst 33342 (Blue)	Calcein AM (Green)	Hoechst 33342 (Blue)*

Diameter: 3mm  
Length: 15mm

Two tunica layer: **Fibroblast & SMC**  
Cross-section: Enlarged view: Three tunica layer: **Fibroblast & SMC & Endothelium**  
Side section:

Labels in images: Glass, Scaffold, Derma bond, 5 mm, 500 μm, 50 μm, Mono-layered endothelial cell.

15

### Conclusion

- Successfully fabricated a multilayer structured blood vessel, with length = 15mm, diameter = 3mm, thickness = 380μm, Young's modulus = 0.78MPa. The blood vessel contains three different cell lines well attached to each other and the scaffold in static station.
- Need to do perfusion test for compatibility of shear stress caused by high flow rate and blood pressure, and monitor the cell attachment and cell viability with different bio/ chem/ mechanical cues.
- For long-term study, the degradation rate of the PLCL and the change of mechanical properties, the replacement of the cell tissues should be monitored as well.

16

### Future Plan & Potential Barrier

- Test the fabricated blood vessels using the perfusion cultivation system.
- Change cell lines as patient/animal specific ones.
- Transplant to animal model for long-term observation and check the degradation of scaffold and viability/ functionality of the construct.
- Most important, the substitution of the scaffold with tissue and the integration of the graft to the body.
- For clinical translation, the first concern is hard for automation, that is, the bio-assembly step should be engineered/ optimized.
- Maximize the functionality of the engineered vascular graft using growth factors (e.g., VEGF).
- Immunogenicity tests will also be necessary if used on patients.

17

### References

- Jeong, S., et al. "In vivo biocompatibility and degradation behavior of elastic poly(L-lactide-co-ε-caprolactone) scaffolds". *Biomaterials* 25, pp. 5939-5946, 2004.
- Matsusaki, M., et al., "Rapid construction of three-dimensional multilayered tissues with endothelial tube networks by the cell-accumulation technique," *Adv Mater*, vol. 23, pp. 3506-3510, 2011.
- Sajoscha Sorrentino and Hermann Haller, "Tissue Engineering of Blood Vessels: How to Make a Graft", in "Tissue Engineering, From Lab to Clinic". Springer, New York, 2011
- Yamagishi, Y., et al., "Microfluidic perfusion cultivation system for multilayer structured tubular tissues," *The 17th international conference on miniaturized systems for chemistry and life sciences*, no. 1213, 2013.

18

### Acknowledgement

- This experiment is done at Arai Lab, Nagoya University, and fully supported by Dr. Taisuke Masuda, Yuka Yamagishi and Mitsuhiro Ukiki.
- My sincere appreciations to Professor Fumihito Arai, Professor Katsuo Kurabayashi at University of Michigan, the JUACEP staff at Nagoya University and IPE (International Programs of Engineering) staff at University of Michigan.

19

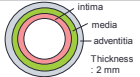


# THANK YOU

---

20

## Appendix

### Mechanical Characteristics

Kinds of artery	diameter	Blood flow	Blood pressure	Blood vessel structure
Aorta	1.5-2.7 cm	63 cm/sec	85-130 mmHg	
Artery	5-9 mm	20-50 cm/sec		
Arteriole	0.2-0.5 mm	5 cm/sec	35 mmHg	
Blood capillary	0.007-0.1 mm	0.05-0.1 cm/sec	15 mmHg	

Target blood vessels  
 Diameter : 2~6 mm  
 Blood pressure : 60~70 mmHg (8000~9300 Pa)  
 Blood flow : 200~500 mm / sec

22

### Compliance

- The concept of "compliance" : "encompassing the changing mechanical properties depending on the hemodynamic pressure within the graft".
- At a given pressure  $P$  in a vessel of diameter  $d$  and wall thickness  $t$ , its Young's modulus ( $E$ ):
 
$$E = \frac{\text{stress}}{\text{strain}} = P \frac{d/2t}{\Delta d/d} \quad (1)$$
- Rearranging equation (1),
 
$$\text{Compliance} = \frac{d}{2Et} \quad (2)$$
- The compliance of the fabricated blood vessel is 5.1, fits the range of a natural artery

### ***The 10th JUACEP Workshop***

**Date:** August 29 (Fri)

**Venue:** VBL Hall, Nagoya University

**Timetable:**

14:00            Opening ~Address from Dean of Graduate School of Engineering~  
14:10 - 17:00   Presentations by UCLA students  
                    (15 mins. presentation + 4 mins. Q&A each)  
17:00 - 17:10   Award Ceremony  
17:30 -            Farewell Banquet

**~Presentation Title~**

**1: Zihe He (P.132)**

“Bonding in Chip Fabrication for Cell Stiffness Measurement”

**2: Tait Dewitt McLouth (N/A)**

“Quantitative Evaluation of Carbon Fiber Content in CFRP Using Microwave Analysis”

**3: Yuan Hung Lo (N/A)**

“Made to Stick: Adhesive Bacterionanofiber AtaA and Quorum Sensing in Bacterial Immobilization”

**4: Mark Kristopher Seal (P.136)**

“Analysis of Solution Growth Conditions on Silicon Carbide (SiC) Polytype”

**5: Yingxia Liu (N/A)**

“Thermal Stress and Strain Analyses of TSV and Microbumps in 3D IC Using Abaqus” (N/A)

**6: Jose Eduardo Gaviria (P.140)**

“Manufacture and Characterization of Boron Oxide Solid Lubricant Using RF Magnetron Sputtering at Low-Vacuum”

**7: Song Dong (P.144)**

“Analysis of Vehicle's Crash Based on Structures' Section Forces”

**8: Yue Huang (N/A)**

“Slip Control for Contact Motion Reproduction”

# Bonding in Chip Fabrication for Cell Stiffness Measurement

Student: Zihe He (Martin)  
 Year: Master 1<sup>st</sup> year  
 Instructor: Fumihito Arai  
 Department: Mechanical Engineering in UCLA  
 Lab: Arai lab in Nagoya University

## Background

- Why cell stiffness?
- Cell stiffness can help identify disease cells and sort them out. A number of pathophysiological states of individual cells result in drastic changes in stiffness in comparison with healthy counterparts. Mechanical stiffness has been utilized to identify abnormal cell populations in detecting cancer and identifying infectious disease.

## Introduction

Former version of the microfluidic chip

Piezoelectric Actuator & Cell Injection Device

## Introduction(Cont.)

## Introduction(Cont.)

Hertzian contact theory

$$P = \frac{4(D/2)^{3/2} \cdot E_c \cdot (\delta/2)^{3/2}}{3(1-\nu^2)}$$

$E$ : Young's modulus  
 $\nu$ : Poisson's ratio  
 $P$ : Force  
 $D$ : the size of the cell  
 $\delta$ : deformation of the cell

$$E_c = \frac{3(1-\nu^2)P}{4(D/2)^{3/2} \cdot (\delta/2)^{3/2}}$$

## Fabrication Process

Three layers:  
 Cover glass layer  
 SOI device layer  
 Holding glass layer

Main steps of chip fabrication:  
 Mask design } Build pattern  
 Photolithography }  
 Etching }  
 Sputtering } Packaging  
 Bonding

### Sputtering

- By first creating a gaseous plasma and then accelerating the ions from this plasma into some source material (a.k.a. "target"), the source material is eroded by the arriving ions via energy transfer and is ejected in the form of neutral particles. As these neutral particles are ejected they will travel in a straight line to substrate

### Sputtering (Cont.)

- We need metallic intermediate layer between cover glass and wafer as circuit, so some method to deposit thin film of metal on cover glass is desired.
- Common methods to deposit thin films:
  - CVD (Chemical Vapor Deposition) & PVD (Physical Vapor Deposition)
  - PVD is more reliable and able to generate smoother film
  - PVD methods:
    - Thermal Evaporation, E-beam Evaporation and sputtering.

### Sputtering (Cont.)

- By first creating a gaseous plasma and then accelerating the ions from this plasma into some source material (a.k.a. "target"), the source material is eroded by the arriving ions via energy transfer and is ejected in the form of neutral particles. As these neutral particles are ejected they will travel in a straight line to substrate

### Sputtering (Cont.)

Deposition	Material	Typical Equipment	Impurity	Deposition Rate	Temperature Range	Cost
Thermal	Al, Ag, Au, Cu, Cr, Ni, Pt, Ti, W, Zn	High Vacuum	High	1 - 20 Å/s	~1000 °C	Low
E-beam	Al, Ag, Au, Cu, Cr, Ni, Pt, Ti, W, Zn	High Vacuum	Low	10 - 100 Å/s	~1000 °C	High

For sputtering: Deposition of Al is around 170 Å/s. Cu is about 320 Å/s

### Sputtering (Cont.)

Evaporation	Sputtering
Low energy atoms (~0.1 eV)	High energy atoms / ions (1 - 10 eV)
High Vacuum	Low Vacuum
Point Source	Parallel Plate Source
Component Evaporate at Different Rate	All Component Sputtered with Similar Rate
Nonconformal, Line of sight process	Conformality Depends on Plasma Conditions

### Sputtering (Cont.)


- Two combinations we used as intermediate layer are shown below:
  - Chromium & Aluminum
    - Chromium works as adhesive layer while aluminum works as conductor
    - We did the sputtering twice, for the first time the film was smooth and acceptable; for the second time there was mossy area as shown
- Resistivity (20 °C):
  - Aluminum : 28.2 nΩ m
  - Chromium : 125 nΩ m

### Sputtering (Cont.)


- Possible reason for the mossy area:
- we were probably getting a columnar morphology, which gives a "massy" white or grey appearance. The columnar structure develops when the film is deposited on a grainy (not smooth) surface or when the film thickness exceeds several hundred nanometers (and there is no concurrent bombardment during deposition)

### Sputtering (Cont.)

- 2. Copper
- For sputtering of Copper on cover glass, we tried both RF sputtering and DC magnetron Sputtering. RF gave us uneven film, but the result from DC magnetron was pretty good.
- Cu Resistivity: 16.78 nΩ m




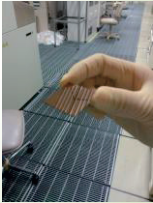
RF (radio frequency) Sputtering System



DC magnetron Sputtering System

### Sputtering (Cont.)

- Parameter and result of coppersputtering

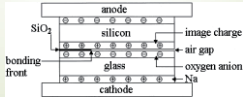



### Bonding

- Bonding affects hermeticity of chip
- Common bonding methods:
  1. Fusion Bonding (Direct bonding)
    - Usually used for bonding of glass and silicon, strict requirement
  2. Anodic Bonding
    - Relatively easy to do, intermediate layer is ok
  3. Eutectic Bonding
    - Need much research in eutectic alloy
    - Ex: Al-Ge, 49/ 51 wt%, eutectic temperature is 419 °C
  4. Diffusion Bonding (Thermo-compression bonding)
    - Require temperature up to 1000 °C , moving parts may be attached



### Anodic Bonding

- Concept:
- 4.2% Na<sub>2</sub>O exists in Pyrex.glass. Na<sup>+</sup> ions in the glass become so mobile that they are attracted toward the cathode
- Oxygen anion moves to the contact surface, and creates positive charge on silicon side
- High electric field combines Si and oxygen anion to get SiO<sub>2</sub>



### Anodic Bonding (Cont.)

- Pretreatment:
- Clean the cover glass with CUTE low pressure plasma system and ultrasonic cleaning system. Then spin-dry it.





CUTE low pressure plasma system (left), supersonic cleaning system (right)



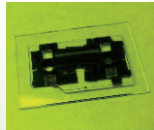
### Anodic Bonding (Cont.)

- Bonding with aluminum film:
- Bonding was a success but there was contaminant inside the cover glass. That white contaminant may be compound of diffused Al ions and oxygen anions, aka  $Al_2O_3$ . Chromium should have performed as diffusion barrier, but diffusion still happened. Bonding with mossy sputtering was a failure.



### Anodic Bonding (Cont.)

- Bonding with copper film:
- Success. Bonding is strong and we couldn't peel with our hand. Though some contaminant extracted on top of cover glass, it could be easily cleaned with piranha solution. However, what the contaminant is remains unknown.
- Unfortunately, the chip was still broken due to unbalanced force.



### Conclusion & Future work

- Anodic bonding with copper film works well, but we still need to figure out where the contaminant was from. Copper might diffuse into wafer and glass, though we didn't notice.
- Bonding with aluminum film is still a possible solution. We can increase the thickness of chromium or change it to TiN.
- We used n-type wafer during the bonding. If we change it to p-type, time needed can be reduced.
- Eutectic bonding and diffusion bonding are still worth attempt.

Wafer	p-type	n-type	Time
Bonding time	1	> 20	20
Time at 100 V	1	-	5
Bonding time	1	-	5
Time at 100 V	1.5	-	10
Bonding time	1.5	-	10
Time at 400 V	1.5	-	10

\*The obtained wafer surface  
 \*The obtained wafer surface  
 \*The obtained wafer surface  
 \*The obtained wafer surface

### Acknowledgement

- Special thanks to Professor Fumihito Arai and my tutor Hirofumi Sugiura. Professor Arai gave me this chance to do research and study in Arai Lab. Sugiura San taught me a lot about chip fabrication and answered a lot of questions in patience. Other lab members helped me with my study, research and life. Thank you.
- Of course, without JUACEP program I could not have such a great chance to stay in Japan for 2 and half months. Thank you, JUACEP.

### Reference

- Wang G, Mao W, Byler R, Patel K, Henegar C, et al. (2013) Stiffness Dependent Separation of Cells in a Microfluidic Device. PLoS ONE 8(10): e75901. doi:10.1371/journal.pone.0075901
- <http://www.ece.nyu.edu/courses/material/EE410-Wms/Part%206%20Thin%20Film%20Deposition.pdf>
- <http://www.ajaint.com/whats.htm>
- <http://www.linkedin.com/groups/Bright-coating-aluminum-sputtering-10-1390797.S.150650823>
- [http://en.wikipedia.org/wiki/Eutectic\\_bonding](http://en.wikipedia.org/wiki/Eutectic_bonding)
- Thomas M.H Lee, Debbie H.Y Lee, Connie Y.N Liaw, Alex I.K Lao, I-Ming Hsing. Detailed characterization of anodic bonding process between glass and thin-film coated silicon substrates, Sensors and Actuators A: Physical, Volume 86, Issues 1-2, 30 October 2000, Pages 103-107, ISSN 0924-4247, [http://dx.doi.org/10.1016/S0924-4247\(00\)00418-0](http://dx.doi.org/10.1016/S0924-4247(00)00418-0).
- [http://www.wafer-bumping.com/documents/techno/thin\\_film.html](http://www.wafer-bumping.com/documents/techno/thin_film.html)
- Diffusion barrier property of TiN and TiN/Al/TiN films deposited with EMCVD for Cu wire connection in ULSI, Young-Hoon Shin and Yukihiko Shimogaki 2004 Sci. Technol. Adv. Mater. 5:399

## Analysis of solution growth conditions on Silicon Carbide (SiC) Polytype

Mark Seal  
JUACEP Summer 2014  
Ujihara Group  
Nagoya University, Aichi Japan

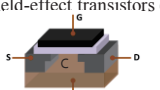
## Outline

- Introduction/Background
- Research Goal
- Methods/Results
- Analysis
- Conclusion
- Future Work

## SiC- a next generation semiconductor

Properties	Si	4H-SiC
Crystal Structure	Diamond	Hexagonal
Energy Gap : $E_G$ (eV)	1.12	3.26
Electron Mobility : $\mu_n$ (cm <sup>2</sup> /Vs)	1400	900
Hole Mobility : $\mu_p$ (cm <sup>2</sup> /Vs)	600	100
Breakdown Field : $E_B$ (V/cm) X10 <sup>6</sup>	0.3	3
Thermal Conductivity (W/cm°C)	1.5	4.9
Saturation Drift Velocity : $v_s$ (cm/s) X10 <sup>7</sup>	1	2.7
Relative Dielectric Constant : $\epsilon_s$	11.8	9.7

- Applications: high voltage power devices, such as metal-oxide-semiconductor field-effect transistors (MOSFET)



## Choosing the 'best' polytype

- Many polytypes of SiC

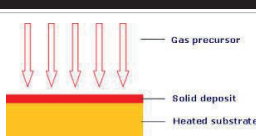
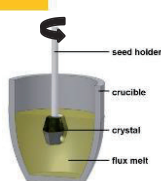
Parameters	3C-SiC	4H-SiC	6H-SiC
Bias Current Density (A/m <sup>2</sup> )	$3.7 \times 10^8$	$3.4 \times 10^8$	$3.5 \times 10^8$
Peak electric field (V/m)	$4 \times 10^8$	$4.25 \times 10^8$	$4 \times 10^8$
Breakdown voltage (V)	110	140	109
Peak frequency (THz)	0.353	0.325	0.350
Peak Conductance (S/m <sup>2</sup> )	$-1.52 \times 10^8$	$-1.65 \times 10^8$	$-1.01 \times 10^8$

- 4H-SiC is the best?
  - Not for MOSFET application
  - "Electron trapping in SiO<sub>2</sub>/3C-SiC systems is suppressed"

H. Uchida et al., Materials Science Forum 717-726, (2012) 311

## Growing Pains

- Epitaxial growth
  - Substrate(Si) mismatch (~20% !)
  - Introduce stacking faults
  - CTE difference
  - Low crystal quality
- Top-Seeded Solution Growth (TSSG)
  - Preferentially grow 3C-SiC

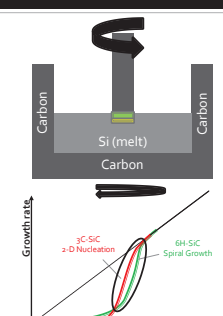



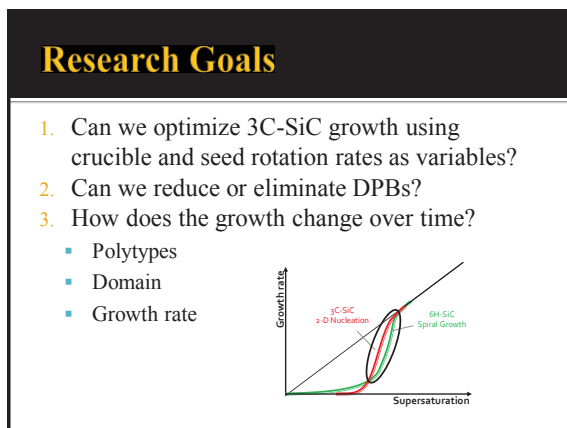
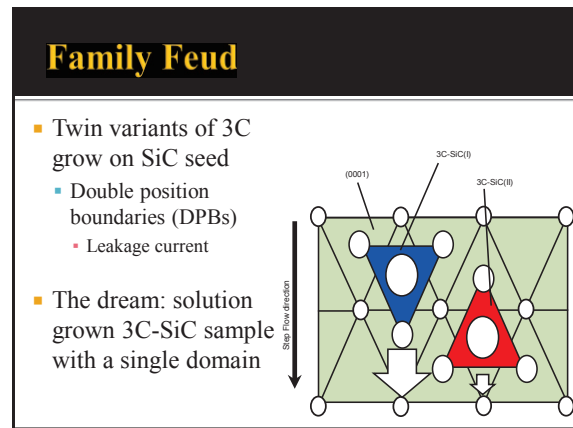
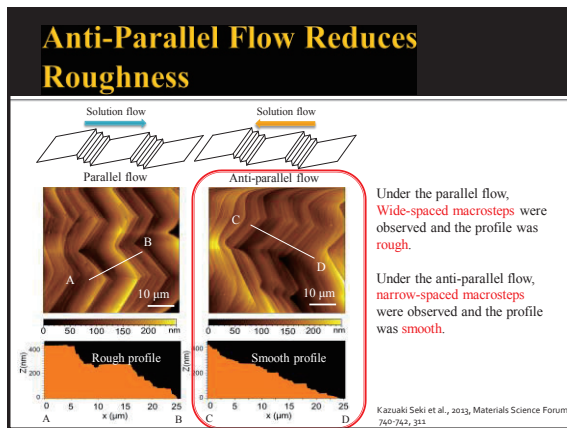
## Furnace Growth Details

- Si source: Si (electronic grade)
- Carbon source: Graphite Crucible
- Seed: 6H-SiC (Si face)
  - Offcut: 4°
  - Direction: (1  $\bar{1}$  0 0)
  - Atmosphere: He:N<sub>2</sub> (100:1)
  - Growth Time: 15 hours
  - Temperature: ~1620 °C

Selectively grow 3C-SiC?

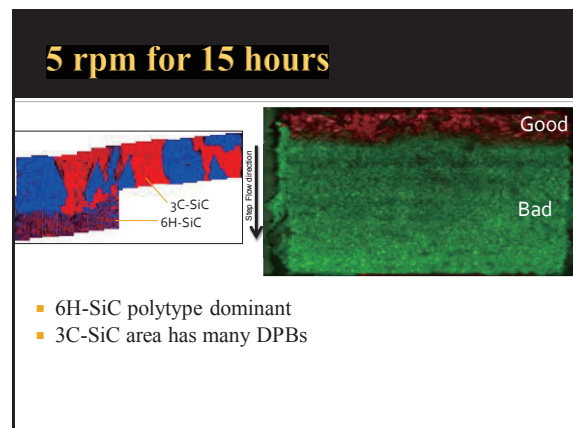
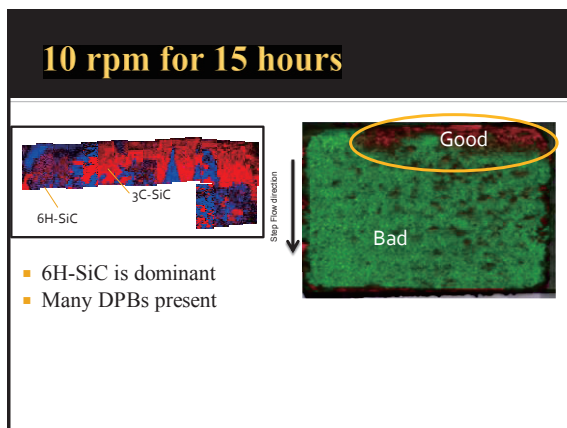
- 3C-SiC 2-D nucleation covers seed surface
- Carbon concentration
  - Rotation speed and concentration profile
  - Temperature



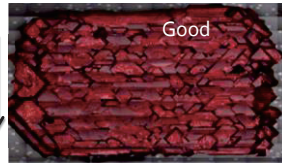
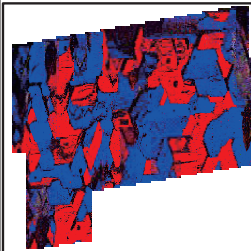


### Previously, on SiC Growth..

Rotation speed (rpm)	Raman	EBSD	Growth Time (hrs)	Comment
40			15	6H Observed near center of sample, mixing issue Many DPBs
20			15	Primarily 3C 6H is dispersed throughout sample Many DPBs



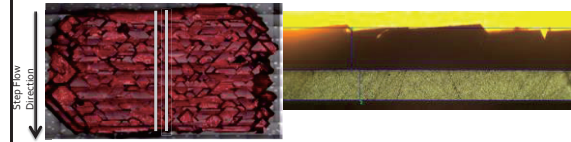
### 10 rpm for 30 hours



Conditions  
 ■ 10 rpm  
 ■ Growth Time: 30 hours

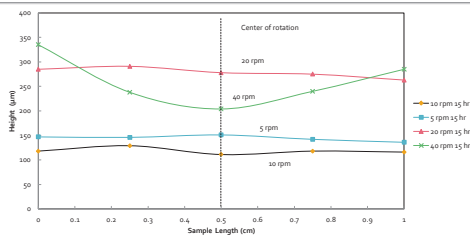
- No 6H-SiC observed!
- Many DPBs present

### Not all growth sites are created equal



- Growth sites near edges experience highest temperature
- Growth sites near the edges experience highest C concentration

### Cross Section Analysis



- 40 rpm: C could not reach center of rotation
- 20 rpm: "Goldilocks Conditions"
- 10, 5 rpm: Not adequate mixing after 15 hours to establish conditions for 3C-SiC growth

### Conclusions

- Mixing speeds of ~20 rpm yielded the most 3C-SiC with the lowest amount of DPBs after 15 hours
- Polytype ratio is a function of growth time
- Doubling the growth time (from 15 hours to 30 hours) appears to allow 3C-SiC to be selectively grown

### Future Works

- Continue exploring rpm effects on 3C-SiC quality
  - 15 rpm for 15, 30 hours
- Transmittance cross section analysis of 10 rpm (30 hours)
  - Ratio of polytypes
  - Growth rates

### Thank you for a great summer!

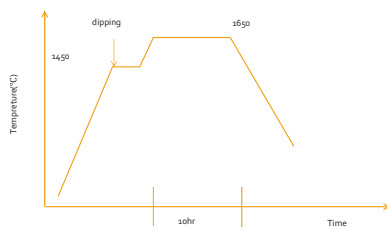
- Mentor: Professor Ujihara
- Crystal Growth Group
  - TA: Shota Yamamoto

## Questions?

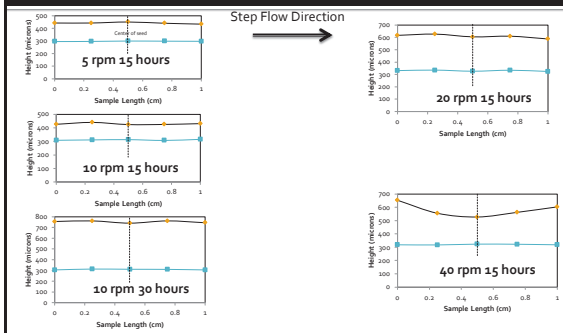
## Analysis and Possible Causes

- rpm  $\geq$  40: too fast
  - C cannot diffuse into the center
- rpm = 20: May be the best
  - Appears to have lowest number of DPBs
- rpm = 10: too slow
  - In 15 hour growth time, C cannot diffuse to seed
  - In 30 hour growth time, different story
- rpm  $\leq$  5: too slow
  - C cannot diffuse to seed


## Dipping Procedure



## Cross Section Comparison



## Cross-section of 10 rpm (30 hrs)



**Manufacture and characterization of Boron Oxide solid lubricant using RF magnetron sputtering at low-vacuum**

Characterization of boron based coatings on Silicon substrate, the manufacturing issues arising from boron coating manufacturing, and viable solutions to resolving the problems.

Jose Eduardo Gaviria, Dept. Materials Science, Graduate School, UCLA  
Supervisor: Noritsugu Umezawa, Graduate School of Engineering, Nagoya University


### Introduction

**Coating Technology**

- ▶ Metal Coatings
- ▶ Diamond-like carbon (DLC)
- ▶ Boron Coatings

**Manufacturing methods**

- ▶ Chemical Vapor Deposition
- ▶ Electroplating
- ▶ Radio Frequency Magnetic Sputtering



### Boron Coatings

**Types**

- ▶ Boron Oxides
- ▶ Boron Nitrides
  - ▶ Hexagonal BN
  - ▶ Cubic BN
- ▶ Boron Carbide
- ▶ Boron nitrogen carbon (BNC)

**Advantages**

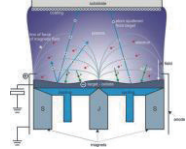
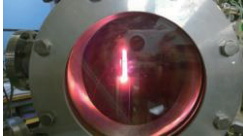
- ▶ Thermal Stability
- ▶ Chemical Stability



### Radio Frequency Magnetic Sputtering

**Advantages**

- ▶ High-melting Point Materials
- ▶ Top-down manufacturing
- ▶ Low maintenance
- ▶ High adhesion
- ▶ High reproducibility

### Initial Idea

**Boron Coatings**

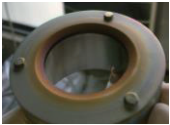

- ▶ Clear advantages over DLC coatings
- ▶ Very little fundamental research
- ▶ Possible compatibility with carbon for hybrid coating systems

**Applications**

- ▶ Steel/Iron based tooling
- ▶ High-temperature Applications
- ▶ Possible use as a intermediate layer for DLC applications

### Problems Encountered

- ▶ Reproducibility
- ▶ Control of environment
- ▶ Manufacturing parameters
- ▶ Measurement of manufacturing variables
- ▶ Boron coating chemical stability
- ▶ Residual stresses

### Applied Solutions

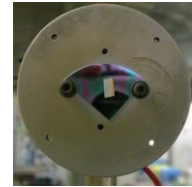
- ▶ Multiple-layer manufacturing
- ▶ Extra measurement equipment
- ▶ Addition of Carbon interlayer



### Manufactured Films

Films manufactured had a variety of different possible modifiers. As such, it was decided on the following manufacturing vectors:

- ▶ Gas composition
- ▶ Pressure
- ▶ Distance
- ▶ Substrate Bias
- ▶ Self-Bias
- ▶ Interlayer
- ▶ Multi-layer application



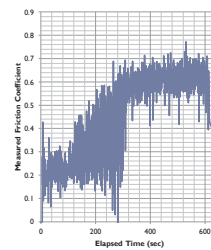
### Methods of Characterization

- ▶ Friction Test
  - ▶ High-temperature
- ▶ Annealing Test
- ▶ Micro-hardness
- ▶ Profilometry
- ▶ Raman Spectroscopy
- ▶ Auger Electron Spectroscopy (AES)

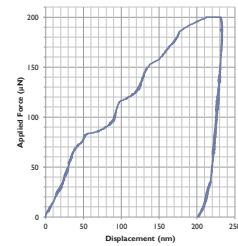


### Friction Test and Micro-hardness

#### ▶ Friction Test

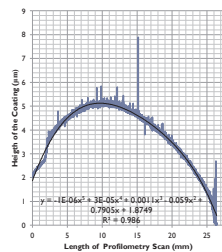


#### ▶ Micro-hardness



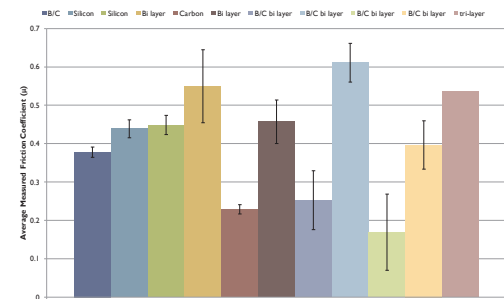
### Profilometry

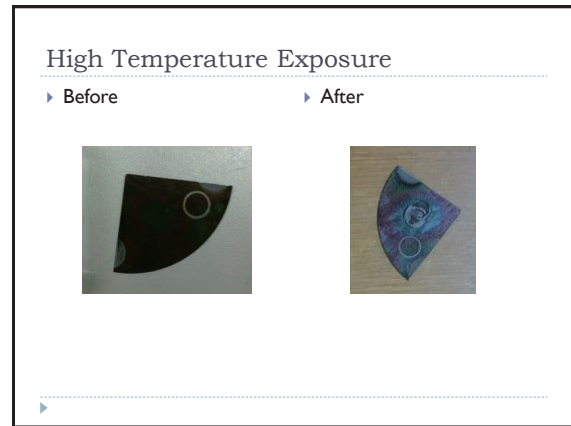
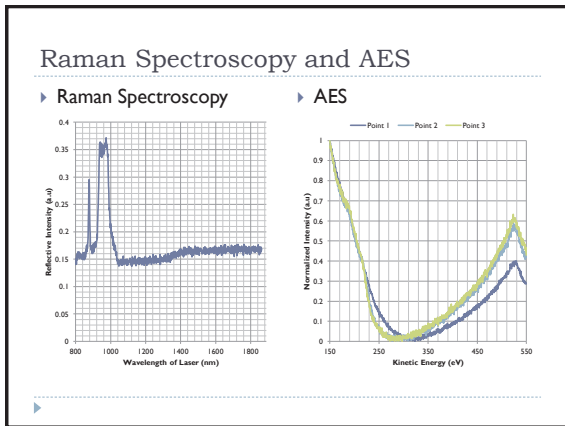
#### ▶ Profilometry




Coating System	Deflection of Substrate (µm) X/Y	Deflection of Coating (µm) X/Y	Calculated Residual Stresses (MPa) X/Y
Bi-layer application of boron film	3.18458 44.9837	-9.83636 -38.1061	-5.312185357 -13.15258943
Tri-layer application of boron film	217.647 247.693	-44.9474 15.8539	-0.720689693 -7.639383222
Bi-layer application of boron film with carbon interlayer	135.4 66.732	-29.613 -15.7694	-8.283334112 -5.142000619

### Different Friction coefficient depending on Material

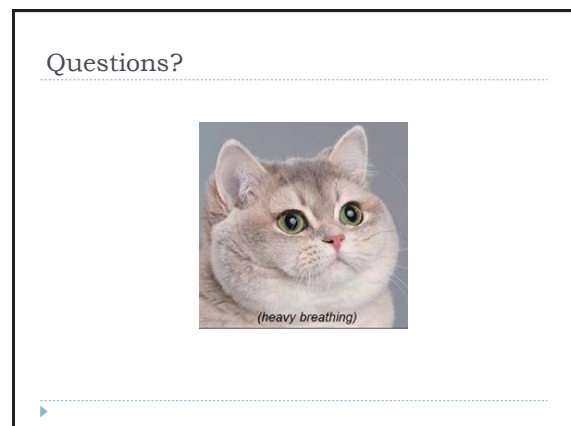




- ### Physical Characteristics
- ▶ Reactivity with atmosphere
  - ▶ Low material strength
  - ▶ High wear rate
  - ▶ Small friction coefficient reduction
  - ▶ Interesting optical characteristics
    - ▶ Fluorescence
  - ▶ High impurity content
- 

- ### Conclusion
- ▶ Reduction of residual stresses by multi-layer application
  - ▶ Ease of manufacture by established methods
  - ▶ Possibility of manufacturing and modifying desired molecular structure
  - ▶ The thermal stability of the coatings is there; however, heat still has a detrimental effect to the coating

- ### Further Work
- ▶ Establishing explanation for optical properties
  - ▶ Modifying manufacturing method to reduce impurities
  - ▶ Testing in high pressure and high temperature environments
  - ▶ Testing on steel/iron substrates
  - ▶ Optimization of manufacturing parameters
  - ▶ Development of BNC coating and characterization
  - ▶ Determining density of coatings






## References

### Images:

- <http://www.polymerdata.ch/Cu/Articles/view/57>
- <http://highpowermedia.com/RET-Monitor/103186-for-games>
- <http://highpowermedia.com/RET-Monitor/103186-for-games>

### Citation:

- [1] Erdemir, A., & Donnet, C. (2006). Tribology of diamond-like carbon films: recent progress and future prospects. *Journal of Physics D: Applied Physics*, 39(18), S311.
- [2] Zhou, Z. F., Bekko, I., Lei, M. K., Li, K. Y., Lee, C. S., & Lee, S. T. (2000). Synthesis and characterization of boron carbon nitride films by radio frequency magnetron sputtering. *Surface and Coating Technology*, 128, 334-340.
- [3] Donnet, C., & Erdemir, A. (2004). Solid lubricant coatings: recent developments and future trends. *Tribology Letters*, 17(7), 389-397.
- [4] Colfer, C. G., & Economy, J. (1995). Oxidative and hydrolytic stability of boron nitride—a new approach to improving the oxidation resistance of carbonaceous structures. *Carbon*, 33(4), 389-395.
- [5] Thomis, M. E., Hartstee, M. P., & McKay, J. E. (1988). The use of surface profilometers for the measurement of wafer curvature. *Journal of Vacuum Science & Technology A*, 6(4), 2370-2371.
- [6] Kubota, T., Tanaka, S., Fushiki, K., & Matsui, H. (2012). Synthesis and fluorescence properties of diazole-boron complexes bearing a  $\beta$ -B-combinats ligand. *Digestive letters*, 44(17), 4682-4685.
- [7] Shreve, A. P., Cherepy, N. J., & Mathias, R. A. (1992). Effective rejection of fluorescence interference in Raman spectroscopy using a shifted excitation difference technique. *Applied spectroscopy*, 46(6), 707-711.
- [8] Trehan, R., Lifshitz, Y., & Rubalis, J. W. (1990). Auger and x-ray electron spectroscopy studies of hBN, cBN, and N+ 2 on irradiation of boron and boron nitride. *Journal of Vacuum Science & Technology A*, 8(6), 4028-4032.
- [9] Marino, M. J., Hsiao, E., Chen, Y., Eryilmaz, O. L., Erdemir, A., & Kim, S. H. (2011). Understanding run-in behavior of diamond-like carbon friction and preventing diamond-like carbon wear in humid air. *Langmuir*, 27(20), 12702-12708.
- [10] Kawai, H., Suzuki, C., Kitamura, M., Sano, N., Ueda, Y., & Nishikawa, M. (1999). Internal stress induced in the process of boron coating. *Journal of nuclear materials*, 266, 1108-1112.





名古屋大学  
NAGOYA UNIVERSITY

## ANALYSIS OF VEHICLE'S CRASH BASED ON STRUCTURES' SECTION FORCES


D. Song  
University of California, Los Angeles

## Background

- The vehicle deceleration directly affects occupant injuries
- The collapse of the passenger compartment is important since it relates with survival space of occupants.


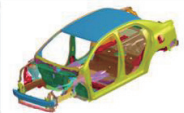
**Both vehicle deceleration and passenger compartment strength are important.**




2

## Background

- The relation between vehicle's compartment deceleration and the structure section forces in the process of frontal crash is useful to analyze crashworthiness.
- The deceleration of the passenger compartment was generated by the force transmitted to the firewall - the structural forces and the engine contact forces.


**The section forces of the vehicle's structures at different impact velocities were investigated.**



3


## Outline

1. Full Frontal Crash Impact Test
2. FE simulation
3. Section Force Analysis
4. Passenger Compartment Collapse
5. Conclusions





4

## 1. FULL FRONTAL CRASH IMPACT TEST

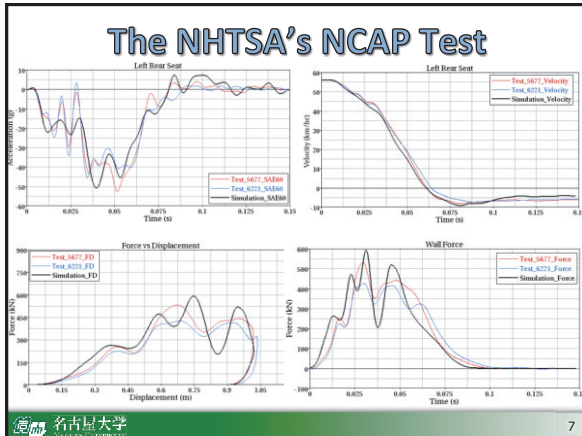


5

## Full Frontal Crash (56 km/h)

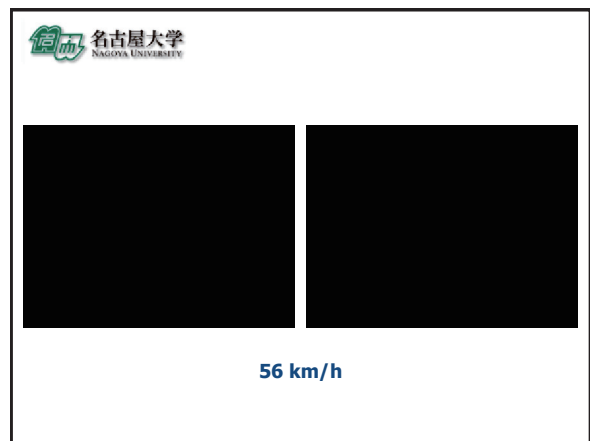
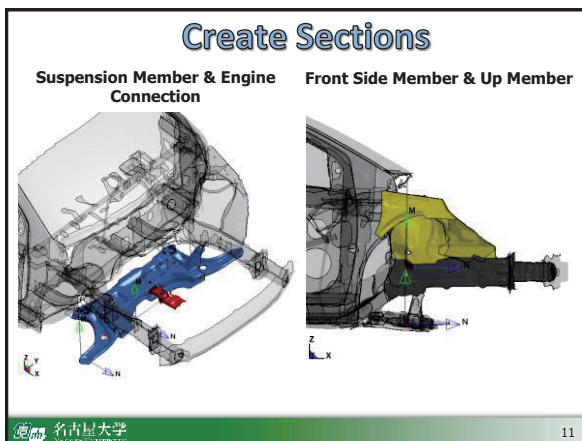
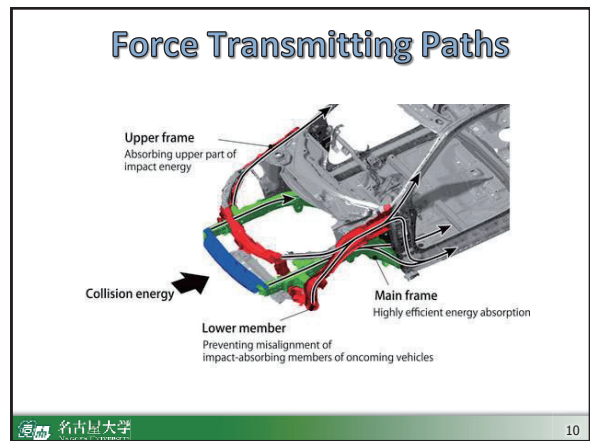
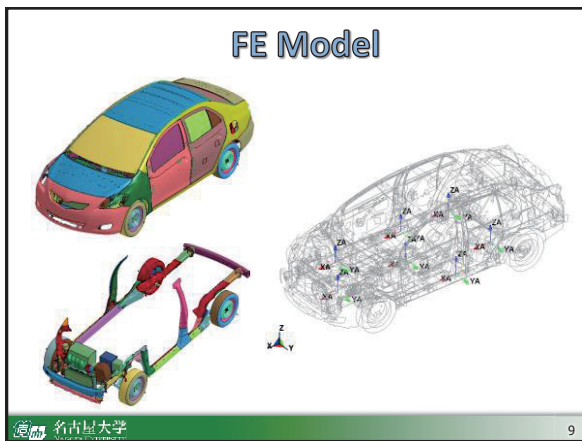



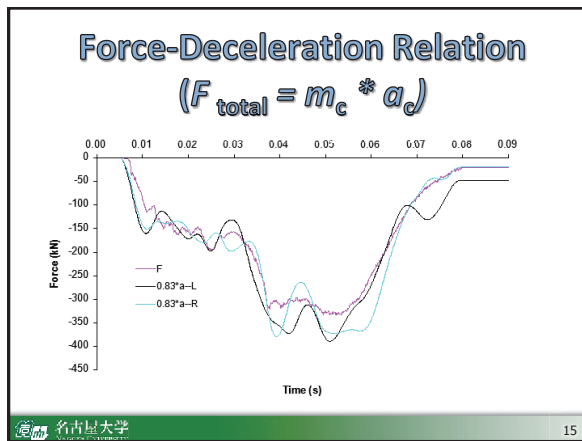
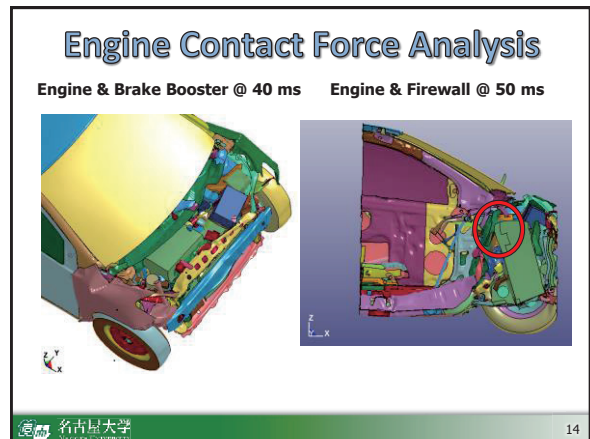
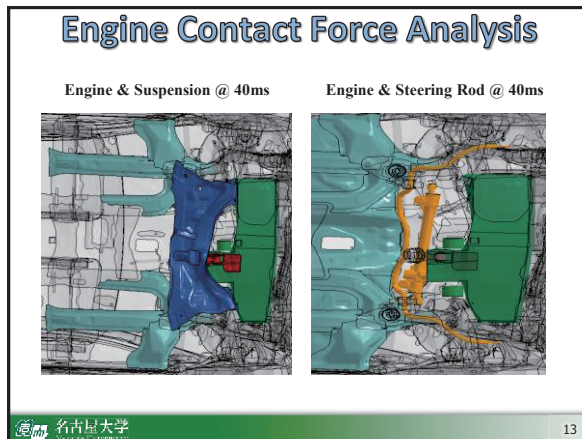
6



## 2. FE SIMULATION

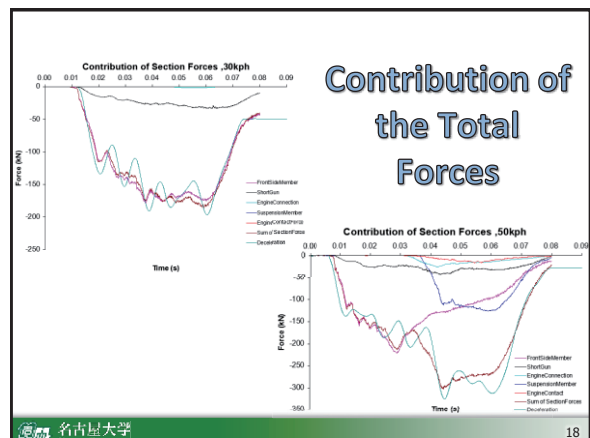
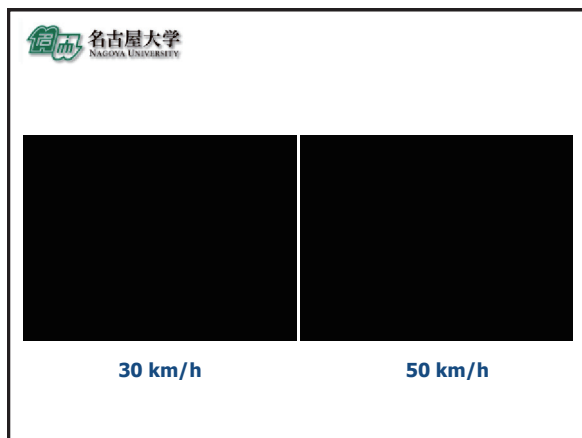
名古屋大学 8

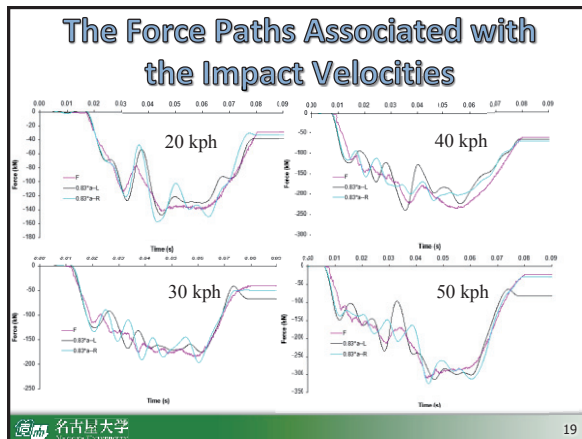




### 3. SECTION FORCE ANALYSIS

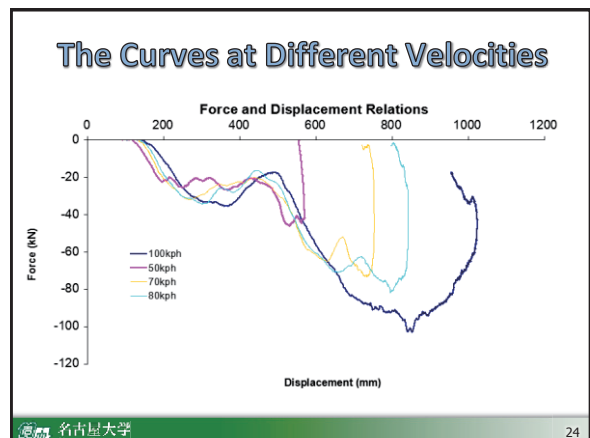
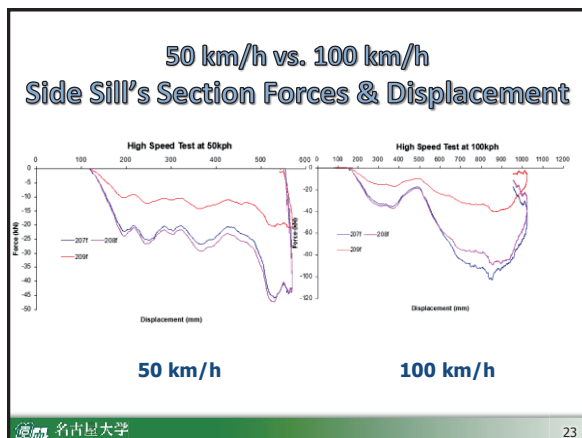
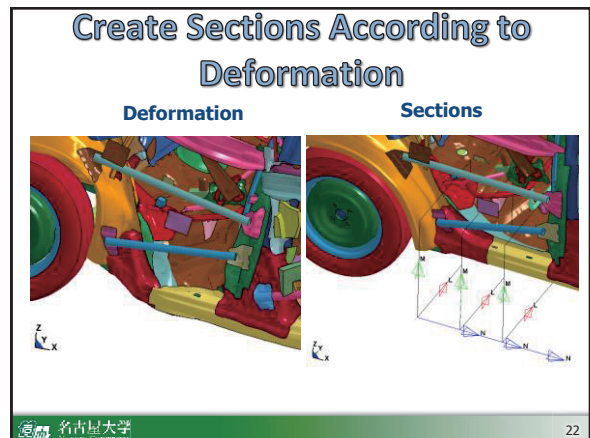
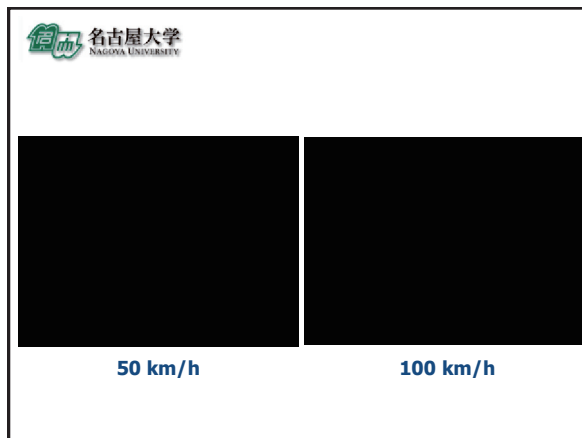
名古屋大学 16

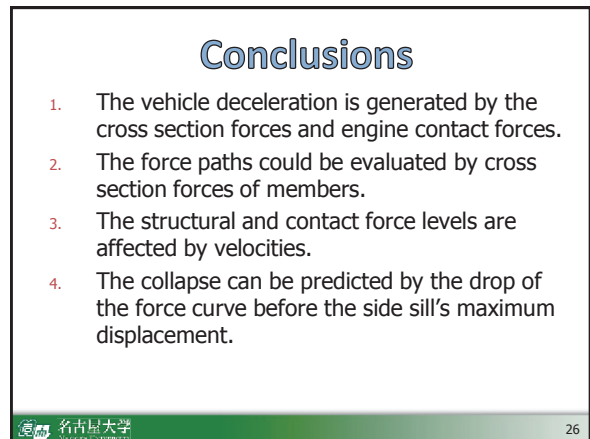
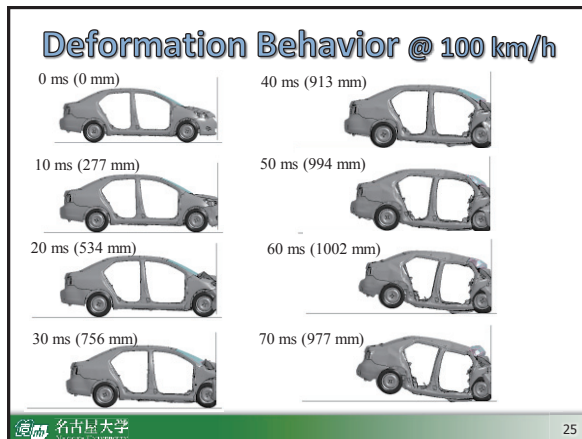




## 4. PASSENGER COMPARTMENT COLLAPSE

20





## **2-f. Final Presentation of Medium-term Students**

### **Antonio Martinez**

**Date & Time:** December 10 (Wed), 11:30-

**Venue:** Room 488, IB Building, Nagoya University

**Presentation Title:** "Acceleration Sensing: Design of Elevator Recognition and Displacement Estimation Algorithm and Implementation on Smartphone"

(P.150)

### **Elvia Cortes**

**Date & Time:** December 16 (Tue), 13:00-

**Venue:** Room 371, Engg. Bldg. 2, Nagoya University

**Presentation Title:** "Performance of an Applied-field MPD Thruster" (N/A)

## Acceleration Sensing: Design of Elevator Recognition and Displacement Estimation Algorithm and Implementation on Smartphone

Research project conducted by  
Antonio Martinez  
under JUACEP program  
at Professor Kawaguchi's Laboratory  
Nagoya University, Graduate School of Engineering, Department of Computer Science and Engineering  
December, 2014

## iOS App

- Name: ↑ ElevatorRecog ↓
- Platform: iPhone and iPad
- Consists of 3 tabs: Acquisition, Recognition, and Calibration
- This project: Acquisition



Design of Elevator Recognition and Displacement Estimation Algorithm and Implementation on Smartphone Antonio Martinez ©2014


## “Acquisition” Phase

- Purpose: To acquire diverse elevators' acceleration data via crowdsourcing to help future development of 'Recognition' phase
- It consists of:
  - Data Collection: 3-axis accelerometer readings
  - Data Storage: Use SQLite database and convert data for export
  - Data Processing: Run developed algorithm in-phone to estimate elevator displacement
  - Display Results: Show estimates of elevator displacement, speed, and other info

Design of Elevator Recognition and Displacement Estimation Algorithm and Implementation on Smartphone Antonio Martinez ©2014

## Data Collection


- User takes elevator rides with smartphone while following app's directions to collect data
- Steps:
  - Fill out "departing floor" and "arriving floor" info
  - "Start" button: App starts extracting acceleration readings from smartphone's 3-axis accelerometer
  - "Stop" button: App ends data extraction
  - User can "Cancel" or "Save" elevator ride



Design of Elevator Recognition and Displacement Estimation Algorithm and Implementation on Smartphone Antonio Martinez ©2014

## Data Storage

- Store each saved ride in embedded SQLite database
- Convert data into .csv file for export via email



Design of Elevator Recognition and Displacement Estimation Algorithm and Implementation on Smartphone Antonio Martinez ©2014

## Data Processing: Overview

- Developed algorithm for in-phone data processing
- Using collected accelerometer data, algorithm ultimately estimates displacement of elevator
- Process flow:
  - Raw 3-axis acceleration data is combined and filtered
  - Critical points of typical elevator acceleration curve are identified
  - Acceleration / deceleration are calculated in corresponding intervals
  - Velocity is calculated by integrating acceleration over time. Similarly, displacement is calculated by integrating velocity over time
- Error analysis

Design of Elevator Recognition and Displacement Estimation Algorithm and Implementation on Smartphone Antonio Martinez ©2014



### Process Flow: Raw data filtering

- 3-axis data is combined
- Data is filtered using custom running average with n=40 interval

Design of Elevator Recognition and Displacement Estimation Algorithm and Implementation on Smartphone Antonio Martinez ©2014

### Process Flow: Critical points

- Data is binned in windows of length = 50 dt
- Four points are identified

Design of Elevator Recognition and Displacement Estimation Algorithm and Implementation on Smartphone Antonio Martinez ©2014

### Process Flow: Acceleration / Deceleration Calculation

- Curve is divided in 3 acceleration segments
- Initial Acceleration
- Mid Acceleration
- Final Acceleration

Design of Elevator Recognition and Displacement Estimation Algorithm and Implementation on Smartphone Antonio Martinez ©2014

### Process Flow: Displacement estimation

- Curves are transformed to geometrically equivalents for simplified calculation of integrals over time
- Velocity corresponding to initial segment is calculated and integrated over whole span to estimate displacement
- Based on testing, post-processing adjustment using second degree polynomial curve fitting is used to improve estimation

Design of Elevator Recognition and Displacement Estimation Algorithm and Implementation on Smartphone Antonio Martinez ©2014

### Data Processing: Error Analysis

Departing Elevator	Arriving Elevator	Direction	ACTUAL Displacement (meters)	ESTIMATED Displacement	Error BEFORE adjustment (%)	ESTIMATED Displacement	Error AFTER adjustment (%)	
Ride #10	1	5	UP	9.60	9.55	-0.5%	9.59	-0.2%
Ride #11	1	5	UP	11.30	11.21	-0.8%	11.32	0.2%
Ride #10	5	10	UP	10.00	10.96	9.2%	10.76	-1.3%
Ride #12	5	10	UP	10.00	10.17	1.7%	10.76	6.7%
Ride #13	1	10	UP	36.30	35.15	-3.2%	36.20	-0.3%
Ride #14	1	10	UP	36.30	35.49	-2.2%	36.19	-0.3%
Ride #10	5	1	DOWN	9.60	9.56	-0.4%	9.60	0.0%
Ride #10	5	1	DOWN	11.30	11.22	-0.7%	11.32	0.2%
Ride #11	10	5	DOWN	10.00	10.01	0.1%	10.05	0.5%
Ride #10	10	5	DOWN	10.00	10.71	7.1%	10.76	6.6%
Ride #12	10	1	DOWN	36.30	35.87	-1.2%	36.26	-0.1%
Ride #13	10	1	DOWN	36.30	35.88	-1.4%	36.10	-0.3%
Ride #14	10	1	DOWN	36.30	35.88	-1.4%	36.10	-0.3%

Design of Elevator Recognition and Displacement Estimation Algorithm and Implementation on Smartphone Antonio Martinez ©2014

### Display Results

- Direction of ride, i.e. UP or DOWN
- Estimated Displacement in meters
- Estimated time
- Initial Acceleration
- Estimated average speed

Design of Elevator Recognition and Displacement Estimation Algorithm and Implementation on Smartphone Antonio Martinez ©2014

## Future Development

- Perform further testing on various elevators
- Improve app user friendliness based on feedback received
- Implement accelerometer calibration to improve displacement estimation
- Improve algorithm after vast amount of data is taken
- Implement "Recognition" tab

Design of Elevator Recognition and Displacement Estimation Algorithm and Implementation on Smartphone

13

Antonio Martinez ©2014

## References

- Berchtold M., Budde M., Gordon D., Schmidke H. R., Beigl M., ActServ: Activity Recognition Service for Mobile Phones, 2010 International Symposium on Wearable Computers (ISWC), 1-8, 2010.
- Brezmes, T., Gorricho, J.L., and Cotrina, J., Activity Recognition from accelerometer data on mobile phones, IWANN '09: Proceedings of the 10th International Work-Conference on Artificial Neural Networks, 796-799, 2009.
- Györfi, N., Fabian, A., and Homanyi, G., An activity recognition system for mobile phones, Mobile Networks and Applications, 14(1), 82-91, 2008.
- Koshimizu, K., Kamioka, E., Estimation of User's Behavior for Realizing Just-in-time Services, IEICE-MoMuC2009, 108, 2009.
- Apple iPhone and Apple iPad app development. 2013. Apple Inc. [www.apple.com](http://www.apple.com).

Design of Elevator Recognition and Displacement Estimation Algorithm and Implementation on Smartphone

14

Antonio Martinez ©2014

<3>

Reports & Questionnaires  
on JUACEP Program

## Findings through JUACEP

**Name:** FU-LONG CHANG

**Affiliation (Dept & Univ):**

**Participated program:** Short (Summer) 2014

**Research theme:** A Novel Control System Design for Robust Assist Systems

**Advisor at Nagoya Univ:** Prof. Susumu Hara

**Affiliation (Dept.):** Mechanical Engineering



In these three months, I spend a lot of time staying in the lab and do some research topic I am not familiar with. At the very beginning, I have a little bit struggle with the programming of my simulation model. Fortunately, I overcame it very quickly and came out with a solution of my research topic later. After first month, I developed almost all of the theory of my algorithm and finish up all the simulations. At the second month, I start to write my research report and I am going to submit part of my paper to a conference, CACS. The rest of it is going to submit to IEEJ.

This is my first time coming to Japan, every thing is very exciting and interesting. I went to a lot of places like Nagoya Castle, or somewhere far from here such as Osaka, Kyoto, or Tokyo. I have tried many new food like Japaness pizza, or Japaness green tea. It is so nice. Beside, I know more about Japaness culture and their working style. Three of my professors are very nice to me, and give me many advices about researching or some fun places. I always hanging out with my labmates, and go to bar having some small beer. I am so surprised about the alcohol Japanese people can drink in one time.

Furthermore, I am an independent travel lover. I believe that Japan is the country that most suitable for self-travel. First of all, Japan is one of the safest countries in the world. I once lost my wallet in my trip to Kobe. Fortunately, I get it back very fast. Second, every Japanese are very kind and very willing to help people who get lost. Like when I get lost at Tokyo, and I ask a pedestrian for help. He is so kind that he help me find the address of my hotel, and he also bring me to the hotel. All of them are so nice.

I really appreciate every people in this program. My professors, my labmates, my TA, and most important the Juacep Office. Mrs Chiharu and Mrs Tomoko really help us a lot, and very kindly help us with many problem we have. Thanks every people in this program and the Nagoya University and University of Michigan to give me such a awesome experience in Japan.

## Findings through JUACEP

**Name:** Taehee Jang

**Affiliation (Dept & Univ):** Department of Electrical Engineering,  
University of Michigan

**Participated program:** Short (Summer) 2014

**Research theme:** Design of a Multifunction Probe Used for Microwave AFM

**Advisor at Nagoya Univ:** Prof. Yang Ju

**Affiliation (Dept.):** Mechanical Science and Engineering



I joined Prof. Yang Ju's group for 3 months and my research topic was the design of multi-function probe used for microwave AFM. I have studied the basic concepts and applications of M-AFM. In order to improve the performance of previous M-AFM probe tip, I have designed the new M-AFM probe tip by using the Microwave simulation tool and compared with the results of the previous probe tip. In addition, the M-AFM is able to measure the force according to the different materials. Thus, to figure out the kind of forces, I have driven the force equation to calculate electromagnetic force from the probe tip.

During this period, I could enjoy not only researching about M-AFM as well as interacting with many people in Japan. I had many Japanese friends in the Nagoya University and we had good time together. We saw baseball game with other friends in Nagoya Dome. When I joined this program, I felt nervous because I can't speak Japanese well. But, Japanese friends taught Japanese language and have a lunch together. Although my Japanese is improved, it is not enough to discuss with others. Through this program, I am motivated to continue to study Japanese. Besides of the research in Prof. Yang Ju's lab, I traveled with other friends around Nagoya. We have been to Nagoya castle and Osu temple and went to hot spring to take a bath in Nagoya. In addition, there are many activities in this program. We visited the Toyota Company and INAX museum for field trip, and we had BBQ in the sea. Except that, we had hand craft session to assemble the combust engine, and then we tried to start our assembled engine. Moreover, there are many interesting lectures that we could attend.

Finally, I could have a lot of experiences for both research and life in Japan through the JUACEP program. I could know more about Japan and I have gotten very good impressions for Japanese people and company.

## Findings through JUACEP

**Name:** Songyao Jiang

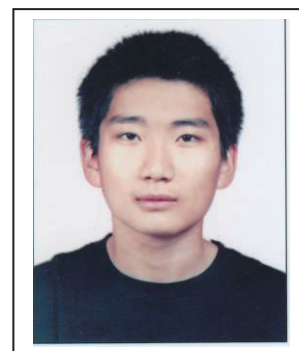
**Affiliation (Dept & Univ):** EE:S University of Michigan

**Participated program:** Short (Summer) 2014

**Research theme:** Load Frequency Control

**Advisor at Nagoya Univ:** Prof. Suzuoki

**Affiliation (Dept.):** Electrical Engineering and Computer Science



After more than two months research in the lab. The strongest feeling of mine is that Japanese people are all very hard working. Some people in my lab come before 10 am and work until 10 pm every day. All the students and staff in my lab are also very serious to their job.

Japanese people are also very polite. The clerks of convenient shops usually say a lot of Japanese honorific to me. People on the street also say a lot of thank you and sorry to each other. They make themselves a good image to me. In general, I think most Japanese people are very kind and helpful.

The only problem is that Japanese student are not good at speaking English. Professors' proficiency of English are much better than students'. I feel difficult to communicate with some Japanese students. I was wondering why this happens in Japan which is a modern advanced country with high technology. Do they need to read English paper for academic purpose? Do they post English paper in any English Journals?

After these days, as I experienced, I find an answer to these questions. Japan has a complete academic environment. There are many academic journals published in Japan. As Japan is an advanced country, Japanese journals are in very good quality. Therefore, Japanese students are used to read Japanese papers in their studies. In most cases, it is not necessary for them to read English paper for reference. In addition, many important foreign journals are translated into Japanese and published officially. This provides a good way for them to read foreign journals in Japanese. I believe the above lead to the situation that it is not that necessary for Japanese student to learn English. So the average English level of Japanese student is poor.

However, this situation depends on the major area of student. In some area, where academic communication is more frequent, for example biology, the average level of English proficiency is much higher. The number of international students is also a symbol of the frequent communication with foreign countries.

During my study in the lab, I attend some meetings with the lab members. One kind of meeting is held every week. In such meeting, students report their recent progress of researches. After the presentation of students, professors will ask a few questions and discuss with them. All the members will gain knowledge in such meeting. Another kind of meeting is when the master students report their total progress of their final thesis to the professors. This kind of presentation is more formal. For 1st year master, the presentation is about the direction and plan of thesis including some basic concepts. The presentation of 2nd year students are very detailed. The duration of the presentation is also much longer than those by 1st year masters. The presentation is mainly about the part they have already completed including the theories, references, experiments and results. They present their ideas and methodologies to the audience. I think the 1st year master students could benefit a lot from that. Unfortunately, the presentations are all in Japanese. I could only read the Kanji and understand 40% of the presentation.

## JUACEP Experience

**Name:** Charles Lesmana Sie

**Affiliation (Dept & Univ):** Electrical Engineering, University of Michigan

**Participated program:** JUACEP 2014

**Research theme:** Human Activity Sensing and Recognition

**Advisor at Nagoya Univ:** Prof. Nobuo Kawaguchi

**Affiliation (Dept.):** Computational Science & Engineering, Nagoya University



This stay is not a brand new experience for me because this was my second time in Japan. Compared to the first one, I definitely had a better look into Japanese daily life and habit due to daily interactions with Japanese students in the university. My short enrolment in the JUACEP program has opened my eyes to different culture and lifestyle, inside and outside of my research lab.

I joined Professor Nobuo Kawaguchi Lab to work on a Human Activity Sensing and Recognition themed research. My research is titled a Correlation Coefficient Method to Count the Number of Human Steps. One of the students in the lab was working on another method to count steps, and he was a major help by providing his method's strengths and weaknesses. My research has been a very enjoyable and fulfilling. The coefficient correlation method is a very robust method to detect one human step over a long period of recording time. It overcome some of the weaknesses that the previous method possessed.

Since the beginning of my stay, the staff and fellow students had given me ample of support and help. They assisted me in learning java programming language, the lab's preferred programming language, and getting familiar to the application that the lab has been developing for the past years. It was good to obtain that information early, so that I would be able to get some background knowledge before I started my summer project. The weekly meeting of the lab was very helpful because I could always present my progress report in to the whole lab and obtain very useful feedback and suggestions from other students and staffs.

The lectures, which were organized by JUACEP, were very helpful to keep current on the technologies that are being developed by Japanese companies. These seminar type classes gave very informative overview about the manufacturing methods developed by industries in Japan. In addition, the handcraft exercise class was a very interesting experience as all the students were able to disassemble and assemble a miniaturized engine. It was very satisfying feeling to hear the roar of my engine at the end of the class.

Outside of my work, I also enjoyed my time doing other activities in Japan. These include sightseeing, visiting temples, and trying Japanese cuisine. My lab mates are also a very welcoming group of people. We enjoyed talking about different cultures, favorite movies, and favorite drinks. I also made many Japanese and other foreign friends outside of my lab. They made my stay in Japan very enjoyable and memorable. This experience of working and living in Japan is definitely one of a kind and I will cherish this memory for a very long time.

## Findings through JUACEP

**Name:** Jin-Gen Wu

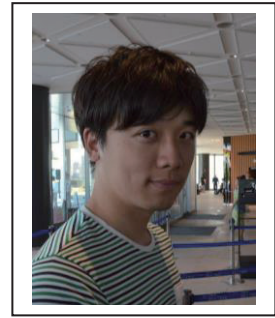
**Affiliation (Dept & Univ):** Mechanical Engineering, Michigan University

**Participated program:** Short (summer) 2014

**Research theme:** Automated Steering System for Obstacle Avoidance  
based on Potential Field Method

**Advisor at Nagoya Univ:** Prof. Tatsuya Suzuki

**Affiliation (Dept.):** Mechanical Engineering



My research topic in Nagoya University is automated steering system for obstacle avoidance based on the potential field method. I gained a lot of valuable experience and learned new skills at Suzuki lab, such as learning C# programming for the controller.

I like the culture of Japan, and I also appreciate the innovative technology in Japan. Travelling in Japan is always what I hope to do. By participating this program, I can not only stay and travel in Japan but also learn the cutting edge of technology in the field of mechanical engineering, especially in the vehicle area.

During these few months, I traveled to many cities in Japan frequently.. The most impressive place is Kyoto. In Kyoto, there are many beautiful temples and castles. I really admire the unique style of those temples and castles. More importantly, I learned a lot of knowledge in the field of vehicle from the research at Suzuki lab, not just constrained in the field of the automated steering system. I also learned the “trajectory planning for automated parking”, “stop movement control with model predictive control”, and so on. I believe all things I learned and all experiences I gained in Japan must have positive impact on my future career.





## Life Experience in Japan

**Name:** Hanyi Xie

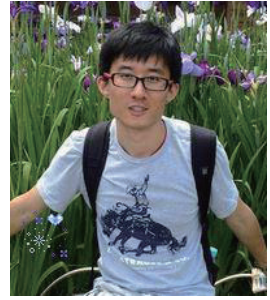
**Affiliation (Dept & Univ):** Mechanical Engineering, University of Michigan

**Participated program:** Short (Summer) 2014

**Research theme:** Friction and Wear of 3D printed materials

**Advisor at Nagoya Univ:** Prof. Noritsugu Umehara

**Affiliation (Dept.):** Mechanical Science Engineering



I think I am really lucky to get involved in Prof. Umehara's lab. Not only because this lab is a pioneer in tribology area, I can learn advanced technology here; but my TA as well as anyone in this lab, is always really kind to help me solve problems, answer my concerns, and teach me to use the advanced machines.

During the weekdays, we have Japanese class in the morning, and come back to the lab doing research in the afternoon. Weekend time is used to travel to places out of campus. Kyoto is a beautiful city full of ancient shrines. The ceremony for prayer is very typical. In addition, Shirakawa-go leaves me deep impression since the countryside is so silent and clean. On rainy days, wind is cool and air is fresh. We can see the clean stream everywhere, as well as the big fish in water. The most impressive events are the Haru semi and Natsu Ryoko with my lab members. This is my first time living with local Japanese. We played games, chatted through the night, swam in the sea, enjoyed the hot spring, tasted seafood BBQ, drank a lot.etc. In my opinion, the beautiful scenery is attractive; but more "shiwase" thing is living together with people in my lab. At that moment, I felt I was closest to native Japanese culture.

The JUACEP program also provides us many opportunities to learn not only the technology but culture in Japan. The Toyota Motor Factory visit gives us a sense of view how the car is assembled from every component and what is the related manufacturing flow chart. During the handcraft exercise, the process of disassembling and assembling is really helpful for us to understand the detailed structure of the rotary engine and the theoretical principles. In the INAX museum, we created paintings on the small toilet, visited the history museum of ceramic development. The seaside BBQ is really impressive since we sit along the coast, watched the beautiful scenery and cooked sea foods by ourselves.

## Findings through JUACEP

**Name:** Yang Yong

**Affiliation (Dept & Univ):** Biomedical Engineering, University of Michigan

**Participated program:** Short (Summer) 2014

**Research theme:** 3D Fabrication of Nanostructure

**Advisor at Nagoya Univ:** Prof. Fumihito Arai

**Affiliation (Dept.):** Nagoya University, Micro-nano Systems Engineering



First of all, I would like to express my appreciations to everyone who helped me to participate in this program, that includes, but no limited to Professor Kurabayashi, staff from JUACEP office (Nagoya University), staff from the IPE office (UM) and the Graduate Education Committee of the Biomedical Engineering department (UM). My case was very complicated and it was almost impossible for me to come to Nagoya University. However, everyone tried their best to help me and eventually I did make it. I can write a four-page essay by only describing this hard and long process. I am truly honored to be part of this program.

I learned a lot at my host lab. My major is not an exact match to my host lab's research direction. I major in Biomedical Engineering with focus on biotechnology and my host lab is mainly working on micro-nano system. I was very worried at first while my tutor was very nice to help me with my project. I built my confidence in working in an unfamiliar area and translate my knowledge to real solutions. One most important thing I learned from my lab mates is their hard-working and enthusiasm towards their work. People usually come at around 10am and most of them stay till 11pm or later, even on weekends and holidays. Not only the students, the professors also come to lab on weekends. I think this could be one reason why Arai Lab is one of the best in this area.

One big pity for me is that I only know little Japanese from the Japanese classes. My lab's discussion meetings and research meetings are all in Japanese and really hard for me to fully understand, though their PPT slides are in English. Even though, I am really impressed with their delicate designs of biorobotics and strategies in solving problems. Most of my Japanese lab mates are very shy and some of them are not very confident in speaking English. To be honest, I felt lonely in the first two weeks. Then I tried to talk to them and found out they are very kind and willing to help as long as I ask. We talked about Japanese comics and differences between Japanese and American course/degree system and campus life.

I really enjoy the series of lectures in production engineering in automobile industry and the field trip to Toyota Motor Factory. I learned the concept of "Jidoka" and "Muda" from the lectures by an engineer from Toyota and saw how "Jidoka" is applied and how "Muda" is avoided during manufacturing process at the factory. Japan is famous and respected for its engineering. JUACEP offered us great opportunity to learn from that.

Not only from the lectures or the field trip, but also from the ordinary life, I noticed the unique characteristics of Japanese engineering, that is, Japanese engineers pay lots of attention to details and quality. For example, even the toilet brush here has a better design than the ones I saw in China and America.

The JUACEP mentioned a term, "academic culture". I think this program is a perfect one for us to experience the academic cultural differences between America and Japan. I will demonstrate a few observations based on my lab.

The Japanese society is strictly hierarchical, even including the academy. Each lab has one professor and several associate and assistant professors. In the lab, people call each other family name only with a suffix ("sensee" for professors, "san" for same or higher "levels", "kun" for male lower "levels") for respect.

Female researchers/engineers are rare in Japan. There are only a handful females in our lab building that there is only one female bathroom in the building. Among all 9 labs which host UM students, my lab has the max number of girls (5, 3 of them are Japanese) and we have not yet heard of any female Japanese professors here. I think one reason is that we are all engineering majors and most Japanese girls do not prefer studying engineering. My tutor is also a girl and I think she is no worse than other male students.

We also visited several places, such as Kyoto, Tokyo and Osaka on weekends. We enjoyed the sights, Japanese food and Japanese culture and history, moreover, nice Japanese people. Last weekend, we went to Tokyo and we tried to buy bus tickets to Fuji Mount using the Loppi at a Lawson store. The instructions on Loppi is in Japanese and we had to ask the staff for help. The staff could not speak English, while a customer heard us and he came to help us. He said he just started to learn English and we wrote down the Kanji and numbers to communicate in addition to English. In order to help us, he called the bus service center and reserved tickets for us. He then wrote down the detailed information for picking up the tickets and explained three times to us to make sure we understand. The whole process took half an hour and he was just a stranger. This is just one instance of nice Japanese people. Thanks to these people, they made our trip not only great but also warm like home.



世界遺産・白川郷合掌造り集落



My "Japanese grandma" 美子姑姑 and me

There are a lot to talk about regard to this program. I will share my experience and my thoughts with all my friends. I enjoy my time here and really appreciate this opportunity. I hope I can come back to Japan again after this program and I will keep learning Japanese.

## **AMAZING RESEARCH LIFE IN JAPAN**

**Name:** Yingrui Zhan

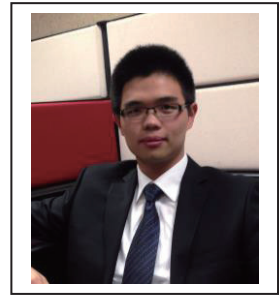
**Affiliation (Dept & Univ):** Dept of Mechanical Engineering, University of Michigan

**Participated program:** Short (Summer) 2014

**Research theme:** Cold forge spot bonding of Aluminum and Copper Sheets

**Advisor at Nagoya Univ:** Prof. Takashi Ishikawa

**Affiliation (Dept.):** Dept of Materials Science and Engineering



On May 12th, 2014, my research life in Nagoya University began. Filled with curiosity and tension, I arrived at Chubu Centrair International Airport. The pouring rain couldn't alleviate my excitement. The warmth from Japanese students and dormitory staff also made me feel the amity of Japanese people. In addition, I would like to thank JUACEP for providing me with round-trip flight and accommodation at Nagoya University, especially considering high living expenses in Japan.

On the second day, my research work officially started. I am working in Professor Takashi Ishikawa's Material Forming and Processing Lab. Professor Ishikawa has long been famed for his research in metal deformation field and he used to be the chairman of The Japan Society for Technology of Plasticity. With such high prestige and rigorous attitude towards research, Professor Ishikawa is very kind and humble in personal though. The atmosphere and working environment of lab are fantastic. Every Japanese student shows a lot of politeness and amity. And the lab has a lot of simple fitness equipment and a sofa bed for students to relax themselves. To my surprise, there is even a public iPad for everyone to play games. Unlike the stereotypical impression of Japanese people that they are all workaholic, my lab shows a well balance between work and relaxation.

After getting myself familiar with the office, I had chance to work on those advanced materials processing machines affiliated with my lab. My research theme is about cold forge process and needs to use Press machines, Servopulser and Scanning Electron Microscope. Professor Ishikawa's lab provided me with everything I need and I had a great time working with my Teaching Assistant. Her meticulousness and proficiency, just like the impression Japanese people have left on me for a long time, were fundamental for achieving our research goal. In fact, Japanese companies and research facilities have an extremely high level in research of metal materials deformation and processing, which is partly resulted from the shortage of natural resources in Japan. In contrast to the United States, Japanese scientist and engineers are still paying a lot of attention on traditional engineering areas and trying to make every use of them. And this is one prominent characteristic of Japan- use less to achieve more. Probably this idea better fits our earth.

Three months of life in Japan is not very long, but long enough for me to experience Japanese culture and history. In all, Japan and America seem like on the two opposite ends, not only for exterior differences like skin colors, language systems, driving on the left or right, but interior aspects including thinking mode, attitude towards other people. However, as long as I am from China, it is not a big problem for me to be adjusted to Japanese lifestyle. In addition, Japanese people always show huge tolerance and kindness to foreign people. This advantage, I think, is the inevitable result of high civilization. Therefore, during my stay in Tokyo, Osaka and Kyoto, I always had a great time wandering streets and visiting gorgeous scenery spots.

Finally, I would like to thank JUACEP again for giving me this precious opportunity to closely look at Japan and its culture. Gaining a deeper understanding of Japan, I may choose to work for a Japanese company in the future. And this experience is my lifelong treasure.

## Findings through JUACEP

**Name:** Chiyang Zhong

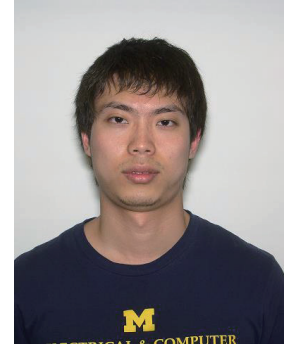
**Affiliation (Dept & Univ):** EECS University of Michigan

**Participated program:** Short (Summer) 2014

**Research theme:** Development of Current Suppression Equipment in Low Voltage DC Distribution System

**Advisor at Nagoya Univ:** Prof. Matsumura

**Affiliation (Dept.):** Electrical Engineering



Before attending the JUACEP program, I had always wanted to come to Japan. I believe like me, many people learn about Japan from its animations. Everything seems so interesting on screens and they just keep drawing us to this mysterious country in the east. Finally one day I saw this opportunity and grasped it. So here I am, in Japan, a magical place.

As this is a summer research program and I did not come here as a tourist, most of the time is spent in the laboratory doing research. However when I have time during weekends, I would travel to nearby places. So far I have been to some major cities in Japan, such as Kyoto, Osaka, and Tokyo. They are all very nice places to visit. Kyoto is famous for its existence as an old-time capital city. Its Matcha products are very tasty and I have grown quite fond of them. Osaka is a place for people to indulge themselves in Japanese food. When it comes to food, most Japanese people would recommend Osaka. It has several blocks of restaurants, full of traditional Japanese food, such as Okonomiyaki, Takoyaki, Sushi, and Ramen. I even tried some balloonfish at Osaka, which was a once-in-a-lifetime experience. As for Tokyo, it is the modern capital of Japan. Shopping and experiencing the culture of Japanese animation are recommended. Some other towns or villages are also worth seeing, like Nara and Shirakawa.

The downside of Japan is that English is not very popular here. Places lacking English signs and people only speaking Japanese are the major problems for travels. However Japanese people are very nice and polite. Although they cannot speak or understand English, they would still try their best to help. After arriving in Japan, I took a short Japanese class which only had ten lectures. It was helpful, but too short to make any difference in communicating with locals. Unlike mechanical engineering labs, which are full of international students, the electrical engineering lab I am in only has Japanese students. I think this is the main reason why the students in those labs can speak English quite well, while I can hardly communicate with my labmates. In this sense, my lab experience is not as good as others. Nevertheless, my professors and labmates are very nice and they offer help whenever I have questions. I have learned a lot through research because of them.

Finally I would like to talk a little about the culture. It is pretty much the same as what is presented in Japanese animations. I'm glad that I had the opportunity to attend one of the festivals held in Nagoya. To attend traditional events, people always dress in Kimonos, which are so pretty, especially for ladies. Some of the activities are also very cultural and fun. I really have had a great time participating in those events.

Generally speaking, this summer research program has not only helped me learn more in research, but also let me experience this wonderful culture. Three months seem to have gone so fast and it is sad that I need to leave so soon. I really hope I could come back sometime in the future.

## Findings through JUACEP

**Name:** Dong, Song

**Affiliation (Dept & Univ):** Mechanical Engineering, UCLA

**Participated program:** Short (Summer) 2014

**Research theme:** Vehicle Crash Safety

**Advisor at Nagoya Univ:** Prof. Mizuno Koji

**Affiliation (Dept.):** Mechanical Science and Engineering



This short summer program provides a great opportunity to me. In terms of my major, mechanical engineering, Japan is a well-developed country in this industry. Many famous companies such as Toyota are well known all over the world. Thus, participating to the JUACEP Summer Program 2014 gave me a precious opportunity to accumulate professional practical experience.

My research in Prof. Mizuno's lab is the great and helpful experience to my career. I can feel the comfortable and harmonious Japanese lab's condition. The tutor and lab mates are friendly and full of passion. They are always glad to help me whenever I met questions during my research. Their work-life balance also impressed me. After the long-time work, they will share experience with each other during a coffee break, including the questions they met in the research and other funny stories. This is also a kind of collaboration, which promotes the research progress and lets people refresh.

Although I do not know Japanese, I still did a lot of excursions during the two-month study. The colorful life in Nagoya makes me full of energy. During these trips, I am attracted by the Japanese culture. Nagoya is a city that famous for its history. The classic places, such as Nagoya Castle and Atsuta Shrine, are really impressive. My lab mates gave me many suggestions to explore the beautiful city. The harmonious lab environment and wonderful city are the reason why I enjoy my every day in Japan. During the holidays and weekends, I went to many other cities, such as Osaka, Nara, Kyoto and so on. I found different Japan through these trips, which is a well-preserved traditional and high-tech modern country. I can feel the traditional culture and Japanese history through the numerous temples. Meanwhile, the smart buildings and other high-tech devices on the streets are amazing.

All these fantastic experiences are came from JUACEP program offered by Nagoya University. I can gain academic knowledge through the research in the lab. The guidance of Prof. Mizuno helps me improve myself, which is of great important to my future career. On the other hand, the daily life in Japan makes me feel different culture and life style. Participating the JUACEP program is a valuable treasure to my life.

## Findings through JUACEP

**Name:** Jose Eduardo Gaviria

**Affiliation (Dept & Univ):** Material Science and Engineering at UCLA

**Participated program:** Short (Summer) 2014



**Research theme:** Manufacture and Characterization of Boron Oxide Solid Lubricant using RF Magnetron Sputtering at Low-Vacuum Pressure

**Advisor at Nagoya Univ:** Prof. Noritsugu Umehara

**Affiliation (Dept.):** Mechanical Engineering



I didn't know what to expect when coming to Japan initially for the JUACEP program. I had no idea if the time that I would be there in Japan would be mostly spent in the guest laboratory working or just trying to overcome the language barrier while doing everyday activities. However, once I arrived in Japan, it became quite clear that this would be an unforgettable experience. I have travelled quite a bit beforehand and quite enjoy it, but never before had it been such a perfect balance of work, cultural exchange, and discovery. During my time in Japan, I worked on a project that I had very little background in. I learned a new set of skills, while being mentored by very capable individuals. I also was welcomed by my mentors with open arms and learned more about Japanese culture. The lectures and learning opportunities arranged by the JUACEP office were insightful and easy to follow. The rest of the time that I was not in the laboratory or attending lectures, I was spending with other students from my program, or just myself, travelling and seeing all that Japan had to offer. The culture, the food, and the typical Japanese way of thinking. Thought there are a lot of differing cultural norms, everyone, even strangers, were very courteous even when I committed a faux-pas. They would even teach me and explain what I had done so I could better present myself in the future and not commit the same mistake twice. All and all, I knew before I started the program that I wanted to come to Japan at one point in my life either to improve my career or just to travel; however, after spending the time I did in Nagoya and all the interactions with the people I met in that time, I can't wait to get another excuse to come back once more and do it all over again.

## Findings through JUACEP

**Name:** Zihe He

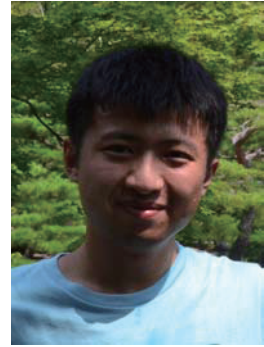
**Affiliation (Dept & Univ):** Mechanical Engineering and Science

**Participated program:** Short (Summer) 2014

**Research theme: Bonding in Chip Fabrication for Cell Measurement**

**Advisor at Nagoya Univ:** Prof. Fumihito Arai

**Affiliation (Dept.):** Mechanical Engineering and Science



When I heard about JUACEP program, I contacted our UCLA professor immediately for detail of this program. Fortunately, my application was approved and I could finally see the real Japan with my own eyes. In the past, I could only know about Japan through media and stories of other people, which may have been dyed with bias. This trip gave me an objective image of Japan, which is very important for understanding of a country. I met many helpful Japanese people, did research with Japanese students, visited places of interests and etc. These two and half months in Japan are exciting and must be the best summer vacation I have ever had.

After I settled down, the first thing that impressed me was how much effort Japanese people made to improve quality of life. Since population density is high in Japan, limited space is another restriction factor that engineers need to keep in mind in products design. For example, those powerful toilets can show that Japanese people care a lot about others. I believe the standard toilets in Japan with washing system can be rarely seen in other countries. Besides, changing cover of the water tank into a tub is a very cool idea to save space and water. Sensors are used very often to save water and energy. In the dormitory we lived in, lights in public rooms are all automatic, so we would not forget to turn off the lights. These are small facts of saving water and energy, but can show the consciousness of environment protection.

Sanitation is another indicator of quality of life. We can tell whether a city is advanced or not if we pay attention to how clean the streets and restrooms are. The garbage sorting rules in Japan may be the most complex in the world. After we moved into the dorm, we were really shocked by the garbage sorting things. However, as time goes by, we are used to them now. If we think deep into those rules, someone needs to do garbage sorting anyway. When everyone in this country is devoted to reducing burden on the sanitation system, this country can definitely be clean and beautiful.

Good environment and clean streets can obviously benefit the tourism. On the weekends, we had time to visit other cities and enjoy the beauty of Japanese culture. We saw many pretty shrines and temples in Kyoto. They had been there for hundreds of years but still looked magnificent. We had delicious takoyaki and okonomiyaki in Osaka, and fed deer in Nara. We went to Gifu and watched the best firework I had ever seen. At this moment, we are planning to visit Tokyo during Obon Holiday and I'm looking forward to it.



Though we can't see sakura blossom or momiji in summer, various festivals in different cities made this trip to Japan completely worthwhile. Of course, I learned a lot about MEMS by doing research in Nagoya University, which might affect my career path in the future. I'm glad I joined JUACEP program and I really had a great time in Japan.

## Findings through JUACEP

**Name:** Yue Huang

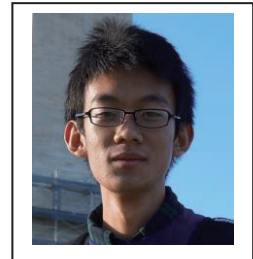
**Affiliation (Dept & Univ):** Department of Mechanical Engineering,  
University of California, Los Angeles

**Participated program:** Short (Summer) 2014

**Research theme:** Slip control for contact motion reproduction

**Advisor at Nagoya Univ:** Prof. Yoji YAMADA

**Affiliation (Dept.):** Mechanical Science and Engineering,  
Nagoya University



The experience at Nagoya University as a member of JUACEP was really amazing. Three-month is too short for me cause I enjoyed both the research and life here.

For the research, I conducted a project related to the wearable robot in Prof. YAMADA's lab. This project is a combination of material science, control system, manipulator control, 3D printing and C language programming. Since I focused on the MEMS field when I was at UCLA, most knowledge and skills related to my research here are new to me. At the beginning, I felt kind of difficult to deal with some tasks such as using Linux system and modeling the friction state of dummy skin. However, Prof. Yamada is very kind and helpful. He was always very patient to give me some instructions and advice. Besides, my TA and labmates also taught me a lot. Thanks to their kind help, I could get familiar with my research more quickly than I expected. In addition, the lectures of Production Engineering and Toyota Motor Factory trip made me impressed by the advanced manufacturing techniques in Japan. The handicraft exercise was also very interesting as well as meaningful.

I also enjoyed my spare time here with my friends and labmates. Japanese people are very polite and hospitable. I joined the activities of lab such as barbecue and drinking in TV tower beer garden, and I enjoyed the time with them a lot. I was also fortunate to visit many places with my friends. We watched sumo games in Nagoya, experienced the traditional Japanese culture in Kyoto, played with deer in Nara, enjoyed delicious food in Osaka, and saw the gorgeous fireworks in Gifu. We relaxed ourselves during the trip, and at the same time, we experienced the Japanese culture and Japanese people's kindness.

Generally, the entire experience here was very impressive and unforgettable. I made a lot of Japanese friends here, and they made me feel home. I hope to express my gratitude to JUACEP for providing me with this great opportunity. I believe this experience will be very useful for my future study and career.



## Findings through JUACEP

**Name:** Yingxia Liu

**Affiliation (Dept & Univ):** MSE, UCLA

**Participated program:** Short (Summer) 2014

**Research theme:** Thermal Stress and Strain analyses of TSV and microbumps in 3D IC using Abaqus

**Advisor at Nagoya Univ:** Prof. Nobutada Ohno

**Affiliation (Dept.):** Department of mechanical science and engineering



I had a really wonderful experience during my stay in Nagoya University. I'm sure this period will be my precious memory and even when I am old I will still remember all those good days in this period with smile on my face.

First I am really grateful for Prof. Ohno's patient guidance to me. I don't have a background in mechanics. Prof. Ohno always explains some basic knowledge to me patiently. TA Mr. Banno helped me a lot in getting familiar with software Abaqus. Without their help, it would be really difficult for me to get into the field of mechanical simulation which is totally new for me but important to my future research.

The field trip to Toyota and the workshop impressed me a lot. I have never thought about how a car is made and was astonished when went to Toyota factory. The scene I saw was really like a Hollywood movie. There were robot arms, solder sparks and the assembly line. The robots acted at a high accuracy. Standing in the factory made me think that it was really fancy to study engineering and I became more respect to those products of human scientific and technological developments. The workshop of painting toilet is even more interesting. At first I thought it was so funny to paint a toilet. Then I found it interesting and especially interesting because we painted together with friends. They all have some amazing ideas. One student from UM even painted Van Gogh's sunflower, making the toilet like a masterpiece.

In the weekends some friends from UCLA always went to explore the city of Nagoya together. We have also been to some other cities like Nara, Osaka and Kyoto. We also enjoyed sumo tournament in Nagoya. I am impressed that Japan has so many trees. There are trees almost everywhere. The scenery is very beautiful. There many stories in our trip, like we were starving to death but have to walk along the street of Kyoto to find a restaurant. Those stories seem funny when I thought up again. The following is a photo to show our happy stay at Nagoya.



## お疲れ様です!

**Name:** Yuan Hung Lo

**Affiliation:** UCLA Bioengineering

**Participated program:** Short (Summer) 2014

**Research theme:** Bacterial Adhesion and Quorum Sensing

**Advisor at Nagoya Univ:** Prof. Katsutoshi Hori

**Affiliation (Dept.):** Biotechnology



My tutor and good friend and I on top of Gifu-cho.

Coming into Japan I had no idea what to expect. I knew less Japanese than a 2-year-old, I was hardly prepared for my research project, and Nagoya was a faraway place I had only seen on Google maps. Honestly, I wasn't feeling too hot about venturing into a world that was so different from home. But as I type this and reflect on these past few weeks, those worries have become only a faint reminder of how much has changed this summer. Japan is strange in the most wonderful way possible. Simply put, there is no place quite like Japan.

Everything in Japan feels distinctively Japanese. The people, the streets, the food, and even their appliances have a recognizable "Made in Japan" feel to them. Their versions of Subway sandwich somehow tastes better than the original, and their water sprouting, odor eliminating toilets are second to none in functionality. And if Japanese things feel different than those in the US, then Japanese people are in an even starker contrast to Americans. The politeness and hospitality displayed by the Japanese people everywhere (and I mean everywhere) never failed to amaze me. Coming from LA, initially I could not believe what I was experiencing. However, it wasn't long before I started to enjoy and appreciate this harmonious culture.

Another quality of Japanese people I admired was their attention to detail. Everything in my apartment was well designed and made with clear intentions. Nothing was wasted, and nothing was superfluous. In lab, my lab mates took incredibly detailed notes, laying out clear goals for each experiment and presenting data in a clear and organized manner that could be understood by someone just picking up the notebook. Furthermore, when I was getting a hair cut, the haircutter executed every cut with precision and purpose, as if he was performing an important ritual. These may be mundane and insignificant examples, but they exemplified just how deeply precision and meticulousness are entwined within the Japanese culture.

Their attention to detail carried over to the way they cared for the environment, which really resonated with the environmentalist in me. The way Japanese cared for their community changed not just my ideas about sustainability; they changed my conception of what it meant to live harmoniously with my surroundings. Everywhere I went I saw people diligently recycle their trash, even down to the plastic packaging. When I went to watch hanabi along the Nagara-gawa River in Gifu, I read that the local communities would volunteer their time to clean up the river after every event. Unsurprisingly, as I learned over the course of this summer, this collective environmentally conscious mentality was also present in the way Japanese people approach biotechnology and bioengineering.

My research at Nagoya University concerned bacterial adhesion proteins and quorum sensing with applications in environmental biotechnology. It utilized the metabolism of microorganisms for non-toxic industrial production, and is an important technology for sustainable development. The engineered microorganisms can be used in biodegradation of toxic chemicals, wastewater treatment, and bioremediation. Furthermore, biofuels, such as bioethanol and methane, can be produced via metabolism of organic wastes. My time in Hori lab was a great opportunity for me to see how Japanese labs conduct research. I also learned many useful molecular and cellular biology lab techniques for studying bacteria. I believe the experience will help me professionally after I return to the US as I try to set up collaborations between Hori lab and labs in UCLA.

My experience with JUACEP far exceeded my initial expectation. Despite the short amount of time, I have learned so much and had so much fun. Words cannot describe how grateful I am for this opportunity. Finally, after an adventurous two and a half months here in Nagoya filled with immense professional and personal enrichment, I am happy to say, without any reservation, お疲れ様です!

## Findings Through JUACEP 2014

**Name:** Tait McLouth

**Affiliation (Dept & Univ):** Materials Engineering, UCLA

**Participated program:** Short (Summer) 2014

**Research theme:** Microwave Analysis of CFRP for Carbon Fiber Content

**Advisor at Nagoya Univ:** Professor Ju

**Affiliation (Dept.):** Mechanical Engineering



I was initially hesitant about staying at Nagoya University for the summer of 2014, as I wanted to build my engineering skills as much as possible in preparation for graduate school and I thought the best way to do this would be through a summer internship. However, now that I have participated in the JUACEP program I can confidently say that I made the right choice. Not only was my stay here good for my engineering ability, but the complete immersion in a new culture helped me grow in more ways than one. I learned [part of] a new language, ate delicious Japanese food, made new friends, and learned more than I could have at any internship in California.

The culture of Japan was one of my favorite parts of the program. During the weekdays the other UCLA students and I would focus on our research efforts, and sometimes eat out for dinner. However, once the weekend came around we would go on 2-3 day long excursions around Japan to places like Kyoto, Nara, Takayama, and many others. These trips were so interesting because once we left Nagoya, we were on our own. It was up to us to decide where we wanted to go and what we wanted to do in all of these foreign cities, and that is what made it so exciting. The language barrier initially posed some problems, however with the basic Japanese we learned in class, and also the ability to read both Hiragana and Katakana (with the added Kanji knowledge of the Chinese students from UCLA), we were able to travel around fairly well. Going to local bars in Osaka, feeding the deer in Nara, and biking around Kyoto gave us some great memories we will not soon forget.

As I mentioned earlier, the weekdays were when we worked, but that did not mean we didn't enjoy ourselves. The food in the school cafeteria was fantastic, and my lab mates were extremely friendly. Going out to play baseball, soccer, and basketball were just a couple of the ways we were able to bond, but also eating together, playing otokogi janken, and talking in lab were very enjoyable. After working in the lab, it was not uncommon for some of us to go to an Izakaya in Motoyama. Similar to an American bar, except with better food, Izakayas were a great opportunity to get to know each other on a more personal level. The work week became just as enjoyable as the weekends did as we got further along in the program and more accustomed to the Japanese lifestyle.

The research itself may have been the most difficult part of the program. I felt that ten weeks was not enough time to adequately start and finish a brand new research project. However, this was not necessarily a bad thing, as the limited time frame pushed us to work harder and think more critically. The language barrier on equipment's software and communication with other members of the lab also posed additional problems, however as an engineer it is our job to be able to work around problems like these and make the best of the situation. I think that these additional problems only motivated us more to work on our research.

I think that participation in the JUACEP program has really taught me a lot about Japanese culture and also improved my problem solving abilities. This will have a positive impact on the research I do down the road, and will hopefully put me in a better position for finding a job in the coming years. I am glad that I chose to come to Japan, and I will wholeheartedly recommend the program to anyone who is looking for something productive and exciting to do during the summer.

## Findings through JUACEP

**Name:** Mark Seal

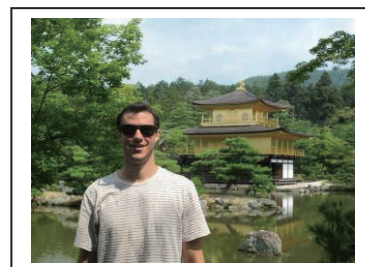
**Affiliation (Dept & Univ):** Materials Science, UCLA

**Participated program:** Short (Summer) 2014

**Research theme:** SiC Solution Growth

**Advisor at Nagoya Univ:** Prof. Ujihara

**Affiliation (Dept.):** Materials Science



It's hard to believe it's already almost been ten weeks. I sit puzzled, sifting through lists of potential words to describe this summer in Japan but perhaps what's most telling are the words that are absent from my search: boring, tedious, and redundant.

I don't mean to say that it was a walk in the park, lab work always has its ups and downs. But these past weeks have flown by faster than any in recent memory and I have so much to be thankful for.

First, to the Nagoya University staff and students for making me feel instantly welcome. From the first day in lab, I was able to participate in research with my mentor. My background is from a slightly different field, but both my student mentor and advising professor were patient while I adapted to the rhythm and culture of their lab group. Although ten weeks is a laughably short amount of time to perform a complete research project, I feel I was able to contribute and work semi-independently, even if the language barrier made things slow going at times.

I'd be lying if I said that weekend trips weren't the highlight of my summer. The temples in Kyoto, the food in Osaka, the fireworks in Gifu, the list goes on and on, but the one constant at every location was the patience and helpfulness of complete strangers. One hundred percent of the times where I was lost or confused, someone would stop and go out of their way to help.

The cultural differences between American and Japanese people are most apparent here. At least where I come from in Los Angeles, relying on the kindness of strangers can be a risky move, but in Japan I was never led astray or taken advantage of (at least that I know of). Combined with working everyday with my Japanese lab members and taking a language class, I have an entirely different and fuller understanding of Japanese culture, and am eager to continue learning. While the Japanese are typically a reserved people, their actions have spoken loudly as a testament to their hospitality.

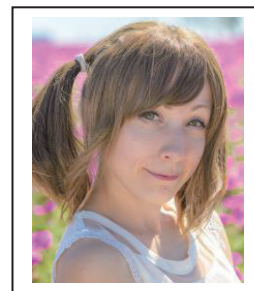
I could write at length about the history of my trip, but its' most interesting impact will be on my future. I'm no longer hesitant to apply for employment positions that involve travel to Japan, or for that matter even applying to Japanese engineering companies. I hope that potential employers will see this trip for what it was; a learning experience on literally every level, from science, to culture, to eating with chopsticks.

## Findings through JUACEP

**Name:** Elvia Cortes

**Affiliation (Dept & Univ):** UCLA

**Participated program:** Medium term (Summer and Fall) 2014



**Research theme:** Effect of Anode Geometry on Steady-State Magnetoplasmadynamics Thruster

**Advisor at Nagoya Univ:** Prof. SASOH

**Affiliation (Dept.):** Aerospace Engineering

Japan is well known for its brilliant innovative technology, while the graduate school of Engineering at Nagoya University has outstanding research facilities. Having the opportunity to be part of this society through the JUACEP program has helped me grow as an engineer and researcher. During my six month stay in Nagoya University I have learned a lot about electric propulsion under the guidance of professor Sasoh, my teaching assistant and lab mates. I learned about how the magnetoplasmadynamic(MPD) thruster works, its acceleration methods, and using this knowledge as well as previous research I designed an optimized MPD thruster. This was then manufactured, and I learned to set up the lab equipment necessary to run tests on the MPD thruster. It was a great experience to finish this project, from the preliminary trade studies, designing, manufacturing and finally experimenting.

Through this internship I was able to experience everyday life and work ethics here in Japan. Every Tuesday morning we had a seminar in Prof. SASOH's lab where each student showed their current progress in research. This was very educational because it helped broaden my knowledge of my own study by learning about other student's research. I have also seen how enthusiastic and hardworking Japanese students are about their work. It is part of this culture to work hard and at the same time relax once in a while. I went to several Izakayas with my lab mates and had a great time socializing and building strong relationships with colleagues. Outside of lab, something that amazed me about Japan is how polite, humble and kind everyone I had the opportunity to interact with was.

The JUACEP program contained many great activities: I learned a lot about production engineering through the seminars that were provided, enjoyed the assembly of the internal combustion engine and finally had an amazing experience in our field trip to see the Toyota plant and the sea side BBQ. The Japanese class helped re-enforce previous knowledge I had of the Japanese language and I learned many useful common every day phrases.

In terms of my career, this program has helped me in many ways. When I first came to Japan I was very shy and scared of public speaking, some qualities that are detrimental to my future engineering career. After presenting my research every week to the entire lab I no longer have a fear of public speaking. Interacting with students from a different culture helped me grow as a person and improved my communication skills. I have also learned a great deal about myself: I really enjoy international collaboration and learning about other cultures. This has motivated me to find a job in an international company in the future.

Traveling around Japan has also been an important part of my experience here. I have been to Kyoto, Nara, Hiroshima, Shirakawago, and Tokyo, truly stunning locations. I also experienced the beautiful Japanese natural environment by seeing autumn leaves at Koorankei and winter sakura at Obara village. Finally, I took part in this culture by wearing a Yukata to the fireworks festivals and visiting the beautiful onsen in Takayama. Through the JUACEP program I have grown as an individual, gained an immense amount of knowledge about research, the Japanese culture and language, and seen many beautiful and historic places that Japan has to offer.

## Findings through JUACEP

**Name:** Antonio Martinez

**Affiliation (Dept & Univ):** Electrical Engineering, UCLA

**Participated program:** Short (Summer) 2014

**Research theme:** Human Activity Recognition using Smartphone

**Advisor at Nagoya Univ:** Prof. Nobuo Kawaguchi

**Affiliation (Dept.):** Department of Computer Science and Engineering



One of the things I most enjoyed from the JUACEP program has been the research lectures. Researchers from well-known companies and institutions come to the Nagoya University campus to offer a research lecture about the work they are currently engaged on. For instance, I enjoyed the research lecture of Professor Toshio Hirota, a visiting professor from Waseda University, who talked about technological innovations for sustainable mobility. Another part of the program that I truly appreciate was the engine assembly/disassembly. This hands-on activity was not only fun, but also very interesting as we were able to closely learn the basic engineering principles seen on an engine.

I found my lab to be unexpectedly big. It has about fifteen members and three professors. Most of my lab mates are undergraduate students, but there are also master's and PhD students. The lab has a good feeling of camaraderie, which is one of the aspects I like the most because this has a positive effect on teamwork, especially in a research setting like this.

I was glad to find that Nagoya University has a beautiful and large campus, the Higashiyama campus that is, where the graduate school of engineering is located at. There are many facilities to serve the students, like cafeterias, convenience stores, coffee shops, etc. Also, there is a gym, which I've been using regularly. In general, the campus area is in a nice and quiet location of Nagoya.

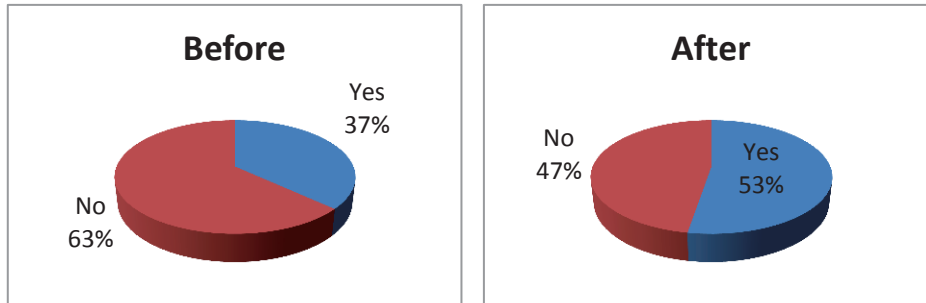
Life in Nagoya has been enjoyable in many aspects, with the exception of the summer weather. It was really hot and humid, but the good thing was that there was always air conditioning on most places, including my lab, and my room. Nagoya is centrally located in Japan. That made it easy to travel not far distances to visit interesting places like Kyoto, Osaka, Tokyo, among others. Even within Nagoya there are many places to visit, like the Nagoya castle, several temples, and even the Nagoya zoo.

I believe having participated in the JUACEP program will not only have an impact on my future career as a researcher, but also, on my life. I have been able to observe the differences and similarities on how a research lab functions here in Japan compared to a lab back home in the US. This definitely will improve my own research practices in the future. Similarly, the cultural differences I have experienced in Japan will enrich the way I see life and will help me appreciate contributions of other cultures to my own.

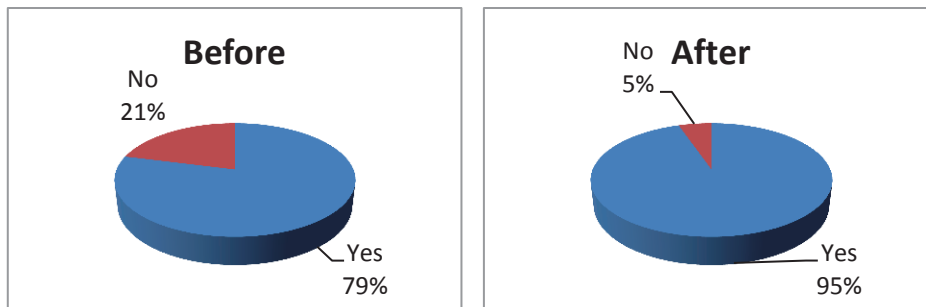
### 3-b. Questionnaires

*\*For Q1-4, we asked the same questions BEFORE and AFTER the program.*

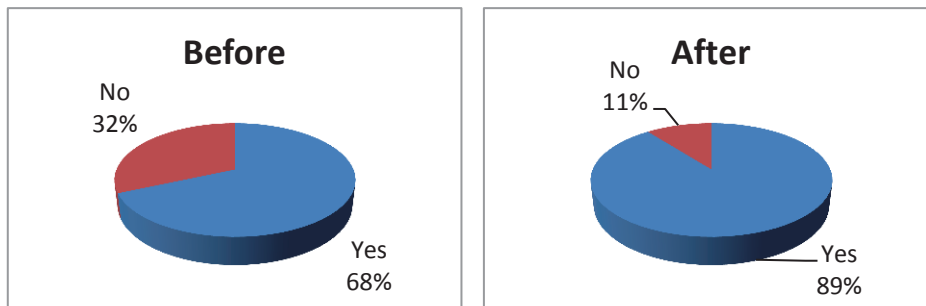
**Q1: Are you interested in studying at a Japanese University for PhD?**



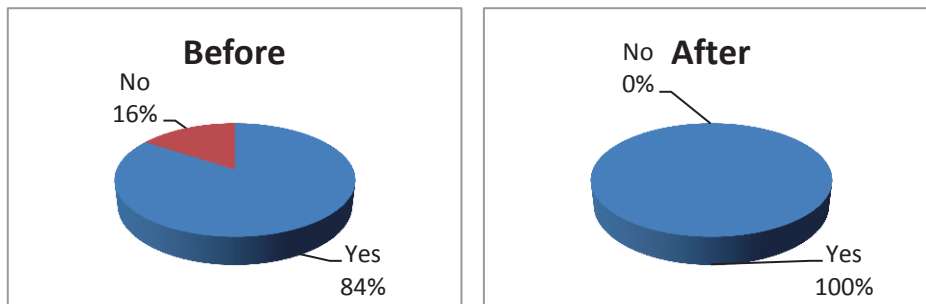
**Q2: Are you interested in working at a Japanese company in USA?**



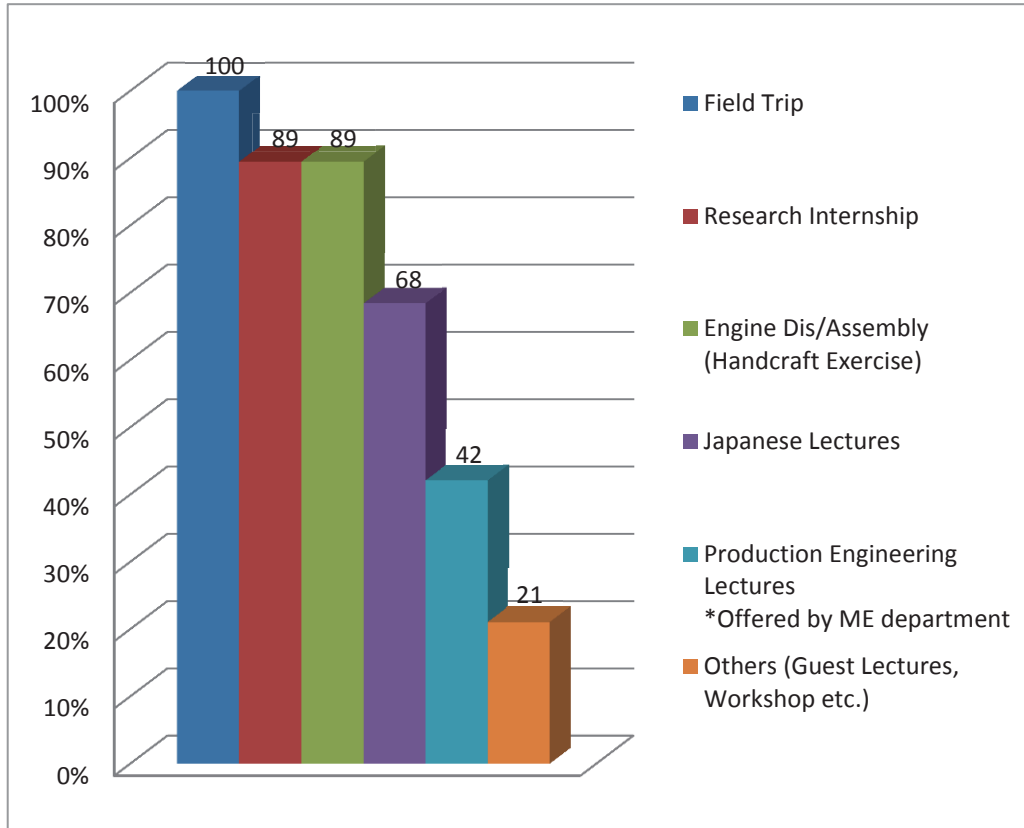
**Q3: Are you interested in Working at a Japanese company in Japan?**



**Q4: Are you interested in working at a non-Japanese company in Japan?**



**Q5: Which programs of the JUACEP did you like?**



**Q6: In what did you find difficulty? What could be improved?**

**Time limitation (10 weeks) of research internship**

- It may have been an insufficient amount of time to come into a foreign country to start a new topic, come up with an experiment, and gather data.
- Instead of each student starting a brand new project to work on, we could work with a current student, helping them with their research that is already established. This would have eased any stress some of the students were feeling as we progressed through the program.
- 10 weeks may not be long enough to do deep research.

**Time limitation (10 lectures) of Japanese lectures**

- Only 10 classes in one month are not enough. Most of the things taught have been forgotten by the end of the stay.
- If JUACEP offers optional session such as open discussion sessions hosted by the TAs or Japanese student volunteers (for example, the students who will go to UM or UCLA) would be great.
- Offering at least 3 days/week lessons for the whole length of the internship would be much appreciated because Japanese people don't have a good command of English compared to other developed countries, therefore, knowing Japanese becomes imperative.



Production engineering lectures

- *A more interactive speaker-audience atmosphere would be more conducive to the audience staying awake.*
- *The language barrier made the lectures hard to understand although each topic is very interesting. The lecturers are from famous companies so more practical case studies would be great.*

Language barrier

- *The English of some students in the group is not very good and my English is also not good. So there is a little difficult to communicate.*
- *Communicating in local people was difficult especially at first.*

Providing more information beforehand

- *Giving more information on the Nagoya University International Program office would be nice since they usually hold cultural exchange events for international and Japanese students at Nagoya University.*
- *Receiving information and tips on traveling before arriving in Nagoya would be useful since most students will be traveling around Japan. (Ex. discounted railroad tickets for foreigners).*

Field trip

- *More visit to automobile museums and plants as Nagoya is famous for car industry.*

Housing situation

- *Bathroom-sharing dorm housing was a bit shocking. In America, dorm housing is usually exclusive for first year undergraduate students. Graduate students need the privacy and quietness of an apartment-like housing setting.*

#### **Q7. Write comments freely.**

This was a truly remarkable internship and I hope this program will continue in order to provide more students with a great learning experience in terms of both research and Japanese culture.

Generally, this program is awesome. It gives me the opportunity to learn more about Japanese universities and culture. The sub-programs are useful and of great fun. They made my life in Japan more colorful. I would like to appreciate all the JUACEP staffs', professors' and lab mates' help. I learnt a lot from them, and I believe we can become the whole-life friends.

Overall, I really enjoyed the program, and I think it is a great experience. I will definitely be recommending JUACEP to my friends back at UCLA, and I hope that the program can continue so as many students from UCLA and UM can get involved as possible. I previously thought that studying abroad was not an option as an engineer. However, the timing of the JUACEP program over the summer is the perfect replacement for a summer internship, as it provides as much (if not more) engineering experience than an internship would have. I already mentioned what I felt was the one flaw with the program, but that could also just be a rare occurrence that happens with difficult research.

Another part of the program I really liked was the JASSO scholarship. I think that 80,000 yen is a perfect amount of money to allow us the freedom to visit other places in Japan like Kyoto and Tokyo, while also leaving spare money for all the delicious food here. I'm very glad that

this money was offered, as it made the choice to participate in the program very easy! Thank you for giving me this opportunity, I truly enjoyed it.

JUACEP is a good program and I hope there could be more students participating in this program.

I love the program whole-heartedly, and I sincerely hope you guys can keep the program going for years to come so other students will have the privilege of experiencing all the awesome things I experienced!

Thank you very much for providing us with this wonderful opportunity. All the programs are very useful and interesting. Faculty and lab mates here are also very nice and make us feel home. The experience here was so good that I hope I could stay here for a longer time.

I am really grateful to the JUACEP program for giving me this opportunity to come to Japan. I would also like to thank all the staff for making this possible. It truly has been an unforgettable experience for me.

All I want to express is my gratitude for JUACEP and help from the office administrators. Without them, I might never have this opportunity to study in Japan. I really treasure this experience. Hope in the future, more students will benefit from JUACEP!

I love this program. I love Japan.

<4>

## Appendix

## 4-a. Pictures

### -Orientation-



### -Welcome Luncheon-



### -Japanese Language Class-



-Field Trip-



*Toyota Motomachi Plant*



*INAX Museum*



BBQ in Chita Peninsula



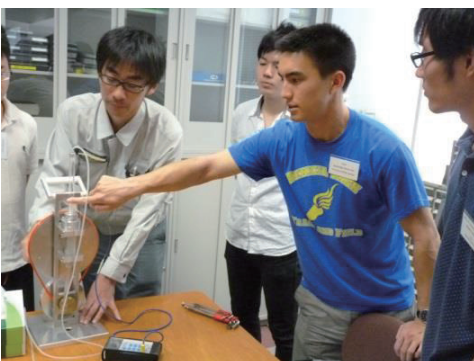
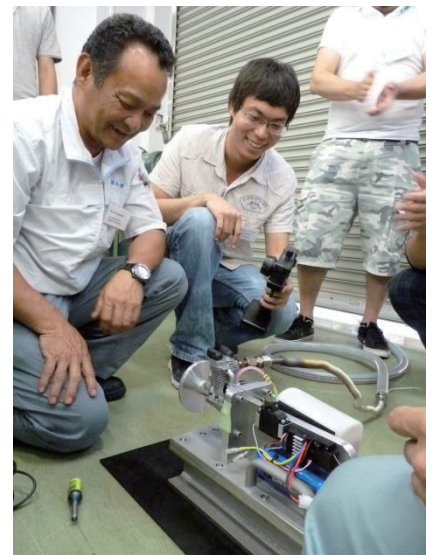
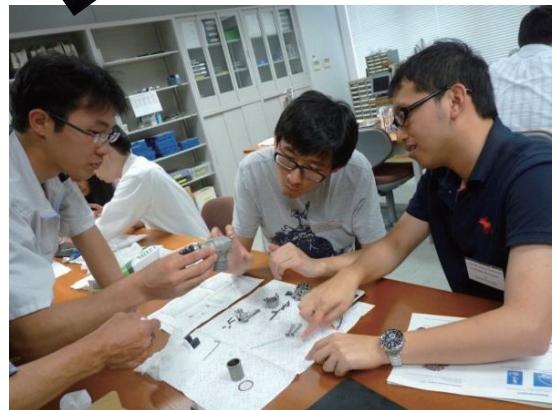
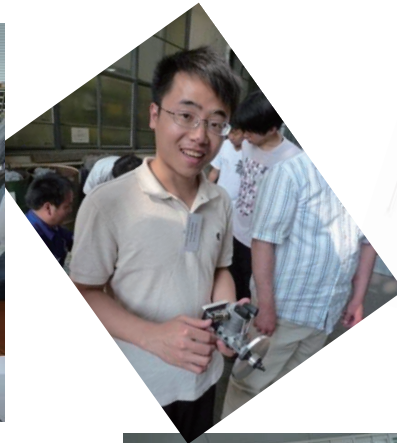
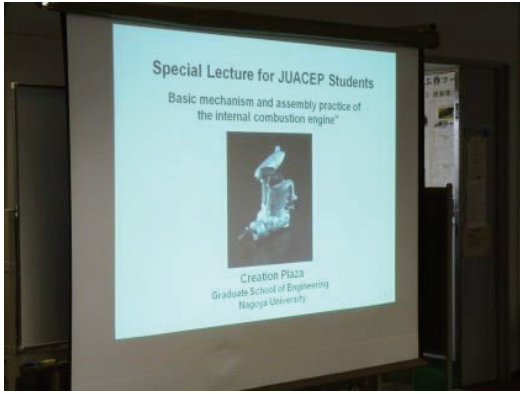
-Round-table Discussion with Prof. Yang-



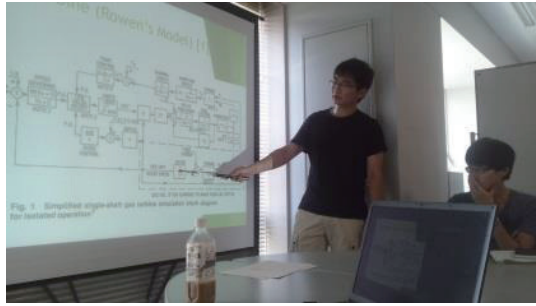
-Meet-up event with NU students-



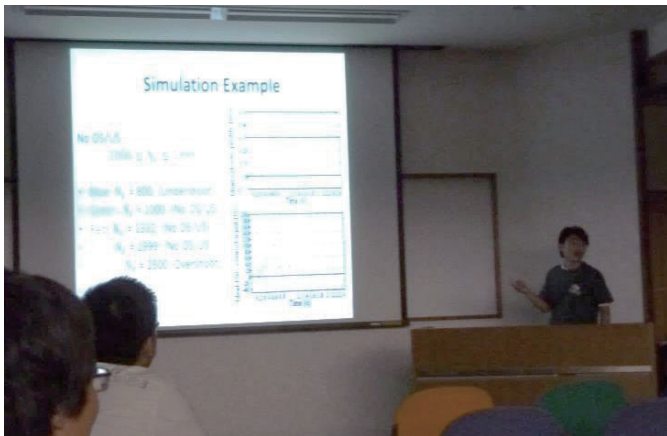
-Handcraft Exercise-



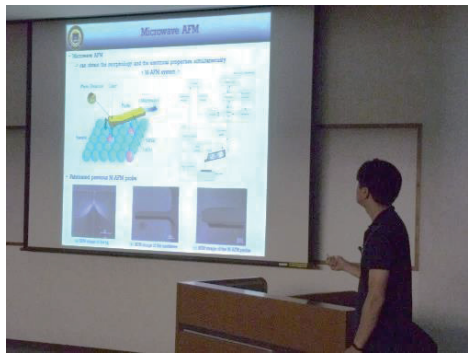
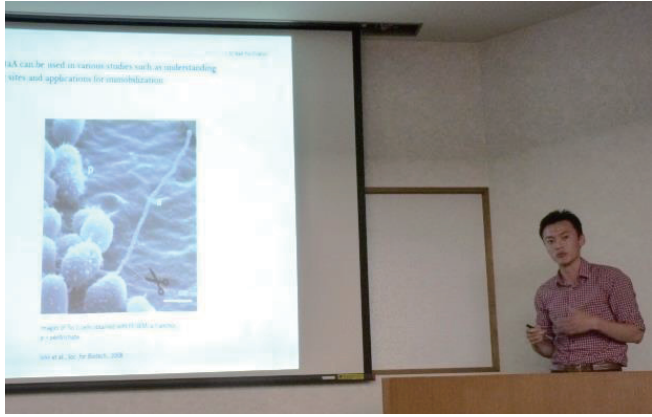
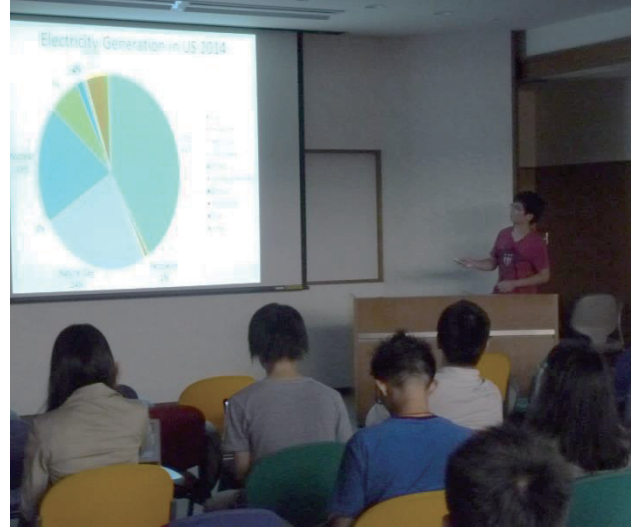
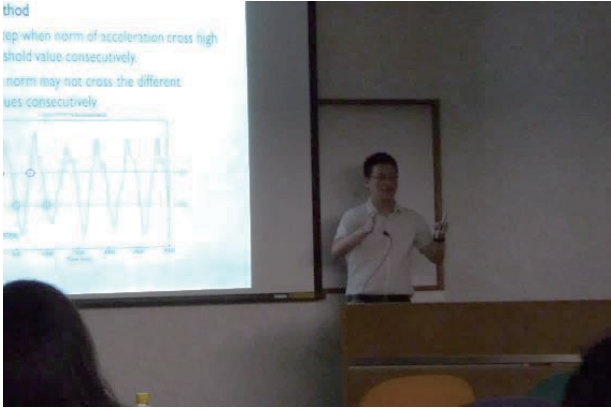
-@ Lab.-



-Workshop-







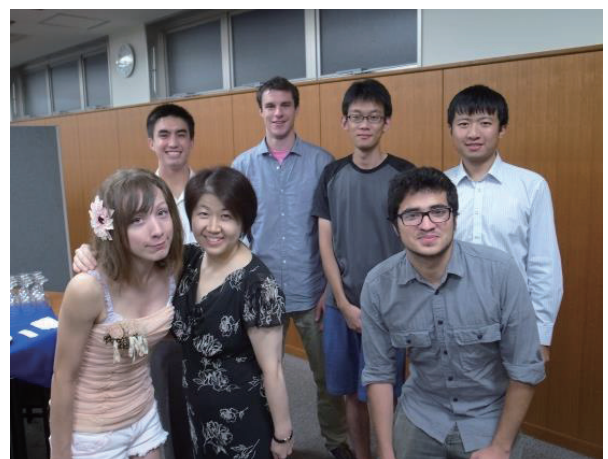
-Awarding Ceremony-

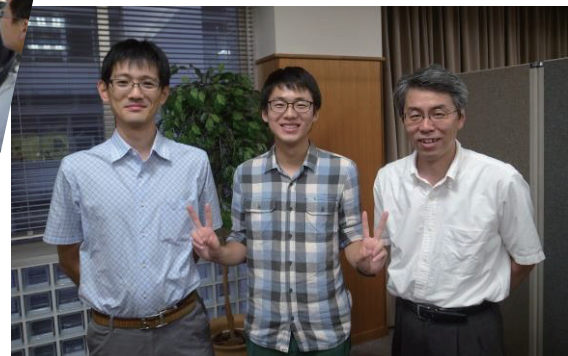
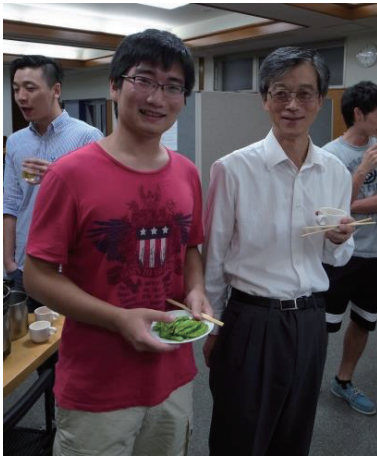


-Final Presentation of 6-month course students-



-Farewell Party-





## 4-b. Handout Materials

*Orientation Agenda*

JUACEP Summer Program 2014



*Tuesday, May 13, 2014 for UM students*

10:00 --ES 032, 3F, ES Bldg--

Reception: payment of admission fee, health insurance and Japanese textbook

10:30 **Orientation**

Welcome address from JUACEP Leader

Introduction of faculty, staff and participating students

*Academic Information*

- A) Schedule
- B) Japanese Language Class
- C) Handcraft Exercise
- D) Introduction to Production Engineering
- E) JUACEP Seminars
- F) Field Trip – Toyota, INAX Museum
- G) 3 Reports (Research report, Scholarship report, Finding through JUACEP)
- H) Evaluation

*Life Information*

- A) Promise
- B) Housing
- C) Use of PC on Campus – set up with each TA
- D) Student ID Card
- E) Medical and Health Care
  - Medical Services
  - Health Precautions
- F) Student Life
  - Refuse Disposal at Nagoya University
  - Public Transportation in Nagoya City
  - If involved in a Traffic Accident
  - Compliance with Japanese Law
  - Safety Guide
  - Culture Shock
  - Differences in Academic Culture
  - Cope with Stress
  - Harassment

11:40 **Introduction of the lab mentors and TAs**

~Picture time~

12:00 **Welcome lunch** --Restaurant Chez Jiroud, 1F, ES Bldg--

~Welcome from the dean of Graduate School of Engineering ~

-----

*Wednesday, May 14, 2014*

13:00 --ES031, 3F, ES Bldg --

Receiving stipend and tuition fee payment



***Tuesday, June 17, 2014 for UCLA students***

10:30 --ES 021, 2F, ES Bldg--

Reception: payment of admission fee, health insurance and Japanese textbook

11:00 **Orientation**

Welcome address from JUACEP Leader

Introduction of faculty, staff and participating students

*Academic Information*

- A) Schedule
- B) Japanese Language Class
- C) Handcraft Exercise
- D) Introduction to Production Engineering
- E) Field Trip – Toyota, INAX Museum
- F) 3 Reports (Research report, Scholarship report, Finding through JUACEP)
- G) Evaluation

*Life Information*

- A) Promise
- B) Housing
- C) Use of PC on Campus – set up with each TA
- D) Student ID Card
- E) Medical and Health Care
  - Medical Services
  - Health Precautions
- F) Student Life
  - Refuse Disposal at Nagoya University
  - Public Transportation in Nagoya City
  - If involved in a Traffic Accident
  - Compliance with Japanese Law
  - Safety Guide
  - Culture Shock
  - Differences in Academic Culture
  - Cope with Stress
  - Harassment

11:40 **Introduction of the lab mentors and TAs**

~Picture time~

12:00 **Welcome lunch** --Restaurant Chez Jiroud, 1F, ES Bldg--

~ Welcome from faculty of JUACEP ~

-----

***Wednesday, June 18, 2014***

13:00 --ES032, 3F, ES Bldg --

Receiving stipend and tuition fee payment

## Students Life Information

### Housing

#### **International Residence Yamate**

(10 minutes' walk from Higashiyama Campus)

Address: 165 Takamine-cho, Showa-ku, Nagoya 466-0811, Japan

Phone: 052-835-5575 (office)

Facilities: This is a three-story building with 106 single rooms (approximately 15m<sup>2</sup>).

It houses a lounge, a recyclable trash area, two laundry rooms, mail boxes, and an administrative office.

Each room is furnished with a bed with bedding(\*), desk, chair, desk lamp, open closet, storage shelf, air conditioner, Internet connection, TV connection, wastepaper bin, sink, induction heating (IH) cooker (1), microwave oven, refrigerator-freezer, ventilation fan, unit bathroom/ toilet and curtains (2 sets), etc.

(\*)Bedding: Set for each room comprises quilt (1), blanket (1), bedpad (1), pillow (1), quilt cover (2), bedsheet (2), pillow slip (2).

Three Japanese graduate students live on each floor in International Residence Yamate as tutors.

### PC & ID

#### **Use of PCs on Campus**

Wireless internet connection is available on campus including the Satellite PC Lab in the main library, and other areas on campus. If you want to connect our lap top PC to Nagoya University Wireless Network

(NUWNET), please go to 'ECIS computer web page' (<http://eee.ecis.nagoya-u.ac.jp/computer/instr.html>)

After receiving your ID and password, you must take the online Information Security Training and pass the test within a week. To pass the test, you must score at least 80% and retake the test until your score 80% or above.

#### **Student ID Card**

A student ID card has many functions. It will let you into the university libraries, and with the card you may borrow books from the library. The card lets you get student discounts at museums, theatres and so on.

### Medical and Health Care

#### **1. Medical Services**

If you suffer from continuous headaches, a loss of appetite, or you cannot sleep well, etc., you should seek the advice of a doctor before the condition gets worse. These symptoms may be a sign of fatigue or

exhaustion. They may also be psychological or psychosomatic symptoms, which are treatable by specialist doctors. In addition to taking care of your own health, please pay attention to your friends' health and encourage them to see a doctor, if they are feeling unwell.

**(1) The Health Administration Office** Students can undergo physical examinations, receive health advice, first-aid and arrange psychiatric counseling at this facility. There is no charge for using any of these services.

Tel: 052-789-3970

[Office Hours for Health Services]

Treatment	Time	Mon	Tue	Wed	Thu	Fri
Physical Examinations & First-Aid	10:00 – 11:30	○	○	○	○	○
	13:30 – 16:30	○	○	○	○	○
Psychiatric Counseling	10:00 – 12:00	○	○	○	○	○
	13:30 – 16:30	○	○	-	○	○

\*Note: Appointments are necessary for psychiatric counseling services. Please call the office 052-788-6276 for appointments.

The Health Administrative Office is open between 9:00 - 12:00, 13:00 - 17:00 for first aid.

## **(2) Calling an Ambulance**

Telephone 119 or press the RED button on a public phone for connection, free of charge. Although it is possible to speak English, it would probably be helpful for you to say the following: **Kyukyusha** (ambulance) **o onegai shimasu. Basho wa** (your location) **desu.** (I am calling for an ambulance. I am at...location.) This number is also used for requesting fire engines (**shobosha**). In Japan, ambulances are available 24 hours a day, free of charge.

## **2. Health Precautions**

### **(1) Food Poisoning**

Great care should be taken with regard to eating habits during the extreme summer weather in Japan. To avoid food spoilage, check the expiration date before buying food, apply heat to raw foods and be careful not to keep food in the refrigerator for an excessive amount of time. To guard against food poisoning, always wash culinary items with hot water. In the past, there was a frightening outbreak of O-157, a bacterial food poisoning disease. There was also an incident where students enrolled at Nagoya University were poisoned by eating wild mushrooms.

### **(2) Necessary measures to prevent the spread of infectious diseases**

If you are traveling from Japan to another country, please seek travel advice regularly until the time of departure. Please follow the basic rules of hygiene to avoid being infected.

The Ministry of Foreign Affairs of Japan: <http://www.anzen.mofa.go.jp/>

World Health organization: <http://www.who.int/en/>

## Student Life

### **1. Refuse Disposal at Nagoya University**

A sorting system for refuse disposal is used at Nagoya University. There are trash cans for “combustible refuse”, “incombustible refuse”, and recycle bins for “empty bottles”, “empty cans”, and “PET bottles” all over campus. In addition, there are boxes and a reverse vending machine near the Co-op. The sorted refuse will be recycled. Newspapers or magazines are collected by recycle companies. Used paper products such as used copy paper are collected and recycled. Students are kindly requested to be mindful when they throw away their rubbish and to use the correct bins to help waste reduction and the reuse of recyclable materials.

### **2. Public Transportation**

#### 1. Subway and City Bus Tickets:

- ① Manaca: Manaca is a pre-paid pass that can be used for both subway trains and buses operated by Nagoya City. Various types of Manaca can be purchased. It can be used for Meitetsu buses and trains, Aonami lines, Yutorito lines and Toyohashi railroad. It is a rechargeable card.
- ② One-day ticket: One-day tickets allow for unlimited rides for one day. One-day tickets for all bus, subway, and bus & subway routes are available. Ticket, Donichi-Eco-Kippu, that can be used on Saturdays, Sundays, holidays and the 8th of every month can be also purchased.

These tickets include a discounted admission fee for some tourist facilities in Nagoya city such as Nagoya Castle or the Tokugawa Museum.

They can be purchased at any subway station. For further information, refer to the following website:

<http://www.kotsu.city.nagoya.jp/> (Japanese)

#### 2. Useful Links:

The following websites provide information on available transport services, time-tables, etc..

HYPERDIA: <http://www.hyperdia.com/en/>

### **3. If involved in a traffic accident.**

If you are involved in a traffic accident, remain calm and do the following:

1. If anyone is injured, dial 119 for an ambulance.
2. Move any dangerous including vehicles, off the road to prevent other accidents.
3. Report the accident immediately, even if it is small, to a nearby police station and obtain a report of the accident.



4. Write down the license plate number of the car concerned as well as the name, address and age of the driver, after requesting to see his/her driver's license.
5. If there are witnesses, write down their names, addresses and telephone numbers.
6. Make detailed notes of the accident and take photographs, if possible.
7. See a doctor, even if you think that you are all right, because sometimes symptoms can take time to occur.
8. Consult your insurance company as soon as possible.

#### **4. Compliance with Japanese Law**

During their stay in Japan, any student who commits a crime, misdemeanor or any other illegal act, will be subject to legal procedures according to Japanese Law. Nagoya University also takes strict disciplinary measures against students who commit crimes or misdemeanors, and may expels them from university.

##### (1) Prohibition of Narcotics

In Japan, the possession and sale, for personal use or otherwise, of all narcotics and any illegal substances are strictly prohibited. If offered, refuse them. If leaving Japan temporarily, never agree to look after a stranger's luggage at the airport.

##### (2) Drinking and Smoking Restrictions

In Japan, people aged under 20 are not allowed to drink or smoke. Smoking is not allowed in many places, including stations, public facilities and within the campus. Nagoya city has special zones where smoking on the street is banned. If found smoking there, you will be fined.

Driving a car, riding a motorcycle or bicycle after drinking any amount of alcohol is a serious offence in Japan, and can also cause accidents. Never drive after drinking. Those who accept a ride in a car that is driven by a drunk driver or those who offer alcohol to a driver are all subject to punishment under Japanese law.

##### (3) Others

Whilst inside a shop, removing product wrappers, price tags or putting products into pockets or bags before actually paying for them may be treated as an attempt to shoplift in Japan. Talking loudly on your mobile phone or chatting with friends in public places, such as on a train, can cause disturbance in Japan.

#### **5. Safety Guide**

Japan is not as safe as most people think. There is the risk of crime anywhere in the world, including Japan. This is what you can do avoid problems.

- ◆ Avoid going out alone at night and keep away from deserted places.
- ◆ Many bag-snatchings occur in Nagoya. Keep your handbag close when walking on the street.
- ◆ Do not answer phone calls from unknown numbers. Do not open the door to strangers, even if they claim that they are representing certain companies. Lock and chain the door of your apartment when you are at home.
- ◆ There are deserted or dark places on campus which you should avoid. There is the risk of theft inside

and outside of buildings. Please always protect your property.

## **6. Culture shock**

Although “culture shock” is generally understood as a temporary shock felt when confronted by different cultural customs, ways of thinking and behavior patterns, it actually refers to a psychological state of depression caused by a succession of failure experiences in unfamiliar social situations. Culture shock is temporary and everybody goes through it to some extent in the process of cultural adaptation. General symptoms of culture shock include negative feelings such as: losing self confidence, feeling depressed, attributing all failure to yourself, feeling that nobody understands you, feeling inadequate, etc. Accordingly, you may lose all motivation to talk with Japanese people or to attend classes. Most of these psychological reactions are, again, very natural in the process of cultural adaptation. Please take time to cope with each single event in your life, and you will be able to overcome these emotions sooner or later.

## **7. Differences in “academic culture”**

It is widely accepted that different values, behavioral and communication patterns exist from culture to culture. However, we often fail to realize that there are also differences in “academic culture”, such as expected roles of academic advisers and students, classroom communication, evaluation criteria, etc. Such differences can also be a major cause of your stress. For example, the relationship between academic adviser and advisee is considered particularly important at the graduate level education in Japan. Some knowledge of the Japanese academic culture will help you achieve your goal more smoothly.

## **8. Cope with Stress**

If you feel pressured by stress or lose confidence in your ability to study, you should think about releasing yourself from these negative emotions. Achieving good results in your studies may take a certain amount of time, and ought to be viewed as an accumulative process. Sometimes, you will need to take a break. If you feel tired, do not push yourself too hard and try to enjoy some of your favorite foods, recreation, and physical exercise. It is also recommended that you talk with your friends, academic adviser, or international students advisors/counselors. Moreover, please do not consider the process of cultural adaptation solely as a cause of stress; you can learn tremendously about various cultures, including your own, from this process.

< Visit the office of ECIS Advising & Counseling Services >

If you feel that you cannot deal with stress or feel a sense of isolation or frustration, do not hesitate to ask for help from international counselors at the ECIS Advising & Counseling Services. There is an international student counselor who will support your personal and psychological concerns. A discussion with an international student counselor can help achieve a useful perspective on culture shock and insights into Japanese culture.

ECIS Advising & Counseling Services (7th floor, West Wing of IB Bldg.)

<http://www.isa.provost.nagoya-u.ac.jp/en/>

## **9. Harassment**

Nagoya University has set up a Harassment Consultation Center to prevent and eliminate the occurrence of any kinds of harassment, such as sexual harassment and academic harassment. Professional counselors deal with inquiries with utmost respect for their clients' feelings and wishes. Where the necessity arises, claims will be referred to the Committee for the Prevention of Harassment for investigation and arbitration. The Harassment Consultation Center works on issues of any degree of gravity. If you observe someone suffering from any kind of harassment, you may also come and report the case. In addition to the Harassment Consultation Center, each School at Nagoya University has appointed a faculty member as contact person (cf. see below). For English language consultation, you may visit the representative at the Education Center for International Students (ECIS). All consultation will be kept strictly confidential.

Nagoya University Harassment Consultation Center (Appointments by fax or E-mail)

Tel: 052-789-5806 (9:30-16:00)

Fax: 052-789-5968

E-mail: [sh-help@post.jimu.nagoya-u.ac.jp](mailto:sh-help@post.jimu.nagoya-u.ac.jp)

URL: <http://www.sh-help.provost.nagoya-u.ac.jp/>Contact persons at each School (including ECIS)

URL: <http://www.sh-help.provost.nagoya-u.ac.jp/pdf/madoguchi.pdf>>

# Campus Map

## Higashiyama Campus



### Main Buildings

- 1** Administration Bureau Buildings
- 2** Toyoda Auditorium / Symposion
- 3** Nagoya University Museum
- 4** University Library (Central Library)
- 5** Noyori Conference Hall
- 6** Noyori Materials Science Laboratory
- 7** Akasaki Institute

### Graduate School / School Buildings

- 8** Graduate School / School of Engineering Buildings
- 9** Engineering and Science Building (Central Building of Graduate School of Engineering / Particle and Astrophysical Science Building)
- 10** Graduate School / School of Science Buildings
- 11** Graduate School of Mathematics Building
- 12** Science and Agricultural Building
- 13** Graduate School of Bioagricultural Sciences / School of Agricultural Sciences Building
- 14** Environmental Studies Hall  
-Graduate School of Environmental Studies
- 15** Graduate School / School of Economics Building
- 16** Graduate School / School of Law Building
- 17** Graduate School of International Development Building
- 18** Graduate School of Education and Human Development / School of Education Building
- 19** Integrated Research Building (Arts and Social Sciences)
- 20** Graduate School / School of Letters Building
- 21** Central Building for Liberal Arts and Sciences  
-School of Informatics and Sciences Building  
-Institute of Liberal Arts & Sciences
- 22** Building A for Liberal Arts and Sciences
- 23** Graduate School of Languages and Cultures Building
- 24** Graduate School of information Science Building

### Centers / Institute Buildings

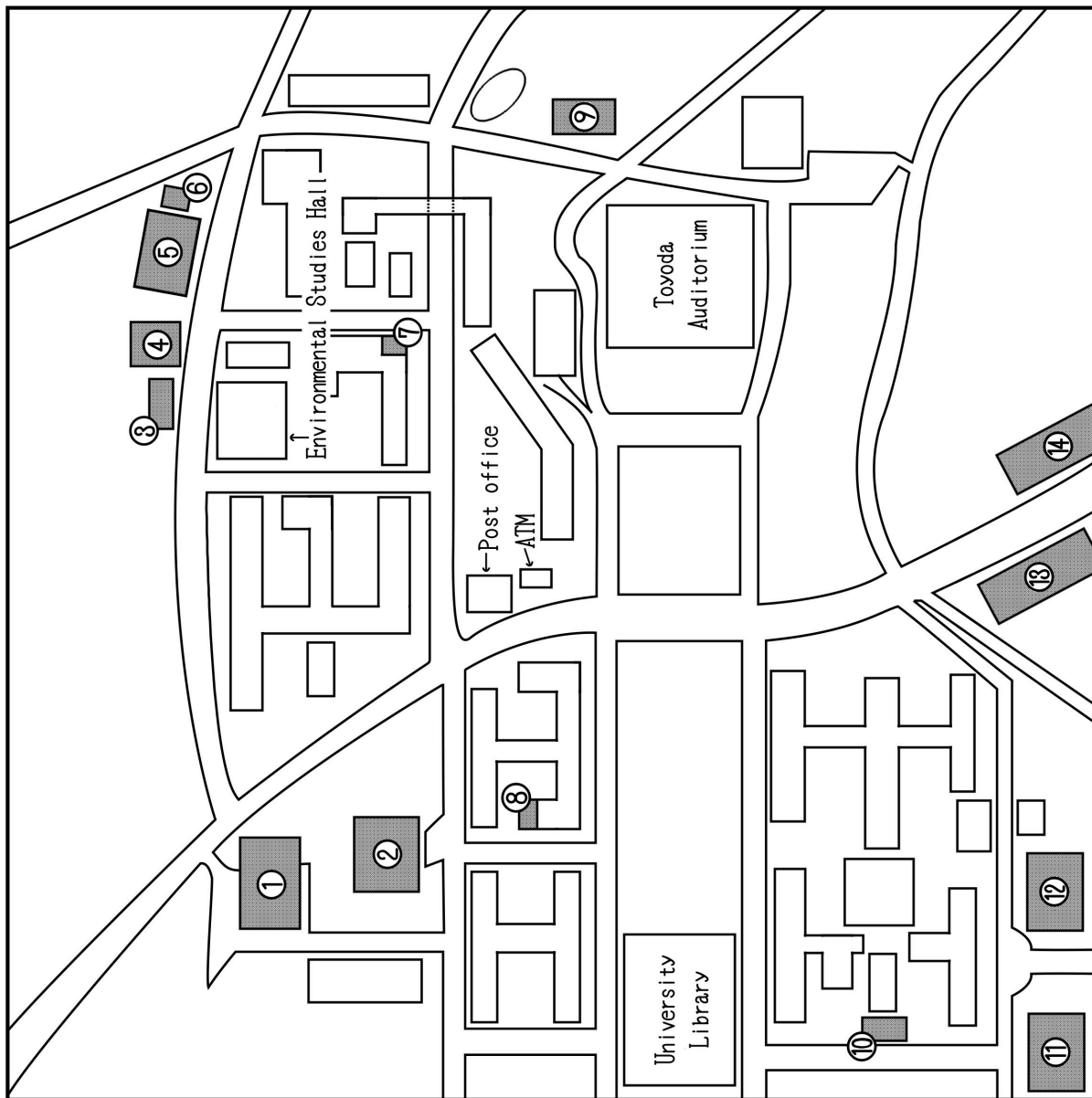
- 25** Center for Developmental Clinical Psychology and Psychiatry
- 26** Center for the Studies of Higher Education
- 27** Education Center for International Students
- 27.2** Advising & Counseling Services, ECIS
- 28** Center for Asian Legal Exchange
- 29** Information Technology Center
- 30** Kobayashi-Maskawa Institute for the Origin of Particles and the Universe (KMI)
- 31** Research Center for Materials Science
- 32** Bioscience and Biotechnology Center
- 33** Radioisotope Research Center
- 34** Research Institute of Environmental Medicine
- 35** Hydrospheric Atmospheric Research Center
- 36** Institute for Advanced Research Hall
- 37** Solar-Terrestrial Environment Laboratory
- 38** Eco Topia Science Institute
- 39** International Cooperation Center for Agricultural Education
- 40** Research Laboratory Building
- 41** Research Center of Health, Physical Fitness and Sports

### Conference Halls & Galleries

- 42** Noyori Conference Hall
- 43** Noyori Materials Science Laboratory, Lecture Hall
- 44** Engineering and Science Building, ES Auditorium
- 45** Science South Building, Sakata & Hirata Hall
- 46** Environmental Studies Hall, Lecture Hall
- 47** Integrated Building (IB), Lecture Room
- 48** Graduate School / School of Economics, Conference Hall
- 49** Graduate School of International Development, Auditorium
- 50** Integrated Research Building (Arts and Social Sciences), Conference Room

# DINING MAP

- ①Hokubu Shokudo / Cafeteria
- ②Shichimittei / Cafeteria
- ③Cafe Fronte / Coffee Shop
- ④Dining Forest / Cafeteria
- ⑤Restaurant Haranoki
- ⑥Rikei Shop / Convenience Store
- ⑦Craig's Cafe / Coffee Shop
- ⑧IB Cafe / Coffee Shop
- ⑨Shokuin Shokudo / Cafeteria
- ⑩Family Mart / Convenience Store
- ⑪Friendly Nanbu / Cafeteria
- ⑫Nanbu Shokudo / Cafeteria
- ⑬Hello Kid / Hamburger Steak Restaurant
- LAWSON / Convenience Store
- Bento Man / Lunchbox Shop
- Botantei / Chinese Restaurant
- ⑭Cafe Terrace Cremes / Coffee Shop
- Tsubovakitei / Grilled-meat (yakimiku) Restaurant
- Kourantei
- GRAN PIATTO / Italian Restaurant





## Hospitals around Nagoya University (※English OK)

### *Nagoya Daini Red Cross Hospital*

Address: 2-9 Myoken-cho, Showa-ku, Nagoya

Tel: (052) 832-1121

Mon-Fri: 8:00-11:00

Closed on Sat, Sun, holidays

### *Watanabe Clinic*

Address: 1F Nikkou Yamate-dori Building, 3 -9-1 Yamate-dori, Showa-ku, Nagoya

Tel: (052)861-3450

Mon-Sat: 9:00-11:30

Mon, Wed-Fri: 16:00-17:30

Closed on Sun, holidays

### *Kai Clinic*

Address: 32-2 Myoken-cho, Showa-ku, Nagoya

Tel: (052)836-9136

Mon-Sat: 9:00-12:00

Mon-Wed, Fri: 18:00-20:30

Closed on Sun, holidays

### *Yamate Dermatologist*

Address: 2-9-1 Yamate-dori, Showa-ku, Nagoya

Tel: (052)836-4115

Mon, Tue, Thu-Sat: 9:30-12:30

Mon, Tue, Thu, Fri: 16:30-19:30

Sat: 14:30-17:30

Closed on Wed, Sun, holidays

### *Fujimi Dentist*

Address: 139 Yagotohujimi, Showa-ku, Nagoya

Tel: (052)835-3200

Mon-Wed, Fri, Sat: 9:30-12:30

Mon-Wed, Fri, Sat: 14:00-19:00

Closed on Thu, Sun, holidays

